

https://dspace.org/

Creation of transgenic chicken for production of human therapeutic proteins in ovo

Hyman, Sophia Yekara

2023
https://hdl.handle.net/10539/35717

Downloaded from a DSpace repository. https://dspace.org/



Creation of transgenic chicken for production of human therapeutic proteins *in ovo.*

By Sophia Yekara Hyman

(1659440)

Dissertation

Submitted to the Faculty of Science,

University of the Witwatersrand, Johannesburg,

in fulfilment of the requirements for the degree

Master of Science

Supervised by: Prof Natalya Nikitina

Johannesburg, February 2023

Declaration

I declare that this dissertation is my own, unaided work. It is being submitted for the Degree of Master of Science at the University of the Witwatersrand, Johannesburg. It has not been submitted before for any degree or examination at any other University.



13th day of February 2023 at Johannesburg

Abstract

The transgenic chicken *in ovo* expression platform for production of pharmaceutical proteins, presents a more cost-effective, high-yielding alternative to current cell-based production systems. The aim in this project was to contribute towards developing a transgenic chicken bioreactor that will ultimately express high levels of therapeutic protein, Tenecteplase, in place of endogenous egg white proteins Ovalbumin and Ovomucoid *in ovo*. The gene-editing approach was CRISPR-Cas9 gene drive constructs in isolated chicken germ cells. The Ovalbumin- and Ovomucoid-specific gene drive constructs were generated through multiple PCR, restriction digests and cloning procedures. Chicken PGCs, extracted from blood of stage 14-17HH embryos, were propagated *in vitro* upon chicken embryonic fibroblast feeder cells. PGCs exhibited typical spherical morphology and stained positive for germ cell surface marker SSEA-1 in fluorescence immunocytochemistry. Unfortunately, gene drive constructs failed to produce desired transgene integration following transfection and antibiotic selection of PGCs. In busulfan-based sterilisation, endogenous PGCs were reduced significantly by 70% using 1.5µg/µl busulfan ($P<0.05$). Donor PGCs injected into day 3 embryonic vasculature were not detected in gonads of previously sterilised embryos at day 6 incubation; likely due to the sup-optimal fluorescent-vector-based tracking of donor PGCs or injection via unreliable mouth-controlled pipette. Future work must investigate manipulating the various factors influencing gene editing at target loci, including cell conditions and pathways favouring HDR, accessible chromatin states for CRISPR-Cas9 machinery, gRNA design, and donor gene drive template conformation. These preliminary experiments, towards production of a transgenic chicken bioreactor, have provided valuable resources and insight for achievement of this pursuit.

Acknowledgements

I would first like to thank my supervisor, Prof Natalya Nikitina, for her guidance and support, with full enthusiasm and encouragement, throughout this project. I am grateful to have benefited from her wealth of knowledge and experience, which made navigating the, at times, daunting tasks of this project possible. I am grateful for and proud of the knowledge I gained and techniques I accomplished during the time I worked in her lab.

To my lab mates, thank you for your advice, patience and moral support. I would also like to acknowledge WITS for the funding of this degree.

Lastly, this dissertation would not have been possible without the unconditional love and support of my parents and two sisters. These accomplishments are because of them and I am forever grateful.

Table of Contents

Section 1: Introduction *13*

1.1 An introduction to protein expression systems 13

1.2 Transgenic animals as a bioreactor 19

1.3 The transgenic hen protein expression platform 21

1.4 Genetic engineering techniques for creating transgenic chicken: past and present 23

1.5 Primordial germ cells: the key to creating transgenics 26

1.6 Sterilisation of recipient embryos for replacement of the germline 32

1.7 Genome editing in chickens: a targeted approach 34

1.8 The therapeutic protein of interest: Tenecteplase 42

1.9 Aims and Objectives 43

Section 2: Methods *45*

2.1 Preparing the OVA and the OVM gene drive constructs with cloning 45

2.1.1 Overview of cloning strategy for generation of the OVA gene drive 45

2.1.2 Overview of the cloning strategy for generation of the OVM gene drive 50

2.1.3 Agarose gel electrophoresis 59

2.1.4 Restriction enzyme digestion 59

2.1.5 Gel extraction 59

2.1.6 DNA cleanup 60

2.1.7 DNA ligation 60

2.1.8 Bacterial transformation 61

2.1.9 Plasmid extraction 61

2.2.0 PCR procedures and preparation of templates for modifying gene drives 62

2.2.1 PCR amplification and cloning of the mouse *HSPA2* promoter 62

2.2.2 PCR preparation of antibiotic resistance fragments and DNA assembly of Puromycin into the OVA gene drive 65

2.2.3 NEBuilder HiFi DNA assembly 69

2.2.4 PCR and cloning for generating the OVM gene drive 72

2.2.5 Replacing the gRNA cassette in the OVM gene drive 72

2.2.6 PCR preparation of antibiotic resistance for assembly of Neomycin into OVM gene drive 73

2.2.7 Replacing the CBh promoter with *HSPA2* promoter in the OVM gene drive 74

2.2.8 Addition of 5' and 3' OVM homology arms 74

2.2.9 Plasmid midiprep 74

2.3 Animal Ethics 75

2.4 Acquisition and incubation of chicken embryos 75

2.5.0 Establishment of culture of primary chicken embryonic fibroblasts 76

2.5.1 Maintenance of CEF cultures 77

2.5.2 Cryopreservation of CEFs 77

2.5.3 Preparation of CEF feeder layers 77

2.5.4 Isolation of male PGCs from embryonic vasculature to establish primary culture 78

2.5.5 Maintenance of PGC primary culture 79

2.5.6 Passaging PGCs and replenishing the CEF feeder layer 79

2.5.7 PCR-based Sexing of embryos 80

2.6 Verifying PGC identity by immunocytochemical staining 81

2.7 Partial sterilisation of chicken embryos 82

2.7.1 Removal of PGCs from chicken embryos using busulfan 82

2.7.2 Assessing sterilisation efficiency in embryonic gonads 83

2.7.3 Processing Embryo Gonadal tissue for Cryosectioning 83

2.7.4 Cryosectioning of gonadal tissue samples 84

2.7.5 Immunohistochemistry of gonadal tissue sections 84

2.7.6 Statistical analysis of busulfan ablation 85

2.8.0 Antibiotic kill curves.....86

2.8.1 Statistical analysis of kill curves.....87

2.9.0 Transfection Procedures.....87

2.9.1 Electroporation of PGCs.....88

2.9.2 Lipofection of PGCs.....89

2.9.3 Puromycin selection of transfected PGCs.....89

2.9.4 Neomycin selection of transfected PGCs.....90

2.9.5 Screening transfected PGCs.....90

2.9.6 Repopulation of PGCs in sterilised embryos.....94

***Section 3: Results*.....95**

3.1 Preparation of the OVA and OVM gene drives.....95

3.1.1 Successful amplification of Puromycin antibiotic resistance sequence.....95

3.1.2 Molecular cloning: insertion of Puromycin into OVA gene drive via NEBuilder HiFi DNA Assembly.....96

3.1.3 Successful Amplification and cloning of the Mouse *HSPA2* promoter into the OVA gene drive.....98

3.1.4 Constructing the OVM gene drive: replacement of the gRNA cassette via cloning.....99

3.1.5 Successful amplification of Neomycin antibiotic resistance gene.....100

3.1.6 Molecular cloning: insertion of Neomycin into gene drive with NEBuilder HiFi DNA Assembly.....101

3.1.7 Cloning: insertion of *HSPA2* promoter into the OVM gene drive.....102

3.1.8 Cloning of OVM 5' and OVM 3' Homology arms onto the OVM gene drive..103

3.2 Isolation and culture of primary PGCs.....104

3.3 Determining optimal busulfan concentration for PGC depletion in embryos.....109

3.4 Determining Puromycin and Neomycin sensitivity of PGCs.....113

3.5 Transfection of PGCs with modified gene drives, eSpCas9 construct, and mRFP-tol2 construct shows the desired HDR-mediated integration did not occur.....115

3.6 Repopulation of busulfan-ablated embryos with PGCs transfected with mRFP-tol2 tracer.....119

Section 4: Discussion*.....*122

4.1 Isolation and culture of primary PGCs 122

4.2 Sterilisation of embryos by busulfan injections 124

4.3 Attempting to restore PGC population in sterilised embryos 126

4.4 Assessing the activity of CRISPR gene drives in PGCs.....130

Conclusions and Future Work.....133

Supplementary*.....*137

References* *147

Appendices*.....*174

List of Figures

Figure 1.1. Migration of PGCs in the early developing embryo.
Figure 1.2. The final OVA and OVM gene drive constructs and their features, to be constructed and used for editing PGCs.
Figure 1.3. Mechanism of action of CRISPR-Cas9 gene drive.
Figure 1.4. Inheritance of a specific allele via gene drive results in Super-Mendelian inheritance.
Figure 2.1. Features of the base gene drive to which various modifications could be made.
Figure 2.2. Steps for modifying the Zeocin antibiotic region in the OVA gene drive.
Figure 2.3. Steps for replacing the CBh promoter in the OVA gene drive.
Figure 2.4. Cloning steps for inserting new OVM gRNA cassette into the OVM gene drive.
Figure 2.5. Steps for adjustment of the Zeocin antibiotic and surrounding region in the OVM gene drive.
Figure 2.6. Strategy for replacing the CBh promoter in the OVM gene drive.
Figure 2.7. Cloning steps for addition of the OVM 5' HA into the OVM gene drive.
Figure 2.8. Cloning steps for addition of the OVM 3' HA into the OVM gene drive.
Figure 2.9. pMiniT 2.0 cloning vector containing HSPA2 insert.
Figure 2.10. The principle of DNA assembly of fragments utilizing sequence homology between adjacent fragments.
Figure 2.11. The stock eSpCas9(1.1)-T2A-Puro vector.
Figure 2.12. The stock pCI-neo vector.
Figure 2.13. Position of primers for creating overlapping regions in antibiotic and associated fragments.
Figure 2.14. The new OVM gRNA cassette for insertion into the OVM gene drive.
Figure 2.15. Main points of extraction of blood containing PGCs from HH14-17 embryos.
Figure 2.16. Setup of busulfan injection into stage X embryos.
Figure 2.17. mRFP-tol2 vector construct
Figure 2.18. The HDR PCR product positions at the OVA and OVM loci.
Figure 3.1. PCR amplification of fragments used for antibiotic DNA assembly in the OVA gene drive.
Figure 3.2. Overlap extension PCR amplification of assembled 3'UTR-SV40-Puromycin fragment.

Figure 3.3. Preparation of the OVA gene drive for replacement of antibiotic by double restriction digestion.
Figure 3.4. Restriction enzyme digestions verifying insertion of assembled Puromycin into the OVA gene drive.
Figure 3.5. PCR amplification and restriction digestion of the mouse HSPA2 promoter.
Figure 3.6. Double restriction digestion of OVA gene drive verifying HSPA2 insert.
Figure 3.7. Restriction digests confirming cloning the new OVM gRNA cassette into the OVM gene drive.
Figure 3.8. PCR amplification of fragments for antibiotic DNA assembly of OVM gene drive.
Figure 3.9. Preparing the OVM gene drive for replacement of antibiotic by double restriction digestion.
Figure 3.10. Restriction enzyme digest verifying DNA assembly of Neomycin into the OVM gene drive.
Figure 3.11. Double restriction digestion of OVM gene drive verifying HSPA2 insert.
Figure 3.12. Restriction digests of gene drives and HAs for cloning of the OVM homology arms into the OVM gene drive.
Figure 3.13. Direct PCR Sexing of chicken embryo samples used for PGC extraction.
Figure 3.14. Culture of male primary chicken PGCs together with growth inhibited CEFs.
Figure 3.15. Immunofluorescence staining of PGCs.
Figure 3.16. Immunohistochemistry using SSEA-1 for detection of PGCs in gonadal tissue sections of embryos treated with different busulfan concentrations.
Figure 3.17. Proportion of PGCs remaining in embryos after treatment with different busulfan concentrations.
Figure 3.18. Survival rate of embryo groups treated with different busulfan concentrations.
Figure 3.19. PGC kill curve after treatment with different Puromycin concentrations.
Figure 3.20. PGC kill curve after treatment with different Neomycin concentrations.
Figure 3.21. PGCs co-transfected with gene drives and mRFP-tol2 tracer.
Figure 3.22. PCR-based screening for HDR-integration or NHEJ at the OVA and OVM loci in transfected PGCs.
Figure 3.23. PCR-based detection of constructs within transfected PGCs.
Figure 3.24. PGCs transfected with mRFP-tol2 tracer construct.
Figure 3.25. Fluorescence imaging of repopulation of exogenous PGCs in gonads of busulfan ablated embryos.

List of Tables

Table 1.1. Summary of expression platforms for therapeutic protein production.

Table 2.1. Restriction enzyme digestion setup.

Table 2.2. Ligation reaction setup

Table 2.3. Primer pair for amplification of Mouse *HSPA2* promoter fragment.

Table 2.4. PCR reaction setup for *HSPA2* promoter using MyFi DNA Polymerase.

Table 2.5. PCR cycling conditions for amplification of mouse *HSPA2* promoter.

Table 2.6. Colony PCR cycling conditions for the *HSPA2* promoter in pMiniT 2.0.

Table 2.7. Primer pairs for amplification of fragments to be used in antibiotic DNA assembly.

Table 2.8. Q5 Hot start High Fidelity PCR reaction setup for amplification of four individual fragments for antibiotic assembly.

Table 2.9. Q5 Hot start cycling conditions for amplification of individual fragments to be used in antibiotic DNA assembly.

Table 2.10. Cycling conditions for overlap extension PCR of OVA gene drive-relevant antibiotic region.

Table 2.11. NEBuilder HiFi DNA Assembly reaction setup for replacement of Zeocin region in gene drives.

Table 2.12. Cycling conditions for overlap extension PCR of OVM gene drive-relevant antibiotic region.

Table 2.13. Taq PCR reaction setup for sexing PCR.

Table 2.14. Sexing PCR cycling conditions.

Table 2.15. Electroporation conditions for PGCs performed with the BTX Harvard ECM 830 Square Wave electroporator.

Table 2.16. Contents of the DNA-lipid complex lipofection reactions for addition to PGCs.

Table 2.17. Primer pairs for 3' and 5' HDR integration assessment.

Table 2.18. Platinum SuperFi II DNA Polymerase PCR setup for screening editing in PGCs.

Table 2.19. Cycling conditions for amplification of 3' and 5' HDR integration amplicons.

Table 2.20. Primer pairs for NHEJ assessment.

Table 2.21. Cycling conditions for amplification of NHEJ amplicons.

Table 2.22. Primers for detecting constructs in transfected PGCs.

List of Abbreviations

ACK: ammonium chloride potassium

bFGF: basic fibroblast growth factor

BSA: bovine serum albumin

BSC: biosafety cabinet

CEFs: chicken embryonic fibroblasts

CHO: Chinese Hamster Ovary

CRISPR: Clustered Regularly Interspaced Short Palindromic repeats

DMSO: dimethyl sulfoxide

DSBs: double-stranded breaks

FACS: fluorescence activated cell sorting

FBS: foetal bovine serum

gRNA: Guide RNA

HA: homology arm

HAs: Homology arms

HDR: homology-directed repair

HH: Hamburger and Hamilton

HSPA2: Heat shock protein 2

LIF: leukaemia inhibitory factor

MACS: magnetic activated cell sorting

NCDs: Non-communicable diseases

NHEJ: non-homologous end joining

OVA: Ovalbumin

OVM: Ovomucoid

OVT: Ovotransferrin

PAS: periodic acid-Schiff staining

PBS: phosphate buffered saline

PFA: paraformaldehyde

PGCs: primordial germ cells

RFP: red fluorescent protein

SCF: stem cell factor

SSEA-1: stage specific embryonic antigen-1

TBSTD: Tris-Buffered Saline TWEEN DMSO

UV- ultraviolet

Section 1: Introduction

1.1 An introduction to protein expression systems

The possibility for establishing a transgenic animal bioreactor is one of the most important emerging research areas in the field of human therapeutic protein production. Complex therapeutic proteins, used for treating a wide range of human diseases usually related to protein absence or malfunction, constitute a significant portion of the biopharmaceutical industry (Usmani *et al.*, 2017; Owczarek, Gerszberg and Hnatuszko-Konka, 2019). The rising prevalence of many non-communicable diseases (NCDs) with the potential for targeted treatment with protein therapeutics, means an increased demand for these products (Gakidou *et al.*, 2017; Vos *et al.*, 2020). The global burden of NCDs is evident in its annual contribution to 74% of deaths worldwide. The four major diseases (cardiovascular disease, cancers, chronic respiratory diseases, diabetes) and others responsible for most of these premature deaths caused by NCDs usually require protein therapeutics for treatment as often times life-saving interventions (Gakidou *et al.*, 2017; Vos *et al.*, 2020). NCDs more greatly affect those in low- and middle-income countries where the majority of NCDs occur. Access to these costly therapeutics in these low-resource settings is a problem that strains an individual's already limited resources and may even force them into poverty (Gakidou *et al.*, 2017; Vos *et al.*, 2020). Affordable, accessible protein therapeutics are paramount. Advances in recombinant DNA methods have not only made production of human therapeutic proteins possible but have also allowed for the modification and enhancement of therapeutic protein function (Grillberger *et al.*, 2009; Strohl, 2015). The large-scale production of therapeutic proteins has been performed in various expression platforms; however, these systems are generally limited by high costs, relatively low yields, production time, limited scalability or inability to produce biologically and structurally appropriate and safe complex protein therapeutics (Dingermann, 2008; Bertolini *et al.*, 2016; Herron *et al.*, 2018). Thus, protein therapeutic availability has not necessarily translated into accessibility or affordability. The transgenic chicken may be the solution to these limitations.

Conventional protein expression platforms have been developed including bacteria, yeast, mammalian cells, insect cells, transgenic plants, and animals. The principle determinant of production platform choice is its bioactivity. The biological characteristics and structure of the product produced by the host are fundamental for production of the desired therapeutic protein. These structural and biological attributes are important for the efficacy, safety, and

immunogenic implications in patients (Grillberger *et al.*, 2009; Solá and Griebenow, 2010; van Beers and Bardor, 2012). Immunogenicity can sometimes be life-threatening in patients and eliminating possible causes which arise from expression systems is a priority in biopharmaceutical production. At present there is a heavy dependence on cell culture expression platforms, however not all proteins can be produced in this system with the same level of success, which provides incentive for further research into alternative expression systems (Bertolini *et al.*, 2016; Owczarek, Gerszberg and Hnatuszko-Konka, 2019; Tripathi and Shrivastava, 2019; Tihanyi and Nyitray, 2020; Kulagina *et al.*, 2021). Furthermore, there still remains much to be learned in attempting to manipulate various expression systems' capabilities towards the desirable high-yielding, low-cost platforms they have the potential to become, and the scope for improvement is large.

Some of the first recombinant proteins were produced in bacteria. This facilitated advances in treating diabetes using recombinant insulin produced in *E. coli* (Goeddel *et al.*, 1979). At the time, this protein expression was profoundly more advanced and improved insulin supply compared to the pre-recombinant-era technology whereby biologics were extracted from natural sources (usually bovine or porcine) (Landgraf and Sandow, 2016). Bacteria-mediated insulin expression was the therapeutic protein breakthrough that set the stage for discoveries in various expression systems. Subsequently, recombinant forms of the therapeutic have been developed to improve its activity (Brogard, Blickle and Paris-Bockel, 1985; Maikawa *et al.*, 2020).

The use of the bacterial system did not stop there. Bacteria have since been used to produce many FDA-approved products ranging from hormones (human growth hormone, insulin analogues, glucagons), to interferons and interleukins (Babaeipour, Shojaosadati and Maghsoudi, 2013; Nausch *et al.*, 2013; Bis *et al.*, 2014; Arif *et al.*, 2015; Hwang *et al.*, 2016; Song *et al.*, 2017; Pal *et al.*, 2018). Bacteria, specifically *E. coli,* are preferred for their fast growth and production setup, as well as low costs. Maintaining bacterial cells requires relatively simple, low-cost, low-input media components such as yeast extract, tryptone, glycerol, sodium chloride and other salts (Francis and Page, 2010; Rosano and Ceccarelli, 2014; Jia and Jeon, 2016). However, bacteria are unable to perform most human-like post-translational modifications such as splicing, phosphorylation, or proper protein folding- all inherent properties of human proteins. This means that additional steps need to be taken to

incorporate genes already without the introns in the bacteria host and engineer the host to acquire the protein modifying properties. This inability to mimic typical complex human protein therapeutic processing, such as renaturation or folding, is a drawback due to the reduced bioactivity and immune response-stimulating properties that can arise (Hermeling *et al.*, 2004; van Beers and Bardor, 2012; Baeshen *et al.*, 2015).

One of the most common, complex post-translational modifications is glycosylation, of which there are different types. Species- and cell-specific glycosylation patterns are important for their impact on efficacy, half-life and immunogenicity of protein products (Hermeling *et al.*, 2004; Solá and Griebenow, 2010; van Beers and Bardor, 2012). The absence of appropriate native glycosylation of proteins in *E. coli* has led to the introduction of synthetic glycosylation pathways via engineering of the cells and inducing expression of glycosylation enzymes. This demonstrates the potential for manipulation of bacterial expression systems. However, reduced biological activity and high costs of endotoxin-related purification procedures remain a limitation (Mamat *et al.*, 2015). Furthermore, retrieving proteins from this system is a challenge as insoluble aggregates form, which requires costly purification processes that decreases yield (Chrunyk *et al.*, 1993; Peternel and Komel, 2011; Gupta *et al.*, 2017). When too much of a recombinant protein is expressed by bacteria, cell stress and protein insolubility further compound this issue (Peternel and Komel, 2011; Zeng and Yang, 2019; Bhatwa *et al.*, 2021). The bacterial expression system has many benefits and has been widely adopted, yet limitations linked to balance between cost and yield can be difficult to navigate in large-scale protein production setups. The system is limited as to the types of proteins that could be successfully produced (predominantly small peptides).

Other eukaryotic cell-based systems explored are yeast, with the most common being *S. cerevisiae* or *P. pastoris.* Like bacteria, this is a relatively low-cost system; quick to setup; allows for fast transition into the production phase, and scalability to large bioreactor cultures (Ferrer-Miralles *et al.*, 2009; Nielsen, 2013; Vieira Gomes *et al.*, 2018; Tripathi and Shrivastava, 2019). Yeast expression systems are superior to bacteria in that they possess the cellular machinery for performing post-translational modifications (such as glycosylation, O-linked phosphorylation, acetylation, and disulphide bonds) and in genetically modified yeast, N-glycosylation is also possible. However, these glycosylations are slightly different to human patterns, hence many groups still engineer the yeast to produce more human-like glycosylation

(Choi *et al.*, 2003; Cheon *et al.*, 2012; Hamilton *et al.*, 2013; Vieira Gomes *et al.*, 2018). Yeast-produced proteins also lack the endotoxin-contamination associated with production in bacterial hosts (Kulagina *et al.*, 2021). Another major advantage is that the yeast-based system also secretes recombinant protein into the media, simplifying purification procedures and reducing overall costs (Nielsen, 2013; Mamat *et al.*, 2015). Yet the risk of the overexpression of recombinant protein causes a burden to the cells and can result in the end-product not forming correctly (Mattanovich *et al.*, 2004). Examples of therapeutic protein products which have been expressed by yeast systems include blood factors, growth factors and cytokines (Martínez *et al.*, 2012; Carcao *et al.*, 2018; Kulagina *et al.*, 2021). While the yeast expression system is beneficial for producing a more structurally human-like protein therapeutic than bacterial systems, obtaining high-quality purified protein is still difficult in many yeast-based expression systems.

The baculovirus-insect cell-based expression system is gaining increasing approval as a eukaryotic cell-based host for production of recombinant proteins (Felberbaum, 2015; Yee *et al.*, 2018). The innate ability of baculoviruses to infect certain species of insect cells, and thereby transfer foreign DNA, was the founding principle of this expression system (Hong *et al.*, 2022). This means that setup of this platform is relatively straightforward. The process involves design and construction of a recombinant baculovirus expression vector followed by delivery of recombinant baculovirus DNA to insect cells and purification of recombinant protein product (Cox, 2021; Hong *et al.*, 2022). The assembly of the recombinant Baculovirus vector carrying the transgene of interest is easily and quickly performed through various methods such as DNA assembly or cloning (Cox, 2021; Hong *et al.*, 2022). A major advantage of this system is the capacity for the baculovirus vector to carry large transgenic sequences (Chen *et al.*, 2011). The system is relatively quick to setup and recombinant protein can be obtained in relatively short amounts of time due to the rapid growth rate of insect cell lines (Hong *et al.*, 2022). Insect cell lines such as those obtained from *Spodoptera frugiperda* and *Trichoplusia ni,* are increasingly being used to produce licenced protein therapeutics for humans (van Oers, Pijlman and Vlak, 2015; Hong *et al.*, 2022). For example, protein-based cancer vaccines and protein-based influenza vaccines derived from the baculovirus-insect system have been approved for human use (Cox and Hollister, 2009; Cox, 2012; Felberbaum, 2015; van Oers, Pijlman and Vlak, 2015). Despite the numerous advantages of the baculovirus-insect expression system, it is still important to acknowledge its limitations. While several appropriate protein-folding and post-translational modifications are possible within the system

(such as phosphorylation, glycosylation and ubiquitination), certain post-translational modifications common in complex protein therapeutics (such as the human-like N-glycosylation) cannot be correctly completed in insect cells (Breitbach and Jarvis, 2001; Palmberger *et al.*, 2012; van Oers, Pijlman and Vlak, 2015). Furthermore some of these insect-specific post-translational modifications are immunogenic and therefore render the recombinant product inappropriate for use in humans (Mabashi-Asazuma *et al.*, 2014). Hence, insect cells are engineered to produce proteins with more human-like glycosylation patterns (Okada *et al.*, 2010; Palmberger *et al.*, 2012; Mabashi-Asazuma *et al.*, 2014). In addition, despite the ease and speed of scalability of the system, higher recombinant protein yields are desirable for commercial products where there is higher demand (Felberbaum, 2015; Tripathi and Shrivastava, 2019). For more complex proteins, scaleup requires time-consuming optimisation processes (Irons *et al.*, 2018). Furthermore yield optimisation is a challenge given that expression levels of insect-produced therapeutic proteins are negatively impacted by insect cell lysis following viral infection (Yee *et al.*, 2018). Significant progress has been made to develop strategies to delay insect cell lysis and hence promote insect cell survival and higher levels of recombinant protein expression for extended periods of time (Steele *et al.*, 2017; Fernandes *et al.*, 2020; Zhang *et al.*, 2021). Overall when producing less complex proteins, the system is cost-effective due to the ease of upscale and adaptability to large-scale growth conditions, as well as the low-level biosafety requirements compared to mammalian cells (Chen *et al.*, 2011; Felberbaum, 2015; Cox, 2021). The main cost-limiting factors are the upfront funds required for large bioreactors and the purification processes which reduce product yield (Felberbaum, 2015). Ultimately, the system is still under constant investigation to provide different approaches for optimisation of recombinant protein production.

Plants have been demonstrated as potential hosts for recombinant therapeutic protein production at three different levels of expression: via cells, tissue, or through the production of a whole transgenic plant. The vast potential for restricting expression of the recombinant protein to a compartment of the plant (the leaves, fruit, seeds or roots) makes is easier to collect the protein. Plants are also capable of producing certain post-translational modifications (N-glycosylation), however some of these modifications are non-human-like which raises the need for genetic modifications to the host prior to therapeutic protein production (Loos and Steinkellner, 2014; Yao *et al.*, 2015; Fischer *et al.*, 2018). A major disadvantage of the plant expression system is the potential for product contamination with pesticides, metabolites or

even pollen which requires post-production purification that further drives up costs (Yao *et al.*, 2015; Tripathi and Shrivastava, 2019). Overall, the plant expression system is a more cost-effective alternative and possesses greater potential for scalability when compared to eukaryote-based mammalian systems (Yao *et al.*, 2015; Łojewska *et al.*, 2016). Although few have been approved for human use, a successful example of a plant-cell-based protein therapeutic is human recombinant β-glucocerebrosidase produced in carrot cell cultures. This protein has reached commercial-scale production and was FDA-approved for treating Gaucher disease (Shaaltiel *et al.*, 2007). Ultimately plant-cell-culture expression systems' low yields compared to what is required for economic feasibility, has inhibited their commercialisation.

The limitations of previously discussed systems which are in many ways ameliorated by mammalian cell systems, have led to large-scale investment in and adaptation of and reliance on mammalian cells in the field of therapeutic protein production. Importantly, mammalian cell-based expression systems are able to produce structurally complex proteins with more human-like properties. Post-translational modifications, folding and processing are achievable within the mammalian cell-expression system in a manner that has positive implications on the proteins' function and compatibility with human bodily systems (van Beers and Bardor, 2012; Tripathi and Shrivastava, 2019). The downside is that genetically engineering mammalian cells and delivery of the transgene for heterologous protein expression is far more complex and slower relative to bacterial or yeast systems (Tripathi and Shrivastava, 2019). Furthermore, the subsequent workflow towards upscaling protein production involves the selection and screening of a single clone that shows stability and high protein expression levels. This takes time (Browne and Al-Rubeai, 2009; Priola *et al.*, 2016; Tripathi and Shrivastava, 2019).

The dominant mammalian cell line used is the Chinese Hamster Ovary (CHO) cell line, responsible for the majority of therapeutic protein production (Lalonde and Durocher, 2017; Stolfa *et al.*, 2018). Impressive cell line evolution has been achieved through intense research and genetic manipulation. This has resulted in expression levels that outperform many other cell lines across species with reports of up to 3-10g/L of product. However, in practice, purification procedures usually cause yield to drop well below this level in large bioreactors (Dahodwala and Lee, 2019; Tihanyi and Nyitray, 2020). Furthermore, the cost per gram of product produced is also relatively high and scale up of protein production in bioreactors

(which can be ten to one thousand litres) is expensive and takes time (Dyck *et al.*, 2003; Soler and Houdebine, 2007).

Today this cell line is favoured for its stability and growth even at large-scale industrial levels, as well as its ability (sometimes via forced genetic manipulation) to carry out glycosylation patterns similar to humans. The CHO cells have proven amenable to genetic modifications and adapt well in large-scale growth conditions (Dahodwala and Lee, 2019; Tihanyi and Nyitray, 2020). On the other hand, genomic rearrangements and gene expression changes can occur, which, coupled with the intense expression demands of the cells, over time can decrease their stability, product output and product quality (Fischer, Handrick and Otte, 2015; Feichtinger *et al.*, 2016; Li *et al.*, 2016). Furthermore, CHO cells can produce non-human-like glycan structures on proteins. This impacts immunogenicity of the protein produced (Bosques *et al.*, 2010). Perhaps the most significant obstacle in this expression system is the costs of setting up the large CHO cell bioreactor. This requires significant upfront investment alone of approximately US$600 million for a standard facility with six 15 000L bioreactor tanks, which can undoubtedly be an impediment to its establishment (Johnson and Merck & Co, 2017). The downstream effects of this and the entire cost of manufacturing on the end price of a pharmaceutical protein is significant (Puetz and Wurm, 2019). Given that multiple factors affect the pricing of protein-based biopharmaceuticals, it is worthwhile to find alternatives in the upstream manufacturing or production process to attempt to reduce prices for creating access to these drugs in developing countries. Numerous advantages related to productivity at large-scale industrial levels and ability to perform glycosylation have made the cell line a favourite, yet the cells are constantly under investigation for improvement. The need for an economically feasible, high-yielding expression system for quality protein therapeutics exists and has thus shifted the focus of some towards the transgenic animal bioreactor.

1.2 Transgenic animals as a bioreactor

Harnessing the innate high-level expression systems (secretory systems) existing in animals is an attractive prospect for the field of therapeutic protein production. Exponential advances in gene editing technologies have made this prospect tangible. Transgenic animals have the potential to address attempts to increase yields and avoid the inflation of associated costs. By restricting expression of the therapeutic protein to secretory tissue, scientists are able to obtain the therapeutic protein expressed by mammary glands in milk or by tubular glands in albumen

(egg white) (Harvey and Ivarie, 2003; Maga *et al.*, 2006; Lillico *et al.*, 2007; Houdebine, 2009; Herron *et al.*, 2018; Kwon *et al.*, 2018).

For some time, transgenic animal hosts such as cows, rabbits, goats, sheep, and pigs have been or are being studied to produce recombinant proteins in their milk (Wright *et al.*, 1991; Maga *et al.*, 2006; Yang *et al.*, 2008; Zhang *et al.*, 2008; van Veen *et al.*, 2012; S.-Y. Lee *et al.*, 2020). However, very few of these proteins have been approved and implemented commercially for treating human disease. Human-like post-translational modifications are a primary advantage of the animal expression platform. However, there is the possibility that some post-translational modifications may cause an immune response or reduced activity in the human recipient (Gil, Velander and Van Cott, 2008). There are also complex ethical considerations which arise from creating these transgenics, especially when the protein being expressed is active and might have harmful effects on the health of the host (Massoud *et al.*, 1996). Different groups have shown successful expression of protein without harmful side effects that have been FDA-approved: recombinant antithrombin produced in goat milk and C1 esterase inhibitor produced in rabbit milk (Adiguzel *et al.*, 2009; van Veen *et al.*, 2012). There are disadvantages to utilising larger mammals, such as goats, for recombinant protein production systems. Larger mammals do not produce a large number of offspring (approximately 1 to 2 for goat; 8 for rabbit; 10 for pig; 1 to 2 for sheep; 1 for cow); gestation times are lengthy (for example 9 months for a cow; 5 months for goat); and lactation only begins close to birth of offspring (Houdebine, 2009). While significant improvement in protein expression levels are achieved compared to cell culture systems, the estimated recombinant protein produced per litre of milk in a single year is still low. Approximately 5g/L of recombinant proteins is produced in a lactating goat yielding 4kg per year (Houdebine, 2009). This would require significant scaleup (establishment of large herds of hosts) to achieve economically feasible levels of product, especially for diseases where there is higher demand or need. Larger mammals also require more maintenance in terms of space and feed which makes scaleup a costly issue (Herron *et al.*, 2018). Furthermore, the purification of end product in transgenic animal milk-expression systems is difficult and further increases production expenses (Harvey and Ivarie, 2003; Houdebine, 2009; Kwon *et al.*, 2018). Despite the notable advantages and potential of this system relating to cost and product yield, difficulties in creating transgenic animal platforms which are safe for host and recipient have prevented the commercial implementation of transgenic animal platforms. Avian models and their potential

for producing high-volume protein-containing eggs (from which the therapeutic protein of interest may be extracted), are considered a unique alternative. Transgenic chickens are emerging as the feasible frontrunner in this field.

1.3 The transgenic hen protein expression platform

A laying hen possesses the qualities needed to overcome the current obstacles of recombinant therapeutic protein expression platforms. Specifically, an *in ovo* expression system, whereby the transgenic hen lays an egg containing therapeutic protein, could provide the high-yield, low-cost system that is at present lacking. The egg white protein in the egg expressed by the tubular gland cells of the laying hen's oviduct magnum acts as the potential target for restricting expression of recombinant proteins (Harvey and Ivarie, 2003; Lillico *et al.*, 2007; Herron *et al.*, 2018). The desire to do so is driven largely by the high levels of expression which might be achieved. A single egg can hold approximately 3.5g of egg white protein, of which 64% can be replaced and thereby converted into recombinant protein. Considering that one hen lays an average of 300 eggs per year the potential for high levels of recombinant protein production exists (Kovacs-Nolan *et al.*, 2000; Harvey and Ivarie, 2003; Lillico *et al.*, 2007; Herron *et al.*, 2018).

The layer hen also provides a naturally sterile environment for protein storage *in ovo*, as well as endogenous protease inhibitors in egg whites which act to protect and preserve functionality of proteins for extended periods of time (Rapp *et al.*, 2003). The purification of protein products from egg white is also not as complex or costly as that from mammalian milk systems which contain high lipid and protein content (Harvey and Ivarie, 2003; Kwon *et al.*, 2018). In contrast to the domestic farm animals discussed previously, the chicken has shorter generation time, can produce high numbers of offspring and may easily expand their flocks from founder hosts (Rapp *et al.*, 2003; Lillico *et al.*, 2007; Herron *et al.*, 2018). The extremely advantageous property of more human-like glycosylation patterns of chickens, compared to other transgenic animals, is also expected to have reduced immunogenic and increased protein activity implications (Raju *et al.*, 2000; Lillico *et al.*, 2007). Since it is known egg white protein consists mainly of products from the ovalbumin (OVA), ovomucoid (OVM), ovotransferrin (OVT) and lysozyme genes we can target them for editing and replacement with a desirable recombinant protein under the control of endogenous regulatory elements such as promoters. The OVA gene is responsible for over half of egg white protein produced (~54%) per egg and OVM accounts

for approximately 10% of the egg white (Kovacs-Nolan *et al.*, 2000; Lillico *et al.*, 2007). Attempts have been made to target these genes with varying success. The strategy for their targeted editing and replacement with a recombinant protein will be discussed in detail later.

The costs of creating and maintaining a transgenic chicken flock is economically more feasible. In addition to the potential for easy and rapid upscaling of production (including by artificial insemination), structures for farming and egg collection are well-established. Thus, the cost of setup for scalability is significantly cheaper than that required to establish and maintain the common mammalian cell culture bioreactors (Harvey and Ivarie, 2003; Rapp *et al.*, 2003). The transgenic chicken facility can follow existing, standard, specific-pathogen-free (SPF) protocols in a closed rearing system to avoid disease outbreak in transgenic flocks (Bahrami *et al.*, 2020). Biosafety is important as infectious diseases can negatively impact on the egg laying capacity of laying hens (Hassan and Abdul-Careem, 2020). It is also important to consider that egg production can decrease with age of chickens and may be reduced when chickens are stressed (sudden changes in environment and living conditions) (X. J. Wang *et al.*, 2017; Pires *et al.*, 2021). Nevertheless, during the upscale process there is no need to worry about inconsistency and changes in quality of recombinant product produced as in large cell culture bioreactor tanks (Li *et al.*, 2016). The numerous advantages of the transgenic chicken system can be seen in table 1.1, which also provides a summary and comparison of the properties of the various expression platforms. In theory the transgenic chicken bioreactor is ideal.

Table 1.1. Summary of expression platforms for therapeutic protein production. The properties of each system are measured on a relative scale. L=low; M=medium; H=high; L/M=low to medium; M/H=medium to high. The dash indicates the property is not applicable in that system.

Property	Bacteria	Yeast	Baculovirus-insect	Plant	Mammalian Cells	Transgenic	
						Animals	Hen
Product yield	M	M/H	M	M/H	M	H	H
Cost/ investment	L	L	M	L	H	H	L
Scaling up capacity	H	H	H	H	L	L	H
Folding, Post-translational modifications	-	L/M	M	M	H	H	H
Glycosylation	-	L/M	L/M	L/M	H	M/H	H
purification cost	H	M	M	H	H	H	M
Product quality (biological activity)	L	L/M	M	M/H	M/H	H	H

1.4 Genetic engineering techniques for creating transgenic chicken: past and present

The creation of therapeutic proteins using a chicken model has been examined through the manipulation of different chicken anatomy and the investigation of various methods for delivering gene constructs into cells that give rise to germ cells (oocytes or sperm). Genetic modifications can be made directly to the embryo or indirectly to blastodermal cells, stem cells, primordial germ cells (PGCs) and spermatogonial stem cells. The methods for producing transgenic animals have included virus-based gene delivery; DNA microinjection or non-viral vectors; and transfer of modified donor nucleus into enucleated oocyte. The distinctive reproductive system of birds has rendered some of the techniques, which have been used successfully to create mammalian transgenics, inappropriate. This has led to the need for developing alternate methods to produce a transgenic chicken.

DNA microinjection has been used in other mammals to efficiently create transgenics, but its application in chickens has proved challenging. This process involves the injection of genetic constructs into fertilised zygotes, which are then transferred to a recipient female or transfer of modified nuclei into enucleated oocytes (Keefer *et al.*, 2001; Schilit *et al.*, 2016). The chicken is not well-suited to these methods. In the reproductive system of hens, the development of the

fertilised zygote occurs already in the hen's reproductive system soon after fertilisation and continues to develop into the blastodermal stage by the time of oviposition. This means a hen would have to be sacrificed to extract the zygote or ovum from the oviduct (Perry, 1988; Sang, 1994, 2004). The large amount of egg yolk surrounding the zygote makes it difficult to identify and microinject DNA into the pronuclei, and survival rates are low (Perry, 1988; Sang, 1994, 2004). Because zygote formation and development begin already in the reproductive system, this means that upon oviposition there are approximately 50 000 cells which make up the blastoderm (Woodfint, Hamlin and Lee, 2018). Furthermore, only a very small portion of blastoderm cells give rise to the germ cells capable of transmitting modified DNA to progeny and targeting only these specific cells at this point of development is difficult (Mozdziak *et al.*, 2003; Woodfint, Hamlin and Lee, 2018). Nevertheless, microinjection was shown to be achievable. A mosaic transgenic rooster was created via microinjection of transgenes into the germinal disc of zygotes in 1994 (Love *et al.*, 1994). Despite successful microinjection, the rate of transmission of modified DNA through the germline was extremely low (at only 3.4%). Thus, breeding transgenics to obtain the desired genetically modified offspring is further required in such a case. More recent use of this technique has been to create transgenic chicken through injection of a lentiviral vector into the subgerminal cavity of early stage X embryos, however, recombinant protein expression levels were extremely low (55μg/ml) and the germline transmission rate was less than 1% (Kwon *et al.*, 2018). The main limitation with this method of creating germline transgenesis, as opposed to whole animal transgenics, is the inefficient and unpredictable outcome. This renders the technique an undesirable pursuit for its lack of reproducibility and low efficiency in chicken models.

Other available alternatives are the use of non-viral vectors or viral vectors. Viral vector systems have been proven as efficient methods to deliver and express transgenes in target tissue in chickens. Viral vectors containing transgenes can be engineered to enhance target specificity or expression levels. Those which have been adapted for creating transgenics are mainly distinguished by their ability to integrate into the host genome. One of the first virus-mediated gene transfers in chickens used the retroviral vector from avian leukosis virus to deliver the transgene lactamase into the subgerminal cavity of stage X embryos (Harvey and Ivarie, 2003). Although the resulting expression levels in egg whites were low and varied (with a maximum 0.2μg/ml achieved), the principle of virus-mediated transgene delivery and expression was successfully demonstrated in this model. Another important takeaway from these findings

revolves around the random integration of the viral vector-containing transgene into the host genome. The differences in the level of transgene expression strongly suggested that the positional effect or site of integration and sequences in the surrounding region can cause repression of transgene expression. This points to a common limitation among many types of randomly-integrating viral vector systems: where there is the problem of host silencing of the transgene and low, inconsistent rates of germline transmission exists (Harvey and Ivarie, 2003). Findings from other studies using retroviral vectors further support concerns about the production of a low frequency of transgenics and offspring and low levels of transgene expression (at a maximum of 2.7μg/ml) (Mozdziak *et al.*, 2003; Rapp *et al.*, 2003). Additionally, these studies demonstrated the effects of using ubiquitous promoters to drive transgene expression. The ubiquitous promoter showed that transgenes can be expressed in egg white. However, the expression levels were too low to meet the threshold for commercial viability. Interestingly, while ectopic expression outside the magnum-oviduct was not detected in these cases, there has been a report of non-tissue-specific expression of transgenes in the blood. This was damaging to the health of the chicken (Kwon *et al.*, 2018). For this reason, the regulatory sequences of the egg white genes, such as the OVA and OVM promoter sequences, are essential for restricting expression to the oviduct. The OVA promoter sequence has been well-documented. When employed for driving transgene expression through viral-vector mediated transfer, the promoter showed tissue-specific control of expression in various studies (Lillico *et al.*, 2007; Byun *et al.*, 2011; Liu *et al.*, 2015; Kwon *et al.*, 2018). Again, inconsistent and low levels (at a maximum of 426μg/ml) of transgene expression were a major limitation of this method. Nevertheless, these findings are important as they demonstrate that expressing biologically active proteins, that might normally be detrimental to other transgenic bioreactors' health, is possible in the transgenic chicken system as the protein remains in the confines of the closed egg environment.

Despite the successful instances of producing transgenics with viral vectors, further limitations exist. The size of the transgenic sequence is limited in many vector systems. This places restrictions on the choice of protein selected for production (Byun *et al.*, 2011). Coupled with the fact that the tissue-specific promoters which are essential for inclusion in construct design are large, leaves little room for the protein sequence (Byun *et al.*, 2011; Liu *et al.*, 2015). As mentioned previously the random integration of transgenes not only impacts variation in expression levels, but also potential health concerns for the host, as integration into unwanted

regions that possess oncogenes for example is a risky and a serious concern for implementing this system (Rapp *et al.*, 2003; Lillico *et al.*, 2007; Liu *et al.*, 2015).

An alternative gene transfer method is the non-viral vector system. This is not as effective due to the fact that the DNA construct usually remains in the cytoplasm and is not stably integrated into the genome but rather is lost during the development of embryos as the cells divide (Naito, Sakurai and Kuwana, 1998). The rise of targeted gene-editing strategies which may rectify these issues is a promising avenue, for further discussion in section 1.7. The targeted gene editing is expected to assist in overcoming the main obstacle of low rates of transgenesis in the founder generation. This means a homozygote (at more than one locus) can only be obtained feasibly when the founder mutation rate is high enough for interbreeding within founders. If not, a further F1 generation needs to be bred via crossing of founders with wild types. This ultimately leads to a more time-consuming, labour-intensive process with a large number of chickens required (Lillico *et al.*, 2007; Byun *et al.*, 2011). The lack of efficiency and consistency in generating transgenics with these methods has shifted the focus towards modification of the germ cells of chickens with targeted gene-editing technologies. This is achieved because of the unique development and migration of PGCs in the early developing chicken embryo.

1.5 Primordial germ cells: the key to creating transgenics

Much attention has been given to the transfer of chicken PGCs for production of transgenics. This method may allow one to overcome the issues of low germline transmission efficiency and problems of founders being mosaic. These cells, the only ones capable of transmitting the entire genome of an organism to progeny, are the undifferentiated progenitors of mature gametes (oocyte or spermatocyte) (Kim and Han, 2018). From the time of fertilisation, PGCs employ a unique development process and route of migration in the developing embryo that allows for their isolation. Figure 1.1 depicts the origins of and migration of PGCs in the developing chicken embryo. This knowledge is important for understanding how we can exploit convenient PGC isolation for *ex vivo* manipulation, before re-introduction into recipient embryos, to generate germline transgenics. Following fertilisation, the PGCs can be found as a cluster in the area pellucida (the starting line for the PGC migration journey). Chicken PGCs first migrate toward the germinal crescent. Thereafter they enter and circulate in the extraembryonic blood vessels between Hamburger and Hamilton (HH) stages 12-17 and peak

at HH15-16 (Hamburger and Hamilton, 1951). The critical difference to mammals, who utilise somatic tissue for migrating PGCs, is that in chickens the PGCs utilise the blood vessels to migrate towards the genital ridge between HH18-21, before finally settling in the gonads (Fujimoto, Ukeshima and Kiyofuji, 1976; Ginsburg and Eyal-Giladi, 1987; Han and Park, 2018; Kim and Han, 2018).

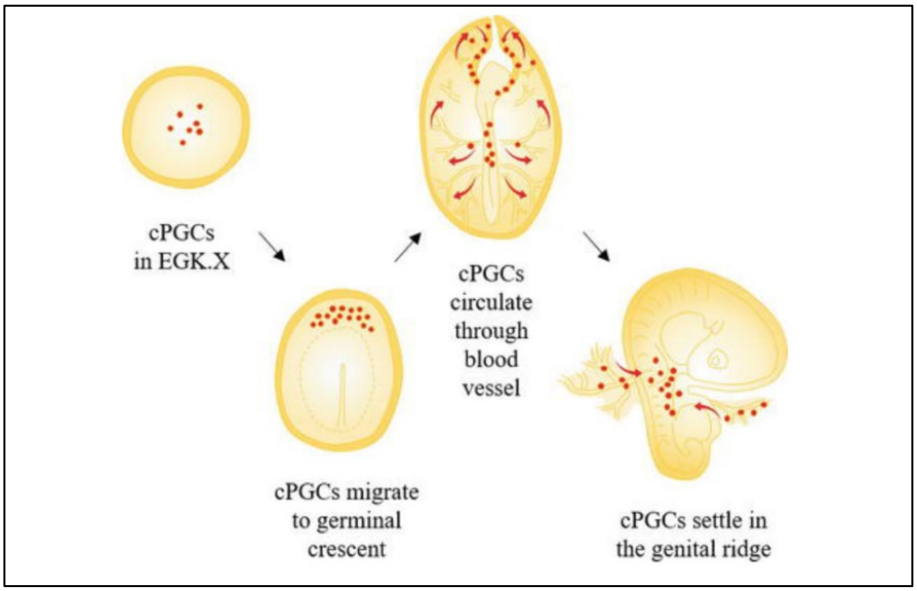

Figure 1.1. ***Migration of PGCs in the early developing embryo.*** *Adapted from Han and Park (2018).*

There are therefore multiple developmental stages from which we can extract the PGCs for *ex vivo* applications. These include: the germinal crescent of HH4-8 embryos, the blood vessels of HH14-17 embryos, the gonadal ridge of the HH26-28 embryos, and the gonads at HH26-31 embryos (Tang *et al.*, 2007; Nakajima *et al.*, 2011; Nakamura *et al.*, 2011; Song *et al.*, 2014; Chojnacka-Puchta *et al.*, 2015; Szczerba *et al.*, 2020; Szczerba, Kuwana and Bednarczyk, 2021). The cells can also be isolated through various methods and maintained in culture. When choosing the source of PGCs the different factors to consider include: variations in the concentration of cells; purity of cells; purification processes required post-extraction; and complexity of equipment or reagents required. Regardless of source of isolation, *in vitro* propagation is essential.

The Stage X embryo, which contains the least amount of extractable PGCs, is not feasible for *in vitro* culture applications (Bednarczyk *et al.*, 2018). Thus, focus is turned towards blood and gonadal PGCs. To isolate PGCs from the bloodstream, the use of a fine glass needle and pipette

has been shown by several groups to be successful in drawing blood from the blood vessels of the embryo (van de Lavoir *et al.*, 2006; Nakamura *et al.*, 2010; Naito, Harumi and Kuwana, 2012; Oishi *et al.*, 2016; Tonus *et al.*, 2016; Han and Lee, 2017; Szczerba *et al.*, 2020). These tools are a low-cost method for PGC extraction and can be implemented at a research-lab level. This technique requires acquisition of skills for successful manipulation of delicate blood vessels and can be a labour-intensive, time-consuming process. Furthermore, when considering the fact that the number of PGCs in circulating blood varies, is relatively low compared to gonadal PGCs, and that the complete blood PGC population is not retrievable, the yield of the procedure is low (Szczerba *et al.*, 2020; Szczerba, Kuwana and Bednarczyk, 2021). Despite these limitations, the bloodstream is a popular source of PGCs owing to the minimal processing or purification procedures needed, and the high purity of PGCs obtained without contaminating somatic cells. The blood cells which accompany the PGCs in extraction are not maintained in favourable conditions and when cultured on feeder cells with PGCs, do not adhere and are removed in cell culture media changes (Szczerba *et al.*, 2020). In this research project, the bloodstream was used as the PGC source in chickens.

The alternative source to blood-derived PGCs, gonadal PGCs, has been explored and implemented in transgenic applications (Tajima *et al.*, 1998; Park *et al.*, 2003, 2015; Nakajima *et al.*, 2011; Chojnacka-Puchta *et al.*, 2015; Szczerba *et al.*, 2020). For gonadal PGC isolation, proteinases such as trypsin-EDTA have been used to digest the gonadal tissue and culture the PGCs together with other gonadal cells (Park and Han, 2000; Szczerba *et al.*, 2020). Hence, enzymatic digestion does not provide highly purified PGC isolates. It has also been shown it is possible to collect gonadal PGCs using phosphate-buffered saline (PBS) without calcium and magnesium ions, to dissociate the PGCs from other somatic cells. This results in a considerable increase in culture purity compared to enzymatic digestion (Nakajima *et al.*, 2011) .This method of PGC isolation is fast, simple, low-cost, and relatively high-yielding. This is beneficial for transgenic applications requiring high cell numbers. However, important limitations, which were considered in this project, for creating a pure line of transgenic PGCs include the risk of contaminating cells and relatively low post-extraction purity levels compared to blood-derived PGCs. Hence, the blood served as the source of PGCs.

There are several available PGC purification procedures which exist with certain advantages and disadvantages. The following procedures have been employed to separate PGCs from

somatic cells or blood cells: Nycodenz gradient (a non-toxic substance) was used to obtain a 70% purity of blood PGCs by Zhao and Kuwana (2003); Percoll density gradient was used by Oishi (2010) to achieve an impressive 94% live-cell recovery rate; ammonium chloride potassium (ACK) lysis buffer, which targets red blood cell contaminants, was shown to increase PGC purity more rapidly than no purification, by up to 92.9% in culture (Yamamoto *et al.*, 2007). The discovery of germ cell surface markers led to the use of Fluorescence-activated cell sorting (FACS) of cells labelled with antibodies against germ cell markers as an efficient method for purifying PGCs (Mozdziak *et al.*, 2005). Magnetic activated cell sorting (MACS) purified gonadal PGCs labelled with antibodies by preferentially separating them from contaminating cells. Yet, in this case purity was still below 50% (Kim *et al.*, 2004). These cell marker-based isolation techniques are costly. Equipment is expensive and requires skilled operators as well as the purchasing of antibodies for each use (Faraghat *et al.*, 2017). The use of density gradient reagents also requires economic investment for relatively few uses, and can be difficult to isolate cells of different densities which stick together (Norouzi, Bhakta and Grover, 2017). The techniques listed here can cause loss of portions of retrievable PGCs as well as have negative effects on their viability (Yamamoto *et al.*, 2007; Faraghat *et al.*, 2017). Given the already low starting amounts of potential PGCs which can be obtained from gonads and blood, purification for isolation is debatable and, in this project, PGCs sourced from blood did not undergo additional purification procedures before being cultured. Once we obtain these PGCs, there are also mechanisms of identification that can be used to verify their isolation. These will be discussed further in this section.

Due to the limitations on the number of potential retrievable PGCs from embryos, and the need for sufficient initial quantities for downstream procedures, *in vitro* PGC propagation is required. Studies which demonstrate methods to culture PGCs over long periods of time, whereby germline potential is maintained, enable *in vitro* PGC propagation. These studies utilised a variety of culture conditions. The first prolonged PGC culture was described by van de Lavoir *et al.* (2006). PGCs drawn from circulating blood were maintained in a medium supplemented with growth factors. The PGCs were grown on buffalo rat liver or mouse fibroblast feeder cells. The media contained basic fibroblast growth factor (bFGF), stem cell factor (SCF) and leukaemia inhibitory factor (LIF). In combination, each of these factors plays an essential role in PGC propagation. The LIF acts to promote the continued undifferentiated form of the PGCs and is essential for maintaining germline potential (Horiuchi *et al.*, 2004;

Tang *et al.*, 2007; Nakano *et al.*, 2011; Farzaneh *et al.*, 2017). The buffalo rat liver feeder cells support this action, as they naturally produce LIF (van de Lavoir *et al.*, 2006). bFGF is important for the proliferation of undifferentiated PGCs in culture; and SCF, whose activity is optimised in the presence of bFGF to promote the undifferentiated state, is also vital for this purpose (van de Lavoir *et al.*, 2006; Choi *et al.*, 2010; Macdonald *et al.*, 2010; Miyahara *et al.*, 2014; Whyte *et al.*, 2015). bFGF also helps to maintain the migratory ability of PGCs (Choi *et al.*, 2010).

The ability of chicken embryonic fibroblasts (CEFs) to produce LIF and bFGF and hence their potential use as a feeder layer to support growth and inhibit differentiation of PGCs makes them an ideal support for PGC growth (Tang *et al.*, 2007). In fact, CEFs have proven to provide the best support for PGC growth *in vitro* when compared to other chicken cells from different origins (Tang *et al.*, 2007). Furthermore, the use of non-chicken-derived homologous somatic cells as feeder layers (such as mouse or buffalo rat liver) has the disadvantage of the risk of transfer of animal pathogens from different species of animal cells, bringing with them immunogenic contaminants as well as the potential to impact downstream transgenic techniques (Tang *et al.*, 2007; Szczerba *et al.*, 2020). The CEFs, which were the chosen feeder cells in this project, can be growth-inhibited via mitomycin-C. Mitomycin-C prevents DNA replication which causes cell cycle arrest (Llames *et al.*, 2015). This prevents CEFs from dividing and overrunning PGCs in culture, while still allowing them to support PGC growth, and CEFS can be replaced continuously as needed by maintaining a CEF culture (Tang *et al.*, 2007). The use of mitomycin-C is an effective, cheaper, less time-consuming alternative to irradiation. Irradiation of cells requires availability of expensive and potentially dangerous equipment, not available for use in this project (Llames *et al.*, 2015). Chicken mesenchymal stem cells collected from bone marrow of chicks have been demonstrated as an alternative source of chicken feeder cells for successful PGC culture. The downside to this method was extraction of cells took place from adult chickens which would likely require higher-level ethical clearance (Li *et al.*, 2019). Furthermore, the protocol for CEF extraction and maintenance of culture had already been established in our lab. Thus, it was easily implementable in this project. The culture conditions employed in this project closely mimic the natural environment of PGCs in chickens and are suitable for maintaining PGCs for applications in transgenesis.

Specific characteristics of PGCs can be used as a tool for identity verification *in vitro*, especially in the absence of purification procedures. In culture, PGCs are large and round and are usually ~15-20μm, and when viewed by darkfield illumination under the microscope, are distinguished by their illumination-causing cell structures (Szczerba *et al.*, 2020; Altgilbers *et al.*, 2021). In this way, rapid identification of PGCs in culture is possible. The most common methods of identification of PGCs in culture employ immunostaining of cell surface markers or periodic acid-Schiff staining (PAS). The PAS staining is a straightforward technique which targets the high glycogen content in the PGC cytoplasm to distinguish them from somatic cells (Jung *et al.*, 2005; Han and Park, 2018). Antibodies raised against cell surface glycoproteins such as stage specific embryonic antigen (SSEA)-1, epithelial membrane antigen (EMA)-1 or chicken vasa homolog (CVH) have since become just as common for confirming PGCs in culture (Jung *et al.*, 2005; Tang *et al.*, 2007; Nakamura *et al.*, 2008, 2010; Han and Lee, 2017). PGC markers are useful in that there are multiple markers expressed throughout the different stages of embryonic development (Kim and Han, 2018). In this study, we utilised a readily available antibody, the anti-SSEA-1 antibody for identification of PGCs.

Following isolation and cultivation of the PGCs, is their transfer to recipient chicken embryos to create germline chimeras. Elucidation of the migration route and timing of PGC circulation in the bloodstream has made this a possibility. The ability to culture PGCs *in vitro* for long periods of time allows for their targeted genetic modification before introducing them to recipients. Delivery of PGCs, isolated from different sources and delivered at various stages of development into recipient embryos, has shown promise for the creation of chimeras. Donor PGC integration into the gonads and subsequent viable progeny have been produced using this technique. A frequently used procedure has been the delivery of isolated PGCs (from blood or gonads) to recipient embryos via the vascular system of HH14-17 embryos. Injection is performed in the dorsal aorta using a glass micropipette and usually a microinjector machine (Naito *et al.*, 1994; Song *et al.*, 2005, 2014; Nakamura *et al.*, 2008, 2010; Oishi, 2010; Han and Lee, 2017). Through this method, the PGCs that show maintained germline potential can migrate to, and settle in, the developing gonads. A simple way to track these donor PGCs and distinguish them from endogenous cells is either by labelling the PGCs with fluorescent dyes which do not harm the cells, or less commonly, by using plasmids encoding fluorescent proteins which act as tracers (van de Lavoir *et al.*, 2006; Nakamura *et al.*, 2010; Song *et al.*, 2014; Woodcock *et al.*, 2019). It is important to note that this technique is technically

challenging- it is difficult to carefully inject the PGCs into small embryonic blood vessels without bursting the vessels and causing significant amount of blood loss that would result in the embryos' death.

An alternative to the delivery of PGCs into embryos, is the delivery of PGCs into adult roosters. This is possible because PGCs are the precursors of gametes. Trefil *et al.* (2017) demonstrated this possibility by showing that spermatogenesis, and hence fertility, was restored by the transplantation of modified donor PGCs into the testes of sterilised adult roosters. In some ways, this route toward transgenic creation is simpler than the vasculature injection required with the embryo route as procedures are not performed on the micro-level. However, they do require a qualified veterinarian and specialised facilities equipped for performing surgeries on adult roosters. Whereas injection into the vasculature of embryos may be performed on a lab benchtop by the researcher. In terms of time, the use of adult roosters might be faster for obtaining transgenic offspring since mating can occur once fertility has been re-established; this can be as soon as 3 months after injection (Trefil *et al.*, 2017). This is quicker and more efficient than modifying an embryo, waiting for hatching, waiting for chick growth until sexual maturity; and only then breeding the transgenic chick to obtain transgenic offspring. However, a greater number of PGCs are needed for injection into adult roosters to achieve transgenesis. This is costly and presents its own time challenges. In the case of this project, PGC injection into the embryonic vasculature was selected for the major reason that far fewer PGCs are needed for injection at the embryo stage compared to the adult stage in chickens, as well as the fact that successful integration into the embryonic gonads can be assessed in HH28-31embryos before hatching (van de Lavoir *et al.*, 2006; Nakamura *et al.*, 2008, 2010; Song *et al.*, 2014; Trefil *et al.*, 2017). This also eliminates unnecessary termination of adult chickens who might not meet transgenic expectations or requirements.

1.6 Sterilisation of recipient embryos for replacement of the germline

The removal of endogenous PGCs in the recipient embryo is just as important as delivery and uptake of modified PGCs to replace the germline. This is performed to reduce the competition between the endogenous and donor cells and to favour donor cell integration in the gonads and transfer to progeny (Nakamura *et al.*, 2008; Woodcock *et al.*, 2019). Various techniques have been reported for increasing the ratio of donor PGCs in the gonads. The most efficient mode

of sterilisation will be beneficial for integration of the modified donor PGCs into recipient embryos and propagation of modified genome onto progeny.

The surgical removal method of removing PGCs takes place in the stage X embryo by removing PGCs from the central area pellucida with a needle (Kagami *et al.*, 1997). Using this technique, endogenous PGCs were reduced and the germline chimeras were created. This technique demonstrates a varying range of efficiency (Kagami *et al.*, 1997). A similar approach involves the physical removal of a portion of PGCs in the blood at a later stage in development before transferring donor PGCs. This is similar to the approach used in this study for isolating PGCs whereby blood is drawn from the recipient embryo. The difference between the surgical removal method and this study's approach is that there is a limit on the amount of blood which can be drawn while maintaining embryo viability. This in turn limits the amount of PGCs which can be removed, thereby affecting the frequency of germline transmission (Naito *et al.*, 1994). Despite the inconsistency or low efficiency of these two techniques, both are beneficial for their minimal equipment needs and reduced costs. Yet, these techniques require the acquisition of specific technical skills for manipulating the embryo at early developmental stages.

Additional methods for embryo sterilisation involve the use of irradiation. This exploits the greater sensitivity of PGCs than other cells to irradiation. Through electromagnetic waves, in the form of ultraviolet (UV) radiation, gamma-rays, or X-rays, we can expose early embryos (usually stage X) to these radiation treatments and deplete native PGCs via DNA-damage-induced cell death (Nakamura *et al.*, 2012; Nakamura, Kagami and Tagami, 2013). A major advantage to these sterilisation methods is that their effects are limited to the endogenous PGCs only while the embryos are exposed to treatment. Thus, transferred donor PGCs delivered later are unaffected (Nakamura *et al.*, 2012). Several studies have proven the effectiveness of these techniques not only in depleting endogenous PGCs, but also in their subsequent creation of germline chimeras (Aige-Gil and Simkiss, 1991; Park *et al.*, 2010; Nakamura *et al.*, 2012). Despite the benefits of these sterilisation techniques related to targeted action against PGC depletion, they require the possession of specific, expensive equipment, which oftentimes, as in our case, is a limiting factor to their adoption. Irradiation may also lead to serious developmental abnormalities (which are difficult to avoid with UV light exposure) and a decline in hatching rates following treatments (Aige-Gil and Simkiss, 1991; Kagami *et al.*, 1997; Song *et al.*, 2005; Nakamura *et al.*, 2010).

The final type of sterilisation involves the use of chemical sterilising agents. The most commonly used agent, busulfan (1,4-batanediol dimethanesulfonate), has been shown to have targeted effects against PGCs when administered into the egg yolk before incubation (Song *et al.*, 2005; Nakamura *et al.*, 2008, 2010; Lee *et al.*, 2013). The side effects (developmental abnormalities, death) of busulfan at high doses are a factor to consider. However, developments surrounding the methods of busulfan administration to allow for delivery in a controlled and timely way, such as through oil emulsions, have reduced these effects. Importantly, busulfan was shown to be effective and suitable for creating recipient embryos that are able to incorporate donor PGCs into their gonads as well as produce donor-derived offspring (Song *et al.*, 2005; Nakamura *et al.*, 2008, 2010; Lee *et al.*, 2013). As reported by these studies, only partial sterilisation and not total depletion of PGCs was possible at busulfan levels that are tolerable to embryos. However, the usefulness of this technique is evident by the successful generation of germline chimeras in these studies. Given the relatively low-resource demands, the technique was explored in this project.

1.7 Genome editing in chickens: a targeted approach

The efficiency of creating transgenic chicken is not only affected by the delivery and integration of modified donor PGCs. The type of gene editing used in the donor PGCs plays an important role in transgenic creation. Many viral and non-viral vectors are a non-target-specific, unpredictable, inefficient form of transgene integration in chickens due to the lack of stable integration in the genome as well as the random nature of integration (Lundstrom, 2018). A more useful system would provide stable integration of the transgene and stable high levels of expression. The targeted genetic engineering technique, Clustered Regularly Interspaced Short Palindromic repeats (CRISPR)-Cas9, could assist in this regard. The principle and practice of CRISPR-Cas9 came about through repurposing and adjusting of a prokaryotic immune system. A specific function of the prokaryotic CRISPR system includes inducing double-stranded breaks (DSBs) at precise or targeted genomic loci to fight off foreign elements in an acquired genetic-memory-based immune system (Bhaya, Davison and Barrangou, 2011; Jinek *et al.*, 2012; Cong *et al.*, 2013; Lin *et al.*, 2014). The endogenous Cas9 endonuclease is directed to the cutting site in DNA by a guide RNA (gRNA). It is this sequence-specific cleavage, together with endogenous cell repair mechanisms, that can be exploited for creating desirable mutations in eukaryotic cells, when the gRNA is specified by the researcher (Jinek *et al.*, 2012; Cong *et al.*, 2013).

To repair the DSBs, one of many endogenous cell repair mechanisms can be activated in the cell. One of two predominant forms of repair, non-homologous end joining (NHEJ) or homology-directed repair (HDR) can be activated in separate DNA repair pathways (Cong *et al.*, 2013; Ran *et al.*, 2013; Lin *et al.*, 2014). The NHEJ pathway re-ligates DSBs in a manner which leaves errors in the form of insertions and deletions (Mao *et al.*, 2008; Heyer, Ehmsen and Liu, 2010). The NHEJ pathway is the dominant repair mechanism active throughout the G1, S and G2 cell cycle phases (Heyer, Ehmsen and Liu, 2010; Lin *et al.*, 2014). In contrast, the HDR pathway is able to produce precise, highly accurate repairs between the break sites using either homologous DNA sequences from homologous chromosomes, sister chromatids or synthetic donor DNA as templates (Lin *et al.*, 2014). It is this precise modification potential that can be exploited for genome editing when we provide the DNA template for repair.

The HDR pathway, although attractive in theory, faces impediments to its utilisation. To begin with, the HDR pathway is in competition with the predominant NHEJ pathway, and it ultimately occurs less frequently (Ran *et al.*, 2013; Maruyama *et al.*, 2015). Furthermore, HDR efficiency varies depending on cell type and even the genomic target and template sequence (Saleh-Gohari and Helleday, 2004; Miyaoka *et al.*, 2016). Despite this, HDR repair has been exploited to produce precise genome editing and integration of transgenes. This has been achieved by providing a repair template of double-stranded DNA constructs that contain homology arms (HAs) complementary to the genomic sequence flanking the insertion sequence (Wang *et al.*, 2015; Zhang *et al.*, 2017; Oishi *et al.*, 2018). Despite these advancements, it is difficult to obtain the desirable HDR integration as cells vary in their abilities to produce HDR or NHEJ, and the various stages in the cell cycle favour different pathways (Lin *et al.*, 2014).

Consequently, researchers have found ways to enhance HDR efficiency and even downregulate NHEJ. An example of a method used to enhance HDR efficiency has been the use of small molecules that act directly or indirectly on different members of DNA repair pathways. These molecules are easily applicable, fast to implement and, importantly, are reversible (Bischoff *et al.*, 2020). Cell-specific activity or sensitivity to such molecules has been suggested and treatment conditions are suspected to work best when cell-optimised (Bischoff *et al.*, 2020; Yang *et al.*, 2020). There are many small molecules which have been investigated by other groups. Two molecules, SCR7 and RS-1, which have been tested in various genome editing

experiments, and whose mechanisms of action are clearly established, were applied in this project and are discussed further in this section.

Direct enhancement of the HDR pathway is achieved with RS-1 as it acts to enhance the binding activity of a key member known as RAD51 (Jayathilaka *et al.*, 2008; Yang *et al.*, 2020). RAD51 is central to the HDR pathway as it is responsible for finding a homologous donor template for repair and strand exchange during repair (Jayathilaka *et al.*, 2008; Yang *et al.*, 2020). RS-1 simply creates a more stable interaction between the RAD51 and the DNA, enhancing its activity. Different groups have shown successful enhancement of HDR in Cas9-induced DNA cutting and repair *in vitro* and *in vivo.* In human kidney cell lines, a significant increase in CRISPR-Cas9-induced HDR, ranging from three- to six-fold, has been achieved with the use of RS-1 (Pinder, Salsman and Dellaire, 2015). Furthermore, the molecule has been applied in animal embryos, such as rabbits, where minimal improvements in HDR were seen (Song *et al.*, 2016).These reports show that levels of HDR achieved were variable and dose- and loci-dependent. Optimisation of treatment in the specific cell is vital where possible.

The second treatment, SCR7, acts indirectly on members of the NHEJ pathway to promote HDR. It does this by binding to and inhibiting DNA ligase IV, a key component of the NHEJ pathway responsible for the joining of broken DNA ends (Lieber, 2010; Yang *et al.*, 2020). Various studies have shown that downregulation of this NHEJ pathway via DNA ligase IV can shift the balance towards HDR-mediated repair. The treatment of various mammalian cells, mouse zygotes, and rats proved the potential to enhance efficiency of HDR (Chu *et al.*, 2015; Maruyama *et al.*, 2015; Ma *et al.*, 2016; Li *et al.*, 2017). A considerable range of different cells and animals have been subjected to RS-1 and SCR7 treatment, however there is currently no evidence of the effects of these small molecules on chicken PGCs or if these molecules cause damage to these cells.

Since there can be variability in the efficacy of small molecules, and SCR7 and RS-1 have shown positive outcomes in some cells and not others, alternative methods for enhancing elements in the HDR pathway should be considered. This has included upregulating the expression of RAD51 or employing a yeast-specific version of RAD51 known to favour HDR (Kurihara *et al.*, 2020). The latter case showed increased HDR efficiency in human kidney cell lines and porcine cells (Di Primio *et al.*, 2005; Shao *et al.*, 2017). Interestingly, when this yeast-

specific analogue of RAD51 is combined with CRISPR-Cas9 in chicken fibroblast cells, targeted sequence insertions increased (Ling Wang *et al.*, 2017). This strategy is one of few emerging alternatives in the battle to promote CRISPR-mediated HDR.

Another approach to promoting HDR, considers the timing of CRISPR-Cas9-induced DSBs and repair. Since we know the timing of the HDR pathway is thought to be restricted to the S and G2 stages in the cell cycle, and repair activation occurs as soon as the DSBs are detected, restricting the expression and hence activity of the Cas9 to cell conditions conducive to HDR-repair is a promising approach (Heyer, Ehmsen and Liu, 2010). It was already shown that a modified version of Cas9 that is less active in the G1 cell cycle phase used in conjunction with cell cycle phase regulators improved HDR frequency significantly in human stem cells (Lomova *et al.*, 2019). However, a variation of the temporal Cas9 expression approach was taken in the design of gene editing constructs in this project, by employing meiosis-specific expression of the nuclease. This is discussed in detail later in this section.

In the context of creating the transgenic chicken, as mentioned above, the integration of a transgene to replace endogenous egg white protein expression can achieve high-yield expression if the entire open reading frames of these genes are replaced with the transgene through CRISPR-Cas9-HDR-mediated repair. Transgenes which fall under the control of the endogenous egg white protein gene enhancers and promoters should provide, in theory, the naturally produced levels of OVA and OVM protein in the egg. This type of gene editing would be superior not only for the high-yield potential but also for the low immunogenicity of the products produced when knocking out endogenous egg white protein expression. Most of the egg's allergenic proteins are those of egg white proteins, with OVM being the major one (Cooke and Sampson, 1997; Caubet and Wang, 2011). The less common egg white protein produced from OVT, accounts for approximately 13% of egg white protein (Lillico *et al.*, 2005). However, the OVT gene in this project was not a target for editing due to reports of embryonic lethality which arise in the homozygous OVT null condition. This indicated OVT's necessity for viability and excludes it from targeted knockout (K. Y. Lee *et al.*, 2020). The low contribution of OVT to egg white protein yield and allergenicity relative to OVA and OVM respectively was the reason I chose to focus on targeting and modifying OVA and OVM in this project (Caubet and Wang, 2011). Egg allergy is a common food allergy affecting more people worldwide. Therefore, the removal of this potential allergenicity from a protein therapeutic is

a major advantage not only for clinical use but also for simplifying and reducing costs of purification in the manufacturing process (Lillico *et al.*, 2005; Caubet and Wang, 2011).

The mechanism proposed for editing of egg white loci involves the use of CRISPR-Cas9 within gene drive constructs, depicted in figure 1.2. These constructs include: a Cas9 endonuclease; gRNA sequences for directing the Cas9 to cleave target DNA sequences; homology arms (HAs); and the transgene coding sequence. The Cas9 in this case is the eSpCas9 adapted from *Streptococcus pyogenes* which is advantageous for its engineered, enhanced target specificity (Slaymaker *et al.*, 2016). The gRNA sequences direct the eSpCas9 to the 5' and 3' ends of the egg white loci open reading frames. Design and evaluation of gRNAs was performed by Prof Nikitina using CRISPOR software. Some of the gRNAs were evaluated in previous studies in the laboratory by Michael Edwards and Chiron Loubser. The coding sequence for the transgene of interest is that of tenecteplase. The DNA sequence was based on the protein sequence obtained from Nordt and Bode (2003). The patent for this sequence has expired and hence its use in this project does not violate any current patents. All these elements are contained within egg white loci-specific HAs. The HAs are 5' and 3' regions flanking the insert DNA sequence. These HAs are complementary to genomic DNA flanking the target loci (OVA or OVM) that will be replaced. These HAs allow for complementary alignment of the gene drive with the target locus, for insertion of the provided gene drive template in place of the target loci. Hence the expression of the transgene will be placed under endogenous egg white protein promoter. The expression of the eSpCas9 falls under a separate promoter. Once initial integration on a single homologue has occurred, the wild type allele on the second homologue can be targeted and converted by HDR using the primary edited allele as template, thereby converting a heterozygote to a homozygote. The mechanism is displayed diagrammatically in figure 1.3.

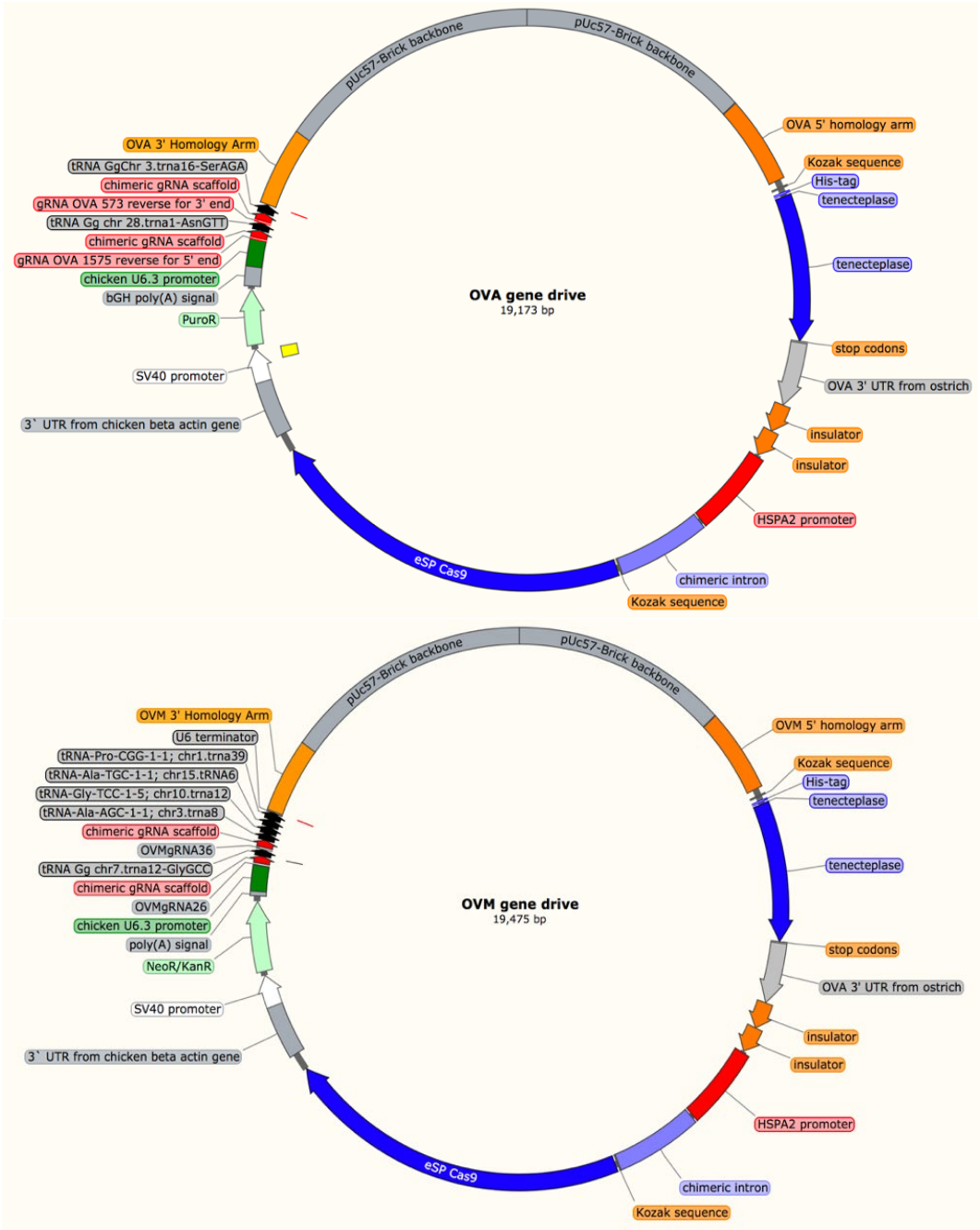

Figure 1.2. ***The final OVA and OVM gene drive constructs and their features, to be constructed and used for editing PGCs.*** *For both gene drives, the vector backbone is the pUc57-Brick Backbone containing sequences for conferring resistance to ampicillin antibiotic and the ORI for cloning purposes. The Tenecteplase gene is shown in blue without any promoter sequence as it will fall under control of endogenous OVA or OVM promoter. The HSPA2 promoter sequence shown in red controls the expression of the downstream eSpCas9 endonuclease shown in blue. The chicken U6.3 promoter shown in green controls the expression of the gRNAs downstream in black and red. The homology arms on each gene drive which are specific to OVA and OVM genomic loci flanking the 5' and 3' end of insert region are shown in each gene drive respectively in orange. For purposes of selection of transfectants the OVA gene drive contains the PuroR sequence (pale green) under control of the eukaryotic SV40 promoter for production of N-Acetyltransferase which confers resistance to Puromycin. The OVM gene drive contains the NeoR/KanR sequence (pale green) under control of the*

eukaryotic SV40 promoter for production of aminoglycoside phosphotransferase from Tn5 which confers resistance to Neomycin. Diagrams made using SnapGene.

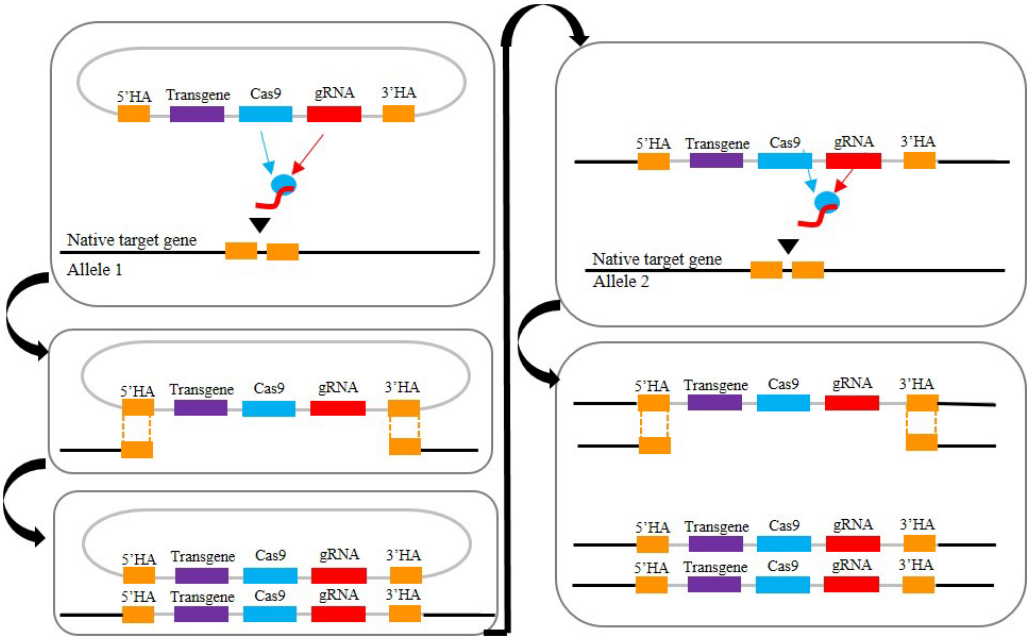

Figure 1.3. ***Mechanism of action of CRISPR-Cas9 gene drive.*** *The plasmid delivered into the cells contains Cas9, transgene, gRNA flanked by HAs homologous to the allele sequence. The gRNA directs Cas9 to cleave DNA at specific site in the locus of one allele. The gene drive is integrated at the locus via HDR. A heterozygote for the gene drive insertion results. The second allele is target via Cas9 and gRNA expressed off the edited allele. The first allele containing gene drive insert acts as a template for repair during HDR for the second allele. Thus, the heterozygote becomes a homozygote when the gene drive is copied onto the wild type locus (second allele). Diagram created in Microsoft PowerPoint, based off that described by Drury et al. (2017).*

In this project, the aim was for the CRISPR-induced HDR-integration steps to be accomplished via specific promoters controlling the timing of Cas9 activity. The initial integration of the gene drive construct within the HAs is not driven by the eSpCas9 expression in this gene drive. Instead, the eSpCas9(1.1)-T2A-Puro vector, with eSpCas9 under the control of the ubiquitous CMV enhancer and chicken β-actin promoter, is responsible (when co-delivered into the chicken PGCs). This vector does not contain HAs and does not integrate into the genome but instead provides initial transient expression of the eSpCas9 protein for targeting loci, and the vector will likely be lost after a few cell divisions. Once the initial HDR-integration has occurred, the conversion of the homologue or sister chromatid is expected to come about due to the meiosis-specific promoter controlling eSpCas9 expression in the homology-arm-containing gene drive integrated at the first allele. The reason behind this is the increased likelihood of HDR-repair pathways occurring in meiotic cells or germ cells than in somatic

cells. In meiotic cells, alignment of homologous chromosomes can take place and NHEJ is downregulated during meiosis in many species (Enguita-Marruedo *et al.*, 2019; Grunwald *et al.*, 2019; Weitzel *et al.*, 2021). Thus, the HDR-mediated integration of the gene drive may occur.

The meiosis-specific promoter chosen in this project was the mouse heat shock protein 2 (*HSPA2)* promoter. The HSPA2 protein itself shows strong conservation across species (Padhi, Ghaly and Ma, 2016). As mentioned previously, targeting the intervention to the times at which HDR is predominant in cells is a useful way to promote HDR-mediated integration of the gene drive. During meiosis, HDR is favoured and given the nature of the gene drive, where breeding or transmission of the drive would take place through the male line, a meiosis specific promoter active during male-specific meiosis is ideal (Weitzel *et al.*, 2021). Though reports proving validity of meiosis-specific promoters *in vivo* are scarce, we opted for an experimentally validated promoter. The *HSPA2* promoter has been experimentally validated to be active predominantly in spermatocytes and spermatids (Dix, Allen, *et al.*, 1996; Dix, Rosario-Herrle, *et al.*, 1996; Dix *et al.*, 1997; Inselman *et al.*, 2009; Bai *et al.*, 2016). This means that by exploiting this form of regulated temporal and tissue-specific expression, we can control the onset of eSpCas9 expression at the edited allele to meiosis in male chicken PGCs (which when re-implanted into chicken will ultimately develop into mature spermatocytes), thereby promoting gene conversion via the HDR-pathway. This would produce an increased efficiency of chimerism in the gonads as well as increase the frequency of gametes transmitting the integrated gene drive to transgenic progeny. This eliminates the need to breed heterozygotes through multiple generations to obtain homozygotes at more than one locus which can be a timely and costly effort. Ultimately the aim is to obtain a hen homozygous for the transgene at all loci, through breeding, which will lay infertile eggs containing therapeutic protein at approximately 2.7g/egg (Lillico *et al.*, 2005). The outcome would be a stable transgenic chicken line, capable of producing high levels of therapeutic protein *in ovo.*

This phenomenon of generating biased and increased inheritance of desired alleles above normal Mendelian ratios, is known as a CRISPR-Cas9 gene drive system. This system is a relatively new development that has been demonstrated, with varying efficiencies, in very few studies on mosquitos, mice and Drosophila melanogaster (Esvelt *et al.*, 2014; Gantz *et al.*, 2015; Hammond *et al.*, 2016; Grunwald *et al.*, 2019; Champer *et al.*, 2020). Figure 1.4 depicts

the principle of what has been termed 'Super-Mendelian Inheritance' where the desired allele in the gene drive is propagated more frequently through generations because the integrated Cas9 at one allele has the ability to cut the wild type allele and copy the drive onto it.

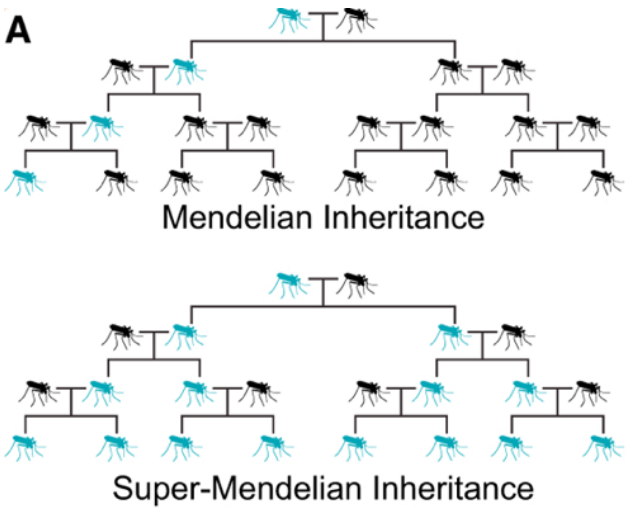

Figure 1.4. ***Inheritance of a specific allele via gene drive results in Super-Mendelian inheritance.*** *The organism carrying the gene drive is depicted in blue. Increased frequency and rate of propagation of the CRISPR-based gene drive is seen in Super-Mendelian inheritance, when compared to regular Mendelian rules where the modified allele has a 50% chance of being passed on to offspring. Adapted from Esvelt et al. (2014).*

Despite the potential the CRISPR-Cas9 gene drive system offers for providing targeted gene modifications, the system is highly variable. There is no guarantee that successful uptake of the constructs by PGCs will produce the expected gene-editing outcomes. Furthermore, this failure to produce HDR-mediated integration of transgenes will only be detected after PGC isolation, propagation and transfection with the CRISPR-Cas9 gene drive constructs. There are a variety of possible causes for this potential failure: gene locus; chromatin state and epigenetic factors at target loci; size and complexity of DNA donor repair-templates; and cell-specific DNA repair pathways (Miyaoka *et al.*, 2016). These limitations are common in the field of CRISPR-Cas9 gene editing systems. This also highlights the field's incomplete control over the system and the imperfect nature of this system in practice.

1.8 The therapeutic protein of interest: Tenecteplase

Therapeutic proteins have become an indispensable tool for treating disease. The recombinant form of tissue plasminogen activator, known as Tenecteplase, in one such therapeutic (Warach, Dula and Milling, 2020; Zitek, Ataya and Brea, 2020). Tenecteplase is used for dissolving

blood clots and is a first-line treatment for cerebrovascular accidents (strokes), which are among the top causes of disability and mortality in South Africa and globally (Maredza and Chola, 2016; Ranganai and Matizirofa, 2020; Akinyemi *et al.*, 2021). Tenecteplase is indicated for use in acute ischaemic stroke during the first 4.5 hours from symptom onset (Warach, Dula and Milling, 2020). This means it should be accessible and easy to store and administer. Despite recombinant Tenecteplase proving the only other cheaper alternative to the standard thrombolytic Alteplase, the treatment is still costly at R2301.13 (South Africa: Department of Health, 2022). Currently, the therapeutic Tenecteplase, engineered to have longer half-life, and increased fibrin specificity, is produced in the common and costly CHO system (Adivitiya and Khasa, 2017). Affordable protein therapeutics, such as Tenecteplase, are essential for the early management of stroke in resource-limited settings such as low and middle-income countries, where the majority of stroke-induced disability and death occurs (Akinyemi *et al.*, 2021). The possibility the transgenic chicken bioreactor offers for producing high-yields of more affordable and accessible protein therapeutics, such as Tenecteplase, makes this study scientifically and clinically significant.

1.9 Aims and Objectives

Aims and Objectives: This project's aims are guided towards the creation of transgenic chicken for therapeutic protein expression *in ovo* by **i**) preparing and transfecting chicken PGCs with generated Cas9-based, egg white loci-specific gene drives and **ii**) evaluating busulfan-based sterilisation for repopulation of gonads in embryos with isolated PGCs.

The following objectives will achieve this:

Objective 1: Prepare egg white loci-specific gene drive constructs via insertion of *HSPA2* meiosis-specific promoter, as well as antibiotic resistance genes, homology arms and gRNA cassette.

Objective 2: Assess and establish a busulfan-based method of sterilisation in chicken embryos for determining the best concentration for sterilisation.

Objective 3: Establish a culture of male chicken PGCs with CEF feeder cells.

Objective 4: Transfection of PGCs with gene drive and general Cas9 expression constructs.

Objective 5: Screen for editing activity of gene drives and Cas9 constructs in transfected PGCs.

Objective 6: Assess PGC-repopulation technique in busulfan-ablated chicken embryos with PGCs transfected with a fluorescent tracer.

Section 2: Methods

2.1 Preparing the OVA and the OVM gene drive constructs with cloning

The stock gene drives which contain elements common to both the OVA and OVM gene drives, and to which modifications were made in order to make them egg-white loci specific, was designed by Prof Nikitina, and obtained from and synthesised by Genscript (figure 2.1). The steps for preparing the new OVA and OVM gene drive constructs involved a series of restriction digests and ligations with cloning with DNA template prepared by PCR and digestion from plasmids. Each gene drive required its own changes to be made to general Cas9 promoters, antibiotic resistance regions, gRNA cassette, and homology arms. Due to the nature of adjusting the gene drive (via restriction enzymes) a specific order for cloning certain elements was followed. The overall sequential steps of restriction digests and ligations for each GD is described briefly below with accompanying diagrams. For all these cloning steps the DNA ligase was employed and DNA fragments for ligation were pre-digested with restriction enzymes. Some DNA fragments required PCR amplification which will subsequently be discussed in detail in this section.

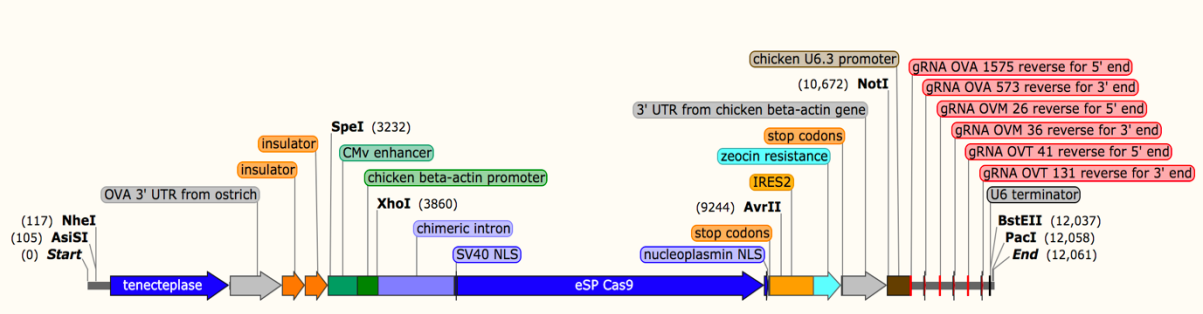

Figure 2.1. ***Features of the base gene drive to which various modifications could be made.*** *Important restriction sites used in cloning are shown. Although the diagram appears linearized, the gene drive is a circular dsDNA structure and features are contained within a pUc57-Brick backbone with Ampicillin resistance and ORI for cloning (not shown here).*

2.1.1 Overview of cloning strategy for generation of the OVA gene drive

For the OVA gene drive the Zeocin antibiotic resistance region was replaced by both restriction enzyme digestion and a HiFi DNA assembly protocol for joining the DNA fragments in a specific order. Zeocin was deemed unsuitable for the purposes of Cas9-based gene drive editing, due to its DNA-damage inducing properties (Tsukuda and Miyazaki, 2013; Lin *et al.*, 2017). The region removed from the gene drives included the Zeocin coding region, part of the associated IRES, as well as the downstream 3'UTR (from chicken β-actin gene). The IRES

was no longer needed since expression of the new antibiotic would be controlled by newly synthesised eukaryotic promoter, SV40, and no longer fall under the same promoter (further upstream) as eSpCas9. The 3'UTR was removed due to the fact that during assembly of antibiotic into the gene drive, the 3'UTR would simultaneously be moved to sit directly upstream of the new antibiotic region (see figure 2.2). Thereafter the general CBh promoter (CMV enhancer and modified β-actin promoter) controlling expression of eSpCas9, would be replaced with the meiosis-specific mouse *HSPA2* promoter. The *HSPA2* promoter was amplified from mouse gDNA extracted from tail tissue and is described in section 2.2.1. For inserting the *HSPA2* promoter into the OVA gene drive double restriction enzyme digestion was performed and gel purified fragments were ligated and cloned. Thereafter the Zeocin antibiotic region was replaced and adjusted with previously prepared Puromycin antibiotic resistance template using HiFi DNA assembly. Figures 2.2-figure 2.3 depict a visual explanation of these cloning steps.

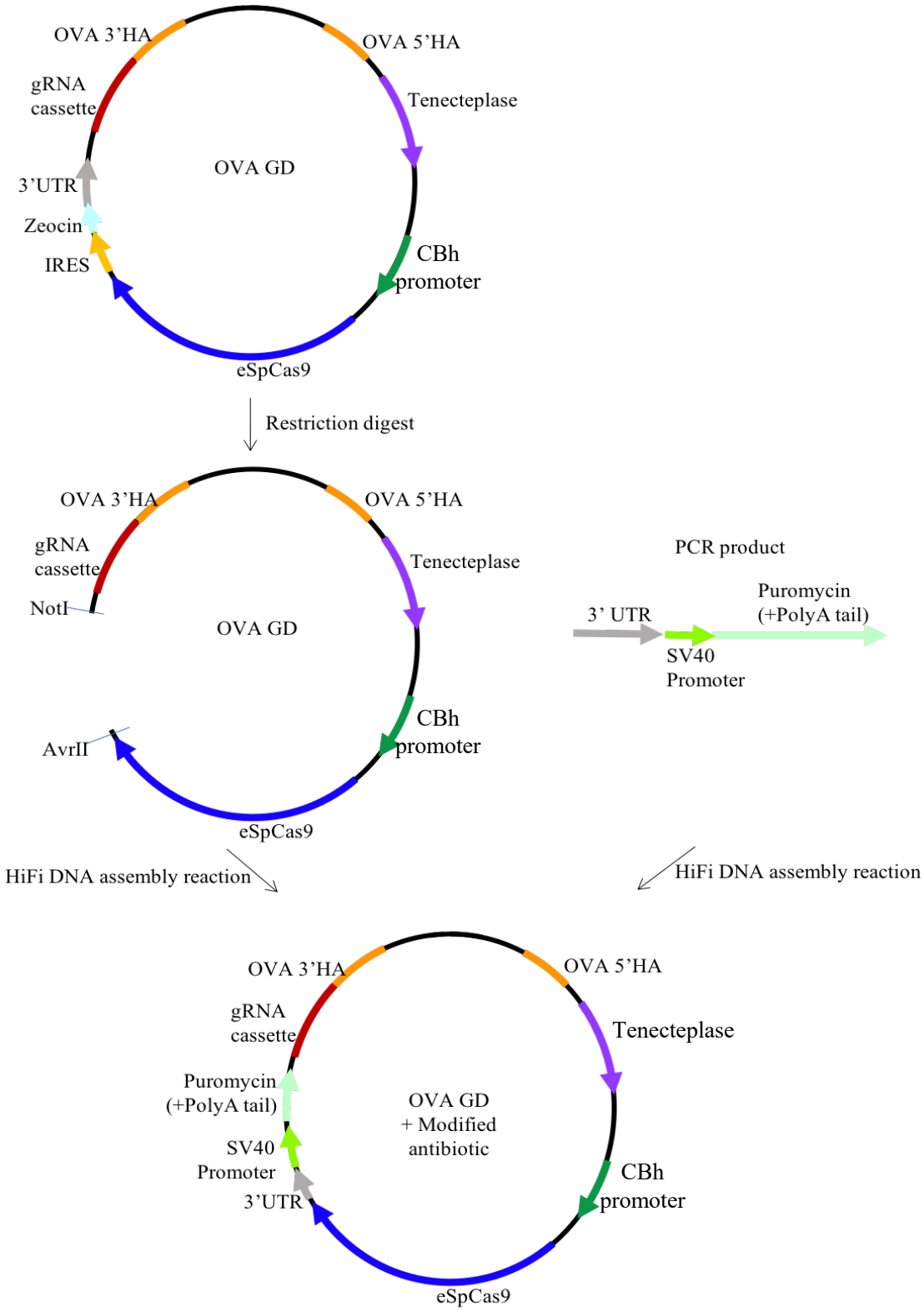

Figure 2.2. Steps for modifying the Zeocin antibiotic region in the OVA gene drive. *The OVA gene drive was digested with AvrII and NotI to remove the Zeocin resistance region, part of the upstream IRES and the downstream 3'UTR. The larger generated fragment was used in the NEBuilder HiFi DNA assembly. The single replacement fragment generated by PCR contained the joined 3'UTR, SV40 Promoter, and Puromycin (with its PolyA tail) and was used in the NEBuilder HiFi DNA assembly. This assembly reaction generated the OVA gene drive with modified antibiotic region that does not conserve the AvrII and NotI restriction sites. This*

modified gene drive can subsequently be carried forward for further adjustment to the CBh promoter.

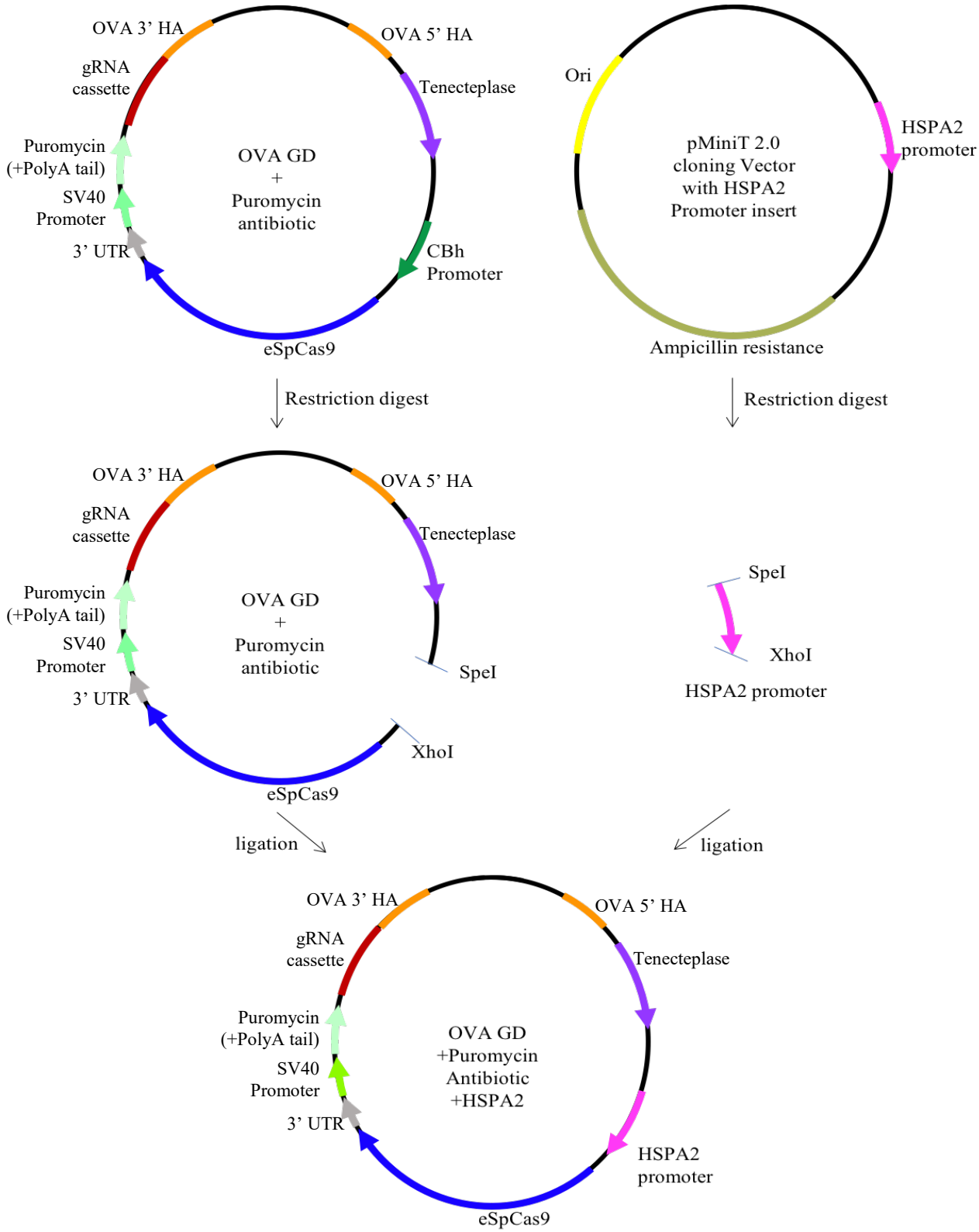

Figure 2.3. ***Steps for replacing the CBh promoter in the OVA gene drive.*** *The OVA gene drive containing newly adjusted Puromycin, and the pMinT 2.0 vector containing HSPA2 were digested with SpeI and XhoI to create sticky ends for ligation. Each digestion created two fragments. The larger fragment generated in the OVA gene drive digestion had the CBh promoter removed and was used in ligation. The smaller fragment (the HSPA2 promoter) digested out of the pMinT 2.0 vector was used in the ligation. The ligation resulted in generation of the OVA gene drive containing HSPA2.*

2.1.2 Overview of the cloning strategy for generation of the OVM gene drive

The OVM gene drive first required insertion of a new OVM gRNA cassette via double restriction enzyme digestion and ligation. Following this, the Zeocin antibiotic region was replaced (as with OVA for reasons explained previously) with Neomycin resistance by employing both restriction digestion and HiFi DNA assembly methods. Next the general CBh promoter (CMV enhancer and modified β-actin promoter), controlling expression of eSpCas9, was replaced with the meiosis-specific mouse *HSPA2* promoter. This too was carried out via double restriction digestion and ligation of the relevant gel purified fragments. Lastly the OVM 5' HA and the OVM 3' HA were ligated sequentially into the gene drive respectively by double restriction enzyme digestions of the cloning vectors, digestion of the OVM gene drive, and ligation of the purified fragments. In all but two cloning steps, fragments were purified by gel extraction before ligation. The exception was in cloning of the HAs where the digested gene drive was instead subjected to PCR cleanup. The diagrams below (figure 2.4-figure 2.8) depict explanations of these cloning steps.

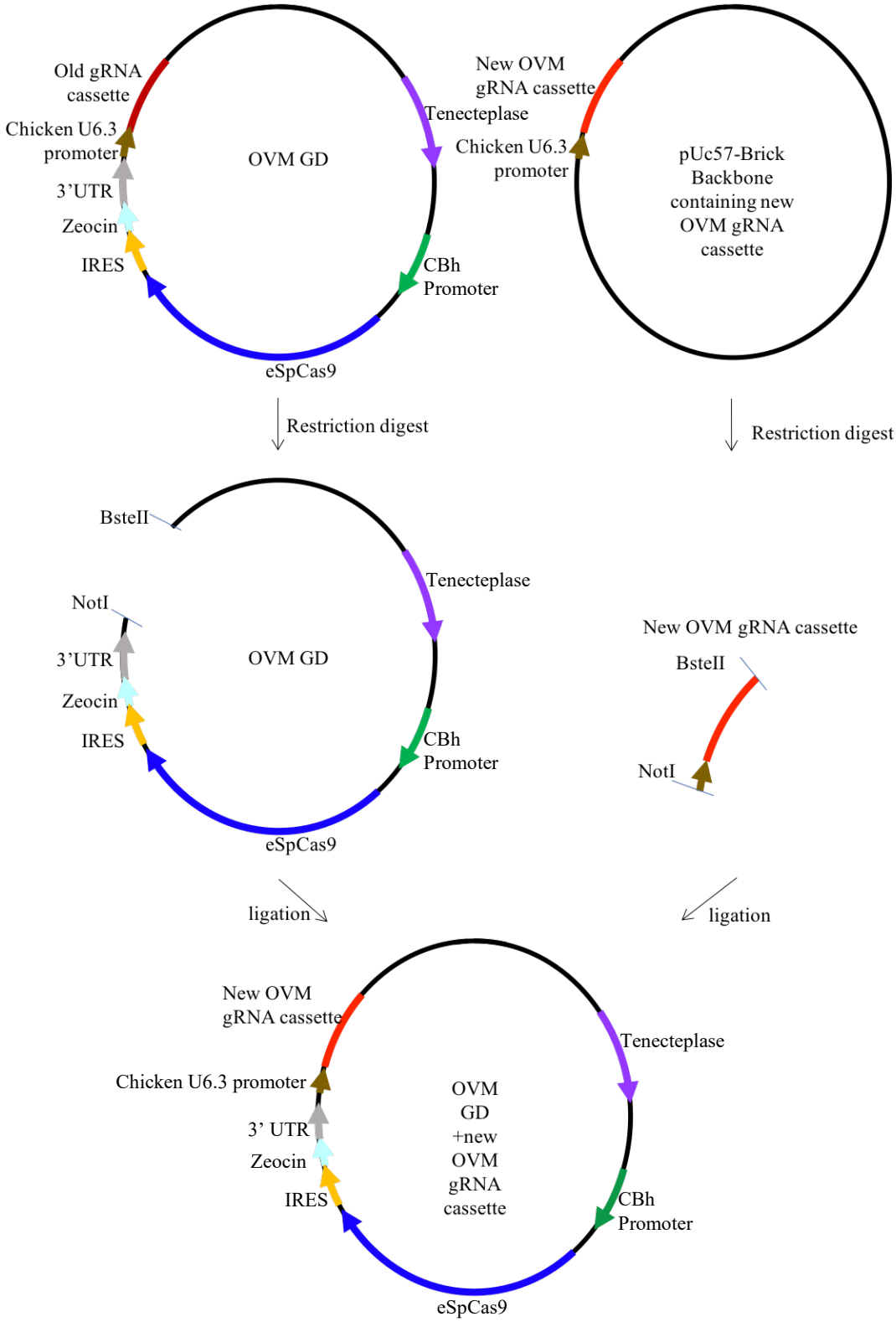

Figure 2.4. Cloning steps for inserting new OVM gRNA cassette into the OVM gene drive. *Both the OVM gene drive and the pUc57-Brick Backbone containing the new OVM gRNA cassette were digested with NotI and BsteII. Each digestion generated two fragments. The OVM gene drive, the larger fragment in its digestion, had the old OVM gRNA cassette along with the upstream Chicken U6.3 promoter removed, and was used in the ligation reaction. The new OVM gRNA cassette was the smaller fragment in its digestion from the pUc57-Brick Backbone and was used for ligation. The digestion created sticky ends for ligation which*

resulted in the generation of the OVM gene drive containing new OVM gRNA cassette. This newly modified gene drive could subsequently be carried forward for adjustment to its Zeocin antibiotic region.

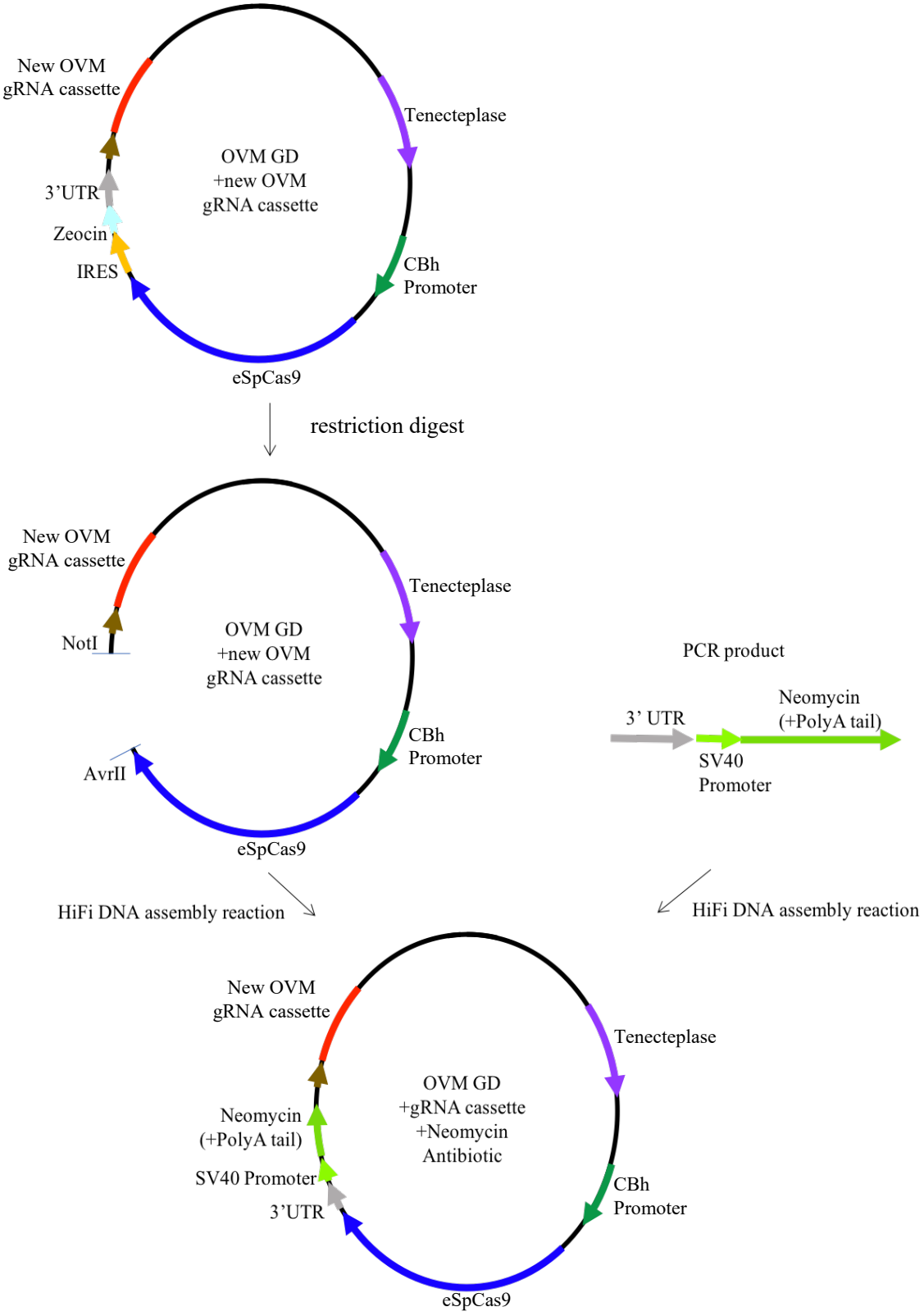

<u>Figure 2.5</u>. Steps for adjustment of the Zeocin antibiotic and surrounding region in the OVM gene drive. *The OVM gene drive containing the new OVM gRNA cassette was digested with AvrII and NotI to remove the Zeocin resistance and associated region. The larger gene drive fragment generated was used in NEBuilder HiFi DNA assembly. The single replacement fragment for the excised region contained the joined 3'UTR and Neomycin (already containing its SV40 Promoter and PolyA tail) and was used in the NEBuilder HiFi DNA assembly. This*

assembly reaction generated the OVM gene drive with modified antibiotic region that does not conserve the AvrII and NotI restriction sites. This modified gene drive would subsequently be carried forward for further adjustment to the CBh promoter.

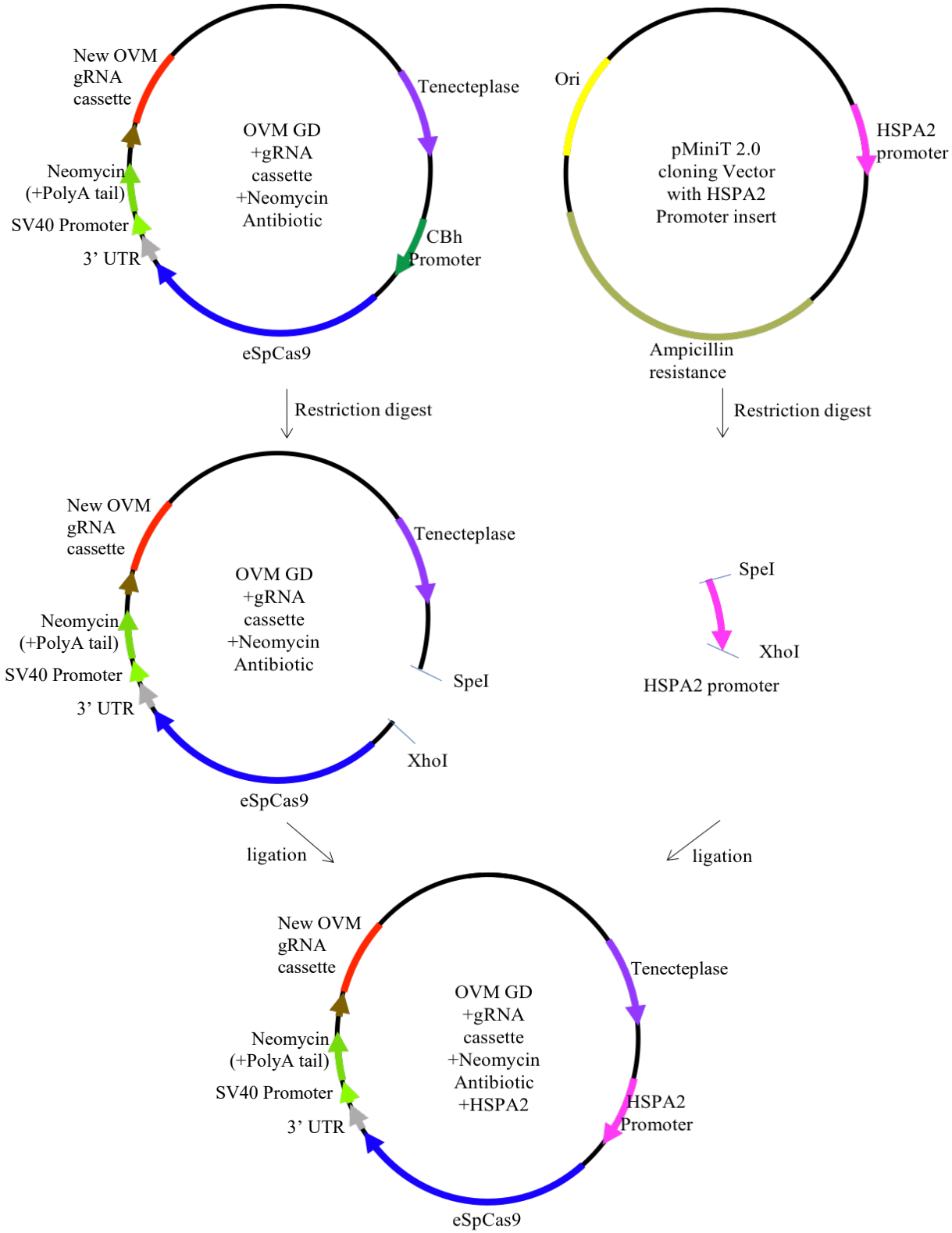

Figure 2.6. ***Strategy for replacing the CBh promoter in the OVM gene drive.*** *Both the OVM gene drive (containing new OVM gRNA cassette and newly adjusted Neomycin), and the pMiniT 2.0 vector containing HSPA2 were digested with SpeI and XhoI to create sticky ends for ligation. Each digestion created two fragments. The larger fragment generated in the OVA gene drive digestion had the CBh promoter removed and was used in ligation. The smaller fragment (the HSPA2 promoter) digested out of the pMinT 2.0 vector was used in the ligation. The ligation generated the OVM gene drive containing HSPA2 promoter.*

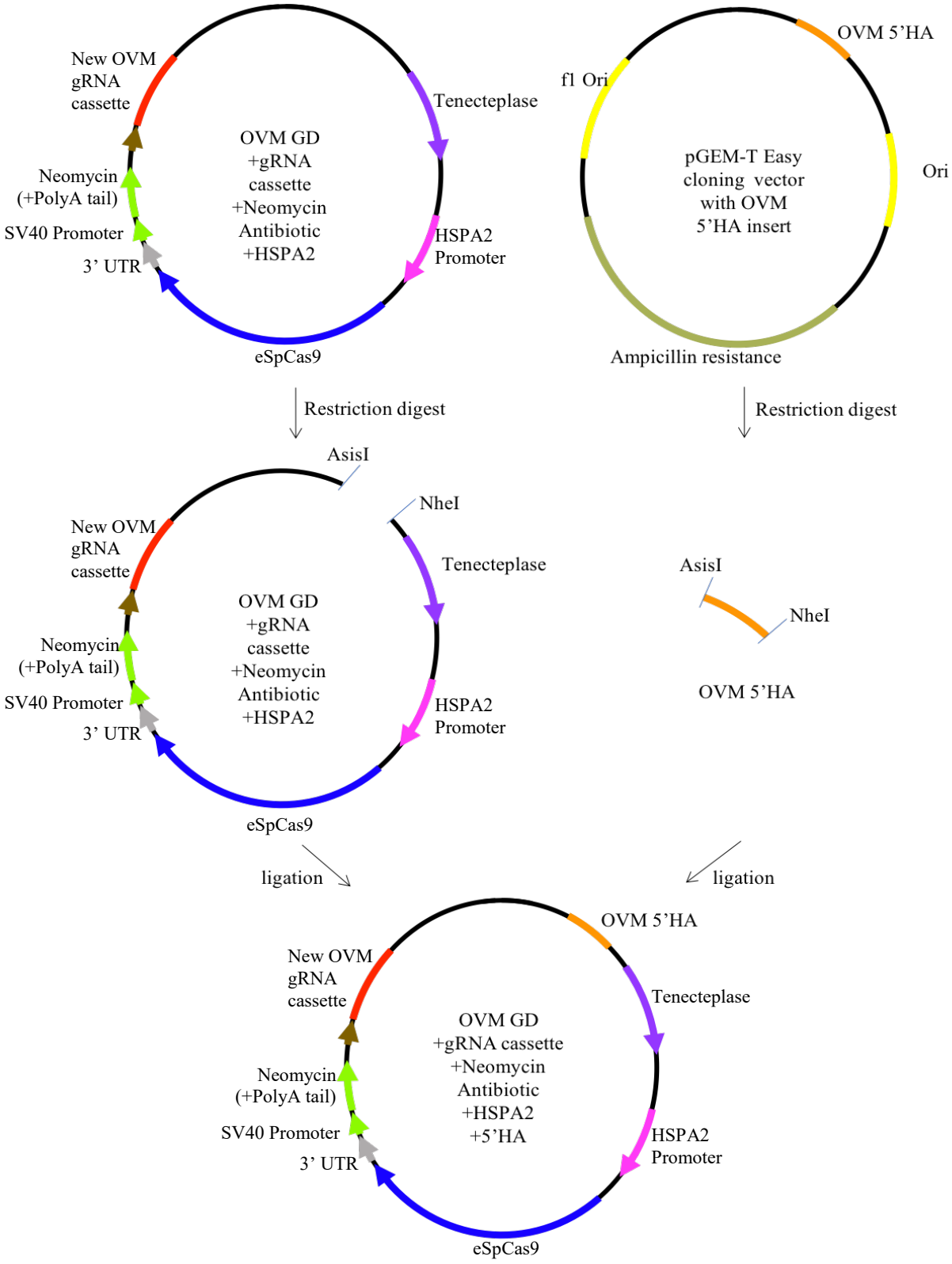

Figure 2.7. ***Cloning steps for addition of the OVM 5' HA into the OVM gene drive.*** *Both the OVM gene drive (containing new OVM gRNA cassette, newly adjusted Neomycin and the HSPA2 promoter), and the pGEM-T Easy vector containing the OVM 5' HA were digested with AsisI and NheI to create sticky ends for ligation. Two fragments were generated by each digestion reaction. The larger fragment generated in the OVM gene drive had a small region (~20bp) removed and the larger fragment was the template for ligation. The smaller OVM 5'*

HA fragment was used in ligation. The ligation generated OVM gene drive containing the OVM 5' HA.

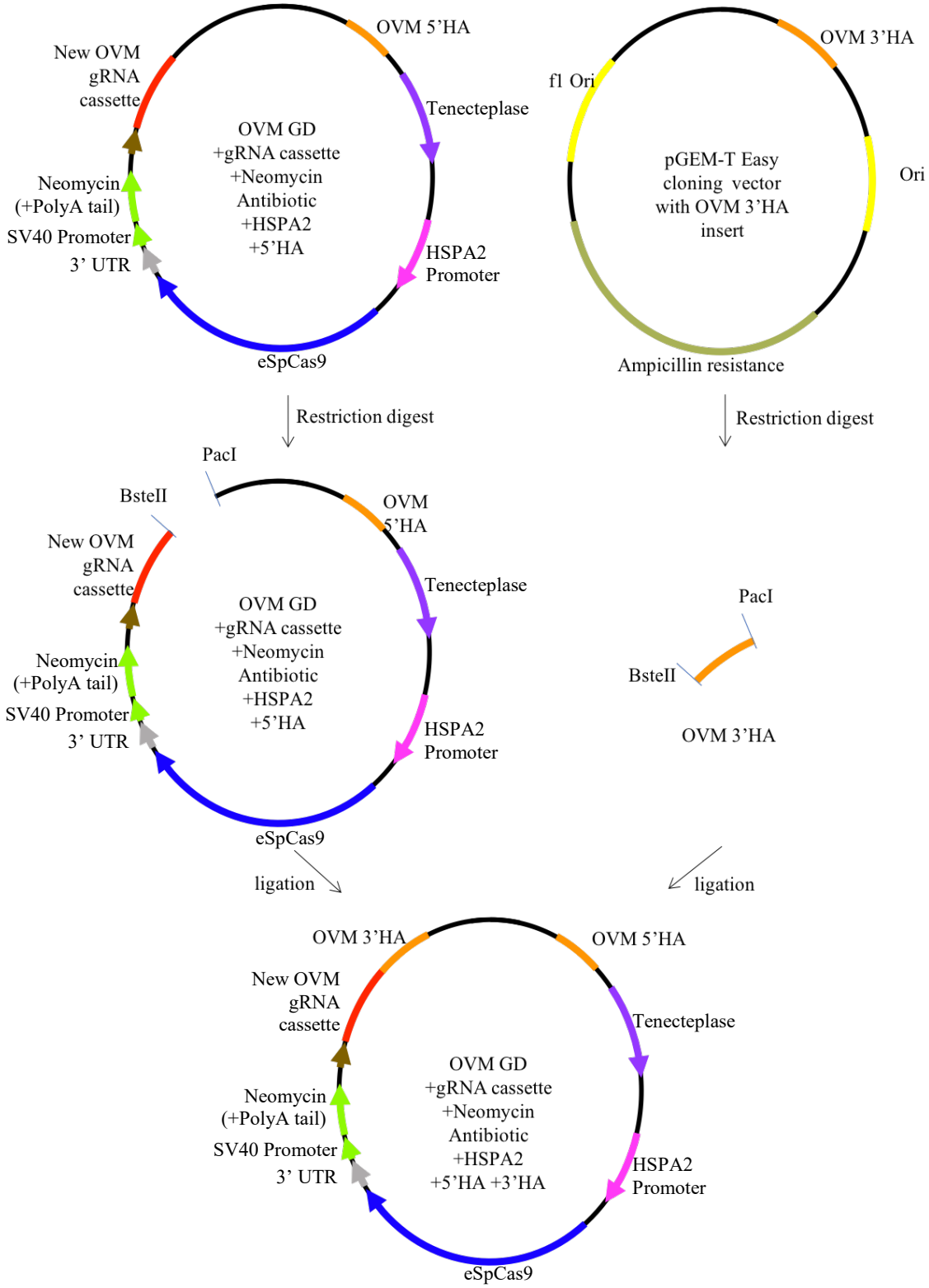

Figure 2.8. ***Cloning steps for addition of the OVM 3' HA into the OVM gene drive.*** *Both the OVM gene drive (containing new OVM gRNA cassette, newly adjusted Neomycin, HSPA2 promoter, and OVM 5' HA), and the pGEM-T Easy vector containing the OVM 3' HA were digested with BsteII and PacI to create sticky ends for ligation. Two fragments were generated by each digestion reaction. The larger fragment generated in the OVM gene drive had a small region (~20bp) removed and the large fragment was the template for ligation. The OVM 3'*

HA, the smaller fragment in its digestion from the pGEM-T Easy vector, was used in ligation. The ligation generated OVM gene drive containing the OVM 3' HA.

2.1.3 Agarose gel electrophoresis

Agarose gel electrophoresis was used for multiple purposes including verifying PCR products, verifying and purifying desired DNA fragments of restriction enzyme digestions, and verifying a check digestion of a ligation reaction. All agarose gels contained 1% agarose in 1X TAE Buffer. Gels included 1µg/ml ethidium bromide (Sigma-Aldrich). DNA samples were stained with 6X loading dye (NEB) before loading onto the gel. The standard NEB 1Kb Plus DNA ladder was run alongside samples on the gel for size verification. Gels were run between 80-110V in 1X TAE Buffer for 30-60 minutes or until the samples migrated more than half way down the gel. Gels were viewed under UV light for image capture using the GelDoc (Bio-Rad).

2.1.4 Restriction enzyme digestion

For all restriction enzyme digestions of DNA performed in this project, whether it be preparation of templates for ligation or confirming a sequence insert after ligation, the protocol of the NEB restriction enzyme's online tool (NEBcloner) was followed. The setup for digestion involved 1-2µg DNA sample in a 25µl or 50µl reaction volume, (table 2.1 below). The digestion reaction was incubated at 37ºC in a water bath or T100^{TM} Thermal Cycler (Bio-rad) either overnight (when preparing ligation templates to ensure complete digestion) or for approximately 1 hour (when assessing ligation success of plasmid extracts). Restriction digestions were verified by agarose gel electrophoresis as described above.

Table 2.1. Restriction enzyme digestion setup. For a 50µl reaction, the volumes were doubled.

Reaction Component	Volume (µl)
DNA sample	1-2µg (depending on stock concentration)
10X rCutSmart Buffer	2.5µl
Restriction enzyme 1(20 000 units/ml)	0.2µl
Restriction enzyme 2 (20 000 units/ml)	0.2µl
Distilled water	Up to total volume of 25µl

2.1.5 Gel extraction

Gel extractions were employed to purify DNA fragments that had been restriction enzyme digested, for subsequent ligation. For all gel extractions the Zymoclean^{TM} gel DNA recovery

kit (ZYMO RESEARCH) or Monarch® DNA gel extraction kit (NEB) was used. Briefly (according to the former's protocol) the gel bands of interest were cut out from the gel using a blade and incubated at 55ºC with 3 volumes of agarose dissolving buffer. The completely dissolved sample was then centrifuged at 17000 x g in a Zymo-Spin™ Column and Collection tube, where it was also washed twice with DNA Wash Buffer and centrifuged again at 17000 x g. The DNA was eluted in 12-30µl pre-heated (to 70ºC) DNA Elution Buffer. The later kit's protocol was similar. In short, the excised gel fragment containing DNA of interest was dissolved at 55ºC in 4 volumes of agarose dissolving buffer. This dissolved sample was centrifuges at16000 x g in a Monarch® Cleanup Column and Collection tube, where it was washed twice with DNA Wash Buffer and centrifuged at 16000 x g. The DNA sample was eluted in 12-30µl pre-heated (to 50 ºC) DNA Elution Buffer. The concentrations of eluted DNA could be obtained via NanoDrop Spectrophotometer (Thermo Fisher) A260/280 readings.

2.1.6 DNA cleanup

The DNA cleanup procedure was performed to purify certain restriction enzyme digested products for ligation- typically these where one of the digested fragments were too small to view by agarose gel and could be removed by DNA cleanup kit. It was also used to purify single digested gene drive samples before transfection. The Monarch® PCR and DNA Cleanup kit was used (NEB) according to its protocol. In short this involved diluting the digested sample with Binding Buffer (2:1 Binding buffer:sample) and spinning it down in the provided column and collection tube at16000 x g for 1 minute. The sample was washed with Wash Buffer twice and centrifuged at16000 x g. The sample was eluted in 12-30µl pre-heated (to 50ºC) DNA Elution Buffer in a fresh 1.5ml or 2ml Eppendorf tube. Again, the concentrations of eluted DNA were obtained via NanoDrop Spectrophotometer (Thermo Fisher) A260/280 readings.

2.1.7 DNA ligation

Ligation (via sticky ends) of digested products was performed with T4 DNA ligase (NEB, M0202S) to modify the gene drives. Ligations were setup as in table 2.2 below and performed at 16ºC. Then 5µl of ligated product was subsequently used in transformation of *E. coli.*

Table 2.2. Ligation reaction setup

Reaction component	Volume (µl)
T4 DNA Ligase Buffer (10X)	2µl
Vector DNA (linearized gene drive)	50-100ng
Insert DNA fragment	According to molar ratio
T4 DNA Ligase	1µl
Nuclease-free Water	Up to total of 20µl

2.1.8 Bacterial transformation

The steps for all transformations, whether using High efficiency NEB 10-beta Competent *E. coli* or High Efficiency NEB Stable Competent *E. coli,* were as follows. The competent cells were removed from -80ºC storage and thawed on ice. Immediately after the cells had thawed, 30-50µl was placed in a 2ml Eppendorf tube on ice, and 5µl of ligation reaction added to it with gentle flicking to mix cells and ligation. The tube was left on ice for 30 minutes and then heat shocked in a 42ºC water bath. The tube was then transferred back to ice for 5 minutes. Approximately 950µl Pre-warmed NEB stable outgrowth media was added to the cell mix which was then incubated for 1 hour at 37ºC with shaking at 250rpm. Following incubation, 100µl of cells was transferred to and spread on a pre-warmed LB agar plate. The plate contained 100µg/ml ampicillin (see Appendices for recipe). The plate was left to incubate overnight at 30ºC. The following day single colonies could be inoculated by selecting and placing in ~6ml LB media supplemented with ampicillin and grown up overnight at 37ºC with shaking at 250rpm. Inoculation was for subsequent plasmid extraction.

2.1.9 Plasmid extraction

Plasmid extractions were performed to determine ligation and transformation success and to obtain purified, cloned plasmid extracts of gene drives or cloning vectors. The protocol for plasmid extraction was an alkaline lysis-based method that had been established in the lab. Before beginning, the relevant buffers (for resuspension, lysis and neutralisation) were prepared (see Appendices for recipes). The liquid culture of interest (grown up from a single colony) grown overnight in LB, was centrifuged at 17000 x g via 2ml at a time three times, each time removing the supernatant. The cell pellet collected at the bottom was resuspended completely in 250µl cold resuspension (Solution I) buffer by pipetting. The cells were then lysed for 2 minutes by the addition of 300µl lysis solution (Solution II) and the sample tube inverted until a white precipitate formed and the solution became clear. The lysis reaction was

neutralised by adding 400µl neutralisation buffer (Solution III). The sample was centrifuged for 5 minutes at 17000 x g following which 700µl of supernatant was transferred to a fresh 1.5ml Eppendorf tube, taking care not to transfer precipitate containing cell debris. After adding an equal volume of Isopropanol to the supernatant, the tube was inverted to mix contents and then incubated for 30 minutes at -80ºC to allow the plasmid to precipitate. The sample was then centrifuged for 5 minutes at 17000 x g and resuspended in Tris-EDTA supplemented with RNAse A (20µg/ml) followed by incubation for 1 hour in 37ºC water bath in order to degrade cellular RNA. After incubation, 300µl of isopropanol (88%) and potassium acetate (0.2M) solution was added to the sample which was then vortexed briefly. The sample was centrifuged, once again at 17000 x g for 5 minutes and the supernatant removed completely, leaving a pellet containing plasmid along the bottom and side of the tube. The pellet was dried by incubation in a heating block and subsequently resuspended in 20-50µl Tris-EDTA buffer (pH 8). The NanoDrop Spectrophotometer was used to confirm concentration and purity ratios, and an agarose gel electrophoresis was used to confirm the size and integrity of the plasmid.

2.2.0 PCR procedures and preparation of templates for modifying gene drives

Various PCR reaction setups and procedures were required for amplification of different products to be inserted into the gene drives, and they are described separately below. For all PCR reactions, thermocycling was carried out in the T100™ Thermal Cycler (Bio-rad).

2.2.1 PCR amplification and cloning of the mouse *HSPA2* promoter

The 926 bp promoter fragment was amplified using primers with restriction sites appended onto their ends in order to clone the promoter fragment in downstream cloning work (Inselman *et al.*, 2009). The forward primer had the *SpeI* restriction site appended onto its 5' end and the reverse primer the *XhoI* restriction site onto its 5' end, along with additional bases for restriction enzyme binding. The primer sequences can be found in table 2.3. The amplification was performed with the MyFi™ DNA Polymerase kit (Bioline), according to its protocol, as a high sequence fidelity was essential and TA overhangs were needed for downstream cloning. Mouse gDNA previously extracted in the lab from tail tissue was used as template for PCR. The PCR reaction setup and cycling conditions are shown below in table 2.4 and table 2.5 respectively. The PCR product was verified by agarose gel electrophoresis before cloning.

Table 2.3. Primer pair for amplification of Mouse *HSPA2* promoter fragment. Restriction sites are underlined in each primer sequence. The amplicon size, which includes appended restriction sites is shown.

Primer	Sequence (5'→3')	Amplicon size (bp)
HSPA2 Mouse Forward	CCGACTAGTAGGAAAGCCGAGGGAGAAAGTT	926
HSPA2 Mouse Reverse	TACCTCGAGAACGTTAGGACGAAAGCGTCAG	

Table 2.4. PCR reaction setup for *HSPA2* promoter using MyFi DNA Polymerase. gDNA extracted from mouse tail tissue was used as template.

Reaction component	Volume (µl)
5x MyFi Reaction Buffer	5µl
Template Mouse gDNA	50ng
Forward Primer (20µM)	0.5µl
Reverse Primer (20µM)	0.5µl
MyFi DNA Polymerase	1µl
Distilled water	Up to total of 25µl

Table 2.5. PCR cycling conditions for amplification of mouse *HSPA2* promoter. The annealing temperature was chosen based on the recommended protocol and using the online IDT Oligo Analyser Tool.

Cycles	Temperature (ºC)	Time
1	95	1 minute
30	95	15 seconds
	56	15 seconds
	72	27 seconds
1	4	Hold

The *HSPA2* promoter fragment was cloned into the NEB pMiniT 2.0 *E. coli* plasmid cloning vector shown in Figure 2.9. This vector is suitable for cloning the single-base overhang PCR product. Using the NEB® PCR Cloning kit and its protocol, the ligation reaction was set up and left to incubate at room temperature (25ºC) for 15 minutes followed by 2 minutes on ice. The reaction contained 25ng of PCR product at a molar ratio of 1:3 (HSPA2 PCR product:pMiniT 2.0). When the vector carries an insert the transformed *E. coli* colony will grow, and those without an insert will not grow due to the uninterrupted toxic minigene within the vector. The resulting ligation reaction was used immediately to transform High efficiency

NEB 10-beta Competent *E. coli* following the protocol discussed previously. Thereafter both colony PCR (Table 2.6) and then plasmid extraction were employed to verify ligation. For colony PCR a pipette tip was used to transfer a small portion of the colony from LB agar plate to the PCR reaction tube. The PCR reaction tube consisted of 5µl Taq DNA Polymerase Mastermix RED (Ampliqon), HSPA2 Mouse forward primer and HSPA2 Mouse reverse primer (1µM each), and distilled water up to a total 10µl reaction volume**.**

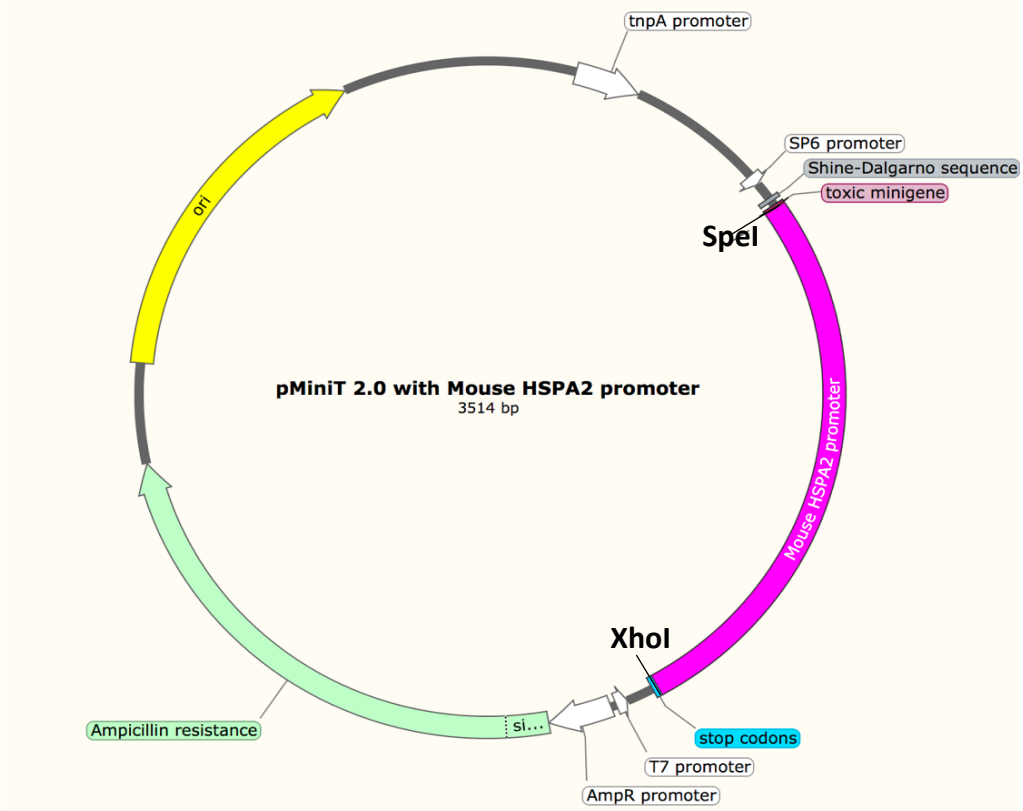

Figure 2.9. pMiniT 2.0 cloning vector containing HSPA2 insert. *The HSPA2 insert shown in pink, disrupts the toxic minigene (also the cloning site) within the vector and therefore permits propagation during cloning. The SpeI and XhoI recognition sites are shown at the ends of the HSPA2 sequence. The vector contains the bla(ApR) marker for selection with ampicillin. Primers for sequencing insert are universal ones within the SP6 promoter and T7 promoter.*

Table 2.6. Colony PCR cycling conditions for the *HSPA2* promoter in pMiniT 2.0. An additional initial cycle step is added for bacterial lysis.

Cycles	Temperature (ºC)	Time
1	98	10 minutes
1	95	1 minute
30	95	15 seconds
	56	15 seconds
	72	27 seconds
1	4	Hold

Additionally, to verify ligation and confirm conservation of restriction sites flanking *HSPA2* promoter, the liquid cultures were subjected to plasmid extraction and subsequent restriction digestion. The pMiniT vector containing *HSPA2* promoter insert, was digested as described before, with *SpeI-HF* (NEB, high fidelity) and *XhoI* (NEB) to verify its size. Conservation of restriction sites is essential for downstream cloning into the gene drives. Due to the necessity for high fidelity sequence of this *HSPA2* promoter, the pMiniT 2.0 extract containing the insert was sequenced before it was cloned into any of the gene drives. Sanger Sequencing (by Inqaba Biotec^{TM}) was performed, with the T7 and SP6 universal primers which are found in the vector flanking the insert (figure 2.9). Thus, the *HSPA2* promoter was ready for insertion into the relevant gene drive at the appropriate cloning step (see section 2.1) via ligation reaction. After performing digestions, with *SpeI-HF* and *XhoI,* of the relevant gene drive and pMiniT 2.0 vector with HSPA2, the gel extracted DNA fragments were ligated overnight at 1:3 (gene drive: *HSPA2*) molar ratio and used in transformation of NEB Stable Competent *E. coli*. Once again plasmid extraction and restriction enzyme digestion with *SpeI-HF* and *XhoI* was performed to screen for successful ligations of single clones. The *HSPA2* promoter sequence in the gene drive was also verified by sequencing (see Supplementary figure 1 and figure 3).

2.2.2 PCR preparation of antibiotic resistance fragments and DNA assembly of Puromycin into the OVA gene drive

The replacement of Zeocin antibiotic in the OVA and OVM (further detail for OVM in section 2.2.3 and section 2.2.6) gene drives with Puromycin and Neomycin respectively employed the use of DNA assembly, and hence required the PCR products of the regions to be inserted. Primers were designed to have the maximum possible overlapping regions with adjacent

fragments essential for DNA assembly of fragments in the desired order (primers in table 2.7). The importance of homologous regions and principle of the NEBuilder HiFi DNA assembly protocol is shown in figure 2.10. This region in the gene drives that needed removal was excised by restriction enzyme digestion using *AvrII* (NEB) and *NotI-HF* (NEB) followed by gel extraction of the linearized gene drive.

The source of the Puromycin resistance coding sequence was a stock vector known as eSpCas9(1.1)-T2A-Puro (figure 2.11) (AddGene, depositer Andrea Németh). The Puromycin sequence could be amplified together with its PolyA-tail, however the source of its promoter, SV40, would be from another stock vector in the lab known as the pCl-neo cloning vector (figure 2.12). The Neomycin together with SV40 promoter was obtained from pCI-neo too. The 3' UTR was amplified using the stock gene drive (figure 2.1). First the four individual fragments (3'UTR, SV40, Neomycin, Puromycin) were amplified separately (table 2.7) and only subsequently joined, where needed, in overlap extension PCR (shown later in figure 2.13 and figure 2.14). This is due to the fact that fewer fragments have a greater chance of assembly in NEBuilder reactions. All PCR reactions were performed using the Q5 Hot Start High-Fidelity DNA Polymerase (NEB, M0491S) in order to ensure high sequence fidelity, and the setup is shown in table 2.8 below. The cycling conditions are given in table 2.9 and table 2.10. The PCR products were verified by agarose gel electrophoresis and purified by gel extraction for subsequent assembly.

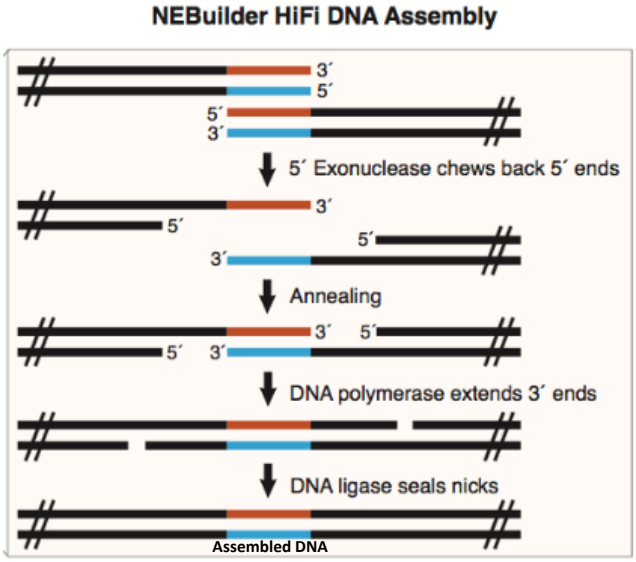

Figure 2.10. ***The principle of DNA assembly of fragments utilising sequence homology between adjacent fragments.*** *The sequence homology between adjacent fragments (in red and*

blue) allow DNA fragments to anneal for the exonuclease to cut back the 5' ends thus creating 3' overhangs. The 3' complementary regions of 3' overhangs on two fragments can anneal and the polymerase will add bases onto the 3' ends using the opposite fragment as template. Adapted from NEBuilder HiFi DNA assembly Manual (New England BioLabs, 2017).

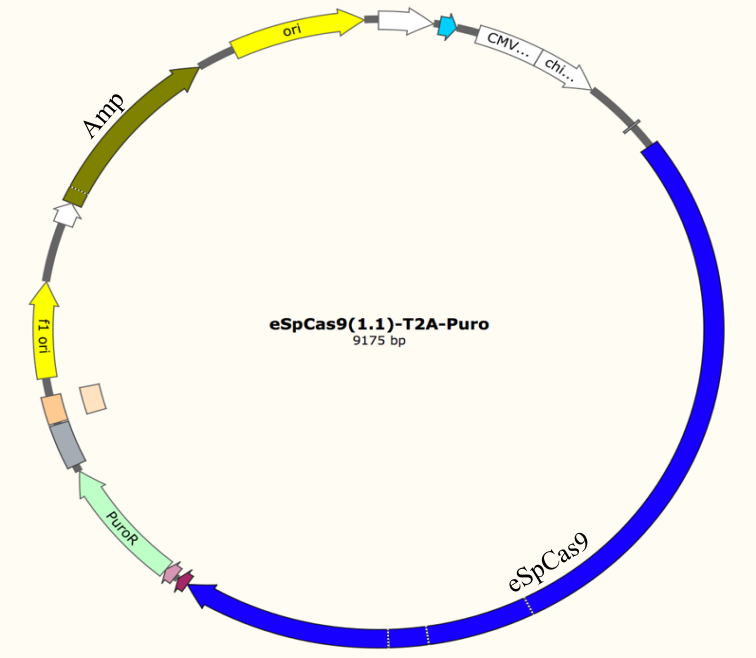

Figure 2.11. ***The stock eSpCas9(1.1)-T2A-Puro vector.*** *The Puromycin sequence with its PolyA tail is shown in green and grey. eSpCas9 is shown in dark blue with its upstream CBh promoter (CMV enhancer and chicken β-actin promoter) in white.*

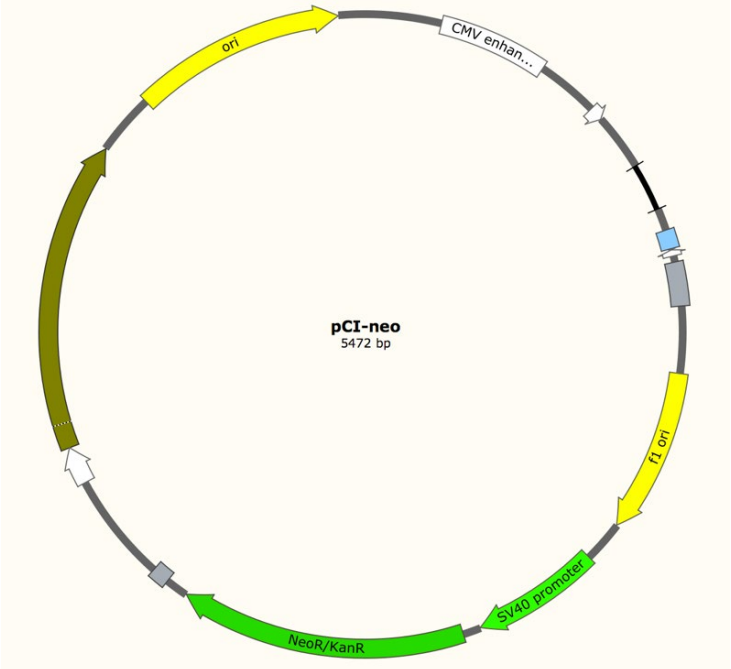

Figure 2.12. ***The stock pCI-neo vector.*** *The Neomycin sequence along with its PolyA tail is shown in dark green (NeoR) and its upstream SV40 promoter in pale green*

Table 2.7. Primer pairs for amplification of fragments to be used in antibiotic DNA assembly. Overlapping regions of adjacent fragments are underlined in each primer and the name and size of each individual fragment is shown. Here the Neomycin fragment includes its SV40 promoter and its PolyA-tail.

Fragment	Primer	Sequence (5'→3')	Amplicon size (bp)
3' UTR	GD 3UTR F	TGTCTTCTTGACGAGCATTCGACTCTG TCACCGGACTG	642
	SV40 3UTR R	CTGGTTCTTTCCGCCTCAGAGCCTCTA TTGTGTGCACTT	
SV40 Promoter	SV40 NEO 3UTR FWD	AAGTGCACACAATAGAGGCTCTGAG GCGGAAAGAACCAG	448
	PURO SV40 REV	GTGGGCTGGTACTCGGTCATGGTGGC TCTAGCCTTAAGT	
Puromycin	SV40 Puro FWD	AACTTAAGGCTAGAGCCACCATGACC GAGTACAAGCCCAC	841
	GD Puro PA rev	TCGGCAGTGCCTGAAGGAGCTCCCCA GCATGCCTGCTATTC	
Neomycin	SV40 NEO 3UTR FWD	AAGTGCACACAATAGAGGCTCTGAG GCGGAAAGAACCAG	1359
	GD NEO PA rev	TCGGCAGTGCCTGAAGGAGCCACAC AAAAAACCAACACACAG	

Table 2.8. Q5 Hot start High Fidelity PCR reaction setup for amplification of four individual fragments for antibiotic assembly.

Reaction Component	Volume (µl)
5X Q5 Reaction Buffer	10µl
10mM dNTP mix	1µl
10µM Forward Primer	2.5µl
10µM Reverse Primer	2.5µl
Template DNA	10ng (depending stock concentration)
Q5 Hot Start High-Fidelity DNA Polymerase	0.5µl
5X Q5 High GC Enhancer	10µl
Nuclease Free Water	Up to total of 50µl

Table 2.9. Q5 Hot start cycling conditions for amplification of individual fragments to be used in antibiotic DNA assembly. *Annealing temperatures for each primer pair was obtained using the online NEB Tm calculator tool. All primer pairs had the same annealing temperature. **The extension time for each amplicon was calculated according to the protocol at 30 seconds/kb. Specifically, the extension times for 3' UTR, SV40, Neomycin and Puromycin were 19 seconds, 13 seconds, 27 seconds, and 41 seconds respectively.

Cycles	Temperature(ºC)	Time
1	98	30 seconds
30	98	10 seconds
	72*	30 seconds
	72	30 seconds/kb**
1	72	2 minutes

Table 2.10. Cycling conditions for overlap extension PCR of OVA gene drive-relevant antibiotic region. Addition of the GD 3UTR F primer and GD Puro PA rev primer was performed in the second stage of cycling. *The first extension time was calculated for the longer Puromycin fragment. **The next extension time was calculated for the fully assembled product at a rate of 30 seconds/kb. The annealing temperature was obtained using the online NEB Tm calculator tool.

Cycle	Temperature (ºC)	Time
1	94	10 seconds
7	94	30 seconds
	72	30 seconds
	72	27seconds *
Remove sample from thermocycler, add primers, return to thermocycler.		
1	94	10 seconds
15	92	30 seconds
	72	30 seconds
	72	59 seconds**
1	72	2 minutes

2.2.3 NEBuilder HiFi DNA assembly

The principle of NEBuilder HiFi DNA assembly, described before, relies on adjacent fragments possessing regions of homology on their ends, which we introduce by appending sequences onto primers. Figure 2.13 shows how primers were designed to create these overlapping homologous sequences. The protocol for DNA assembly of the NEBuilder® HiFi DNA Assembly Master Mix kit was followed. This simply involved setup of the DNA assembly reaction on ice as in table 2.11 using the OVA gene drive with Zeocin antibiotic

region removed (by restriction digestion with *AvrII* and *NotI-HF* and then gel extraction as explained above); and the PCR product template for insertion. Initially the individual PCR products (3'UTR, SV40, and Puromycin), before being joined to one another, were used as template fragments in DNA assembly. However, after failure of NEBuilder DNA assembly using multiple fragments, these PCR products (3'UTR, SV40, and Puromycin) were first joined via overlap extension PCR (figure 2.13). The PCR composition was described previously in Table 2.8. Cycling conditions in Table 2.10 also depict the time point when primer was added. Template DNA (0.2µl) of each individual fragment's PCR product (3' UTR, SV40, Puromycin with its PolyA tail) were added. The joined PCR product acted as the template for DNA assembly with the gene drive in the HiFi DNA assembly reaction. The DNA assembly reaction was incubated in a thermocycler at 50ºC for 1 hour. Thereafter 2µl of the sample was immediately used for transformation with NEB Stable Competent *E. coli* (High Efficiency) as described previously. The following day colonies were selected for plasmid extraction and assessing successful DNA assembly into the gene drive by restriction digestion. The regions were also verified by sequencing (Genscript) (see Supplementary figure 2).

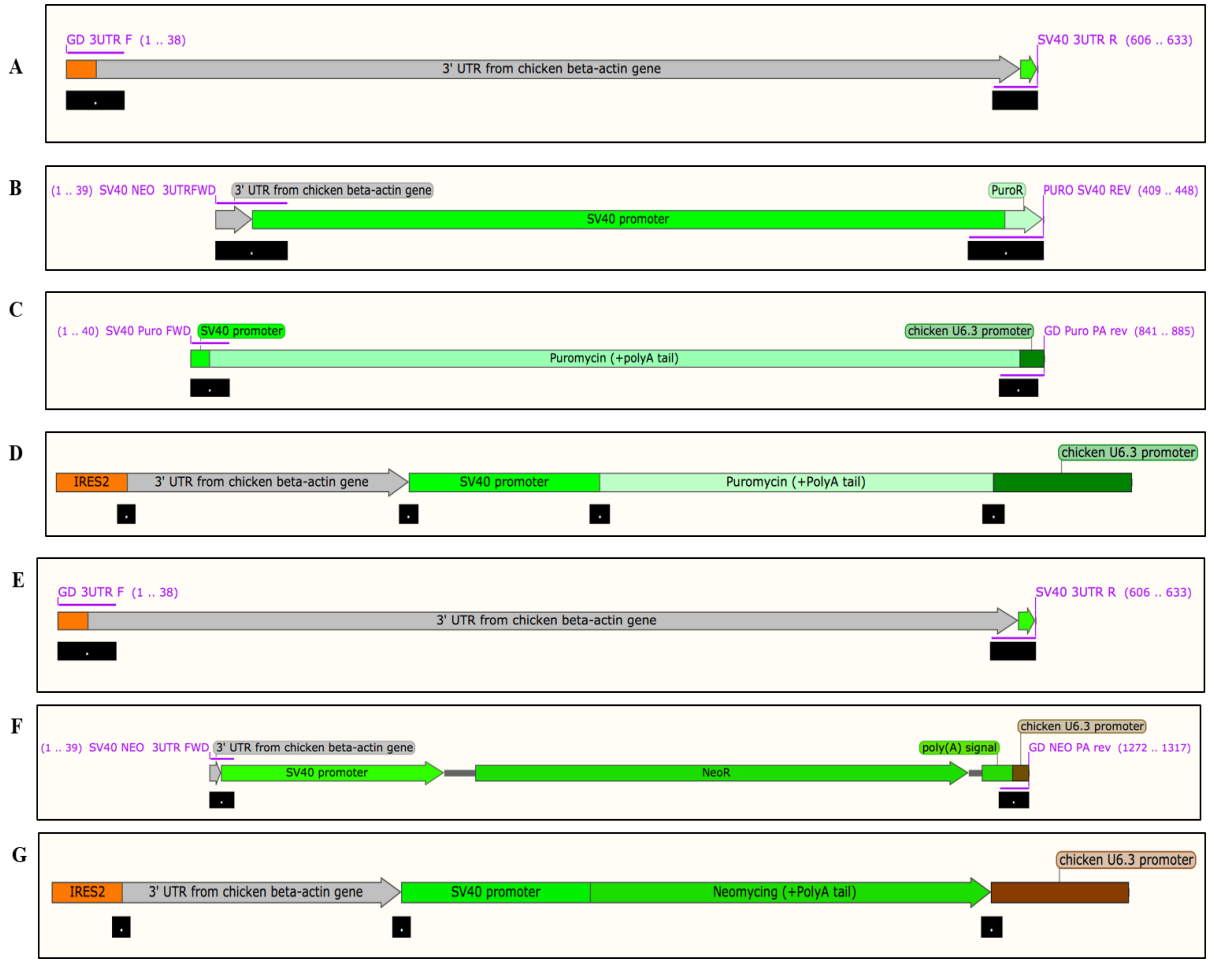

Figure 2.13. Position of primers for creating overlapping regions in antibiotic and associated fragments. *Primers are shown in purple, and regions of homology between adjacent fragments indicated by black block features.* ***A)*** *The 3'UTR fragment at its 5' end contains sequence homology to the upstream IRES in the gene drive (orange), and at its 3' end contains homology with the downstream SV40 promoter (bright green).* ***B)*** *The SV40 promoter at its 5' end contains sequence homology with the upstream 3'UTR (grey) and at the 3' end homology with the downstream Puromycin (pale green).* ***C)*** *The Puromycin (with its PolyA tail) fragment at the 5' end contains sequence homology with the upstream SV40 Promoter and at the 3' end contains sequence homology with the downstream chicken U6.3 promoter (dark green).* ***D)*** *The joined fragments(3'UTR-SV40-Puromycin), with the overlapping regions that allowed for assembly shown in black; this is also the joined region as it would appear assembled into the OVA gene drive between the remaining upstream IRES (orange) and downstream chicken U6.3 promoter (dark green).* ***E)*** *The 3'UTR is the same as in* ***A****.* ***F)*** *The Neomycin fragment (already joined to its SV40 promoter and PolyA tail) contains homology at its 5' end to the upstream 3'UTR (grey) and homology at the 3' end to the chicken U6.3 Promoter (brown).* ***G)*** *The joined fragment (3'UTR-Neomycin) with overlapping regions used in assembly shown in black; this is also the joined region as it would appear in the OVM gene drive between the remaining upstream IRES and downstream chicken U6.3 promoter.*

Table 2.11. NEBuilder HiFi DNA Assembly reaction setup for replacement of Zeocin region in gene drives.

Component	Volume (µl)
Fragments of DNA (gene drive:insert 1:2)	50-100ng (depending sample concentration; adhering to DNA Molar Ratios
NEBuilder HiFi DNA Assembly Master Mix	10µl
Deionised water	Up to total volume of 20µl

2.2.4 PCR and cloning for generating the OVM gene drive

The OVM gene drive was subjected to 4 major changes which required preparation of templates by PCR and restriction digestions. Changes included replacing the gRNA cassette; adjusting the Zeocin antibiotic region with Neomycin antibiotic resistance; replacing the general CBh promoter (CMV enhancer and modified β-actin promoter) controlling expression of eSpCas9 with the meiosis-specific mouse *HSPA2* promoter; and addition of 5' and 3' homology arms.

2.2.5 Replacing the gRNA cassette in the OVM gene drive

The new OVM gRNA cassette, designed and cloned by Prof Nikitina, was chosen as it no longer contained unnecessary regions such as OVT-specific gRNAs, thus making it OVM-specific. The gRNA cassette (along with the upstream chicken U6.3 promoter) (figure 2.14) and the stock gene drive were each digested with *NotI-HF* and *BsteII-HF* (NEB). Ligation of gel purified new OVM gRNA cassette and OVM gene drive was as described previously at a 1:3 molar ratio (gene drive: gRNA cassette). The ligation reaction was used to transform NEB Stable Competent *E. coli* (High Efficiency) and screening for successful uptake of ligated DNA was performed via plasmid extraction and subsequent restriction enzyme digestion. A successfully modified OVM gene drive, verified additionally by sequencing (Genscript) (see Supplementary figure 4), was carried forward for antibiotic modification.

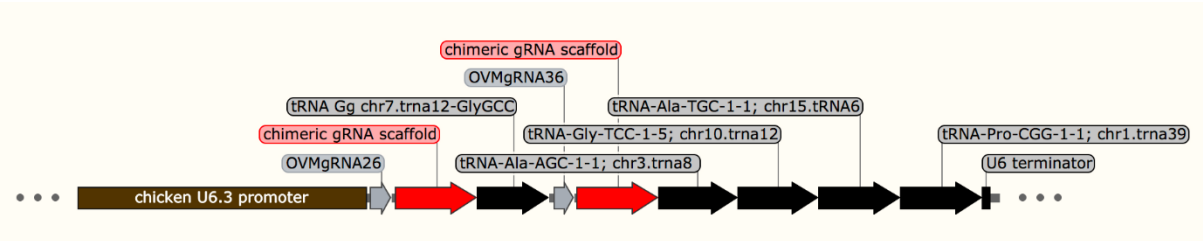

Figure 2.14. The new OVM gRNA cassette for insertion into the OVM gene drive. *The upstream chicken U6.3 promoter is included (brown).*

2.2.6 PCR preparation of antibiotic resistance for assembly of Neomycin into OVM gene drive

Previously the PCR conditions for obtaining the individual fragments (the 3' UTR and Neomycin) for inserting into the OVM gene drive were described (section 2.2.2). The insert 3'UTR and Neomycin fragments were joined via overlap extension PCR. The reaction setup is as described previously in table 2.8 using 0.2µl of each 3'UTR and Neomycin fragment as template. Cycling conditions are shown in table 2.12. The DNA assembly via NEBuilder was setup as in section 2.2.3 with the linearized OVM gene drive (digested *AvrII* and *NotI-HF*) and fully assembled 3'UTR-Neomycin fragment (see figure 2.13 for a diagrammatic explanation). After transformation of NEB Stable Competent *E. coli* with 2µl of assembly reaction, screening for assembled product was performed with plasmid extraction and restriction digests. A successfully modified OVM gene drive, verified additionally by sequencing (Genscript) (see Supplementary figure 4), was carried forward for further modification of the general CBh promoter.

Table 2.12. Cycling conditions for overlap extension PCR of OVM gene drive-relevant antibiotic region. Addition of the GD 3UTR F primer and GD Neo PA rev primer was performed in the second stage of cycling shown in the table. *The first phase's extension time was calculated for the longer Neomycin. **The next phase's extension time was calculated for the fully assembled product at a rate of 30 seconds/kb. The annealing temperature was obtained using the online NEB Tm calculator tool.

Cycle	Temperature (ºC)	Time
1	94	10 seconds
7	94 72 72	30 seconds 30 seconds 41seconds*
Remove sample from thermocycler, add primers to sample, return sample to thermocycler.		
1	94	10 seconds
15	94 72 72	30 seconds 30 seconds 1 minute**
1	72	2 minutes

2.2.7 Replacing the CBh promoter with *HSPA2* promoter in the OVM gene drive

Amplification of the *HSPA2* promoter in preparation for ligation into the OVM gene drive at a 1:3 molar ratio (gene drive: insert) has been described in section 2.2.1. After transformation of the ligation reaction in Stable Competent *E. coli*, the plasmid extract was screened for correct ligation via restriction digest. A successfully modified OVM gene drive, verified additionally by sequencing (Inqaba Biotec^{TM}) (see Supplementary figure 5), was carried forward for addition of the OVM homology arms.

2.2.8 Addition of 5' and 3' OVM homology arms

The homology arms were ligated sequentially onto the gene drive following the protocol explained previously. The difference is that the 5' HA cloning step employs the *AsisI* and *NheI-HF* restriction enzymes and the 3' HA the *BsteII-HF* and *PacI* enzymes. As mentioned previously the digested OVM gene drive was purified by PCR cleanup whereas the OVM 5' HA was gel extracted due to the very small digested sequence (<20bp) removed from the gene drive. Finally, the ligation of cleaned up linearized gene drive and the 5' OVM HA was performed as described before at a 1:3 molar ratio (gene drive: HA) and *E. coli* transformed as before. Once screening for successful ligations by restriction digestion of plasmid extracts took place, the 3' OVM HA was ligated into the OVM gene drive following these steps. This concluded modification of the OVM gene drive, henceforth known as the HSPA2-OVM gene drive.

2.2.9 Plasmid midiprep

In order to obtain plasmid extracts of the final modified constructs known as the HSPA2-OVA and HSPA2-OVM gene drives at high concentrations and in large quantities for downstream transfections, the PureYield^{TM} Plasmid Midiprep System (Promega) was used following the manufacturer's protocol. First, the *E. coli* bacterial cell cultures were allowed to grow in 500ml terrific broth (see Appendices for recipe) until reaching an optical density of at least 2. Optical density was measured at 600nm using an ultraviolet-visible spectrophotometer. The cells were pelleted by centrifugation at 5000 x g for 10 minutes. After removing the media, the pellet was resuspended completely in 6ml cell resuspension buffer followed by a 5-minute incubation in 6ml lysis buffer, with continuous inversion of the sample. Thereafter 10ml of neutralisation buffer was added and the sample inverted multiple times. The sample was centrifuged again at 15000 x g for 15 minutes to pellet cell debris. The supernatant was then transferred carefully

without disturbing the debris to the PureYield™ Clearing Column placed in the top of the PureYield™ Binding column, which were both attached onto a vacuum manifold. The lysate was pulled through both columns by applying the vacuum. The PureYield™ Clearing Column was removed and 5ml of Endotoxin Removal Wash was added to the Binding Column and pulled through using the vacuum. Then 20ml of Column Wash Solution was added and pulled through by vacuum. The membrane inside the column was dried by letting the vacuum run until no ethanol odour could be detected. For the elution step, the binding column was assembled, together with the Eluator™ Device and a fresh 1.5ml Eppendorf tube, onto the vacuum manifold and eluted by addition of 400-600µl nuclease-free water with application of the vacuum. The concentrations of these midi-preps were determined by Nanodrop Spectrophotometer.

2.3 Animal Ethics

For this study all the necessary ethical clearance was obtained from the WITS Animal Ethics Screening Committee. The certification for performing genetic modifications under the Genetically Modified Organisms Act, 1977, was granted to the laboratory by the Department of agriculture, forestry, and fisheries. The work fell under the following permit and registration numbers: AREC 2021/09/02/O and 39.2/Witwatersrand – 20/165 (03/06/2020-03/06/2023). The WITS institutional Biosafety Committee gave the lab ethical clearance under the protocol number: 20190801Lab.

2.4 Acquisition and incubation of chicken embryos

All eggs in this study were SPF fertilized eggs (White Leghorn), obtained and collected from Avi-farms (Centurion, Gauteng, South Africa). Before allowing any eggs to be incubated for the desired duration, they were left overnight on their sides at room temperature on the lab bench top, while also allowing the commercial incubator (Pleysier incubators) to reach appropriate humidity (~65%) and temperature (37ºC). Eggs were allowed to acclimatise overnight for the reason that increased viability is promoted, as discovered previously in the lab.

2.5.0 Establishment of culture of primary chicken embryonic fibroblasts

For all cell culture protocols sterile working conditions were maintained by autoclaving dissecting equipment and continuously wiping down equipment, lab surfaces and benches with 70% ethanol. The biosafety cabinet (BSC; model Esco AC204S8) was treated with UV light before and after each use.

For cultivation of PGCs a direct CEF feeder layer was needed. The CEF feeder layer was established via extraction from day 10 embryos, the protocol for which had been established within the research lab. After ~10 days incubation, the eggs were removed carefully from the incubator, keeping them in their same orientation, wiped down with 70% ethanol and placed within the BSC. Using a sterile 6ml syringe and 20 gauge needle a small hole was made at the sharp and blunt ends of the egg through which approximately 6ml of egg albumen was removed. Cellotape was placed over the egg before dissection, as this helped to prevent egg shell from falling onto the embryo below. A pair of scissors was then used to cut away egg shell to expose the embryo. Using forceps, the embryo was removed through the hole and placed in a Petri dish with 1X phosphate buffered saline (PBS), where the embryonic limbs, head, and viscera were removed with fine forceps. The remaining torso tissue was transferred to and macerated in a petri dish with 1X PBS and then placed into a 10ml Falcon tube containing 1x Trypsin-EDTA. The tube was placed in a shaking incubator at 37 ºC on low speed (~100 rpm) for 30 minutes. Thereafter the tube was left to stand upright until the large chunks of tissue had settled, so that supernatant could be split (1:1) into two 10ml Falcon tubes with an equal volume of 100% foetal bovine serum (FBS). The tube was inverted to mix its contents and subsequently centrifuged at 1000 rpm for 5 minutes to pellet the cells. The supernatant was removed, and the pellet was resuspended in 100% FBS. After repeating the centrifugation step, the pellet in each tube was resuspended in 10ml CEF media (recipe in Appendices). Before CEFs could be plated, an automated cell count was taken for each tube. An equal volume of trypan blue (Sigma) and cell suspension was mixed and allowed to incubate for ~3 minutes before being added to dual chamber slides (Bio-Rad; catalogue number 1450015**)**. A viable cell count was obtained via the TC20 automated cell counter (Bio-Rad). The cells from a single embryo were seeded into multiple 75cm^2 flasks with vented cap at a density of ~2.1 x10^6 cells.

2.5.1 Maintenance of CEF cultures

The cultures of CEFs were incubated in a NuAire NU-5500 Direct Heat CO_2 Incubator at 37°C, 5% CO_2. Sterility was maintained with the use of 70% ethanol on culture flasks each time they were moved between the incubator or BSC. The CEFs were observed regularly for fibroblast morphology and confluency under the inverted compound microscope (NIB-100, Allfine Medlab). Once CEFs had reached a high confluency (~70-80%) they were passaged and either maintained in cell culture (where they were passaged continuously upon reaching ~70-80% confluency) for use as a feeder layer or frozen as stocks. For passaging CEFs, the CEF media was removed and cells were washed with 1X PBS. The cells were then treated with warmed 1X trypsin EDTA and incubated at 37ºC for 5 minutes or until the cells lifted, appearing rounded and detached when viewing with inverted microscope. The trypsin was de-activated by adding CEF media to the flask, and the cells pelleted by centrifugation at ~400 x g for 4 minutes. A cell count was taken (as in section 2.5.0) for plating in 75cm^2 flasks with warmed CEF media to keep a continuous CEF culture to be readily used for CEF feeder layers.

2.5.2 Cryopreservation of CEFs

Cell stocks were prepared for freezing in liquid nitrogen for long-term storage. Once CEFs had reached ~80% confluency they were passaged. A confluent T75 flask was split (1:1) into two-four 2ml cryo-vials. The same protocol for passaging CEFs was followed as described above, except the CEF pellet was resuspended in a specific CEF freezing media (recipe in Appendices) before transfer to a cryo-vial. The cryovials containing CEFs were left overnight in an Isopropanol-filled (Ethanol SA) container placed in a -80 ºC freezer. This ensured a slow cooling rate of -1 ºC/minute. This provides better cell viability after cryopreservation. The following day the samples were stored in liquid nitrogen.

2.5.3 Preparation of CEF feeder layers

For preparation of growth-inhibited CEF feeder layers, CEFs with low passage numbers were chosen (below 10) in order for CEFs to settle, grow rapidly and fulfil their role as a factor-secreting feeder layer to PGCs. CEFs that were maintained in culture and passaged regularly, or frozen stocks could be used. If CEFs in culture were used, they were simply passaged and seeded into a 6 well-plate at a density of ~0.3 x10^6 cells. If frozen stocks were used, they were thawed and prepared as follows. Once the cryo-vial was removed from liquid nitrogen it was thawed immediately on ice and centrifuged for 4 minutes. The media was removed, and the

pellet resuspended in ~200ul of pre-warmed CEF media. A viable cell count was taken before plating in a 6-well plate. The CEFs were left overnight to allow cells to settle. The following day when confluency was optimal for growth inhibition (~60-70%), mitomycin-C (10µg/ml) (Merck) was added to CEFs and left to incubate in the incubator at 37 ºC for 4 hours. Optimal confluency was important. If the confluency was too high growth inhibition might not be complete. Arrest of mitomycin-C treatment was done by removing CEFs from the incubator, discarding the media containing mitomycin-C, then washing with 1X PBS. Once warmed CEF media was added the CEFs were returned to the incubator. For use as a feeder layer, and since these growth inhibited CEFs tend to die off after ~5-7 days, the CEF feeder layers were prepared on the same day that PGCs were to be seeded onto them.

2.5.4 Isolation of male PGCs from embryonic vasculature to establish primary culture

After incubation, HH14-17 embryos were carefully removed from the incubator and wiped down with 70% ethanol. Approximately 6ml of egg albumen was removed from the sharp and blunt ends of the egg through a small hole using a sterile 10ml syringe and 20-gauge needle, to lower the position of the embryo on the egg yolk. A pair of scissors was then used to cut away egg shell, creating a large field of view wide enough to expose and comfortably manipulate the embryo. Prior to cutting away the egg shell, a piece of tape was placed over the egg, to prevent egg shell falling onto the embryo below. While viewing the embryos under compact stereo microscope (Zeiss) blood was drawn (from mainly the dorsal aorta, vitelline arteries, heart) using a sterile mouth pipette to which a fine glass micropipette was attached (figure 2.15). Each embryonic sample of extracted blood containing PGCs was placed separately in its own well of a PCR plate with 50ul pre-warmed PGC media (recipe in Appendices). The plate was covered in parafilm to attempt to minimize cross-contamination while the plate was outside the egg incubator. The PCR plate was kept inside the warmed egg-incubator while awaiting sexing and then pooling of male samples. This served as a temporary holding medium for the blood samples to keep the cells warm and to minimize stress to them. A piece of tissue from the head of each embryo sample was dissected with fine forceps and placed in individual PCR tubes containing lysis buffer with 20mg/ml proteinase K (recipe in Appendices) for application in sexing protocol (in section 2.5.7). After sex determination was completed, male extracted blood was pooled and added onto mitomycin-inhibited CEF feeder cells in a 6-well plate containing supplemented PGC media.

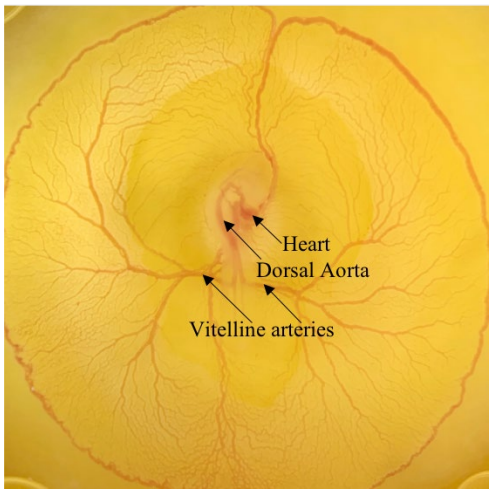

Figure 2.15. ***Main points of extraction of blood containing PGCs from HH14-17 embryos.*** *The blood of embryos was drawn with a fine glass needle and mouth pipette from the vasculature, mainly from the points indicated by labelled arrows.*

2.5.5 Maintenance of PGC primary culture

The protocol for maintaining and propagating a culture of undifferentiated PGCs was adapted from literature. The PGCs were incubated in a NuAire NU-5500 Direct Heat CO_2 incubator in PGC media supplemented with basic fibroblast growth factor (bFGF; 10ng/ml; Sigma), Leukemia inhibitory factor (LIF; 10ng/ml; Sigma), and Stem cell factor (SCF; 5ng/ml; Sigma) (see recipe in Appendices). The PGC media was changed regularly by completely replacing it the following day after seeding so as to help remove egg yolk and blood cells which may have been carried through from dissection. Thereafter half of the media was replaced approximately every 3 days. The PGCs were observed with inverted microscope for growth and morphology as well as confluency and formation of clusters. Sterility was maintained, similarly to CEF cultures. Handling and working with PGC cultures were performed within the BSC.

2.5.6 Passaging PGCs and replenishing the CEF feeder layer

The mitomycin-C-inhibited CEF feeder layers, upon which the PGCs were cultured, were replaced every 5-7 days as they tended to die off. This was achieved by passaging the PGCs together with any few remaining CEF feeder cells to a newly inhibited CEF feeder layer. Wells containing PGCs on CEFs were aspirated of media and then washed with 1X PBS. Pre-warmed 1X Trypsin-EDTA was added to coat the cells, and cells were left to incubate in the incubator at 37 ºC for 10-15 minutes. Following incubation, PGC media was added to the well to inactivate the trypsin. Very carefully, the contents of the well along with aspirated media containing PGCs were transferred to a 15ml falcon tube for centrifugation at 400 x g for 4

minutes. The media was removed with care so as not to disturb the cell pellet, which was subsequently resuspended in 1-2ml of PGC media. An automated cell count could then be taken as described before. The cells were split and seeded onto feeder cells usually at 1:1 ratio. The passaging of PGCs was also based on their proliferation and were usually passaged once confluent.

2.5.7 PCR-based Sexing of embryos

The protocol for determining the sex of embryos was adapted from literature and well established within the lab as it allows for PCR amplification using embryo lysate without DNA extraction (Clinton *et al.*, 2001; Li *et al.*, 2011). The small piece of head tissue dissected and set aside during PGC extraction from each embryo sample was submerged in 100µl lysis buffer and 1µl 20mg/ml proteinase K to digest tissue, on ice. The samples were vortexed briefly to mix contents and then placed in a thermocycler at 55ºC for 15 minutes. The tube was again vortexed and then placed in a thermocycler at 55ºC for 15 followed immediately by 95ºC for 5 minutes. The tubes were then vortexed again and centrifuged until the tissue pellets and supernatant was not too murky. The supernatant was kept for use in PCR. Here the method for detection was multiplex PCR which involved amplification of both sex-specific and control amplicons in a single reaction. The sex-specific sequence is a *XhoI* repeat sequence found on the female-specific W chromosome. The 18S ribosomal gene acted as the control, found in both male and female embryos. The Taq DNA Polymerase Master Mix RED (Ampliqon) was used. The conditions for PCR setup and relevant primer sequences can be found in table 2.13 and table 2.14. The PCR products were visualised via agarose gel electrophoresis.

Table 2.13. Taq PCR reaction setup for sexing PCR. The W primer pair produce an amplicon of 415bp using the Forward (5´CCCAAATATAACACGCTTCACT 3´) and Reverse (5´ GAAATGAATTATTTTCTGGCGAC 3´) primers. The 18S ribosomal control produces an amplicon of 256bp with the Forward (5´ AGCTCTTTCTCGATTCCGTG 3´) and Reverse (5´ GGGTAGACACAAGCTGAGCC 3) primers.

Component	Volume (ul)
Crude DNA extract	0.5
Master Mix	5
0.5uM18S primer (forward and reverse)	1 (0.5ul each)
1uM W primer (forward and reverse)	2 (1ul each)
Distilled water	1.5

Table 2.14. Sexing PCR cycling conditions.

Cycles	Temperature(ºC)	Time
1	94	2 minutes
	94	5 seconds
30	56	5 seconds
	72	5 seconds
1	72	5 minutes
1	4	hold

2.6 Verifying PGC identity by immunocytochemical staining

The extracted PGCs in culture were verified by morphology and PGC markers. This simply involved viewing by inverted compound microscope and monitoring for PGC growth and small cluster formation as described above, and by performing immunocytochemistry. PGCs were characterised by the presence of a specific marker, stage-specific embryonic antigen (SSEA)-1. Since the protocol involved fixation, PGCs' were set aside for the sole purpose of immunocytochemical staining. A single well in a 6-well plate containing PGCs on CEFs was employed as a negative control. All incubation steps requiring a temperature of 37ºC, were carried out in the NuAire incubator. Media was removed from the wells and cells were washed three times for 5 minutes with 1X PBS. Cells were fixed by adding 4% Paraformaldehyde (PFA) to cover the surface of wells, and then incubated at 37ºC for 30 minutes. After removal from the incubator, the PFA was replaced with 1X PBS for three 5-minute washes. Blocking was performed in all wells by incubating cells in 2% filter-sterilised Bovine Serum Albumin (BSA), for 1 hour at room temperature in the BSC. The cells were incubated with mouse monoclonal primary antibody anti-SSEA-1 (1:100; Abcam; ab16285), constituted in 2% BSA, at 37ºC for 2 hours. The primary antibody was omitted from the negative control well, and instead those cells were incubated in 1ml 2% BSA during this time. Following incubation, thorough washing of all wells three times for 5 minutes with 1-2ml of 1X PBS was performed. The remaining steps of this immunocytochemistry protocol were performed in the dark due to use of immunofluorescence. All the cells were incubated with conjugated secondary antibody, Rabbit Anti-Mouse IgG H&L (FITC; Abcam; ab97045), at a concentration of 1:50 constituted in 2% BSA, at 37ºC for 1 hour. Once again thorough washing of the cells to remove unbound antibody was performed with 1X PBS. All cells were counter-stained with 5ng/µl DAPI (4′,6-diamidino-2-phenylindole) for 15 minutes at room temperature. After removing DAPI, a small amount of PGC media was added to coat the bottom of the wells for viewing stain with the

FLoid™ Cell Imaging Station (Thermo Fisher) and for image capturing and analysis. Images were processed using ImageJ ver. 1.53k (Rasband, 2022).

2.7 Partial sterilisation of chicken embryos

The protocol for ablation of endogenous PGCs in chicken embryos was adapted from literature (Song *et al.*, 2005; Nakamura *et al.*, 2008, 2009, 2010; Lee *et al.*, 2013). The embryos were sterilised by busulfan emulsion injection at stage X, with 3 different busulfan concentrations in order to determine the best concentration for ablation, where ablation efficiency was high and survival rate was acceptable. After treatment the number of PGCs in day 7.5 embryos were counted and the viability rate for each concentration assessed.

2.7.1 Removal of PGCs from chicken embryos using busulfan

In preparation for injection, the embryos were placed horizontally overnight at room temperature, in order for the blastoderm to be positioned on top of the yolk. The different busulfan emulsions were prepared immediately before injection into stage X embryos, in order to prevent separation of emulsion components. The oil-busulfan emulsion was made by first dissolving busulfan in dimethyl sulfoxide (DMSO) and then in 50% sesame oil to get the desired dilutions (containing 65µg/50µl=1/3µg/µl, 75µg/50µl=1.5µg/µl, and 85µg/50µl=1.7µg/µl). The emulsions were mixed by passing them through a sterile 0.45µm membrane filter 50 times until busulfan completely dissolved and components were well mixed. The emulsion was also vortexed before use.

Before injection eggs were wiped down with 70% ethanol. A small hole was made in the sharp end of the egg (to avoid puncturing the air pocket at other end) using a sterile insulin needle and 50µl of busulfan emulsion injected into the yolk of the eggs (see figure 2.16 for experimental setup). The hole was then sealed with tape and the eggs placed in the egg incubator. Incubation of embryos occurred at 37ºC and 62-65% humidity. A group of non-treated control embryos were also placed in the incubator and allowed to develop to the same stage. At the end of the incubation period, a count of dead and alive embryos was taken. The count was used to estimate the survival rate for each group. Any embryos with visible developmental abnormalities or stunted growth were noted.

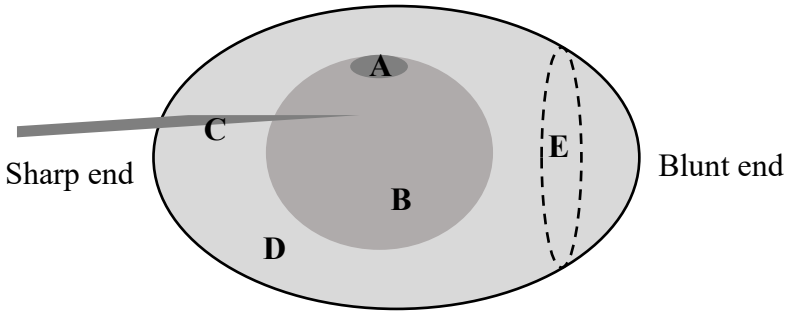

Figure 2.16. ***Setup of busulfan injection into stage X embryos.*** *Eggs remained sealed during injection, apart from the injection site at the sharp end of the egg.* ***(A)*** *Blastoderm.* ***(B)*** *Egg yolk.* ***(C)*** *Needle carrying busulfan emulsion.* ***(D)*** *Egg white.* ***(E)*** *Air pocket. Image created in Microsoft PowerPoint.*

2.7.2 Assessing sterilisation efficiency in embryonic gonads

In order to determine the efficiency of busulfan sterilisation, the PGCs in each embryo sample which had survived and had no observable developmental defects were counted via immunostaining of gonad tissue sections. The busulfan treated and control groups could then be compared to estimate efficiency of the sterilisation method.

For both control and busulfan treated groups the gonads were dissected out the embryo. Similar to before, using sterile dissecting scissors and forceps a hole was made on the side of the egg to comfortably remove the embryo. The vasculature surrounding the embryo was cut away and the embryo transferred to a Petri dish with 1X PBS for dissection under compact stereo microscope. Immediately the embryo was euthanized by decapitation with dissecting scissors and a small piece of soft tissue from the head set aside for sexing PCR as described previously. The limbs, viscera, skin, muscle and all tissue except exposed gonads and attached kidneys were discarded. The remaining tissue was washed in 1X PBS in the dish. The gonads and attached tissue of each sample were transferred to individual 2ml Eppendorf tubes containing 4% PFA for downstream processing.

2.7.3 Processing Embryo Gonadal tissue for Cryosectioning

Before samples were cryosectioned, a series of processing steps were completed. First the samples were fixed by submerging in 4% PFA in 2ml Eppendorf tubes, and left overnight on a shaker at low speed at room temperature. The following day, the PFA was removed, taking care not to damage any tissue, and replaced with 1.5ml of 1X PBS to wash the tissue while horizontally shaking at low speed for 15 minutes at room temperature. Three wash steps were

performed. After washing, the embryos were subjected to a sucrose gradient treatment (a cryoprotectant) over the course of ~3 days. First the embryos were submerged in 5% sucrose and left in the fridge at 4ºC in the upright position overnight or until they had sunk to the bottom of the tubes. This was repeated with 15% sucrose, and then 30% sucrose. The sucrose was removed, and three wash steps were performed with 1X PBS as before. Following the washes, the embryos were immersed in cryomatrix embedding media, taking care to completely cover all tissue and remove air bubbles that could prevent contact of media with tissue. The embryos were left in cryomedia in the fridge at 4ºC overnight to penetrate the tissue. The following day, the samples were placed carefully into silicone freezing moulds filled with cryomedia. The tissue samples were then subjected to flash freezing by submerging the moulds containing tissue in a container of liquid nitrogen for approximately 30 seconds. The moulds were then immediately transferred to -80ºC freezer for about 5 minutes to allow for slower cooling of samples which helps avoid cracking of samples and subsequent tissue damage. Frozen blocks of cryomedia containing tissue samples were stored at -20ºC prior to sectioning.

2.7.4 Cryosectioning of gonadal tissue samples

The frozen embedded tissue samples were placed on the specimen mount in the orientation for cutting tissue sections along the dorsal-ventral axes of the embryos, and in order to obtain a greater number of sections for counting PGCs. Before sectioning, the whole gonads were removed from the -20ºC freezer and placed within the Leica CM1520 cryostat (Leica biosystems) to equilibrate to -16ºC (the recommended sectioning temperature for gonadal tissue). The frozen block of tissue was adhered onto the specimen mount with a small amount of cryomatrix embedding media and also allowed to equilibrate to the cryostat temperature. Upon fixing the specimen mount in place, the block was sectioned at a thickness of 10µm. Using a camel hair brush, the sections were flattened out and transferred to labelled positively charged slides by gently bringing the slide close to the sections. Sections were viewed continuously under light microscope. Every second section within gonadal tissue was discarded to avoid recounting the same PGCs later in immunostaining. Slides were allowed to dry at room temperature and then stored at -20ºC.

2.7.5 Immunohistochemistry of gonadal tissue sections

For immunostaining of gonads and visualisation of PGCs, slides containing tissue sections were allowed to come to room temperature and then rehydrated by placing them in a glass

container filled with 1X Tris-Buffered Saline, 0.1% TWEEN,1% DMSO (TBSTD). After three 15-minute washes in TBSTD, the sections were immersed in 2% BSA for 1 hour of blocking non-specific antigenic sites. The sections were incubated with primary antibody SSEA-1 (1:50) in a sealed humidified container at 4ºC. The primary antibody was added to the slides and prevented from running off by gently placing parafilm over the sections. The parafilm also created a layer for solution to continuously move across all sections on a slide. The humidity was achieved by placing damp paper towels below the elevated slides in the airtight container, and this avoided drying out of sections. Primary antibody was omitted for the negative control to ensure elimination of autofluorescence. The following day the sections were once again washed three times in 1X TBSTD to wash off unbound primary antibody. The remaining steps of this protocol were performed in the dark due to the use of fluorescein conjugated antibodies as well as the light-sensitive DAPI. The slides were then incubated with Rabbit Anti-Mouse IgG H&L (FITC) secondary antibody for two hours at room temperature (Abcam; ab97045; 1:100). Both primary and secondary antibody were suspended in 2% BSA and 50µl of the particular antibody solution added per slide. The sections were once again washed three times in 1X TBSTD and then counterstained by placing DAPI (0.2 µg/ml) suspended in 2% BSA onto the slides, covering in parafilm and incubating for 15 minutes at room temperature. The sections were briefly washed in 1X TBSTD. After allowing to air-dry at room temperature the sections were sealed with a glass coverslip. The sections were viewed using the FLoid^{TM} Cell Imaging Station for image capturing and analysis. Images were processed using ImageJ ver. 1.53k (Rasband, 2022).

2.7.6 Statistical analysis of busulfan ablation

For each sample, PGCs were counted across 20 sections of stained gonadal tissue. Microsoft Excel (version 16.30) program was used for statistical calculations. For survival rate of embryos, Chi-squared test was performed. Anova was used to determine if there was any significant difference in average numbers of PGCs between all groups. If the difference was significant, an additional Tukey's post-hoc test was performed to determine exactly where the significant difference lay, hence confirming optimal concentration of busulfan. A Fisher's exact test of independence was used to determine if there was a relationship between busulfan dose and observed developmental defects. For all statistical tests performed, $P<0.05$ was accepted as statistically significant.

2.8.0 Antibiotic kill curves

The OVA and OVM gene drives were modified to contain Puromycin and Neomycin resistance genes respectively for the purpose of selection and obtaining pure transfected PGC lines. Hence, the optimal selection antibiotic concentration for each antibiotic needed to be determined, since they are cell type dependent. Based on the literature, a range of antibiotic concentrations for each was chosen to treat cells over a period of time. The minimum concentration (which is not toxic early on in treatment) at which cells were killed by the end of treatment (5-7 days) was the optimal concentration. Since the PGCs were cultured on a CEF feeder layer and survival and proliferation of PGCs without growth-inhibited CEFs was minimal, the kill curve was performed on PGCs cultured on growth-inhibited CEFs. To account for the CEFs in the assay, the same kill curve was performed on growth-inhibited CEFs in parallel. Thus, at the end of the assay the cell count of CEFs could be subtracted from the cell count of PGCs on CEFs. This gave an estimated kill curve of PGCs alone. Since the CEFs were growth-inhibited (described previously) they did not proliferate to skew the cell count. For each concentration of PGCs on CEFs and for each concentration of CEFs, triplicate treatments were performed. Puromycin treatment concentrations included 0, 0.25, 0.5, 0.75, 1.0, 1.25, 1.5, 1.75, and 2.0 μg/ml. Neomycin treatment concentrations included 0, 100, 200, 300,400, 500, and 600μg/ml. For both Puromycin and Neomycin the protocol was as follows. In 48-well plates the CEFs were seeded at a density of $0.3x10^5$ cells/ml and allowed to settle for a few hours before growth inhibition with mitomycin-C (described previously). PGC were seeded onto the relevant CEFs at a density of $0.5x10^5$ cells/ml and allowed to settle overnight. The following day the PGC media was removed from wells and replaced with media supplemented with antibiotic at the relevant concentration. The media with relevant antibiotic was replaced every two days and cells were observed under inverted compound microscope for cell death. At the end of treatment (1 week for Neomycin and 5 days for Puromycin) a manual live cell count was taken for each well. Cells were aspirated and trypsinised with 1X Trypsin-EDTA, followed by centrifugation at 400 x g for 4 minutes and then resuspension of the pellet in ~100μl PGC media. Cell suspension was diluted (1:1) with Trypan Blue and loaded onto an Improved Neubauer Haemocytometer with cover slip for viewing and counting by light microscope. The formula used for obtaining the live cell density (when 4 major blocks were counted on the grid) was:

Density= [live cells counted x Dilution Factor]/[number squares counted x volume]

2.8.1 Statistical analysis of kill curves

Microsoft Excel program was used for statistical calculations. A one-way ANOVA was used to determine if there was any significant difference in numbers of cells between all groups. If the difference was significant, an additional Tukey's post-hoc test was performed to determine exactly where the significant difference lies, hence confirming optimal concentration of antibiotic. For all statistical tests performed $P<0.05$ was accepted as statistically significant.

2.9.0 Transfection Procedures

In this study, electroporation and lipofection, for co-transfection of the final modified gene drive constructs (HSPA2-OVA or HSPA2-OVM) together with the general expression eSpCas9(1.1)-T2A-Puro construct (figure 2.11) and mRFP-tol2 construct (figure 2.17) were performed. The mRFP-tol2 construct was included as a form of fluorescent-based tracking of PGCs that would subsequently be injected into recipient embryos. The construct can integrate at low rates if endogenous cell transposases are present, producing low levels of expression of red fluorescent protein (RFP). RFP will be transient under the control of the ubiquitous promoter in the construct. For both transfection procedures the PGCs were lifted from the CEF feeder layer for transfection by pipetting followed by centrifugation at 400 x g, and subsequently transferred back to a growth inhibited CEF feeder layer. An automated cell count was taken as described previously to transfect $1x10^5$ cells. Post-transfection, the cells were also treated with 7.5µM RS-1 (XcessBio) and 0.1µM SCR7 (XcessBio) overnight in order to promote HDR and inhibit NHEJ. These concentrations were chosen based on previous studies in the lab with CEFs. The PGC media was supplemented with both reagents and left overnight before the selection process began. Since the literature for optimal concentrations of RS-1 and SCR7 in chicken PGCs is lacking, the lab's established concentration in CEFs was deemed sufficient.

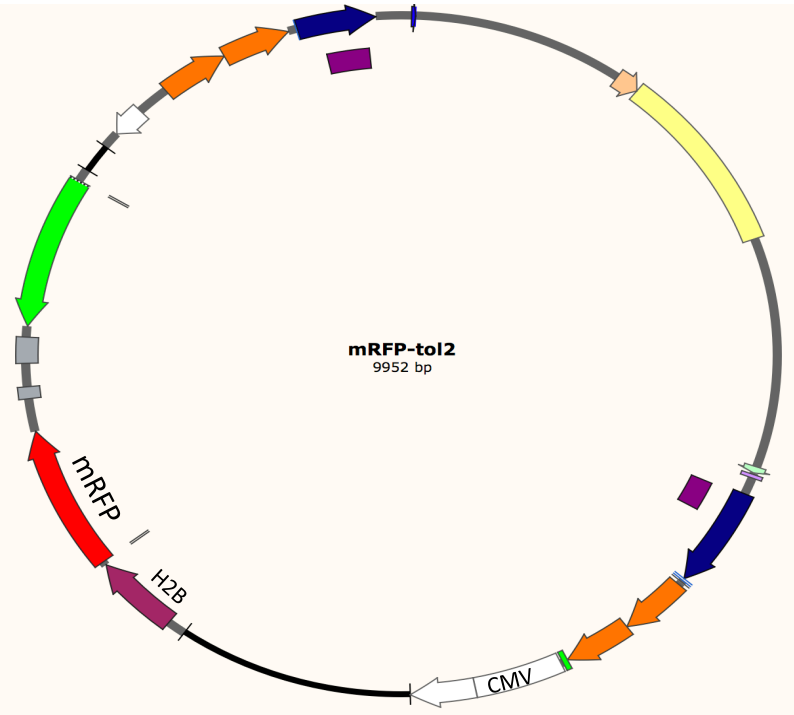

Figure 2.17. ***mRFP-tol2 vector construct****. The monomeric red fluorescent protein is shown in red. The promoter for RFP is CMV. The Tol-2 elements, such as the ITR are included as part of the system that allows for random integration and expression of the RFP. The transposase is not included.*

2.9.1 Electroporation of PGCs

Electroporation procedures for PGCs were carried out using the BTX Harvard ECM 830 Square Wave electroporator (BTX). The pellet of PGCs were obtained from wells with high confluency or clusters and resuspended in 250µl Opti-MEM™ followed by immediate addition of 5µg midiprep-DNA (HSPA2-OVA/HSPA2-OVM Gene drive: eSpCas9: mRFP-tol2 was 3:1:1) and immediate transfer to a 4mm electroporation cuvette for electroporation under conditions given in table 2.15. After electroporation the PGCs were transferred to a 6-well plate containing growth-inhibited CEFs. Cells were treated with RS-1 and SCR7. The cells were left to settle overnight. In certain instances, the HSPA2-OVA and HSPA2-OVM gene drives were linearized before electroporation. This simply involved the preparation of two 50µl reactions of a single digestion of 10µg of each of the gene drives using *PacI* as described previously. After overnight incubation at 37ºC and inactivation at 65ºC, the samples were purified using the Monarch® PCR and DNA Cleanup Kit (NEB) following the manufacturer's protocol before being used for electroporation.

Table 2.15. Electroporation conditions for PGCs performed with the BTX Harvard ECM 830 Square Wave electroporator.

Setting	Specification
Mode	LV
Voltage	240V
Pulse length	10ms
Number of pulses	2
Pulse interval	1s

2.9.2 Lipofection of PGCs

Lipofection procedures were performed using the Lipofectamine 3000 (Invitrogen) according to the recommended protocol. The only difference was that here the PGCs that were pipetted off CEFS for transfection, were lipofected in suspension for a few hours before being transferred to a growth inhibited CEF feeder layer. The lipofection reactions were setup (table below 2.16) and the DNA lipid complexes allowed to form for 20 minutes before being added to PGCs. This procedure used 5µg midiprep-DNA (HSPA2-OVA/HSPA2-OVM Gene drive: eSpCas9: mRFP-tol2 was 3:1:1) diluted in 250µl Opti-MEM^{TM} and 10µl P3000 reagent for each pair of wells (two different lipofection conditions for each OVA and OVM). The PGCs were left to settle overnight.

Table 2.16. Contents of the DNA-lipid complex lipofection reactions for addition to PGCs.

Component	Volume Condition 1	Volume Condition 2
Opti-MEM^{TM} Medium	125µl	125µl
Lipofectamine^{TM} 3000 Reagent	3.75µl	7.5µl
DNA constructs diluted in Opti-MEM^{TM} and P3000 Reagent	125µl	125µl

2.9.3 Puromycin selection of transfected PGCs

The PGCS co-transfected with the HSPA2-OVA gene drive containing Puromycin resistance were treated with Puromycin for selection. This was performed by supplementing the media in wells with 1.75µg/ml Puromycin for 2 days and decreasing to 1.5µg/ml for 2 days after. The cells were allowed to recover briefly before screening.

2.9.4 Neomycin selection of transfected PGCs

The PGCs co-transfected with the HSPA2-OVM gene drive containing Neomycin resistance were treated with Neomycin for selection. This was performed by supplementing the media in wells with 500µg/ml Neomycin for 2 days then 400µg/ml for 2 days. The cells were allowed to recover briefly before screening.

2.9.5 Screening transfected PGCs

To assess for activity of constructs in the transfected PGCs, their gDNA was extracted for performing different PCRs on the target loci. Again, the PGCs were lifted off CEFs by pipetting. gDNA was extracted from cells following the Monarch® gDNA extraction kit (NEB). The primers chosen (Table 2.17 and table 2.20) screen for HDR integration and NHEJ. For HDR the primer pairs amplify over the integrated gene drive, across the homology arms and into the genome at both the 5' and 3' ends (see figure 2.18). All PCR were performed using the Platinum™ SuperFi II DNA Polymerase (ThermoFisher; 12361010). The PCR setup and cycling conditions are shown in Table 2.18, Table 2.19, and Table 2.21. PCR was also setup for detection of various constructs used in transfected PGCs (table 2.22). Available primers were chosen to amplify Puromycin (of the HSPA2-OVA gene drive); Neomycin (of the HSPA2-OVM gene drive); part of the pUc57-brick backbone (of both the HSPA2-OVA and HSPA2-OVM gene drives); and part of the eSpCas9-tol2 construct backbone.

Table 2.17. Primer pairs for 3' and 5' HDR integration assessment. The PCR product is shown along with the annealing temperature. Annealing temperatures were obtained using the online Thermofisher Tm calculator.

Primer	Sequence (5'→3')	Annealing temperature (ºC)	Amplicon size (bp)
OVA 5' HDR Fwd	ACCTGCGTGATACCCCCTAT	60	3447
CDS rev	CCTTGGGATTCCATTGACT		
Puro int fwd OVA	GCAAGAACTCTTCCTCACGC	64	2504
3' HDR Rev	CCTCTGTGTGCTGCTCCTAC		
OVM 5' HDR Fwd	TCCCCTCGAAGGAAACCCATA	60	2255
CDS Rev	CCTTGGGATTCCATTGACT		
Neo int Fwd	ACGTTGTCACTGAAGCGG	63	2585
OVM 3' HDR Rev	ACTGCTTCATCCATCTGCCC		

Table 2.18. Platinum SuperFi II DNA Polymerase PCR setup for screening editing in PGCs. The relevant primers for amplifying either HDR- or NHEJ-specific amplicons can be added to the reactions as shown here.

Component	Volume (µl)
5X SuperFi^{TM} II Buffer	4
Forward Primer	0.5µM final concentration
Reverse Primer	0.5µM final concentration
10mM dNTPs	0.4
gDNA template	5-100ng
Platinum SuperFi II DNA Polymerase	0.4
5% DMSO	1
Distilled water	Up to a total of 20

Table 2.19. Cycling conditions for amplification of 3' and 5' HDR integration amplicons. **The annealing temperatures were obtained based on melting temperatures of primers, and the extension time based on 30s/kb extension ability of the Polymerase. **The OVA 5' HDR and OVA 3' HDR annealing temperatures were 60 ºC and 64 ºC respectively. The OVM 5' HDR and OVM 3' HDR annealing temperatures were 60 ºC and 63 ºC respectively.

Cycles	Temperature(ºC)	Time
1	98	30 seconds
30	98	10 seconds
	**	10 seconds
	72	30s/Kb*
1	72	5 minutes
1	4	hold

Table 2.20. Primer pairs for NHEJ assessment. The PCR product is shown along with the annealing temperature. The annealing temperature was obtained using the online Thermofisher Tm calculator.

Primer	Sequence (5'→3')	Annealing temperature (ºC)	Amplicon size (bp)
OVA NHEJ Fwd	AAGGGTGAAGTACCTGCGTG	65	1826
OVA NHEJ Rev	CAAGGTCTGTCCCATCACCC		
OVM NHEJ Fwd	GTGAAACCGCCAAGAAACCC	65	623
OVM NHEJ Rev	CAGAGTGCGAGATGAACCGA		

Table 2.21. Cycling conditions for amplification of NHEJ amplicons. The annealing temperature was obtained via the online Thermofisher Tm calculator and the extension time based on 30s/kb extension ability of the Polymerase. For the OVA NHEJ product the extension time was 55 seconds and for OVM NHEJ it was 19 seconds.

Cycles	Temperature(ºC)	Time
1	98	30 seconds
30	98	10 seconds
	57	10 seconds
	72	30s/Kb*
1	72	5 minutes
1	4	hold

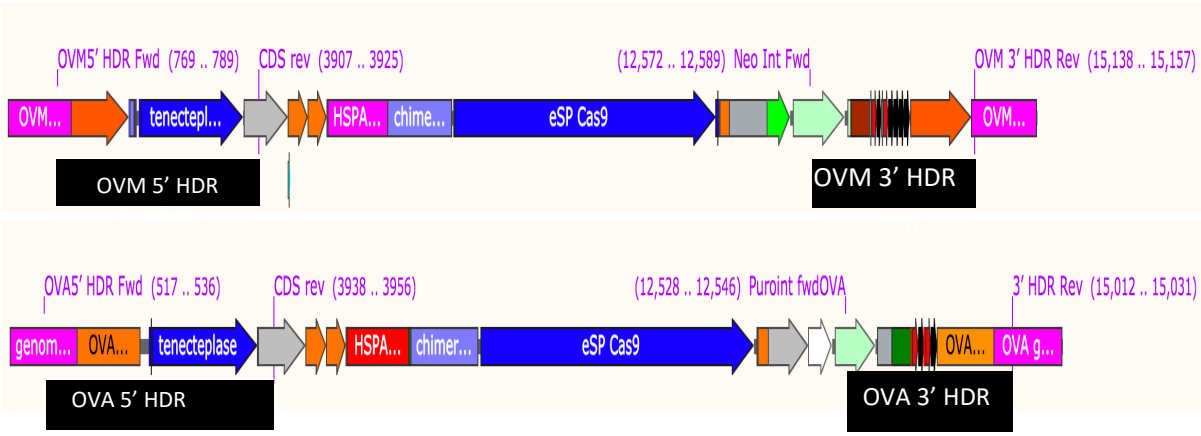

Figure 2.18. The HDR PCR product positions at the OVA and OVM loci. *The 5' HDR integration PCR products and the 3' HDR integration PCR products are shown in black, along with the relevant primers labelled in purple. The genomic OVA (top) or OVM (bottom) DNA flanking the insertion on either end is shown in pink. Diagram created in SnapGene.*

Table 2.22. Primers for detecting constructs in transfected PGCs. Primers detected backbone in gene drives and eSpCas9, as well as Puromycin and Neomycin in gene drives.

Primer	Sequence (5'→3')	Annealing temperature (°C)	Amplicon size (bp)
eSpCas9 backbone forward	GCTATGTGGCGCGGTATTAT	60	2480
eSpCas9 backbone reverse	TCGCAGCGACTCCCG		
OVA/M gene drive backbone forward	ACCTCTGACACATG	60	385
OVA/M gene drive backbone reverse	TTCGAGCTCGGTAC		
OVA Puromycin forward	AAGTGCACACAATAGAGGCTCTGAGGCGGAAAGAACCAG	60	1289
OVA Puromycin reverse	TCGGCAGTGCCTGAAGGAGCTCCCCAGCATGCCTGCTATTC		
OVM Neomycin forward	AAGTGCACACAATAGAGGCTCTGAGGCGGAAAGAACCAG	60	1359
OVM Neomycin reverse	TCGGCAGTGCCTGAAGGAGCTCCCCAGCATGCCTGCTATTC		

2.9.6 Repopulation of PGCs in sterilised embryos

The transfer of donor PGCs into embryos was preceded by busulfan ablation (1.5µg/µl) as described previously. To trace the donor PGCs in recipient embryos, 1µg of mRFP-tol2 vector (figure 2.17) was used in electroporation of these PGCs prior to injection. The PGCs were lifted by pipetting off a CEF feeder layer and electroporated as described in section 2.9.1. The transfected PGCs were viewed for red fluorescence using the FLoid^{TM} Cell Imaging Station. After verification that PGCs took up the tracer plasmid, they were lifted by pipetting and centrifuged at 400 x g for 4 minutes and resuspended in 1X PBS. The recipient ~HH16-17 embryos were wiped with 70% ethanol and had a small hole made in the shell of the side of the egg. A small volume of blood (1-3µl) was drawn for sexing by PCR as described previously. Using a mouth pipette and pulled glass needle 1000 cells in 50µl PBS were injected into blood vessels of male recipients (dorsal aorta, sinus terminalis and vitelline veins). The embryos were sealed with parafilm and allowed to incubate until day ~6 where PGCs have already begun populating the gonads. After incubation, live embryos and any developmental delays or death were recorded. The live embryos showing no deformities were dissected out from the eggs and all tissue except the gonads, kidney and back-torso dissected away with forceps as described previously. The samples were viewed for presence of red fluorescence within the gonads using the Zeiss Axio Imager 2.

Section 3: Results

3.1 Preparation of the OVA and OVM gene drives

Adjustments made to the OVA and OVM gene drives required amplification of regions from various source templates. Cloning was the major method employed to modify the Zeocin antibiotic resistance regions, the general CBh promoters controlling expression of eSpCas9, the OVM homology arms, and the OVM gRNA cassette.

3.1.1 Successful amplification of Puromycin antibiotic resistance sequence

For modifying the OVA gene drive, already containing OVA homology arms, the Puromycin (with its PolyA tail), SV40 promoter and 3'UTR were prepared by PCR, for replacement of Zeocin antibiotic resistance region. The individually amplified fragments have regions of homology between adjacent fragments appended onto their ends. Overlap extension PCR assembled these three fragments prior to NEBuilder HiFi DNA assembly with the gene drive. These three products, before and after their joining, are shown in agarose gels in figure 3.1 and figure 3.2 respectively.

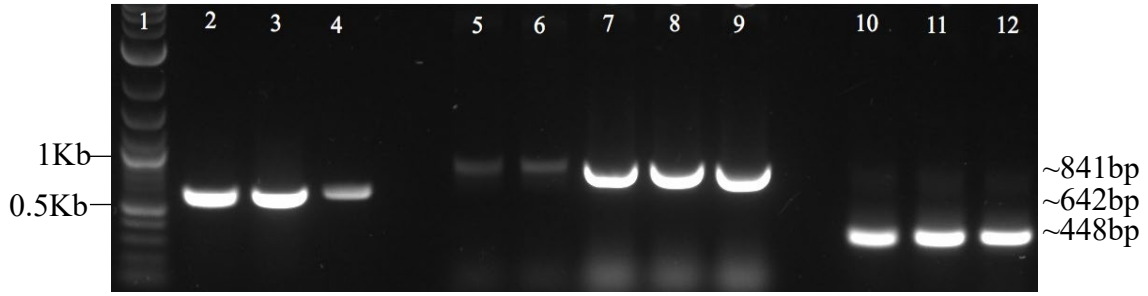

Figure 3.1. ***PCR amplification of fragments used for antibiotic DNA assembly in the OVA gene drive.*** *PCR products were run on a 1% agarose gel stained with ethidium bromide. Lanes 2-4: 3'UTR at ~642bp. Lanes 5-9: the ~841bp Puromycin fragment. The SV40 promoter fragment in lane 10-12, at ~448 bp. Lane 1: NEB 1Kb Plus DNA ladder for size validation. Image captured via GelDoc (Bio-Rad).*

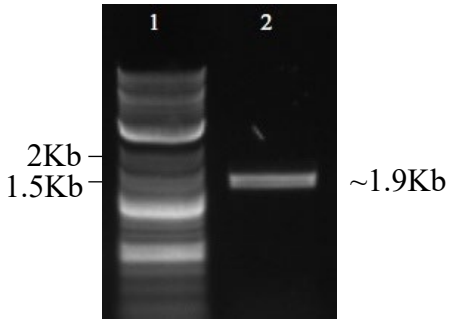

Figure 3.2. ***Overlap extension PCR amplification of assembled 3'UTR-SV40-Puromycin fragment.*** *PCR products of 3' UTR, SV40 promoter, and Puromycin were assembled in this order by exploiting the overlapping regions of adjacent fragments in PCR. This fully assembled DNA product is shown in lane 2 at ~1.9Kb, next to the NEB 1Kb Plus DNA ladder in lane 1. The 1% agarose gel was stained with Ethidium Bromide. Image captured via GelDoc (Bio-Rad).*

The OVA gene drive itself was then prepared for replacement of the Zeocin coding region, part of the associated IRES, as well as the downstream 3'UTR via restriction enzyme digestion (figure 3.3) followed by gel extraction for downstream DNA assembly as explained in section 2. The IRES was no longer needed since expression of new Puromycin antibiotic would be controlled by the eukaryotic SV40 promoter, and no longer fall under the same promoter as eSpCas9.

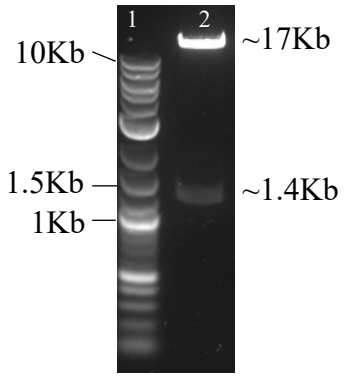

Figure 3.3. ***Preparation of the OVA gene drive for replacement of antibiotic by double restriction digestion.*** *The region for replacement in the gene drive was removed by restriction enzyme digestion with AvrII and NotI-HF and is shown at 1428bp in lane 2. The remaining linearized gene drive fragment was purified by gel extracting the upper gene drive band (~17Kb) in lane 2 with a gel extraction kit. Lane 1 indicates a Molecular weight marker known as the NEB 1Kb Plus DNA ladder. The gel was a 1% agarose gel stained with Ethidium Bromide. Image captured via GelDoc (Bio-Rad).*

3.1.2 Molecular cloning: insertion of Puromycin into OVA gene drive via NEBuilder HiFi DNA Assembly

For assembly of the insertion template (3' UTR-SV40-Puromycin) into linearized OVA gene drive, the NEBuilder HiFi assembly kit was used as previously described (section 2). This

method was possible because this template contained sequences on its ends that were complementary to the flanking sequence in the gene drive. Once the assembly reaction was used in bacterial transformation the plasmid extract was screened for successful assembly via double restriction enzyme digestion with enzymes that flank the insert as well as fall within the Puromycin coding sequence. As expected, the distinct banding patterns between OVA gene drive containing versus OVA gene drive lacking insert was observed. The anticipated digestions can be seen in figure 3.4 and verified successful DNA assembly. There appeared to be undigested gene drive sample, which runs as the largest band size. This partial digestion was likely due to short incubation time employed for a check digestion of a large construct. Due to the necessity of sequence accuracy in gene drive constructs, and to ensure no mutations had arisen during PCR or assembly and cloning that would alter the function of the sequence, this newly adjusted region in the OVA gene drive was also sequenced (Inqaba Biotec^{TM}) and aligned using the Multiple Sequence Comparison by Log-Expectation (MUSCLE) software in MEGA X version 10.1.8 (see Supplementary figure 2).

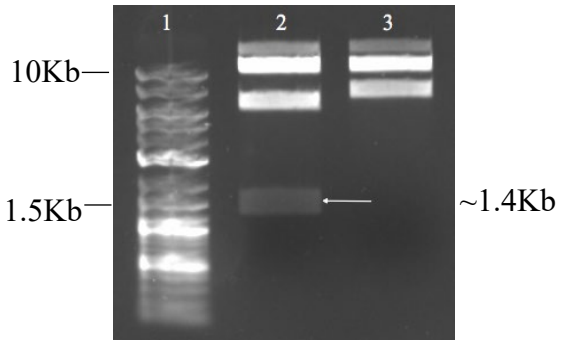

Figure 3.4. ***Restriction enzyme digestions verifying insertion of assembled Puromycin into the OVA gene drive.*** *The plasmid prep containing 3' UTR-SV40-Puromycin (lane 2), and the unadjusted OVA gene drive containing Zeocin (lane 3), were digested using BsteII-HF and XhoI. Lane 2: The top band (~18 Kb) is undigested gene drive, the second band below is a fragment of digestion at the expected ~10.9 Kb band, the third band below that falls at the expected 6Kb. The band indicated by the white arrow in lane 2, which falls at ~1.4Kb represents the digested fragment that comes about because of a BsteII-HF recognition site within the puromycin fragment itself. This band is absent in the Zeocin-containing gene drive in lane 3, which acts as a negative control. Lane 3: the top band (~18 Kb) is undigested gene drive and the second band below is the expected ~10.9 Kb band as in lane 2; the third band differs to the adjusted OVA gene drive and appears instead as one larger band at 7.5Kb and not two smaller bands as in lane 2. The 1% agarose gel was stained with Ethidium Bromide. Image captured via GelDoc (Bio-Rad).*

3.1.3 Successful Amplification and cloning of the Mouse *HSPA2* promoter into the OVA gene drive

The CBh promoter driving eSpCas9 expression in the gene drives needed replacement with the experimentally validated meiosis-specific *HSPA2* promoter. The nature of modifying this region in the gene drive by cloning with restriction digestion and ligation, required the *HSPA2* promoter fragment to be amplified with restriction sites appended onto their ends. The PCR amplification from mouse gDNA was performed as described in section 2 with primers appending the restriction sites (*SpeI-HF* and *XhoI)* onto the fragment. The expected PCR product was confirmed by agarose gel (figure 3.5). The PCR product was cloned into the pMiniT 2.0 *E. coli* plasmid cloning vector as discussed previously in order to plasmid extract and sequence verify the insert as well as grow up large amounts for subsequent cloning into the gene drives. Universal sequencing primers (T7 and SP6) found in the plasmid flanking the insert for sequencing were used to generate reads which were analysed using MUSCLE as before. The sequence was deemed sufficient for downstream application (see Supplementary figure 1).

For replacement of the CBh promoter in the OVA gene drive with the *HSPA2* promoter, restriction digestions with *SpeI-HF* and *XhoI* of both the pMiniT vector containing *HSPA2* and the OVA gene drive were performed. Gel extractions of digested fragments were ligated as previously discussed in chapter 2 (figure 3.5). Once the ligation was used in bacterial transformation the plasmid extract was double restriction enzyme digested with the same enzymes for verifying insert. This revealed multiple clones of OVA gene drive with *HSPA2* promoter inserted (see agarose gel in figure 3.6). Once again, the gene drive was sequenced with primers flanking the insert which ruled out the presence of mutations. Sequencing results were analysed as described above (see supplementary figure 3). The sequence similarity was deemed sufficient thereby concluding the modifications to the OVA gene drive. This generated the final version of the HSPA2-OVA gene drive to be used in transfection procedures.

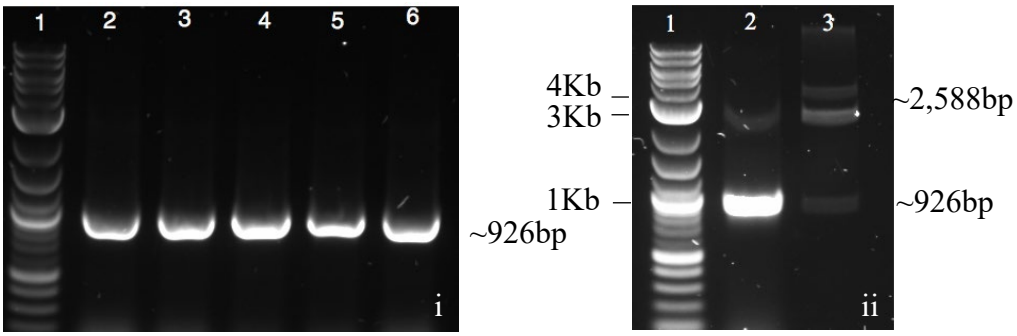

Figure 3.5. ***PCR amplification and restriction digestion of the mouse HSPA2 promoter.*** *The Mouse HSPA2 Promoter fragment was amplified and cloned into the pMiniT 2.0 vector, and the insert verified by colony PCR* ***(i)*** and *double restriction digest with SpeI-HF and XhoI* ***(ii)****.* ***i)****Lanes 2-6: colonies positive for HSPA2 insert.* ***ii)*** *Lane 2: shows a bright band representing the HSPA2 PCR amplicon at ~926bp. Lane 3 shows digestion of the insert (~926bp band) out the linearized pMiniT vector (~2,588bp). The band at ~3-4Kb in lane 3 represents undigested pMiniT with HSPA2 insert. The NEB 1Kb Plus DNA ladder was run in lane 1 on both gels. The gels were 1% agarose stained with ethidium bromide. Image captured via GelDoc (Bio-Rad).*

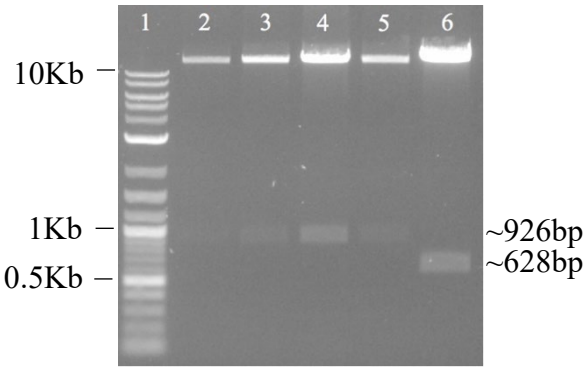

Figure 3.6. ***Double restriction digestion of OVA gene drive verifying HSPA2 insert.*** *Four different clones were digested with SpeI-HF and XhoI verifying replacement of CBh with HSPA2. The unmodified linearized OVA gene drive containing CBh, digested with the same enzymes, was run alongside samples in lane 6 (~628bp) as a control for size comparison of the modified region. Of the four digested clones in lanes 2-5, lanes 3-5 show the HSPA2 band digested out the OVA gene drive. The lane 4 clone's HSPA2 band appears more clearly at ~926 bp than the faint lanes 3 and 5. In lanes 2-5 the linearized gene drive bands appear above the ladder at ~17.8Kb and at ~18.1Kb in lane 6. The standard molecular weight marker was the NEB 1Kb Plus DNA ladder in lane 1. A 1% agarose gel stained with Ethidium Bromide was employed. Image captured via GelDoc (Bio-Rad).*

3.1.4 Constructing the OVM gene drive: replacement of the gRNA cassette via cloning

The gRNA cassette in the OVM gene drive (lacking homology arms) was replaced with an OVM-specific gRNA cassette, meaning OVA and OVT gRNAs were no longer part of the cassette. This new OVM-specific gRNA cassette (together with the upstream U6.3 Promoter) and the OVA gene drive to be modified were isolated by double restriction digestion with the same pair of restriction enzymes. The isolated linearized OVM gene drive lacking old gRNA

cassette and the new OVM gRNA cassette were verified by agarose gel (figure 3.7) and gel extracted for subsequent ligation and transformation of *E. coli* as described previously in section 2. The plasmid extracts upon restriction enzyme digestion show verification of new OVM gRNA insert in the OVM gene drive as the anticipated banding pattern and sizes on the agarose gel was observed (figure 3.7). Once again, the gene drive was Sanger sequenced to rule out the presence of mutations in the cassette (Genscript). The sequence similarity was sufficient for continuation with downstream cloning (refer to Supplementary figure 4).

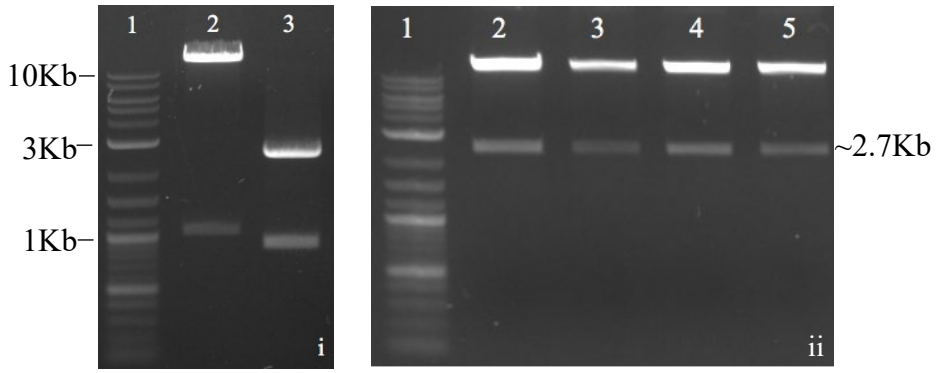

Figure 3.7. ***Restriction digests confirming cloning the new OVM gRNA cassette into the OVM gene drive. i)*** *The OVM gene drive and new OVM gRNA cassette digested with NotI-HF and BsteII-HF. Lane 2: the upper linearized OVM gene drive band appears at ~17.3Kb, and the lower ~1071 bp band represents the old OVM gRNA cassette. The new OVM gRNA cassette attached to the U6.3 promoter is the lower band at ~925 bp in lane 3, and the upper band represents the linearized pUc57 backbone at ~2.7Kb.* ***ii)*** *lanes2-5: Four clones exhibited the anticipated 2.7Kb band which is a region of DNA containing new OVM gRNA cassette, when digested with AvrII and BsteII-HF. The NEB 1Kb Plus DNA ladder was run in lanes 1 on both gels. Gels were 1% agarose stained with Ethidium Bromide. Image captured via GelDoc (Bio-Rad).*

3.1.5 Successful amplification of Neomycin antibiotic resistance gene

The next step in modification of the OVM gene drive, similarly to OVA, was to prepare the fragments of DNA and gene drive for assembly that would replace the Zeocin antibiotic resistance region. Here however the Neomycin antibiotic resistance gene was assembled into the OVM gene drive. The Neomycin (already attached to its *SV40* promoter and PolyA-tail) PCR-amplified product and the 3' UTR PCR amplified product were assembled by overlap extension PCR and purified by gel extraction as previously discussed in section 2. These two fragments, before and after their joining, are shown in the agarose gels in figure 3.8. When it was confirmed the fragments were of correct sizes, they could be purified by gel extraction for use in DNA assembly. The gel extracted DNA was quantified and analysed by Nanodrop spectrophotometer.

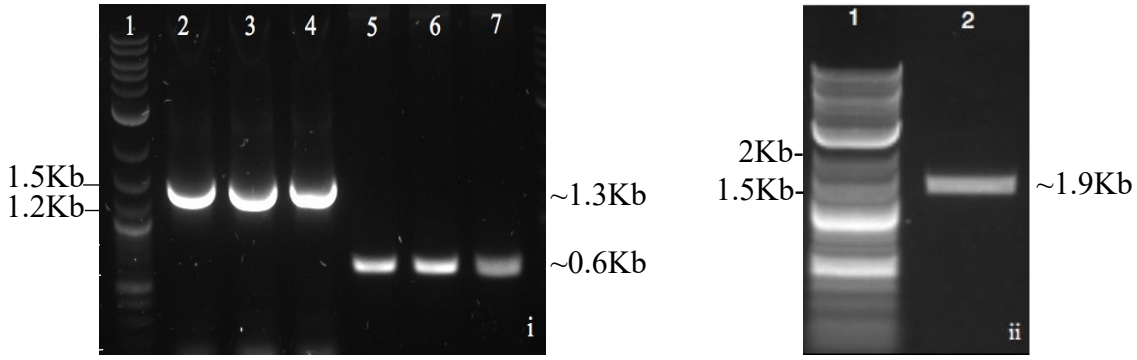

Figure 3.8. ***PCR amplification of fragments for antibiotic DNA assembly of OVM gene drive.*** *PCR products were resolved on 1% agarose gels stained with ethidium bromide.* ***i)*** *Lanes 2-4: Neomycin fragment (with its SV40 promoter and PolyA tail) shown at ~1359bp. Lanes 5-7: the 3'UTR amplicon at 642bp.* ***ii)*** *Lane 2: Overlap extension PCR product of joined 3' UTR and Neomycin shown at ~1.9Kb. PCR products were run alongside standard 1Kb Plus DNA ladder (NEB) in lanes 1 for size validation.*

As with OVA, the OVM gene drive was prepared by removing Zeocin, part of the associated IRES, as well as the downstream 3'UTR via restriction enzyme digestion. This digestion was verified on an agarose gel in figure 3.9. The linearized gene drive fragment was gel extracted for downstream DNA assembly.

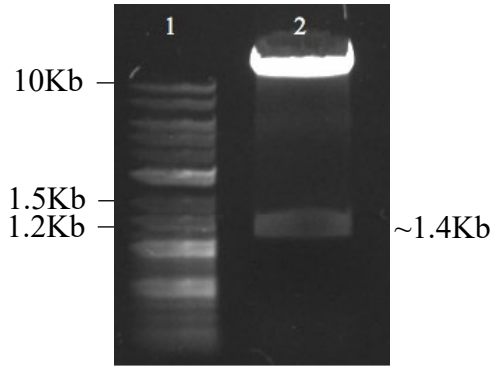

Figure 3.9. ***Preparing the OVM gene drive for replacement of antibiotic by double restriction digestion.*** *The OVM gene drive was digested with AvrII and NotI-HF to remove Zeocin, the 3' UTR and part of the IRES. The removed region is seen at ~1428bp in lane 2. The remaining linearized gene drive fragment was purified by gel extracting the top gene drive band (>10Kb) in lane 2. Lane 1: the NEB 1Kb Plus DNA ladder. The gel was a 1% agarose gel stained with Ethidium Bromide. Image captured via GelDoc (Bio-Rad).*

3.1.6 Molecular cloning: insertion of Neomycin into gene drive with NEBuilder HiFi DNA Assembly

The newly joined antibiotic (3' UTR-Neomycin) fragment and linearized OVM gene drive were assembled using the NEBuilder HiFi DNA assembly kit as previously described (section 2). The triple restriction enzyme digestion of multiple clones of plasmid extraction of the assembled construct confirmed successful DNA assembly. The restriction enzymes employed

flanked the antibiotic region of interest as well as the downstream gRNA cassette confirming the latter's presence too. The digestion produced a cut within the new Neomycin insert and upstream and downstream of this site. In the OVM gene drive containing Zeocin (the negative control), the very same enzyme (*AvrII*) would not produce a cut within Neomycin but rather within the IRES. Hence the digests produced 3 fragments in both cases but of different sizes. The anticipated banding pattern and sizes were observed via agarose gel electrophoresis (figure 3.10). When digested with identical enzymes, the distinct difference in banding sizes between OVM gene drive containing new Neomycin insert and new OVM gRNA cassette and the OVM gene drive still containing Zeocin and old gRNA cassette were visible. This confirmed successful DNA assembly. Sequencing of the assembled region (Genscript), ensured no mutations were acquired during amplification, assembly or cloning. The sequence data was aligned using the MUSCLE in MEGA and the sequence similarity was verified for further modification of a clone (see Supplementary figure 4).

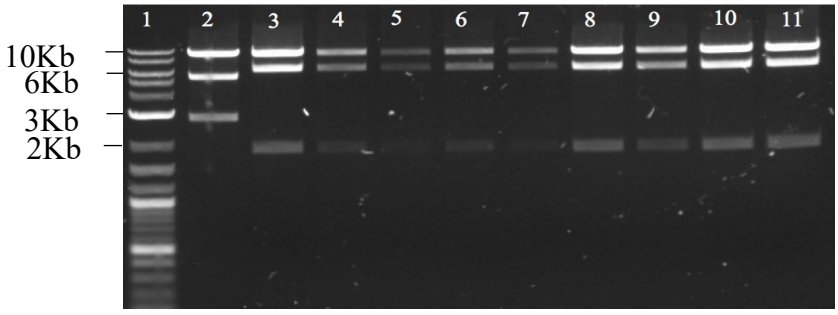

Figure 3.10. ***Restriction enzyme digest verifying DNA assembly of Neomycin into the OVM gene drive.*** *Nine different plasmid-extracted clones showed the 3'UTR-Neomycin insert assembled into the gene drive when digested with BsteII-HF, XhoI and AvrII (lanes 3-11). Lane 2: digested OVM gene drive containing Zeocin and old gRNA cassette. Lanes 2-11: the larger band on top (~9.1Kb) represents the linearized gene drive; the middle band represents the region digested between XhoI and AvrII and the lower smallest band represents the fragment digested between AvrII and BsteII-HF. The middle band is larger (~6.3Kb) in lanes 3-11 compared to lane 2 (~5,3Kb), due to the AvrII restriction site occurring further downstream from XhoI following DNA assembly with Neomycin. The lowest band contains the region with new OVM gRNA cassette and there is a visible size difference between lanes 2 containing the old cassette (~2.6Kb) and lanes 3-11 (~1.8Kb). A 1% agarose gel stained with Ethidium Bromide was employed. Image captured via GelDoc (Bio-Rad).*

3.1.7 Cloning: insertion of *HSPA2* promoter into the OVM gene drive

Following the adjustment of antibiotic resistance, the CBh promoter in the OVM gene drive was replaced with *HSPA2* promoter. The OVM gene drive (figure 3.11) and pMiniT (figure 3.5) were subjected to double restriction enzyme digestion with *SpeI-HF* and *XhoI* for ligation of gel extracted promoter and linearized gene drive. The *HSPA2* promoter insert was confirmed

via restriction digestion of the resulting plasmid extracts. The anticipated banding patterns and sizes produced by digestion were observed on agarose gel verifying successful ligation (figure 3.11). The sequencing of gene drive containing insert with primers flanking the insert ruled out the presence of mutations. The sequence similarity was sufficient for using a single clone in further modifications (see Supplementary figure 5).

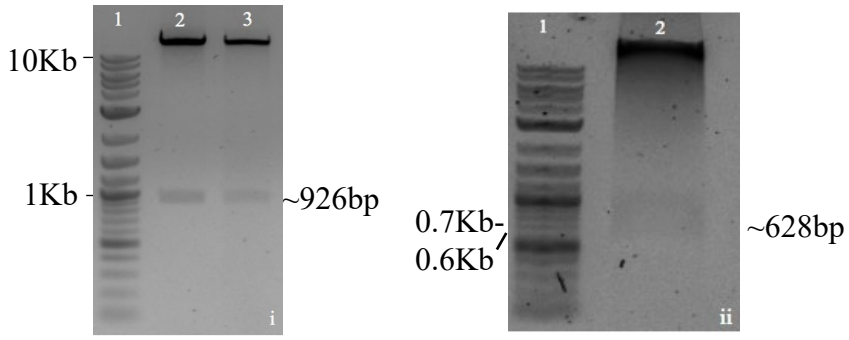

Figure 3.11. ***Double restriction digestion of OVM gene drive verifying HSPA2 insert. i)****Two different clones show HSPA2 inserted (~926bp band) into OVM gene drive (top band) when double digested with SpeI-HF and XhoI (lanes 2-3)* ***ii)*** *The OVM gene drive still containing CBh digested with SpeI-HF and XhoI. Lane 2: the linearized gene drive band at ~16Kb and the faint CBh promoter band at ~628 bp. The standard molecular weight marker for* ***i*** *and* ***ii*** *was the NEB 1Kb Plus DNA ladder run in lanes 1. A 1% agarose gel stained with Ethidium Bromide was employed. Image captured via GelDoc (Bio-Rad).*

3.1.8 Cloning of OVM 5' and OVM 3' Homology arms onto the OVM gene drive

The final modifications of the OVM gene drive were the addition of homology arms, essential components for directing HDR at the OVM locus. The HAs were cloned sequentially into the OVM gene drive. Restriction digests of the OVM gene drive and the pGEM-T Easy Vector (Promega) containing the 5' HA were performed using both *AsisI* and *NheI-HF*. The linearized gene drive and HA fragments were verified by agarose gels (figure 3.12) and purified by DNA cleanup kit and agarose gel extraction respectively, for ligation. Resulting plasmid extracts digested with *AsisI* and *NheI-HF* showed successful ligation as the anticipated banding pattern generated by digestions were observed via agarose gels (figure 3.12). A single clone with insert was used for addition of the next HA in the same manner but with the *BsteII-HF* and *PacI* restriction enzymes. Upon positive screening of both HAs via expected restriction digestions of plasmid extracts (figure 3.12) modification of the OVM gene drive was complete. This final OVM gene drive, with all modifications, used in transfections was hereafter known as the HSPA2-OVM gene drive.

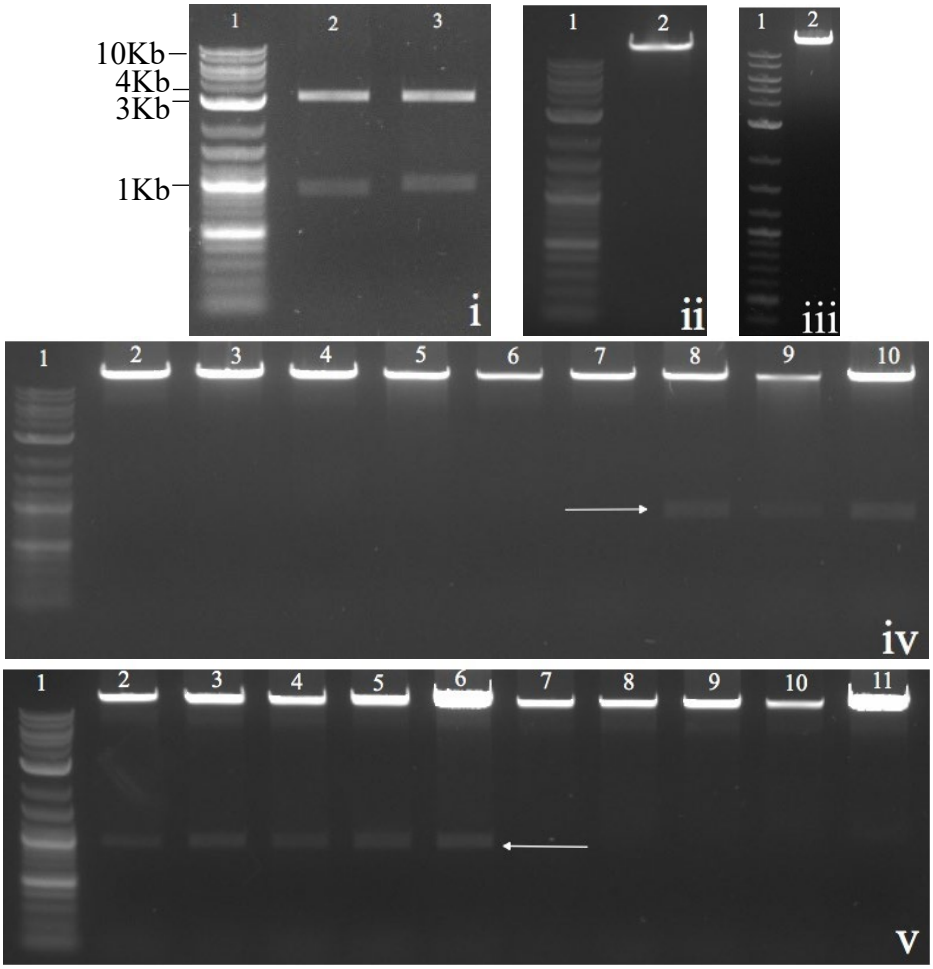

Figure 3.12. ***Restriction digests of gene drives and HAs for cloning of the OVM homology arms into the OVM gene drive. i)****The OVM 5' HA (lane 2 at 902bp) and OVM 3' HA (lane 3 at 952bp) were digested out separate pGEM-T Easy Vectors with AsisI and NheI-HF and BsteII-HF and PacI respectively. The linearized pGEM-T Easy Vectors are represented by the bands at ~3Kb.* ***ii)*** *The OVM gene drive digested with AsisI and NheI-HF produces a large linearized band >10Kb.* ***iii)*** *The OVM gene drive containing the 5'HA digested with BsteII-HF and PacI exhibits the expected single large linearized band (>10Kb).* ***iv)*** *Restriction digestion of the OVM gene drive verifying insertion of the 5' HA (902bp shown by white arrow) in clones in lanes 8-10. Lanes 2-7 detected no 5' HA insertion.* ***v)*** *Restriction digestion of the OVM gene drive (already containing the 5' HA) verifying insertion of the 3' HA (952bp shown by white arrow) in lanes 2-6; lanes 7-11 detected no 3' HA insertion. The NEB 1Kb Plus DNA ladder was run alongside samples in lanes* ***1*** *on all five gels (****i-iv****). Agarose gels were 1% stained with ethidium bromide. Image captured via GelDoc (Bio-Rad).*

3.2 Isolation and culture of primary PGCs

In the course of this project, *in vitro* culture of PGCs has been well developed. A culture system that closely mimics the natural environment in which PGCs find themselves in the embryo was established. Part of this involved employing a CEF feeder layer on which to cultivate the PGCs. The CEFs were extracted from day 10 embryos and maintained in appropriate CEF media as described previously, as well as frozen via cryogenic stocks for continuous replacement of CEF

feeder layers as required. One to two days following extraction, CEFs usually appeared highly confluent (see Supplementary figure 6) and were passaged for creating cryostocks by trypsin-based protocol discussed previously in section 2. In maintaining the CEF culture they were regularly observed and showed typical fibroblast morphology. As the number of passages of the CEFs increased, their growth declined, and they were discarded near passage 10. CEFs were also passaged upon reaching ~80% confluency, this could take anywhere from 2-7 days depending on number of passages the cells had already been through as well as seeding density. For use as a feeder layer, the CEFs were first growth inhibited with mitomycin-C, so the feeder layer would not proliferate and overrun the PGCs in co-culture but could still secrete necessary factors for maintaining undifferentiated PGCs. This was performed by seeding CEFs in a 6-well plate and allowing them to settle overnight. Upon confirming the CEFs were near optimal confluency for growth inhibition (~60-70%), they were incubated with mitomycin-C as discussed in section 2. The growth-inhibited CEFs tended to die off and lift from the plate after 5-7 days, hence they were replenished in co-culture with PGCs (see Supplementary figure 6 for CEF culture figures).

The primary culture of PGCs was established by sourcing PGCs from circulating blood. Isolating PGCs from the bloodstream was achieved by extracting whole blood from embryos. Male PGCs were pooled for cultivation on the same CEF feeder layer in PGC medium supplemented with hormone. Males were identified by PCR sexing using tissue from the head of each sample (n=100). The multiplex sexing PCR (detailed protocol in section 2) amplified the W chromosome specific *XhoI* amplicon in females, and the 18S control gene amplicon in both sexes. The PCR was verified by agarose gels, and an example representative sexing gel, distinguishing male from female samples, given in figure 3.13. The PGCs were maintained in PGC media supplemented with hormones and a gradual growth of PGCs and slow cluster formation over time was observed. The growth of PGCs was best with the support of a CEF feeder layer. The PGCs' identity was confirmed by visualisation of their morphological characteristics such as rounded shapes, and their growth as single cells and small clusters of PGCs in suspension atop the CEF feeder layer, which is characteristic of these cells. Clusters were not common (only small clusters began formation at ~14 days). Many PGCs grew as round single cells that were sometimes loosely attached to the CEF feeder layer and free-floating (figure 3.14). As expected, PGCs appeared to reflect more light under the microscope compared to the underlying CEFs. Additionally, immunocytochemistry was used as a means

of confirming PGC identity. This employed a PGC-specific cell surface marker SSEA-1. Figure 3.15 shows clusters and single PGCs cultured on CEFs, fluorescently stained when fixed, blocked and incubated with primary antibody anti-SSEA-1, and conjugated secondary antibody Rabbit Anti-Mouse IgG, and counterstained with DAPI (detailed protocol in section 2). PGCs positive for SSEA-1 showed green fluorescence when observed with the FLoid™ Cell Imaging Station. This confirmed the successful isolation and culture of PGCs *in vitro.*

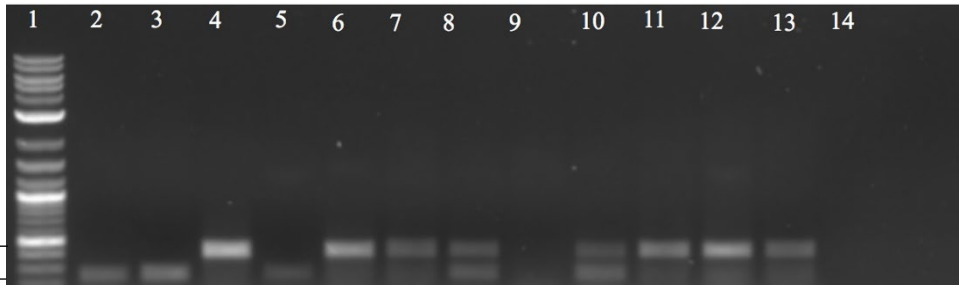

Figure 3.13. Direct PCR Sexing of chicken embryo samples used for PGC extraction. *A representative gel of sex determination in PGC source embryos. Using head tissue from each embryo sample, direct multiplex PCR was performed. The male samples display only the single 18S ribosomal gene amplicon at ~256 bp. Females display 2 bands- the XhoI amplicon at ~415 bp and the single 18S ribosomal gene amplicon. Lane 14 is the no-template control. The samples (lanes 2-13) were run alongside the NEB 1Kb Plus DNA ladder in lane 1. The 1% agarose gel was stained with Ethidium Bromide. Image captured via GelDoc (Bio-Rad).*

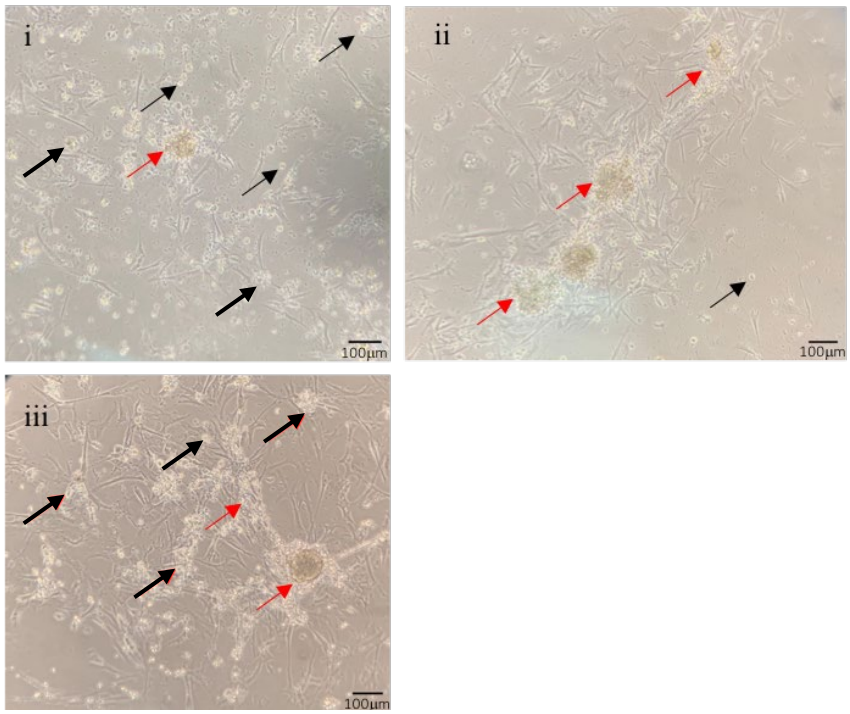

Figure 3.14. Culture of male primary chicken PGCs together with growth inhibited CEFs. *Blood-extracted PGCs were maintained in PGC media supplemented with hormones. Progression of PGCs over time in culture are shown. PGCs are round, some are unattached and some loosely adhere to the CEF cells. PGCs are distinguished by their rounded shape and*

bright illumination. Some of the clusters are indicated by red arrows and single cells by black arrows. ***i)*** *PGCs after 10 days in culture show small cluster formation and single cells are dominant.* ***ii)*** *PGCs after 2 weeks in culture with cluster formation; here the CEF feeder cells were nearing depletion at which point they would be replenished.* ***iii)*** *PGCs after 3 weeks in culture shows continued cluster presence and PGC growth. Scale bars=100μm.*

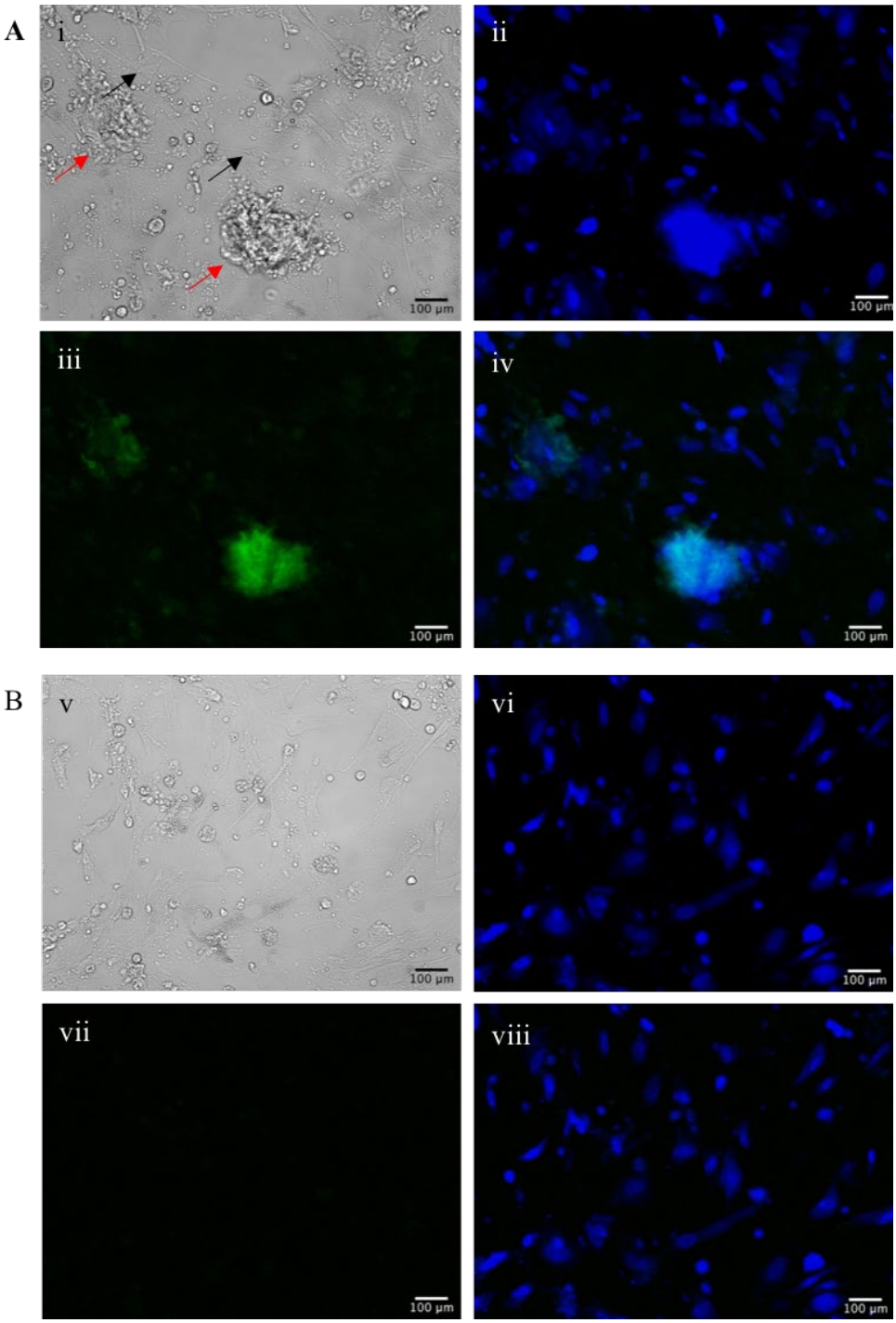

Figure 3.15*. Immunofluorescence staining of PGCs.** *PGCs on growth inhibited CEF feeder cells were fixed and immunostained with primary anti-SSEA-1, and nuclei counterstained with DAPI. SSEA-1 positive PGCs appear green due to the fluorescent conjugated secondary antibody employed.* ***A. i-v) *A cluster as well as singular PGCs on a CEF feeder layer after immunostaining.* ***i)*** *Cells viewed under white light. PGCs indicated by red arrows and CEF feeder cells indicated by black arrows. The CEF feeder layer in this region is not highly confluent and had begun dying off.* ***ii)*** *Cells viewed under blue light for DAPI visualisation.* ***iii)*** *Cells viewed under green light for antibody fluorescence visualisation of PGCs.* ***iv)*** *Merged images of DAPI blue light and FITC green light images.* ***B. v-viii)*** *Cells where SSEA-1 was omitted showed no green fluorescence under green light* ***(vii)****, blue light is shown* ***(vi)****, and merged blue and green* ***(viii)****. Scale bar=100µm. Images captured using the FLoid™ Cell Imaging Station.*

3.3 Determining optimal busulfan concentration for PGC depletion in embryos

The targeted ablation of endogenous germ cells in chicken embryos using busulfan has been previously demonstrated successfully (Song *et al.*, 2005; Nakamura *et al.*, 2008, 2009, 2010; Lee *et al.*, 2013). The aim here was to establish a technique of busulfan-based sterilisation in the lab. In order to do this, the optimal concentration of busulfan (one that has a high ablation efficiency yet is not lethal to embryos) was determined by performing ablation with three different concentrations of busulfan in sesame oil emulsions: 1.3µg/µl; 1.5µg/µl; and 1.7µg/µl. The injection occurred into yolk via the sharp end of stage X embryos. After ~7.5 days of incubation, the survival rate for the different groups was noted. Certain defects, which are known potential side effects of busulfan, such as abnormal development, were noted in 3 embryos that were part of the 1.7µg/µl treatment group (see images in Supplementary figure 7). There was no statistically significant association between busulfan dose and developmental defect occurrence (P=0.19).

Male embryos (confirmed by sexing PCR) with no delay in development or developmental defects were analysed for numbers of surviving PGCs and assessment of ablation efficiency. This was performed via fluorescence immunohistochemistry-based detection of PGC-specific marker SSEA-1 on gonadal tissue sections of the samples. Stained sections were viewed and captured via FLoid^{TM} Cell Imaging Station for analysis. When visually comparing the control and busulfan-treated groups, a decline in PGCs detected by immunostaining was seen as the busulfan concentration increased (figure 3.16). This relationship was quantified, and the efficiency of ablation was determined by counting PGCs on every second section over 20 sections per embryo sample. For each group (1.3µg/µl; 1.5µg/µl; and 1.7µg/µl busulfan) the average number of PGCs (n=5 embryo samples per group) was calculated and compared to the average number of PGCs of the counted control (n=5 embryo samples) as shown in figure 3.17. This gave an indication of PGC reduction. This shows a relationship between surviving PGCs and busulfan concentration. As busulfan concentration increased the individual sample counts and average number of PGCs decreased. The one-way ANOVA revealed a significant difference in PGCs when compared to the control group, and the Tukey's post-hoc test revealed which groups in particular showed significant PGC reduction. When compared to the control, all the busulfan groups showed a statistically significant difference in reduced numbers of PGCs (figure 3.17). The highest number of PGCs were detected in the untreated control (0µg/µl concentration) group. Of the treatment groups the highest number of PGCs were detected in

the 1.3μg/μl group however this was still a moderate reduction of approximately 49% compared to the control. The lowest number of PGCs was detected in the 1.7μg/μl group which was approximately 75% lower than the control group. There was still an impressive 70% reduction in number of PGCs in the 1.5μg/μl busulfan treatment group. The results of the Chi-square test showed that there was no statistical difference in the survival of embryos in the different dosages of busulfan emulsion treatment despite the observation of a trend in counted embryos surviving and sample size meeting minimum test requirements. The 1.3μg/μl busulfan treatment group exhibited the highest survival rate followed by the 1.5μg/μl treatment group and then 1.7μg/μl treatment group (figure 3.18).

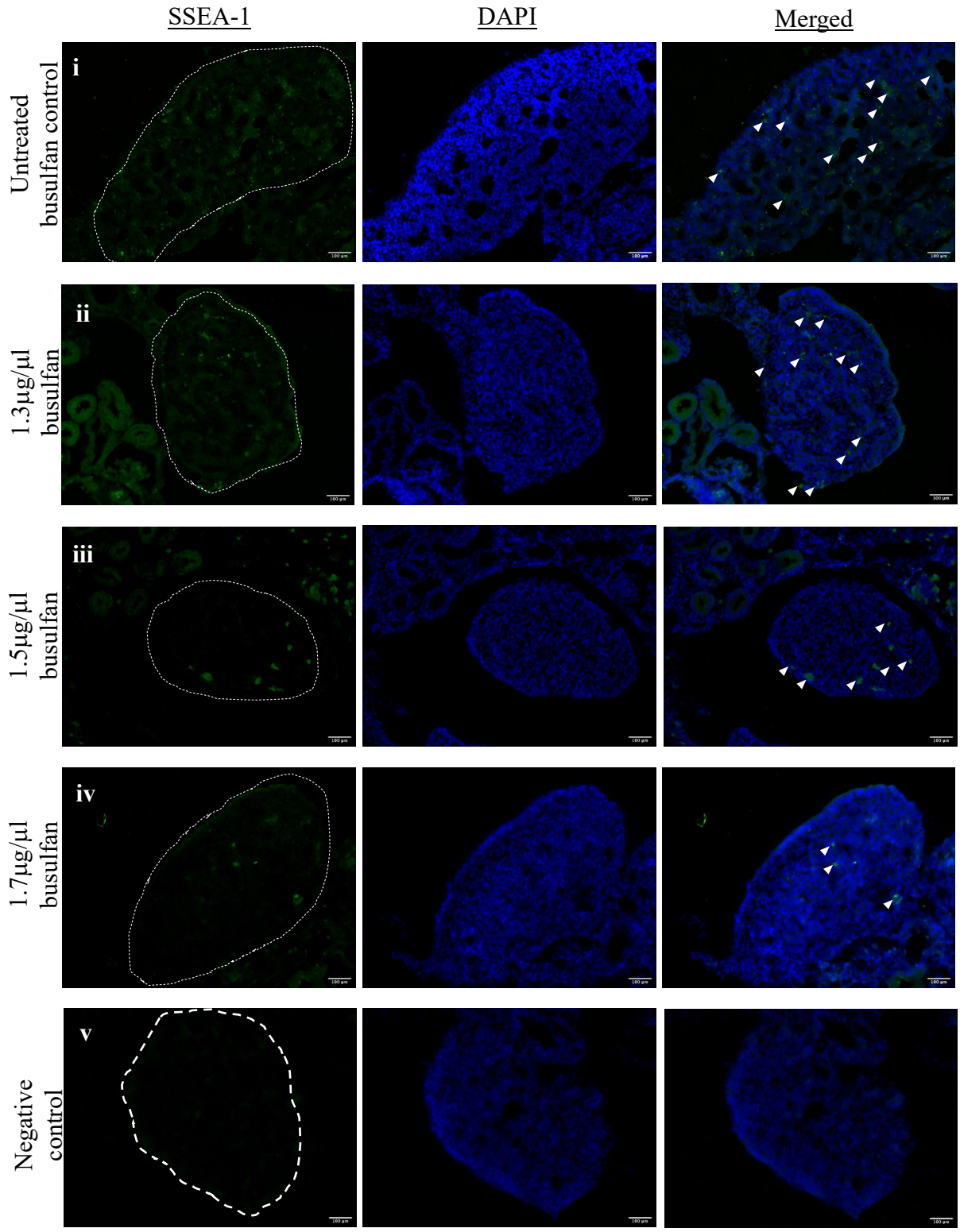

Figure 3.16. Immunohistochemistry using SSEA-1 for detection of PGCs in gonadal tissue sections of embryos treated with different busulfan concentrations. *A single representative gonad from each treatment group is shown. Gonads of embryos dissected at day 7.5 were sectioned (~10µm), fixed on slides and immunostained with primary SSEA-1 antibody and secondary conjugated FITC antibody (green stain), and nuclei counterstained with DAPI. Gonads are outlined in white dotted line and white arrows show SSEA-1 positive PGCs in the gonads.* ***i)*** *Untreated busulfan control.* ***ii)*** *Busulfan treatment 1.3*µg/µl. ***iii)*** *Busulfan treatment 1.5*µg/µl. ***iv)*** *Busulfan treatment 1.7*µg/µl. ***v)*** *Negative control: untreated busulfan control with*

SSEA-1 omitted. Scale bar=100μm. Images viewed and captured via the FLoid™ Cell Imaging Station.

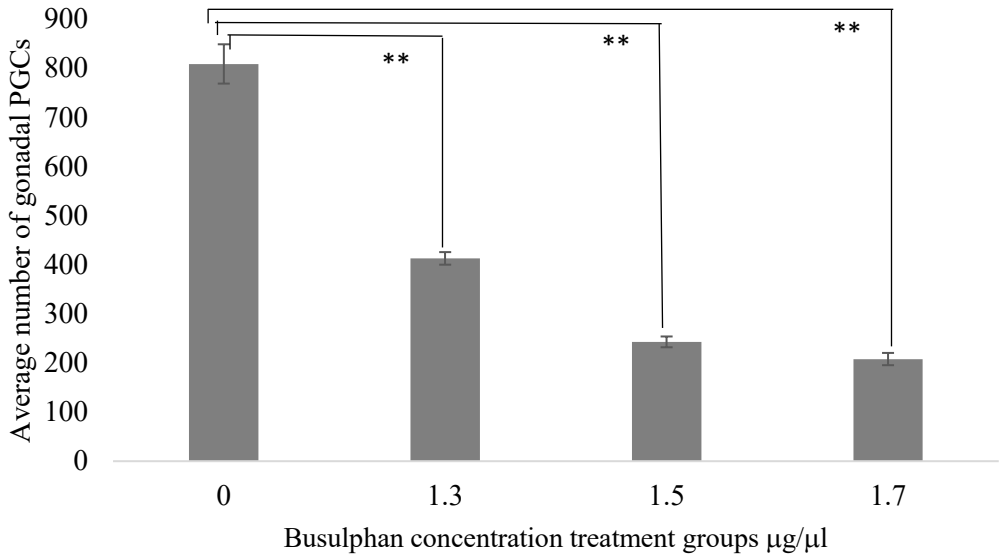

***Figure 3.17*. PGCs remaining in embryos after treatment with different busulfan concentrations.** *The PGCs detected, by SSEA-1 immunohistochemistry, in gonadal tissue sections were obtained over 20 sections per sample across 5 samples in each group. The average PGCs remaining after treatment is plotted for each group. Error bars represent standard error of the mean. The ANOVA between groups generated test statistics F=148.58 and P<0.01. **The post-hoc generated test statistics P<0.01 for all treatment groups compared to the control.*

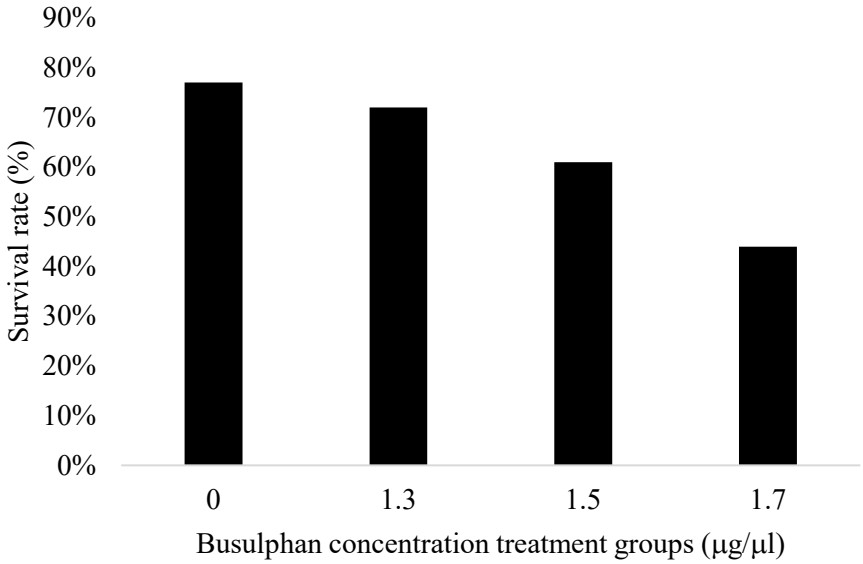

***Figure 3.18.* Survival rate of embryo groups treated with different busulfan concentrations.** *The survival is shown as the percentage of alive embryos at day 7.5 incubation following busulfan treatment. The Chi Square test generated P>0.05 for all treatment groups compared to the control.*

3.4 Determining Puromycin and Neomycin sensitivity of PGCs

In order to determine the minimum concentration for selection of PGCs, the cell viability was measured after treatment with a range of concentrations of Puromycin or Neomycin. The PGCs grown on a growth-inhibited CEF feeder layer, as well as an identical CEF feeder layer alone in parallel were maintained in PGC media supplemented with antibiotic for 5 days (Puromycin) and 7 days (Neomycin) after which a manual viable cell count was taken using trypan blue. Each concentration of the PGCs on CEFs and the CEFs only was performed in triplicate for obtaining averaged counts represented in the Puromycin kill curve in figure 3.19 and the Neomycin kill curve figure 3.20. The PGC curve alone, calculated by subtracting the average CEFs curve from the average PGCs on CEFS curve (at each concentration point), indicated the estimated concentration at which all PGCs were killed after treatment. For the Puromycin kill curve, this was 1.5µg/ml and for the Neomycin kill curve this was 400µg/ml. The ANOVA test performed on the Puromycin PGC kill curve indicated significant difference in number of viable cells between the treatment groups. To pinpoint where this difference lay, and specifically if the optimal concentration group was statistically significant, the Tukey's post-hoc test was performed. The test showed statistical significance in the cell viability at the 1.5µg/ml group (minimum concentration where PGCs killed off by end of treatment) as well as some others compared to the untreated control. The ANOVA performed on the Neomycin PGC kill curve indicated significant difference in number of viable cells between the treatment groups. Once again, the Tukey's post-hoc test was performed which revealed statistical significance at the optimal selection concentration of 400µg/ml (minimum concentration where PGCs killed off by end of treatment) when compared to the control.

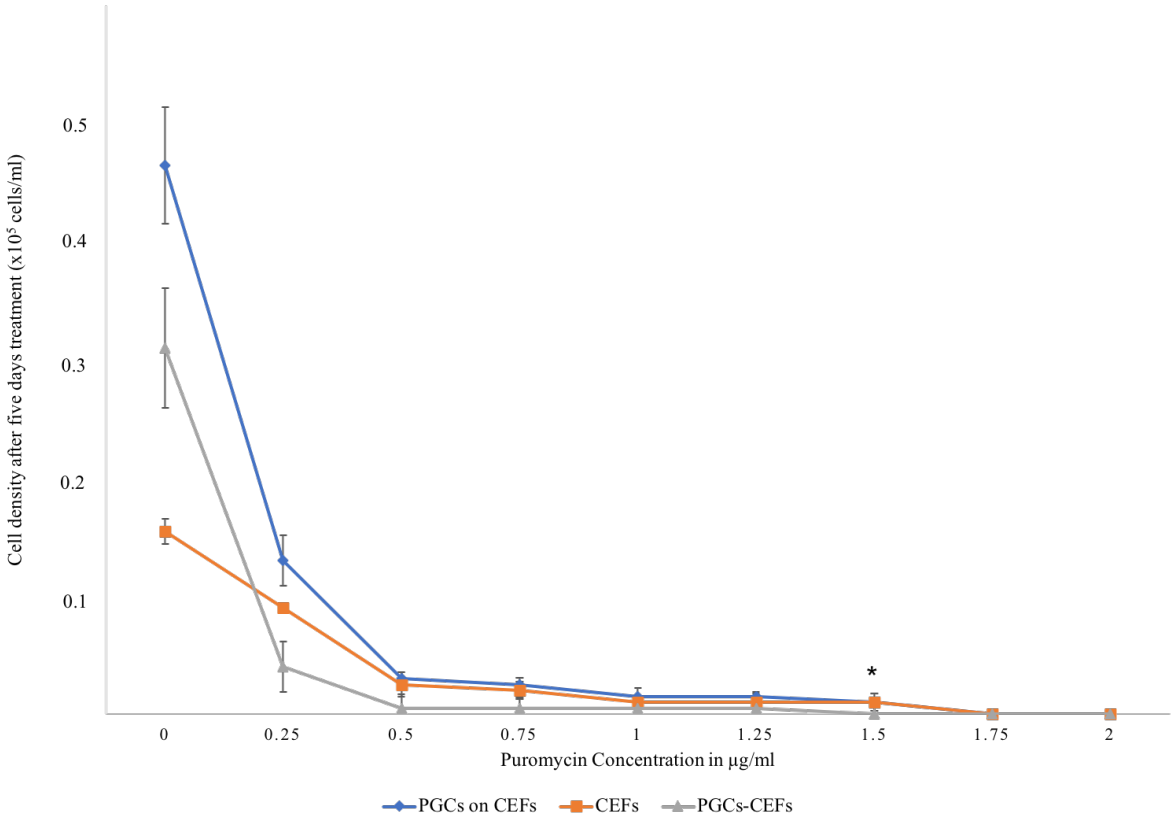

***Figure 3.19*. PGC kill curve after treatment with different Puromycin concentrations.** *After a 5-day treatment of PGCs cultured on CEFs, as well as CEFs cultured alone, with different Puromycin concentrations, live cell counts of replicate wells were averaged and plotted. The plot of PGCs, shown in grey, was extrapolated by subtracting the CEFs from the PGCs on CEFs for each concentration. Error bars represent the standard deviation from the mean at a 95% confidence interval. ANOVA revealed the test statistics F=136.29 and P<0.01. The post-hoc test generated P<0.01 for all the concentrations compared to the untreated control. The optimal concentration was marked with * to indicate significance.*

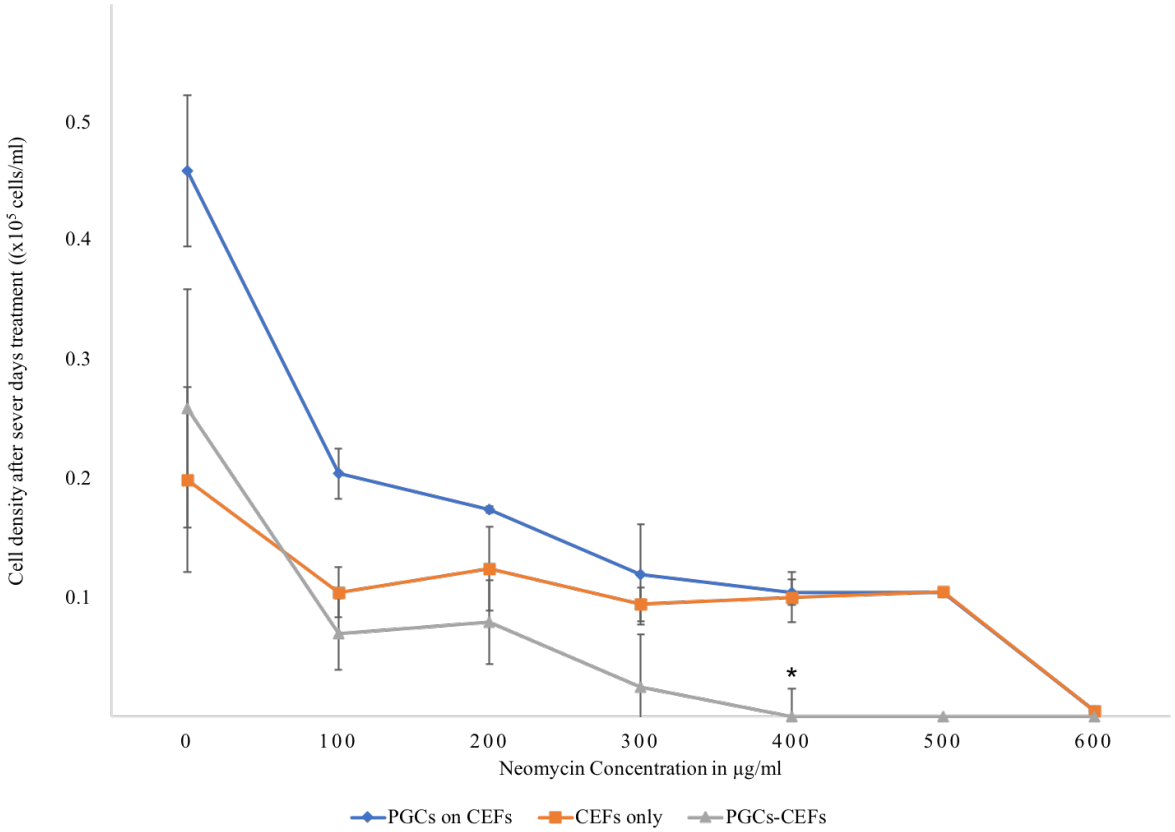

***Figure 3.20*. PGC kill curve after treatment with different Neomycin concentrations.** *After a 7-day treatment of PGCs cultured on CEFs, as well as CEFs cultured alone, with different Neomycin concentrations, live cell counts of replicate wells were averaged and plotted. The plot of PGCs, was extrapolated by subtracting the CEFs from the PGCs on CEFs for each concentration. Error bars represent the standard deviation from the mean at a 95% confidence interval. ANOVA revealed the test statistics F=115 and P<0.01. The post-hoc test generated P<0.01 for all the concentrations compared to the untreated control. The optimal concentration was significant and marked with *.*

3.5 Transfection of PGCs with modified gene drives, eSpCas9 construct, and mRFP-tol2 construct shows the desired HDR-mediated integration did not occur

Following transfection, either by electroporation or lipofection, with HSPA2-OVA or HSPA2-OVM gene drive, eSpcas9 construct, and the mRFP-tol2 construct, cells were treated with HDR-promoting and NHEJ-inhibiting compounds RS-1 and SCR7. Selection with Puromycin (OVA transfectants) and Neomycin (OVM transfectants) was performed as described in section 2. After selection, cells were observed by fluorescence microscope for red fluorescence (figure 3.21) confirming uptake of mRFP-tol2 with the other constructs. Even with antibiotic selection of cells (positive for gene drives), few were observed by fluorescence microscopy that showed successful co-transfection with the mRFP-tol2 too. gDNA extraction, performed after the cells had recovered, allowed for screening of the transfectants by PCR for the desired

HDR integration or for NHEJ. The detailed PCR protocol was discussed previously in section 2, parts of which had been previously performed in the lab. The HDR PCR targeted the 5' and 3' ends of the OVA or OVM integration sites, the NHEJ targeted the single joined region flanking the cutting sites of OVA or OVM. The PCR products were verified by agarose gel electrophoresis shown in figure 3.22 and figure 3.23. Of the HSPA2-OVA electroporated sample and the two HSPA2-OVA lipofected samples with circularised constructs, no editing was detected. For the HSPA2-OVM lipofected samples with circularised constructs no editing was detected, however the HSPA2-OVM electroporated sample exhibited bands on the agarose gel when screening for HDR integration at the 3' end of target OVM locus. The bands however were of unexpected sizes, at ~5Kb and ~1.8Kb, when the anticipated band should be at ~2.5Kb. Two samples where the gene drives were linearized before electroporation, with a single *PacI* digestion, as a means of attempting to promote the desired HDR integration, showed no detectable HDR or NHEJ. In order to rule out the uptake of constructs into the cells as the cause of lack of desired editing, a construct-specific amplicon was amplified off each HSPA2-OVA or HSPA2-OVM gene drive, the eSpcas9 construct, and the mRFP construct in each gDNA sample. In this way these construct PCRs acted as positive controls. The products were verified by agarose gel electrophoresis (figure 3.23) and all three constructs were detected in the gDNA extract of samples.

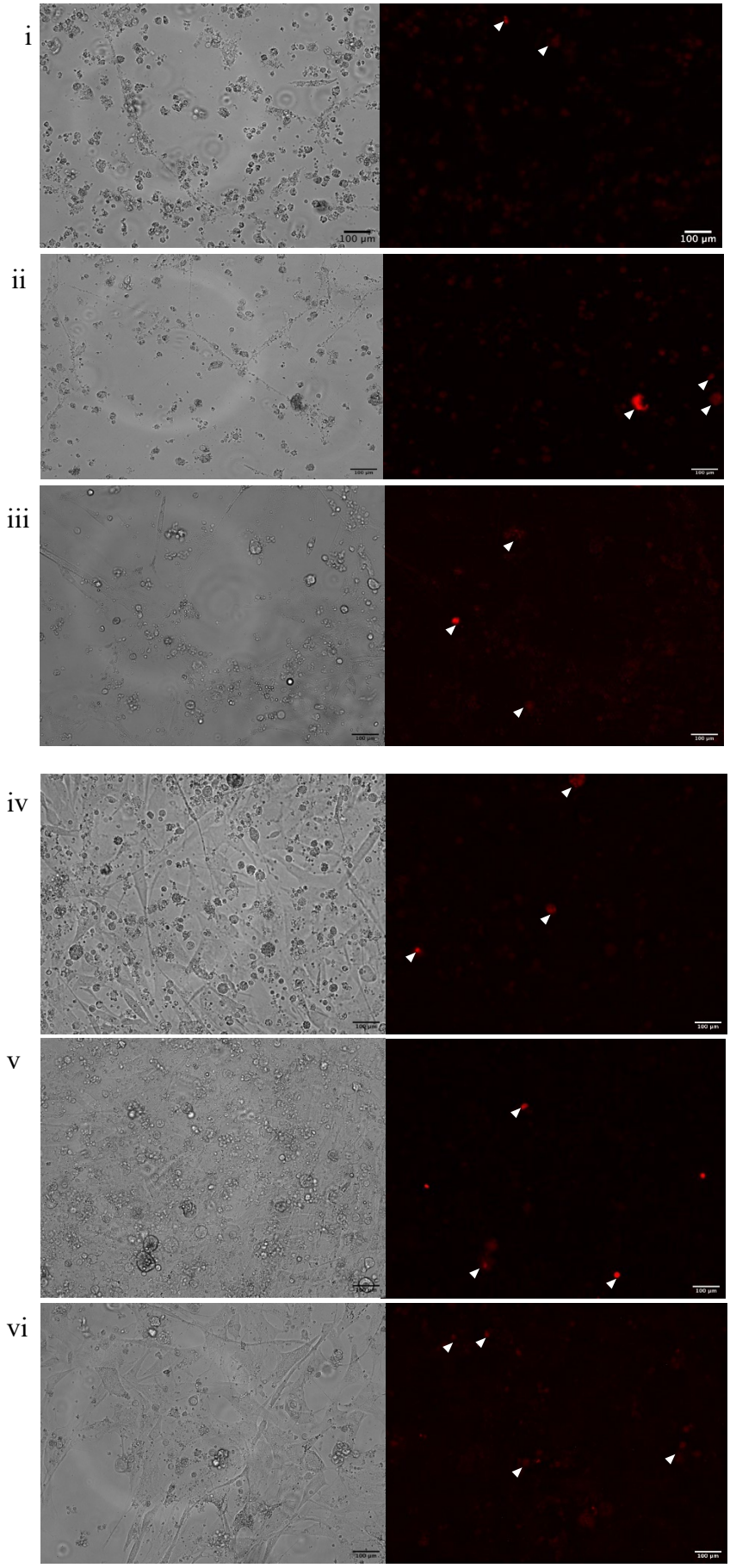

Figure 3.21. ***PGCs co-transfected with gene drives and mRFP-tol2 tracer.*** *Red fluorescence arises due to expression of RFP in transfectants (some are indicated by white arrows).* ***i-iii)*** *The HSPA2-OVA transfectants.* ***iv-vi)*** *The HSPA2-OVM transfectants.* ***i*** *and* ***iv*** *are electroporated PGCs. Lipofection at lower concentrations of lipofectamine are in* ***ii*** *and* ***v.*** *Lipofection at higher concentrations of Lipofectamine are shown in* ***iii*** *and* ***vi.***

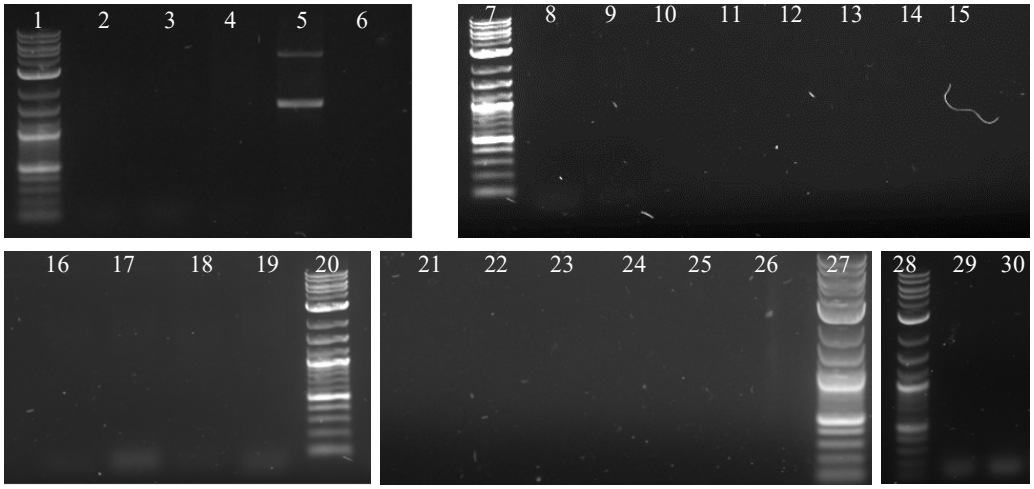

***Figure 3.22*. PCR-based screening for HDR-integration or NHEJ at the OVA and OVM loci in transfected PGCs.** *The gDNA extracted from transfected PGCs was screened for HDR integration at 5' and 3' ends of the integration site or for NHEJ across the integration site by PCR. The only sample exhibiting PCR bands was that of the HSPA2-OVM electroporated sample screened at its 3' integration site in lane 5. The band sizes are ~5Kb and ~1.8Kb. There was no detection of HDR or NHEJ in other samples (either electroporated or lipofected) in lanes 2-4, 8-15, 16-19, 21-26, and 29-30. Lane 6 shows a no-template control. Lanes 1, 7, 20, 27, and 28 show the NEB 1Kb Plus Marker run alongside samples on the 1% agarose gels.*

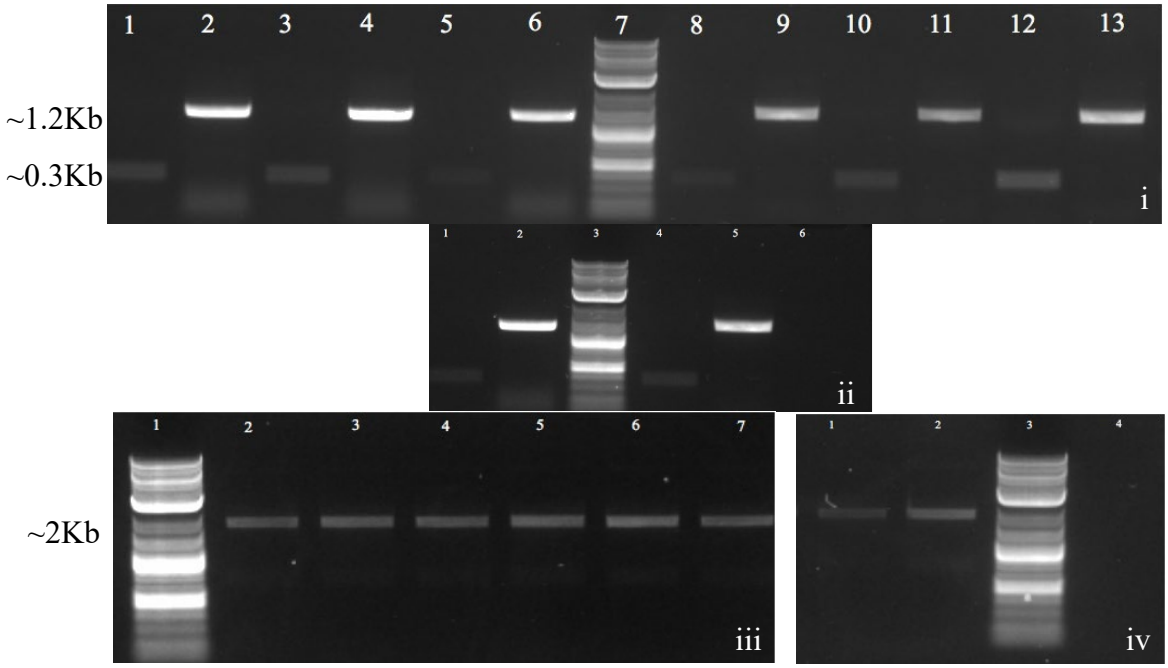

Figure 3.23*. PCR-based detection of constructs within transfected PGCs.** *The gDNA extracted from transfected PGCs was screened for presence of the constructs used in transfection: namely the HSPA2-OVA or HSPA2-OVM gene drive and the eSpCas9 construct. The various PCRs amplified Puromycin (~1.2Kb) of the HSPA2-OVA gene drive, Neomycin (~1.3Kb) of the OVM gene drive, backbone in both the gene drives (~0.3Kb), and the backbone in the eSpCas9 vector (~2.5 Kb).* ***i) *The samples on this gel were transfected using circularised constructs. Lanes 1,3, and 5 show amplicons for the HSPA2-OVA gene drive backbone in electroporated sample, lipofected sample at lower concentrations of lipofectamine, and lipofected sample at higher concentrations of lipofectamine. Lane 2,4, and 6 show amplicons*

Puromycin in the HSPA2-OVA gene drive of these same samples. Lanes 8,10, and 12 show amplicons for the HSPA2-OVM gene drive backbone in electroporated sample, lipofected sample at lower concentrations of lipofectamine, and lipofected sample at higher concentrations of lipofectamine; and lanes 9, 11, and 13 show amplicons of Neomycin in the HSPA2-OVM gene drive of these same samples. ***ii)*** *The samples on this gel were transfected using linearized gene drive constructs. Lane 1 shows amplicon for the HSPA2-OVA gene drive backbone in electroporated sample with its amplicon Puromycin shown in lane 2; the HSPA2-OVM electroporated sample shows the backbone amplicon in lane 4 and the Neomycin amplicon in lane 5. A no-template control where gDNA was omitted was run in lane 6.* ***iii)*** *The eSpCas9 general expression construct was detected in all types of cells transfected with circular construct.* ***iv)*** *The eSpCas9 general expression construct was detected in all types of cells transfected with linearized construct. In all the gels here the 1Kb Plus DNA Ladder was employed as a Molecular Weight Marker (lanes* ***i-****7,* ***ii-****3,* ***iii-****1,* ***iv-****3). All the gels in this figure were stained with Ethidium Bromide. Image captured via GelDoc (Bio-Rad).*

3.6 Repopulation of busulfan-ablated embryos with PGCs transfected with mRFP-tol2 tracer

Preceding injection of exogenous PGCs into busulfan-treated (at 1.5µg/µl) embryos (detailed protocol in section 2) the PGCs were transfected with the mRFP-tol2 tracer. PGCs viewed ~3 days after electroporation with RFP shows the cells took up the construct. Although the efficiency could not be quantified, the amount of red fluorescence in PGCs was observed overall under the red light of fluorescence microscope. Although few, rounded PGCs had formed small clusters positive for RFP (figure 3.24). The mRFP-tol2 tracer did not contain antibiotic resistance needed for selection and therefore PGCs, after recovering, were simply lifted by pipetting for repopulation of day 3 ablated embryos. A small volume of blood (1-5µl) was taken for sexing before injection into recipient male embryos. The injection of cells into the blood vessels was followed by further ~3 days incubation, by which time PGCs have already begun settling in the gonads. The embryo samples which survived (n=4/17) were those where PGCs were injected into the branching vitelline veins. Gonads observed for red-protein fluorescence (figure 3.25) showed no obvious observable red fluorescence in the gonads under fluorescence microscope. No embryos had observable defects.

White light Red light

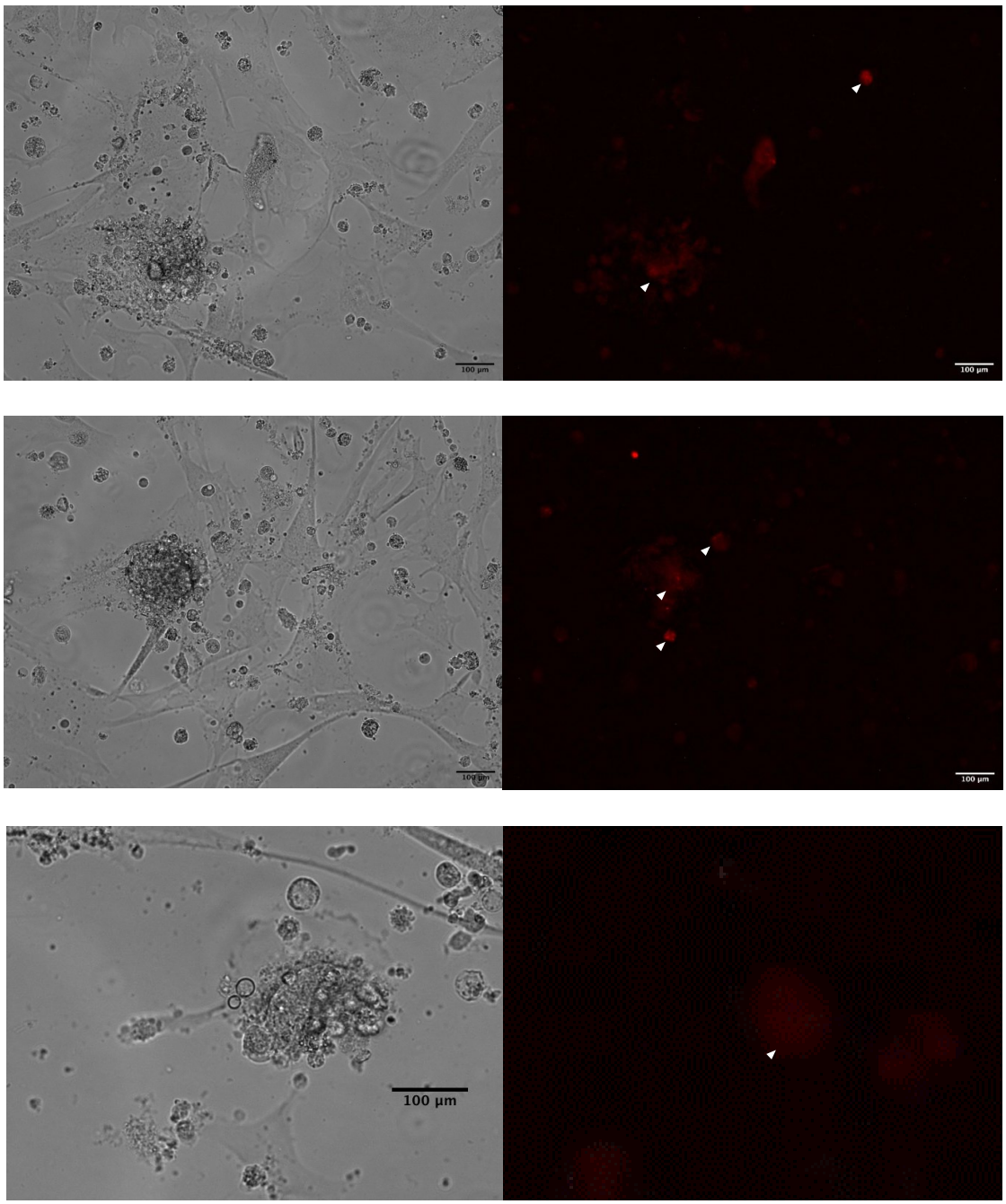

***Figure 3.24*. PGCs transfected with mRFP-tol2 tracer construct.** *After allowing electroporated PGCs to recover on growth inhibited CEFs, they were observed for expression of RFP via fluorescence microscopy. Different images of transfected cells are shown. Clusters and single PGCs (some shown by white arrowheads) were positive for red fluorescence. Scale bar=100µm. Images viewed and captured via the FLoid™ Cell Imaging Station.*



Figure 3.25*. Fluorescence imaging of repopulation of exogenous PGCs in gonads of busulfan ablated embryos.** *PGCs transfected with mRFP-tol2 tracer were injected into the blood vessels of day 3 embryos. Day 6 embryonic gonads are shown.* ***(G) *The gonads are outlined in white dotted lines.* ***(K)*** *Kidneys attached to either gonad.* ***i)*** *Noninjected control embryo.* ***ii)*** *Embryo injected with mRFP-transfected PGCs. Images captured with ZEISS Zen microscope.*

Section 4: Discussion

The production of an *in ovo* transgenic chicken bioreactor, via germline chimeras, requires proficiency in various advanced techniques. This study explored various potential techniques and components involved in the creation of transgenics. The focus of this study was on the techniques capable of modifying germ cells *ex vivo* to deliver transgenes into recipient embryos. While concentrating on the isolation and culture of primary PGCs *in vitro,* and PGC editing through preparation and use of gene drive constructs, the sterilisation and restoration of germ cells in sterilised recipient chicken embryos was explored. Meeting all these conditions for editing and successfully delivering PGCs to obtain germline chimeras is a challenge and it was evaluated in the context of Cas9-based gene editing techniques. An investigation of these procedures in transgenic chicken production will give us insight into the benefits and downfalls of potential avenues towards scalable transgenic chicken production.

4.1 Isolation and culture of primary PGCs

Several studies have reported the successful development of a culture system of PGCs. In this study, the PGCs were sourced from blood of HH14-17 embryos and propagated upon a CEF feeder layer. A hormone-supplemented media composition described in literature was used in order to maintain undifferentiated PGCs in conditions which mimic their natural environment. This is important for preserving the biological identity of the PGCs (van de Lavoir *et al.*, 2006; Tang *et al.*, 2007; Choi *et al.*, 2010; Naito, Harumi and Kuwana, 2012; Miyahara *et al.*, 2014; Tonus *et al.*, 2016). As a commonly employed method for chicken PGC identification, the anti-SSEA-1 antibody identified PGCs positive for the PGC cell surface marker SSEA-1 (Miyahara *et al.*, 2014; Tonus *et al.*, 2016; Kim and Han, 2018). This confirmed the blood-extraction technique to obtain PGCs. PGCs appeared pure after approximately 10-14 days in culture and exhibited typical PGC morphology (figure 3.14). This is in keeping with findings reported in other studies (Tonus *et al.*, 2016; Szczerba *et al.*, 2020). This means yolk and red blood cells and other impurities transferred during PGC isolation from embryos was no longer present in culture by 2 weeks post extraction. Despite previous studies' stressing the importance of the need for explicit purification protocols to obtain high homogeneity of PGC cultures (such as Percoll density gradient, ACK lysis buffer, or FACS) it was decided not to employ these due to the significant subsequent loss of cells (Mozdziak *et al.*, 2005; Yamamoto *et al.*, 2007; Motono *et al.*, 2008). Resource limitations and the costly nature of implementing certain

purification procedures further support this decision. This project demonstrated that any other cells other than the desired PGCs, such as erythrocytes, were eliminated as they were not suited to survival in the culture conditions employed in this study. Thereafter these cells were simply washed away during media changes without the need for depletion of valuable, costly purification reagents such as Percoll.

One of the disadvantages of the blood extraction technique for obtaining PGCs is the low number of PGCs available for isolation from the blood at the onset. This resulted in a slower time to cultivate a sufficient number of PGCs for downstream purposes. The number of PGCs in circulating blood in the embryo not only varies but is considerably lower compared to those available in the gonads (Nakamura *et al.*, 2007; Szczerba *et al.*, 2020; Szczerba, Kuwana and Bednarczyk, 2021). This means a larger number of samples needs to be processed to obtain as much blood containing circulating PGCs as possible. Anand *et al.* (2018) found that the starting concentration of PGCs in culture affects their proliferation and contributes to determining how fast the cell line can be established; a higher starting concentration facilitates a more rapid decrease in the time required to achieve a desired yield. The trade-off between purity and yield in isolating PGCs from the different sources means that if obtaining a relatively large amount of PGCs in a shorter time period is the priority, gonad isolation and extraction might be a preferable alternative. Gonadal PGC isolation is also less time-consuming and laborious than circulating PGC extraction. However, given the high risk of carrying over different contaminating somatic cells in gonadal PGC isolation, and the necessity in this study of a pure PGC line, this method was not utilised (Szczerba et al., 2020).

In this study, the applicability of PGCs to a variety of the techniques, from preliminary experiments testing sensitivity to antibiotics, to confirming post-extraction PGCs' identity with immunostaining, to establishing PGC use in transfection and as donor PGCs in repopulation of gonads, was demonstrated. The various techniques reinforce that many PGCs are needed for transgenic applications. PGCs' sensitivity to antibiotics Neomycin and Puromycin revealed the minimum concentrations for selection of PGCs transfected with HSPA2-OVA or HSPA2-OVM gene drive constructs providing Puromycin or Neomycin antibiotic resistance respectively. The statistically significant, optimal Puromycin and Neomycin selection concentrations were found to be 1.5μg/ml and 400μg/ml respectively (figure 3.19 and figure 3.20). These findings fall within the range of reported studies and is considered to be in

agreement with findings of other studies (van de Lavoir *et al.*, 2006, 2012; Oishi *et al.*, 2016; L. Wang *et al.*, 2017). These preliminary experiments, although caused the depletion of a significant portion of the PGC culture, were necessary.

4.2 Sterilisation of embryos by busulfan injections

The role of endogenous PGCs in creating germline chimeras or transgenics is important. The outcomes and success of populating the gonads with foreign PGCs depends not only on the ability of the exogenous PGCs transferred to migrate to, and settle in, the gonads, but also on the presence of endogenous PGCs. Some studies suggest that the number of endogenous PGCs relative to donor PGCs is a major contributing factor to the efficiency of donor PGC transfer and the efficiency of repopulation of gonads (Nakamura *et al.*, 2008, 2010; Nakamura, Kagami and Tagami, 2013; Woodcock *et al.*, 2019). This is because there may be competition between the two types of PGCs for colonisation of the gonads. If the amount of donor PGCs relative to endogenous PGCs is increased in the chimeric gonads, the frequency of donor PGC transmission is enhanced. The exact relationship between the amount of donor PGCs relative to endogenous PGCs is not consistently defined across studies. Rather a trend of increased proportion of donor PGCs has been observed with sterilisation-based removal of endogenous PGCs (Nakamura *et al.*, 2008, 2010). Thus, in this project, I sought to eliminate the endogenous PGCs in chicken embryos using busulfan.

There are various sterilisation techniques including: gamma irradiation, x-ray irradiation, surgical or chemical methods. Despite their relative efficiency and accuracy, the former three methods require costly equipment or high skills levels which limits their applicability (Kagami *et al.*, 1997; Nakamura *et al.*, 2010, 2012; Park *et al.*, 2010). In this study chemical sterilisation using the chemical sterilant busulfan was used to target endogenous PGCs. As an alkylating agent which selectively targets germ cells in chicken embryos, the busulfan compound has been successfully shown to eliminate PGCs by apoptosis when injected into stage X embryos (Song *et al.*, 2005; Nakamura *et al.*, 2008, 2010; Lee *et al.*, 2013). A sesame oil and DMSO-busulfan-emulsion was delivered into the egg yolk, with the intention to analyse the optimal busulfan concentration for eliminating endogenous PGCs. The busulfan dosage had an effect on PGC survival but not on embryo survival. The optimal busulfan concentration was found to be 1.5 μg/μl (figure 3.17 and figure 3.18).

By analysing the remaining PGCs with SSEA-1-based immunohistochemistry in gonads across the range of three gonadal busulfan-treatment groups, the reduction in PGCs becomes evident. This reduction demonstrated that the sterilisation achieved a 49%-75% removal of PGCs across the busulfan dosages compared to the control (figure 3.17). Other similar sterilisation procedures using busulfan have found varying results for sterilisation efficiency, yet all indicate the trend of increased sterility with increased busulfan dose (Song *et al.*, 2005; Nakamura *et al.*, 2008, 2010). This project's findings correlate with this trend. In the embryos treated with 75µg busulfan, a statistically significant reduction of 70% of PGCs relative to the control was accomplished. This reduction seems close to the 85µg busulfan treatment group which achieved a 75% PGC reduction. To investigate this the two groups were compared. Interestingly when comparing these two groups, although we counted differing numbers of PGCs after treatment, there was no statistically significant difference between the two busulfan concentrations. Thus, when considering which the optimal concentration for most efficient sterilisation was, the embryo survival between the treatment groups and development of teratogenic effects of busulfan were considered.

Busulfan is a teratogen, and even at low doses of exposure, deformities in the chicken embryo can arise (Nakamura *et al.*, 2008; Bischoff *et al.*, 2020). Although administration of the agent early on in development has been shown to act more towards targeting PGCs for elimination, this only reduces but might not eliminate potentially teratogenic effects of residual busulfan in the embryo (Nakamura *et al.*, 2009). The rationale behind using the oil-emulsion to deliver busulfan is based on the fact that the busulfan in the emulsion may rise in the yolk towards the blastoderm because of the lower density of the mixture. This is less harsh to the embryos than direct contact with the blastoderm on top of the yolk (Nakamura *et al.*, 2010). In this study the research lab did not possess the costly equipment (Internal pressure-type micro kit;IMK-20; MCtech) required to emulsify the busulfan-DMSO-sesame oil mixture. While the busulfan appeared completely dissolved using a regular membrane porous filter, it is possible that at the higher dose of 85µg busulfan, precipitation (as was sometimes noticeable before injection) occurred. Precipitation may have led to inconsistent exposure of the embryo to the busulfan (Nakamura *et al.*, 2010; Lee *et al.*, 2013). This potential issue was attempted to be mitigated by continuously passing the emulsion through a membrane filter; regularly vortexing the emulsion before use; and only preparing the emulsion right before injection. Therefore, the effect of the emulsion's preparation on the teratogenic effects to the embryo is not definitive.

Busulfan has been associated with abnormalities in limb development and eye development (Nakamura *et al.*, 2008, 2009). While there were teratogenic effects observed in the embryos exposed to the highest dosage of busulfan in this study, these were not statistically significant (P=0.19). The survival of embryos in different busulfan treatments groups showed no statistically significant difference, despite the drop observed in survival with increasing busulfan concentrations (figure 3.18). However, the minimum sample size requirement for performing this test was met (McHugh, 2013). The embryo survivability for the two highest busulfan concentrations (which achieved sufficient PGC reduction) were well above 50%. This was deemed sufficient in the context of subsequent additional manipulations that affect embryo survivability.

Even though the results were not statistically significant, based on the effect on survival and embryo teratogenic potential of busulfan-mediated sterilisation, the minimum possible dose that still showed promising sterilisation efficiency was chosen in this study. A study by Nakamura *et al.* (2010) found survival reduction and developmental abnormality frequency increased with higher busulfan doses (>75μg). A low embryo survival rate following sterilisation is undesirable for downstream injection of donor PGCs into the vasculature. Thus, together, these two procedures, which cause stress to the embryo, may have a combined negative impact on survival. The findings from this study, together with other reports, suggest that higher concentrations of busulfan affect survivability and developmental defect occurrence, while lower rates have a lower sterilisation efficiency. This led to the conclusion that the 75μg busulfan dose was optimal in the context of this project's experiment.

4.3 Attempting to restore PGC population in sterilised embryos

The roles of endogenous and donor PGCs in creating germline chimeras are both important. The donor PGCs need to be delivered into the bloodstream and retain their biological identity and ability to migrate via the bloodstream to the gonads. Injection into the bloodstream of sterilised embryos has been reported, using various techniques to produce germline chimeras (Song *et al.*, 2005; van de Lavoir *et al.*, 2006; Nakamura *et al.*, 2008, 2009, 2010; Tonus *et al.*, 2016). To investigate this, I thus sought to determine if repopulation could be achieved using the various techniques and tools available in the lab for this study.

In this study, donor PGCs were tracked using a construct employing red-fluorescent protein emission (via mRFP-tol2 plasmid), expressed upon transfection into the PGCs. PGCs positive for RFP expression enable fluorescence-based tracking of injected PGCs *in vivo,* post-injection. Prior to injection into the embryonic vasculature, the embryos had been sterilised using busulfan injection. Different injection sites in the blood vessels were employed and a low survival rate resulted at ~23%. Survival in this study was significantly lower when compared to similar studies (Nakamura *et al.*, 2009, 2010). However, no embryos exhibited any teratogenesis suggesting the sterilisation technique used in conjunction with PGC injection posed low risk to developmental abnormality occurrence. The surviving embryos were those injected at the site of vitelline veins. Amongst the surviving embryos, no visible red fluorescence was detected in the embryonic gonads (figure 3.25). This indicates that no traceable PGCs, following injection into the vasculature, were able to migrate via the bloodstream to populate the gonads.

Several limitations affect the potential for successful repopulation of gonads post-sterilisation. Firstly, the method used in this study to track donor PGCs was difficult to quantify. While it was possible to verify the conditions for obtaining transfectants via electroporation, the efficiency of the technique could not be quantified. PGCs appeared to show mRFP-tol2 construct uptake and subsequent RFP expression (figure 3.24). Yet, it was not possible to propagate a large number of a pure line of mRFP-tol2-transfectants through antibiotic selection. This was regrettably due to an inability to adjust the mRFP-tol2 construct by restriction digestion (for insertion of antibiotic resistance gene) due to time constraints and a lack of the appropriate, required restriction enzymes. Future work should consider the use of antibiotic selection for cultivating these RFP-positive PGCs. A pure line of RFP-positive PGCs would aid in identifying true repopulation in the gonads, as we cannot rule out the possibility that non-transfected donor PGCs (co-injected with RFP-positive PGCs) preferentially inhabited the gonads. These non-transfected PGCs would not have been detectable without fluorescent marker. Additionally, the mRFP-tol2 construct possesses the elements of the tol2 system for random integration into the genome, except for the transposase enzyme. The transposase enzyme, which would normally be delivered via a separate transposase expression plasmid, was not included (Tsukahara *et al.*, 2015). This means stable integration can occur at minimally low levels only in the presence of endogenous cell transposases and expression of the RFP protein was likely transient, under control of the vector's ubiquitous promoter. This

also meant the transfected PGCs needed to be injected into embryos soon after transfection to ensure fluorescent traceability of PGCs in the embryos was still possible in the limited timeframe of the RFP expression. This was a considerable disadvantage, since PGCs did not have much time to recover and the stress imposed on them from electroporation might have had unforeseen negative effects in repopulating the gonads efficiently.

A more stable form of fluorescent labelling would be more practical for tracking PGCs than the available mRFP-tol2 construct. A common, simple tracking system of donor PGCs in recipient embryos- that is the use of fluorescent protein dyes such as PKH26 which labels the PGC membranes prior to injection- has been demonstrated to be an effective alternative (Yamamoto *et al.*, 2007; Nakamura *et al.*, 2008, 2009, 2010; Szczerba *et al.*, 2020). The technique described in these reports for applying the PKH26 dye is relatively straightforward. Thus, a stable form of PGC labelling can be achieved.

The number of PGCs injected and the mode of injection into recipient embryos affect PGC delivery to the gonads. Due to the low numbers of viable PGCs remaining for use in injection after performing kill curves, and transfection procedures, 1000 cells were injected per embryo. The amount of PGCs injected varies considerably across reported studies, yet the optimal numbers for achieving maximum donor PGC integration while maintaining high survivability rates cannot be definitively known in the context of different experimental setups (van de Lavoir *et al.*, 2006; Nakamura *et al.*, 2009, 2010; Oishi, 2010; Oishi *et al.*, 2016). The limiting factor to be noted in this project was that the cell line did not consist of purely-transfected RFP-positive PGCs, therefore the injected PGC cell count before injection was unlikely to be a true representative of the traceable PGCs that were injected; the cell count of traceable PGCs was likely much lower. Given that studies have reported low percentages of initially injected labelled donor PGCs colonising the gonads after injection, this was likely to have caused an underestimation of outcome yield in this project (Nakamura *et al.*, 2011; Miyahara *et al.*, 2014). The low number of detectable donor-PGCs in the gonads may be attributed to suboptimal instrumentation- for example the use of mouth-controlled pipettes and fine glass needles for injecting the cells. The use of manual instruments increases the possibility of haemorrhage or simply leakage of the cells out the blood vessel, as pressure is inconsistent. This means this study's findings related to gonadal repopulation may not be comparable to results reported in studies where methods used to manipulate blood vessels and perform delicate injection

(without bursting blood vessels and killing the embryos) utilise specialised and automated equipment. For example, two almost comparable studies to this study, used costly equipment (namely a microinjector (IM-300)) which is not available in this study's research lab, instead of a mouth-controlled pipette (Oishi, 2010; Oishi *et al.*, 2016). The use of a microinjector enables controlled injection of precise, small volumes of medium containing cells, and controls the pressure settings. The use of specialised equipment such as this is recommended for future work to improve the delivery of PGCs into the bloodstream without causing bleeding at the site of injection, and thus improving study efficiency and productivity.

The sterilisation procedure is another factor to consider in lack of observable PGC repopulation in the gonads. While there were no doubt benefits in terms of the relatively simple, inexpensive method of busulfan-based sterilisation described in this study, there are those who believe that there is the small possibility of leftover busulfan targeting the donor PGCs (Nakamura et al., 2013). However, since the half-life of busulfan has been estimated to be between 10-18 hours *in vivo*, and donor PGC injection occurred long after (~3 days incubation), it is unlikely the busulfan was responsible for lack of detectable repopulation of gonads (Song *et al.*, 2005). Thus, the busulfan sterilisation is unlikely to have a negative impact on this technique.

The amount of PGCs has a significant effect in the repopulation phase and in attempting to understand why it might not have occurred. The relationship between numbers of PGCs delivered into the bloodstream and its effects on survivability and on efficiency of gonadal repopulation varies across reported studies (Song *et al.*, 2005; van de Lavoir *et al.*, 2006, 2012; Nakamura *et al.*, 2010; Oishi *et al.*, 2016; Han and Lee, 2017). Furthermore, these studies vary in the sterilisation techniques used in conjunction with repopulation; and the modes of injection. Therefore, it is difficult to know the sole effects of the numbers of PGCs used in injection, in the context of similar techniques used in this study.

The ability of the PGCs to retain germline competency is essential for migration to the gonads following injection in the embryos. Despite maintaining PGCs in this project according to accepted conditions outlined in literature, it is helpful to know if the PGC culture, even after transfection procedures, showed conserved PGC identity and if the PGC population remained homogenous in terms of retaining an undifferentiated PGC phenotype. In future work it may be useful to evaluate the expression of common germline-associated markers known to be

involved in migration of PGCs and/or conservation of the PGC phenotype and germline potential (Motono *et al.*, 2008). This was not possible due to the low numbers of PGCs remaining at the end of experimental procedures and hence the low template-sample DNA that could be retrieved for performing these PCR-based techniques. This could not be performed before repopulation as it would mean irreversible loss of PGCs.

4.4 Assessing the activity of CRISPR gene drives in PGCs

The last element analysed of the techniques toward transgenic production was that of editing the genome of PGCs. This transgene insertion was targeted at two of the major allergenic egg white proteins- OVA and OVM (Caubet and Wang, 2011). The foundation of this editing approach was CRISPR-Cas9 based gene drives and general Cas9 expression constructs. Generation of the HSPA2-OVA and HSPA2-OVM gene drives was successfully completed through multiple adjustments of various regions in the constructs. The stock gene drive was the basic starting plasmid for multiple variants of this gene drive within the lab. Naturally, changes would arise that need to be made for altering the functions and purposes of the construct and these changes were made via restriction enzyme digestions, ligations and cloning as opposed to commercial synthesis due to the large number of variants and adjustments that occurred. This may pose the issue of mutations arising during the cloning and DNA assembly processes, which was the justification for sequencing the construct at each step of adjustment, especially before their use in transfection experiments with the valuable PGCs. All adjusted elements in the gene drives had perfect sequence identity for downstream transfections (supplementary data). The limiting factor of the restriction digestions and cloning techniques for gene drive modifications was time. The requirement for sequencing at each step of cloning caused lengthy waiting periods in this study. This caused delay in implementation of the gene drive constructs in transfection of PGCs.

The transfection procedures, which involved both electroporation and lipofection, demonstrated the gene drive activity did not produce the desired editing and integration at the OVA and OVM loci. The transfection procedures themselves appeared to have been successful in that all the constructs, namely the HSPA2-OVA/M gene drive; the eSpCas9 general expression construct and the mRFP-tol2 construct, were detected even after antibiotic selection (figure 3.23). This likely indicated that co-transfection of PGCs was successful to a degree, since antibiotic selection (gene drives contain antibiotic resistance) preceded this screening.

Despite this fact, the transfection of PGCs did not yield desired detectable forms of HDR-integration or NHEJ. It was only at the 3' end of the OVM target locus that unexpected forms of editing were shown in the form of an unexpected PCR amplicon (figure 3.22). This could be interpreted as inefficient forms of DSB repair occurring. This result for the OVM locus is on the one hand encouraging for the construct activity (and Cas9 cleavage), yet on the other hand troubling in that it highlights the at times unpredictable or inefficient nature of the DSB repair process.

The repair of DSBs in cells entails complex processes that can be error-prone and result in various forms of insertions and deletions, especially during instances, such as this project, where DNA templates for repair are large (Rodgers and McVey, 2016). Importantly to consider are the modes in which the more favourable forms of HDR repair can be promoted in the cell. In this study the NHEJ-suppressor, SCR7, was used together with the HDR-stimulator RS-1 (Jayathilaka *et al.*, 2008; Lieber, 2010; Bischoff *et al.*, 2020; Yang *et al.*, 2020). These experimentally-validated molecules have been shown to enhance desired forms of DNA repair in various *in vitro* and *in vivo* experiments (Jayathilaka *et al.*, 2008; Chu *et al.*, 2015; Maruyama *et al.*, 2015; Pinder, Salsman and Dellaire, 2015; Ma *et al.*, 2016; Song *et al.*, 2016; Li *et al.*, 2017). However, treatment with these small molecules are not without risks; results are not definitive but can be inconsistent across cell types, target loci and insertion templates; and the activity and effects in chicken PGCs is lacking (Jayathilaka *et al.*, 2008; Chu *et al.*, 2015; Maruyama *et al.*, 2015; Pinder, Salsman and Dellaire, 2015; Ma *et al.*, 2016; Song *et al.*, 2016; Li *et al.*, 2017; Lamas-Toranzo *et al.*, 2020). In this study the concentrations used for treating PGCs post-transfection were based on those previously established in the research-lab in CEFs. Additional work is necessary to determine the optimal concentration and effects of these molecules on HDR efficiency in PGCs specifically. In future work it would be useful to perform transfection experiments in conjunction with a range of RS-1 and SCR7 treatment doses. This would allow for the determination of sensitivity of PGCs to these reagents and the optimal concentrations for efficacious targeting and editing of OVA and OVM loci. While these compounds have shown favourable outcomes for DNA repair in various species, experimental validation in chicken PGCs is lacking. Furthermore, the HDR/NHEJ ratios have been shown to be influenced by gene locus, cell type and even nuclease type (Miyaoka *et al.*, 2016). A difference in effects of these molecules on CRISPR-induced HDR integration across cell types within and between species may indicate differences in expression of members of

the DNA repair pathways. Since data on expression of members of these pathways in PGCs is lacking, the effectiveness of the RS-1 and SCR7 treatments is difficult to assess (Miyaoka *et al.*, 2016). Thus, the success of this application will to some degree depend on determining effects of these molecules on PGCs. Testing these effects would once again require an abundance of PGCs.

Evaluation of the gene drive constructs themselves, reveals noticeable limiting factors which should be investigated in future work. The HSPA2-OVA and HSPA2-OVM gene drives were successfully assembled and adjusted to the needs and aims of this project and future work. However, the resulting large sizes (>19Kb) and complexity of these constructs might prove to be a limiting factor in their application. For instance, the lack of desired editing might be as a result of the complex folding of the structure not being able to assume an appropriate form for cutting and HDR-mediated integration using the supercoiled gene drive as a template. Conformation of donor template (supercoiled plasmid or linearized template) has proven to have varying, and sometimes conflicting, effects on efficiency of CRISPR-induced HDR-integration (Paix *et al.*, 2017; Yao *et al.*, 2018; Zhang *et al.*, 2022). This may provide an explanation of a potential contributor to the unexpected, incorrect HDR occurring in the OVM sample electroporated with circularised, supercoiled gene drive construct. The single cut donor plasmid (the gene drive) did not produce a detectable improvement in HDR in this project. However, given the potential for enhancement of HDR, linearization of donor template in different ways should be explored to determine its effects on HDR efficiency. An alternative technique for promoting the initial HDR-integration step is through the temporal control of gene editing. In this study, the eSpCas9 general expression construct provided the transient eSpCas9 expression for initial cleavage of the target loci. The HSPA2-OVA or HSPA2-OVM gene drives were adjusted to place integrated eSpCas9 under control of the meiosis-specific *HSPA2* promoter. The phases of the cell cycle where HDR is dominant can be leveraged for timing delivery of the eSpCas9 construct and gene drives. This simple technique of forcing cells *in vitro* into the same cell cycle stage via small molecules, such as cyclin D1, has been reported to enhance HDR efficiency considerably in human cells (Lin *et al.*, 2014; Zhang *et al.*, 2017). Similarly, to the RS-1 and SCR7 molecules, it would be ideal to test such reagents in chicken PGCs specifically to determine the effects on germ cells.

Another factor to consider is the impact of chromatin structure on editing efficiency. Besides the impact on the outcome of repair pathway choice in cells, the structure of and hence access to the loci by the CRISPR-Cas9 machinery can be affected too (Chen *et al.*, 2016). Despite other studies demonstrating accessibility to the OVA and OVM loci through their specific CRISPR-Cas9 editing machinery, in the context of this study's CRISPR-Cas9 gene drives and overall treatment of cells with HDR-promoting and NHEJ-inhibiting agents, the effects of these conditions on chromatin state are not known. The gRNA target sites in this study differ to those who have accomplished editing at the OVA and OVM loci (Oishi *et al.*, 2016, 2018). This study's gene drive constructs targeted, for cleavage and hence replacement, a larger portion of the ORFs of the OVA and OVM loci (cleavage occurs further upstream in the genes). While other studies have targeted disruption of the loci via gRNA action further downstream within exons 2 or exons 3 of the loci (Oishi *et al.*, 2016, 2018). Thus, there is the possibility that chromatin state, at the site in which the gRNA target sequence is embedded, in PGCs may play an important role in achieving Cas9 cleavage and editing of loci. This point is especially intriguing when considering the epigenetic patterns can be affected by their environment in which the PGCs are found *in vitro* (Kim and Han, 2018; Szczerba *et al.*, 2020).

Conclusions and Future Work

The processes described here toward the creation of transgenic chicken still require future work. There are further experiments which may be performed. The requirements for large numbers of PGCs from techniques in which cultivation of cells takes longer, and which require expensive resources, mean it may be prudent to explore the more rapid and higher-yielding gonadal PGC isolation and cultivation. The gonadal PGCs can be isolated from day ~6-7 embryos and maintained *in vitro* as performed in this project on a mitotically-inactivated CEF feeder layer (Park and Han, 2000; Park *et al.*, 2003, 2015; Nakajima *et al.*, 2011; Chojnacka-Puchta *et al.*, 2015; Naito, Harumi and Kuwana, 2015). Thus, it will be possible to isolate a relatively larger number of PGCs from a larger available population in the embryo (Chojnacka-Puchta *et al.*, 2015). Although the recovered viable PGCs will be reduced as a result of mandatory purification procedures, the more rapid and less labour-intensive gonadal dissection process means a larger number of input samples can be used as PGC sources. The larger starting PGC concentration will be beneficial for a more rapid cell line establishment (Anand *et al.*, 2018). Alternatively, time- and resource-permitting, the PGCs isolated from blood can be maintained in culture for extended periods of time. van de Lavoir *et al.* (2006) described

cultivation for up to 113 days before injection and successful colonisation of gonads of recipient embryos. This demonstrates the possibility to obtain the necessary amount of PGCs needed across various experiments. This is especially important when experiments require fine-tuning and inevitably results in loss of PGCs.

Furthermore, for the purposes of repopulation, a significant number of PGCs is needed. Given the multiple factors that can affect the outcome of this PGC repopulation there are different experiments which can be performed in future work. First, as mentioned before, an automated microinjector, where pressure settings can be specified and PGCs can be injected into vasculature in a precise, controlled manner, would be ideal as injection with the mouth-controlled pipette proved challenging and inconsistent (Oishi, 2010; Oishi *et al.*, 2016). It might also be valuable to determine (with either automated or manual injection) the effects of cell number on repopulation efficiency. A range of PGC amounts from 100-3000 cells have been used in similar experiments and it would be helpful to determine the effects in the context of this study and equipment and resources available in the research lab (Song *et al.*, 2005; van de Lavoir *et al.*, 2006; Nakamura *et al.*, 2010; Oishi *et al.*, 2016; Han and Lee, 2017). For the labelling of PGCs for tracking their migration after injection into the embryonic vasculature, a higher purity of fluorescent-traceable PGCs would be beneficial. This is aided by antibiotic selection for positive transfectants. This will require an antibiotic resistance gene inserted into the mRFP-tol2 vector by restriction digestion and cloning in the manner performed in this project for gene drive generation (unique restriction digestions and cloning). A perhaps more ideal or convenient form of tracing the PGCs would be to label them with the PKH26 red lipophilic membrane dye, since this can produce a more stable, long-term stain (Yamamoto *et al.*, 2007). This procedure will require incubation of isolated PGCs with the dye to allow incorporation of the red dye into their cell membrane and stopping the reaction with DMEM. This dye has been successfully used in this way to stain PGCs and subsequently deliver them to recipient embryos in transgenic chicken repopulation studies (Yamamoto *et al.*, 2007; Nakamura *et al.*, 2008, 2009, 2010; Szczerba *et al.*, 2020). The long half-life of PKH26 allows for long term staining of the cells, which eliminates concerns over donor PGCs not being detectable and distinguishable *in vivo* over time (Yamamoto *et al.*, 2007). Thus, it will be possible to distinguish donor PGCs in the recipient embryo.

The effects of the donor template's conformation in promoting HDR must be evaluated. This will concern testing linearization (via restriction digestion) of the gene drives at multiple sites prior to transfection, in order to assess if linearization at different sites compared to supercoiled plasmid construct has any effect or enhances access to the template for repair. Certain groups have demonstrated that double cut, linearized donor template considerably improved transgene integration efficiency compared to supercoiled donor plasmid template, in particular experimental contexts (Zhang *et al.*, 2017; Yao *et al.*, 2018). Taking these reports into consideration, double-cut linearized HSPA2-OVA and HSPA2-OVM gene drives at the restriction sites flanking the HAs (*AsisI* and *PacI*) should be tested as donor template for HDR.

Future work regarding design and activity of the gene drive constructs should consider the target sequences for Cas9, directed by the gRNAs, for cleavage. These target sequences may be inaccessible due to heterochromatin structure formation or epigenetic factors in the genomic region. To attempt to address this one might employ heterochromatin relaxers or investigate alternative gRNA designs. Alternative gRNA sequence targets within the region at the ends of the OVA or OVM ORFs can be designed. Alteration of these regions can be performed easily with specification of primers for PCR and cloning techniques. While the ultimate goal is to replace as much of the ORF of endogenous OVA and OVM egg white protein genes to reduce allergenicity, the efficacy and success of binding and cleavage at gRNA target sequences is vital. The range of gRNA target sequences may need adjustment and testing in different regions of exon 1 or even exon 2, similar to reported studies (Oishi *et al.*, 2016, 2018). It would be preferable to exhaust HDR-promoting treatments, via small molecule optimisation, before resorting to gRNA design alterations.

In conclusion, this study has shown an efficient, inexpensive technique for isolation of pure PGCs and their cultivation *in vitro.* As the foundation of the CRISPR-Cas9 gene-editing approach, the PGCs together with the gene drive constructs generated, will serve as an important resource in continuation of this research. Importantly the experiments demonstrated a relatively straightforward, economical method for chemical sterilisation of embryos via busulfan. On the other hand, this study has highlighted the many potential obstacles that hinder the success of PGC repopulation of gonads of recipient embryos, and which might be obstructing the efficacy of gene editing in PGCs. It is now up to future work to investigate methods for providing the conditions for the gene drives to successfully perform editing in

PGCs. From local chromatin structure to exploiting and enhancing endogenous cell repair mechanisms, the possibilities are significant. Across the various techniques it became clear the necessity of a long PGC culture, which requires significant time and resources. These experiments, the PGCs cultivated here and the gene drives generated will serve as valuable resources, findings, techniques and tools for future work in the realisation of a transgenic chicken bioreactor.

Supplementary

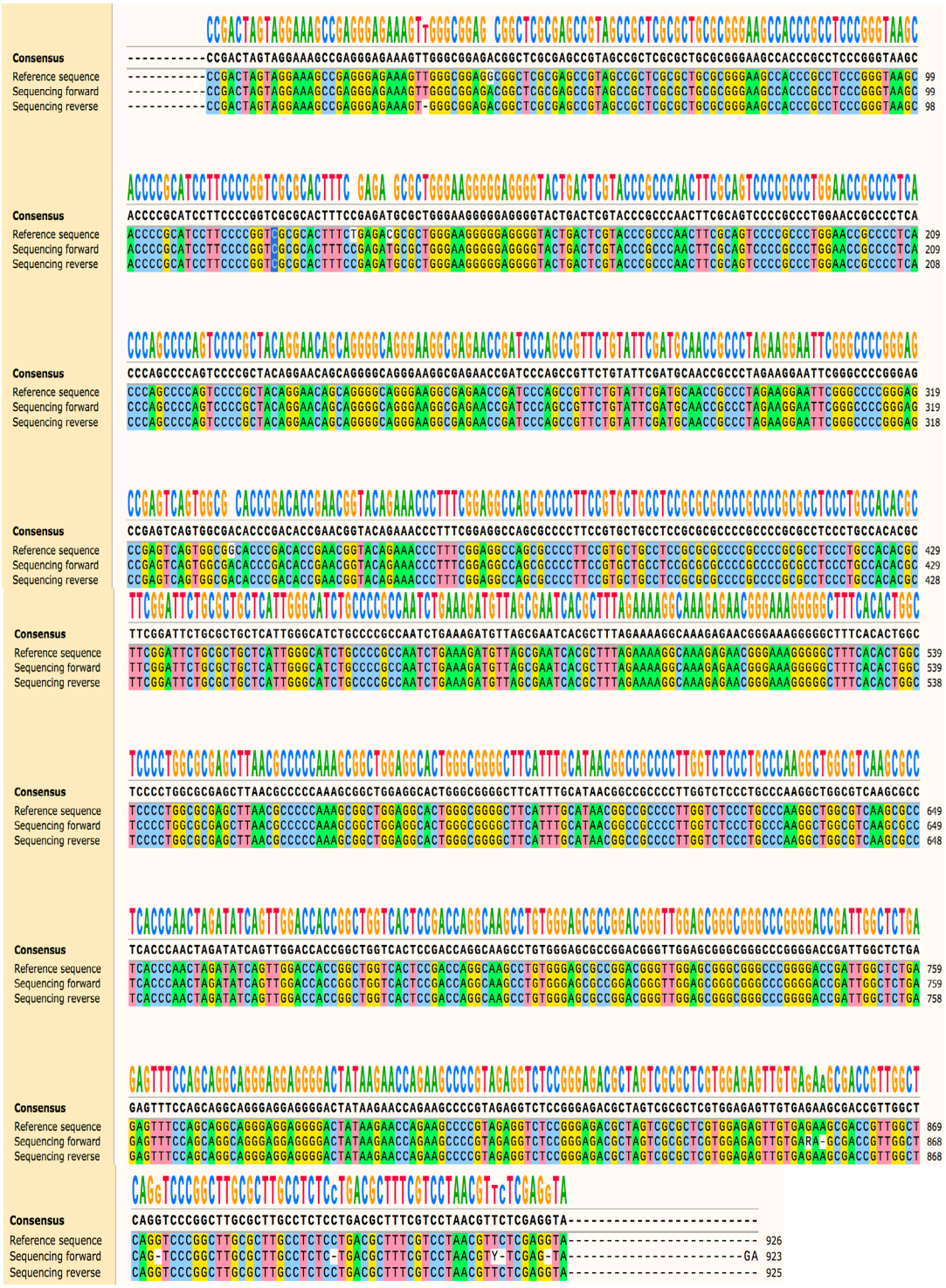

Supplementary figure 1. ***Sequence alignment of the HSPA2 promoter in the pMiniT-vector.*** *The two rows of sequence data were aligned against the reference sequence to give the consensus sequence. Figure produced in SnapGene.*

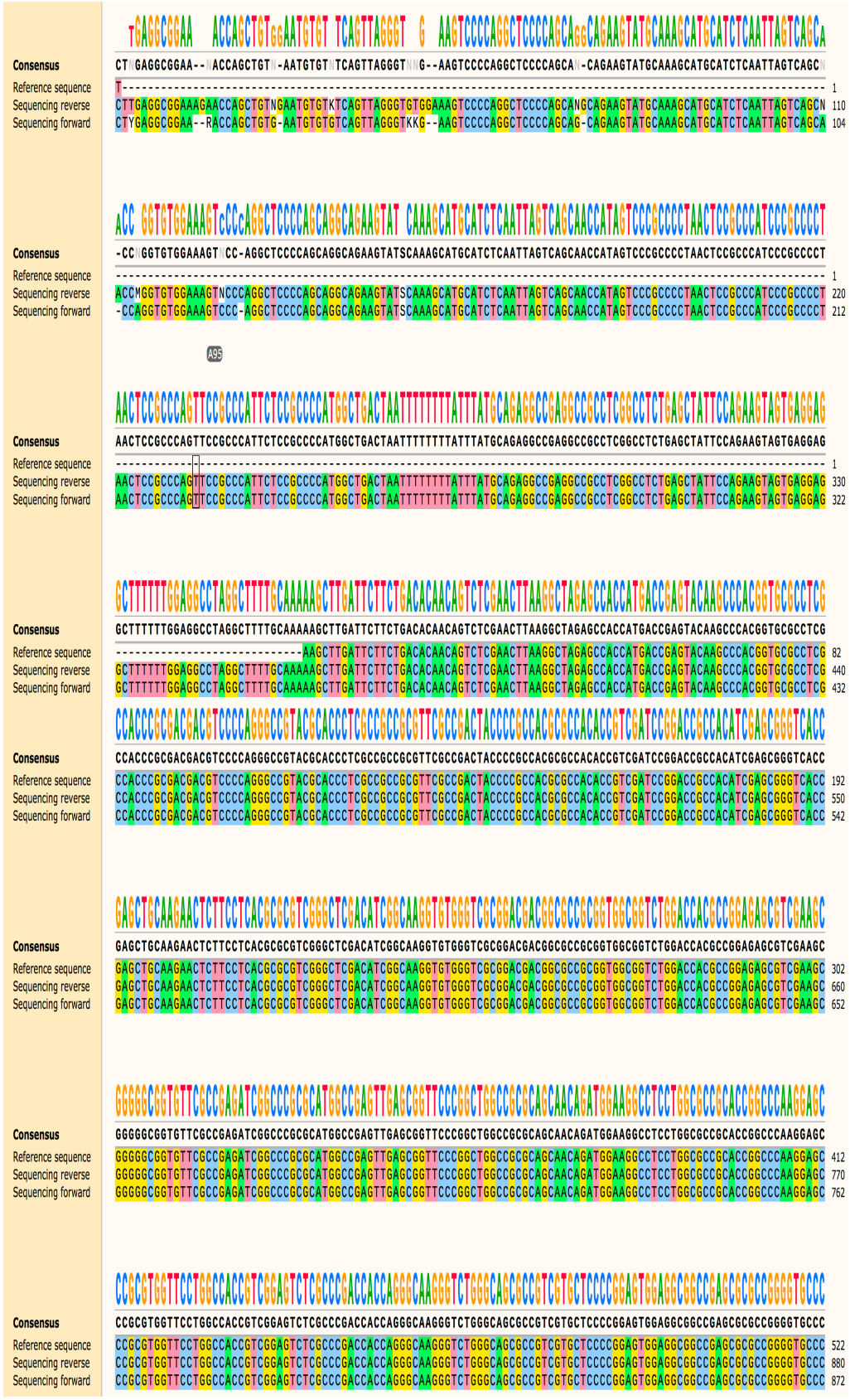
Consensus
Reference sequence
Sequencing reverse
Sequencing forward
A95

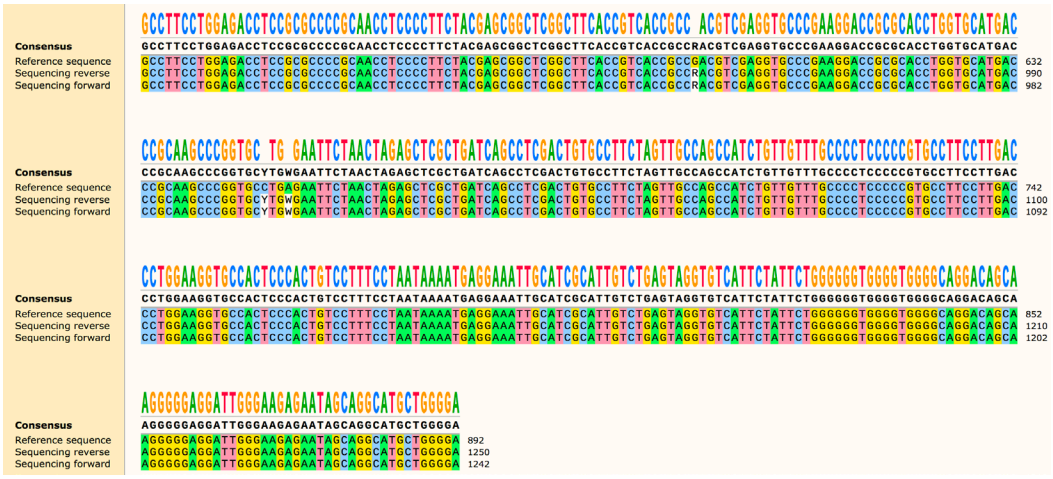

<u>Supplementary figure 2.</u> Sequence alignment of the Puromycin sequence in the OVA gene drive. *The region was sequenced in multiple fragments and aligned against the reference sequence to produce a consensus sequence. Figure produced in SnapGene.*

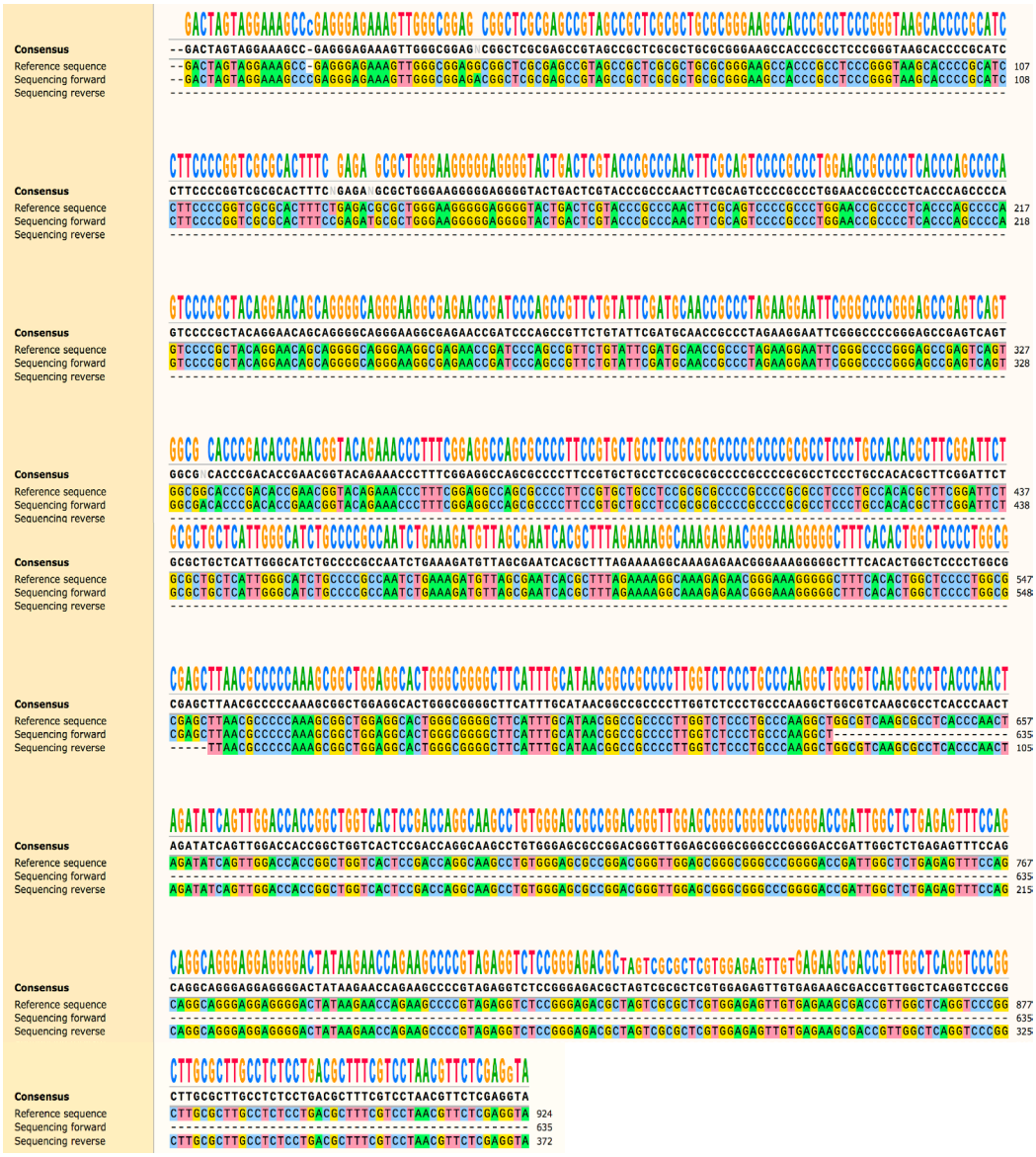

Supplementary figure 3. ***Sequence alignment of the HSPA2 promoter in the OVA gene drive.*** *The two sequences generated in sequencing were aligned against the reference sequence to produce a consensus sequence. Figure produced in SnapGene.*

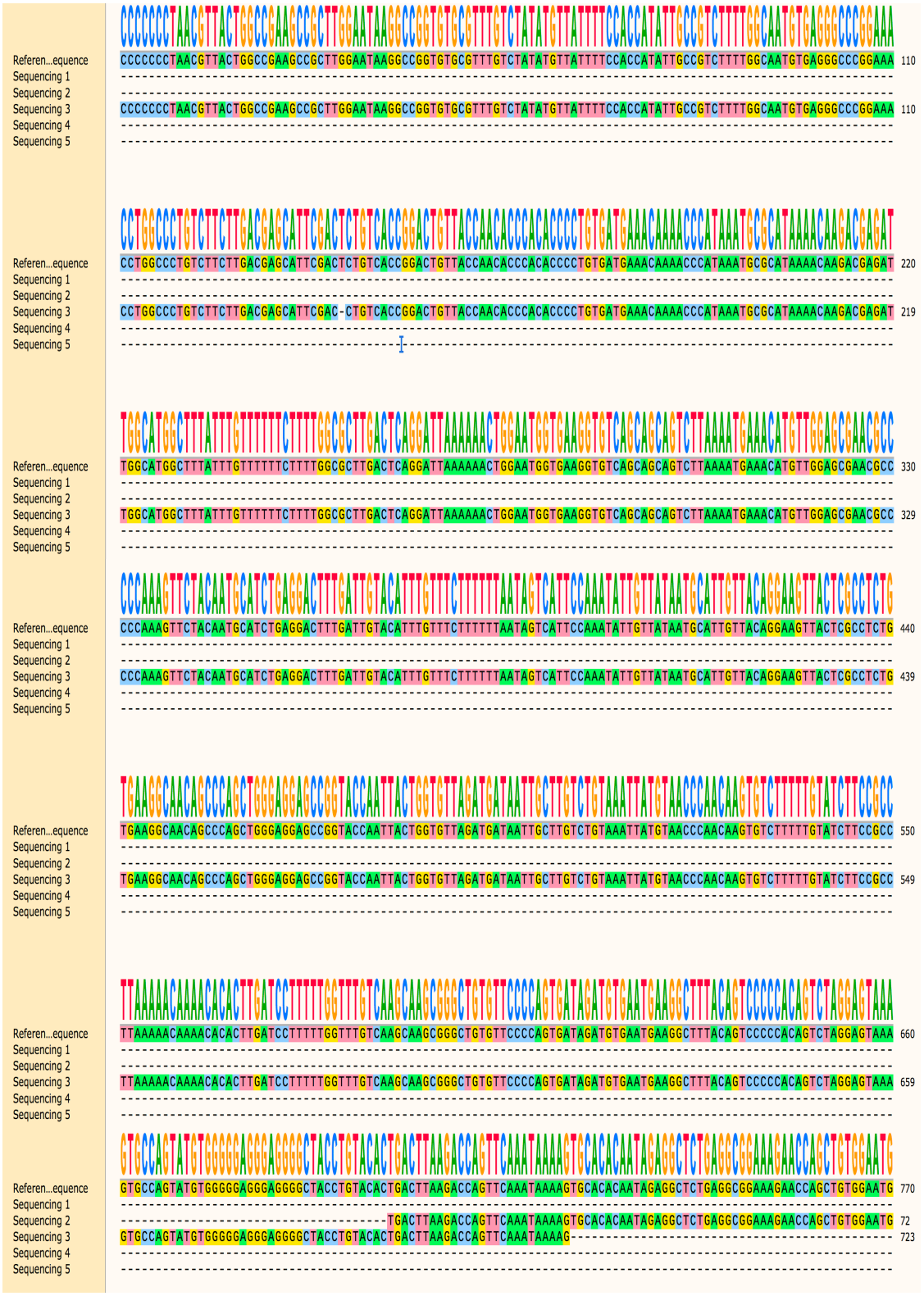
Referen...equence
Sequencing 1
Sequencing 2
Sequencing 3
Sequencing 4
Sequencing 5
CCCCCCCTAACGTTACTGGCCGAAGCCGCTTGGAATAAGGCCGGTGTGCGTTTGTCTATATGTTATTTTCCACCATATTGCCGTCTTTTGGCAATGTGAGGGCCCGGAAA 110
CCTGGCCCTGTCTTCTTGACGAGCATTCGACTCTGTCACCGGACTGTTACCAACACCCACACCCCTGTGATGAAACAAAACCCATAAATGCGCATAAAACAAGACGAGAT 220
CCTGGCCCTGTCTTCTTGACGAGCATTCGAC-CTGTCACCGGACTGTTACCAACACCCACACCCCTGTGATGAAACAAAACCCATAAATGCGCATAAAACAAGACGAGAT 219
TGGCATGGCTTTATTTGTTTTTTCTTTTGGCGCTTGACTCAGGATTAAAAAACTGGAATGGTGAAGGTGTCAGCAGCAGTCTTAAAATGAAACATGTTGGAGCGAACGCC 330
TGGCATGGCTTTATTTGTTTTTTCTTTTGGCGCTTGACTCAGGATTAAAAAACTGGAATGGTGAAGGTGTCAGCAGCAGTCTTAAAATGAAACATGTTGGAGCGAACGCC 329
CCCAAAGTTCTACAATGCATCTGAGGACTTTGATTGTACATTTGTTTCTTTTTTAATAGTCATTCCAAATATTGTTATAATGCATTGTTACAGGAAGTTACTCGCCTCTG 440
CCCAAAGTTCTACAATGCATCTGAGGACTTTGATTGTACATTTGTTTCTTTTTTAATAGTCATTCCAAATATTGTTATAATGCATTGTTACAGGAAGTTACTCGCCTCTG 439
TGAAGGCAACAGCCCAGCTGGGAGGAGCCGGTACCAATTACTGGTGTTAGATGATAATTGCTTGTCTGTAAATTATGTAACCCAACAAGTGTCTTTTTGTATCTTCCGCC 550
TGAAGGCAACAGCCCAGCTGGGAGGAGCCGGTACCAATTACTGGTGTTAGATGATAATTGCTTGTCTGTAAATTATGTAACCCAACAAGTGTCTTTTTGTATCTTCCGCC 549
TTAAAAACAAAACACACTTGATCCTTTTTGGTTTGTCAAGCAAGCGGGCTGTGTTCCCCAGTGATAGATGTGAATGAAGGCTTTACAGTCCCCCACAGTCTAGGAGTAAA 660
TTAAAAACAAAACACACTTGATCCTTTTTGGTTTGTCAAGCAAGCGGGCTGTGTTCCCCAGTGATAGATGTGAATGAAGGCTTTACAGTCCCCCACAGTCTAGGAGTAAA 659
GTGCCAGTATGTGGGGGAGGGAGGGGCTACCTGTACACTGACTTAAGACCAGTTCAAATAAAAGTGCACACAATAGAGGCTCTGAGGCGGAAAGAACCAGCTGTGGAATG 770
GTGCCAGTATGTGGGGGAGGGAGGGGCTACCTGTACACTGACTTAAGACCAGTTCAAATAAAAG 723

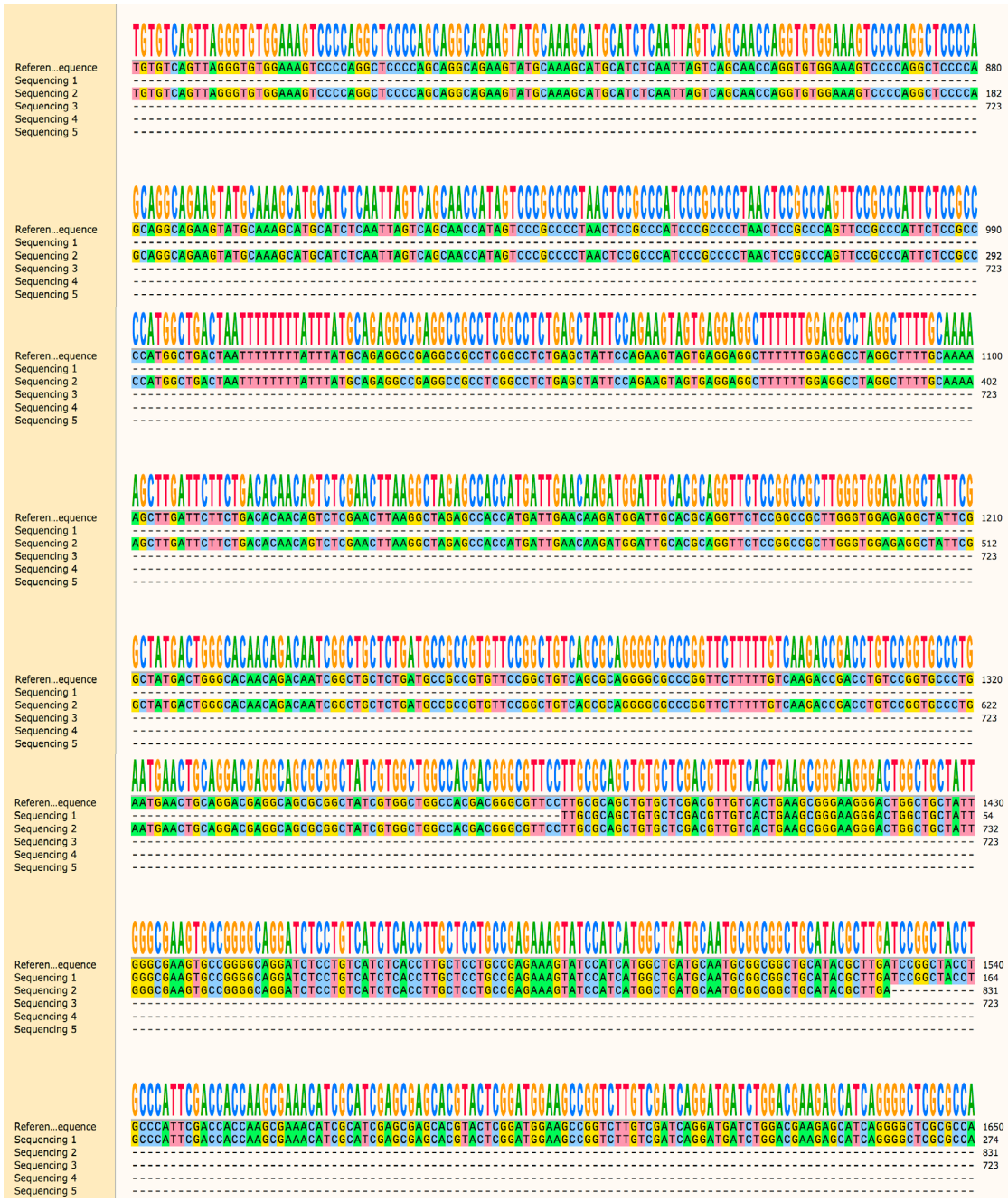
Referen...equence
Sequencing 1
Sequencing 2
Sequencing 3
Sequencing 4
Sequencing 5
880
182
723
990
292
723
1100
402
723
1210
512
723
1320
622
723
1430
54
732
723
1540
164
831
723
1650
274
831
723

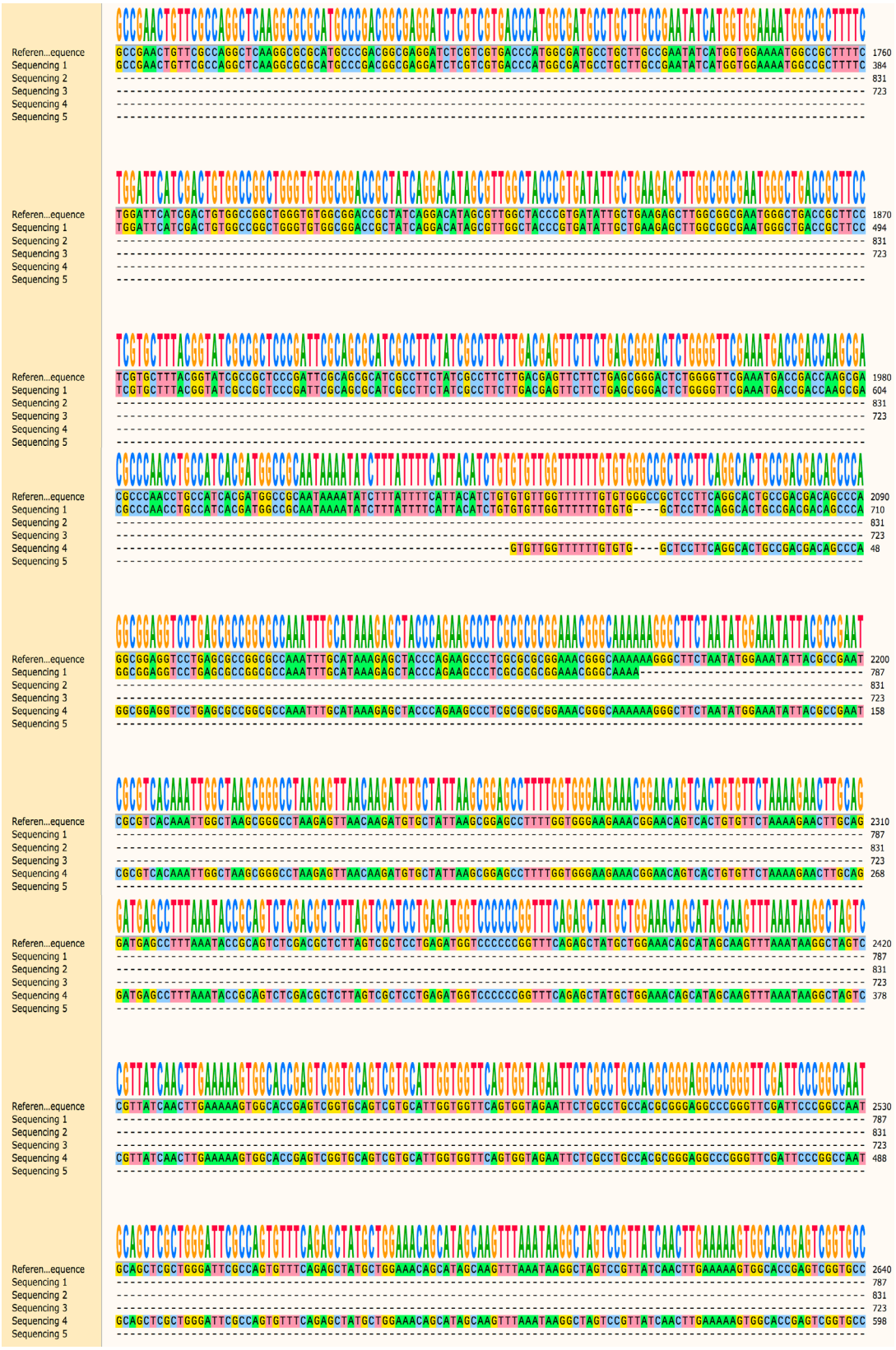
Referen...equence
Sequencing 1
Sequencing 2
Sequencing 3
Sequencing 4
Sequencing 5

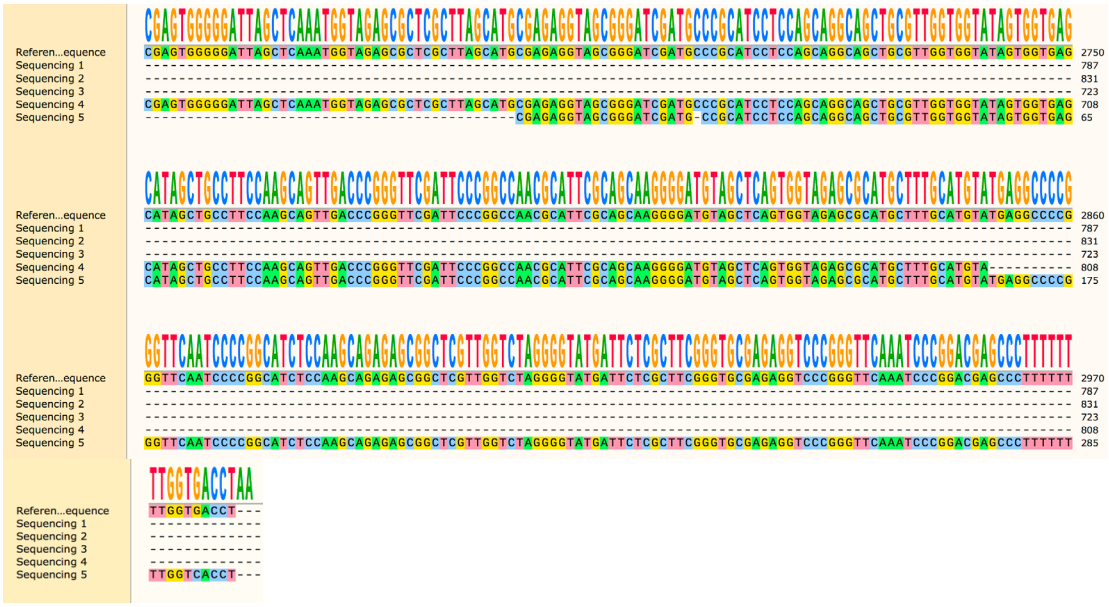

Supplementary figure 4. ***Sequence alignment beginning at Neomycin antibiotic region and ending at the end of the downstream OVM gRNA cassette.*** *The region was sequenced in multiple fragments and aligned against the reference sequence. Figure produced in SnapGene.*

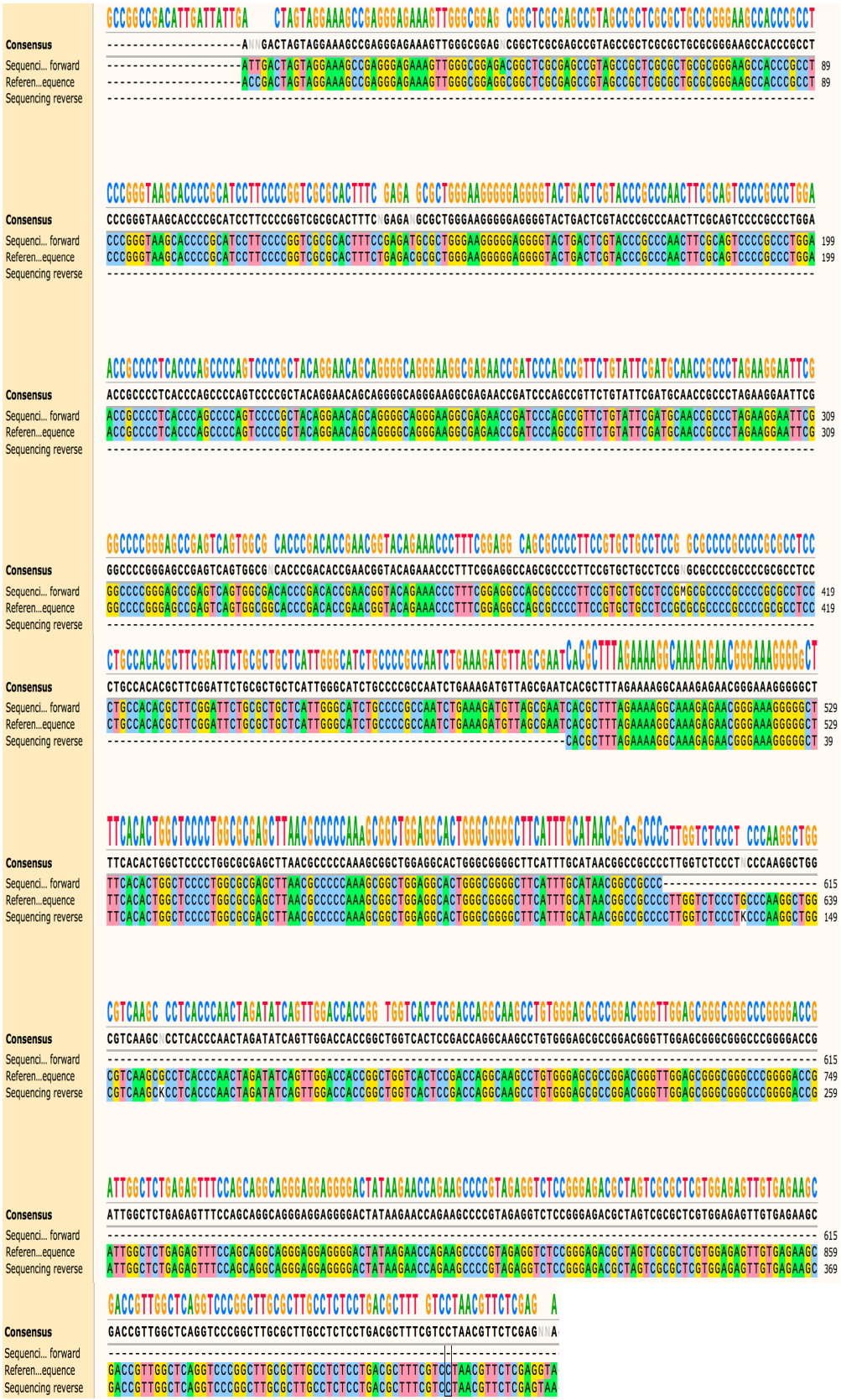

Supplementary figure 5. ***Sequence alignment of the HSPA2 promoter in the OVM gene drive.*** *The two forward and reverse sequences generated in sequencing were aligned against the reference sequence to produce a consensus sequence. Figure produced in SnapGene.*

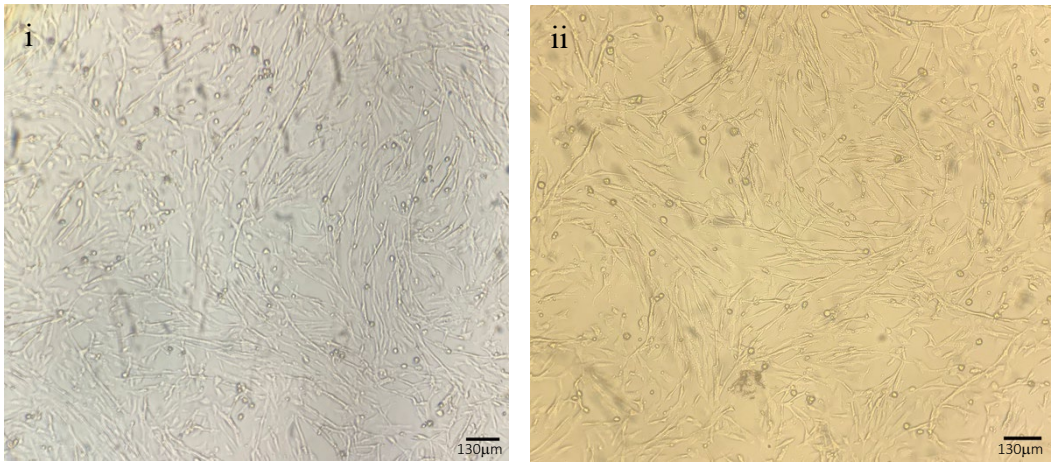

Supplementary figure 6. Cultured CEFs after extraction from chicken embryos. *CEFs were extracted from day 10 chicken embryos and maintained in CEF media.* ***i)*** *CEFs 1 day after extraction from embryos, at passage zero. CEFs appear attached to the plate and exhibit typical fibroblast morphology as well as high confluency of ~80-90%.* ***ii)*** *CEFs prepared for use as a feeder layer: at this confluency of ~70-80% the cells were growth inhibited with mitomycin-C. Scale bar=130µm*

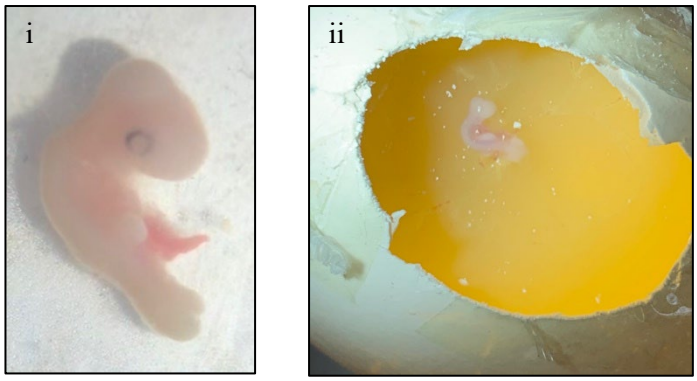

Supplementary figure 7. Developmental defects observed in embryos of the 1.7µg/µl busulfan treatment group. *At day 7.5 embryos showed stunted growth and death at the stage seen in figures. In* ***ii*** *growth is severely stunted and death occurred early in development.*

References

Adiguzel, C. *et al.* (2009) 'European community and US-FDA approval of recombinant human antithrombin produced in genetically altered goats', *Clinical and Applied Thrombosis/Hemostasis: Official Journal of the International Academy of Clinical and Applied Thrombosis/Hemostasis*, 15(6), pp. 645–651. Available at: https://doi.org/10.1177/1076029609339748.

Adivitiya, null and Khasa, Y.P. (2017) 'The evolution of recombinant thrombolytics: Current status and future directions', *Bioengineered*, 8(4), pp. 331–358. Available at: https://doi.org/10.1080/21655979.2016.1229718.

Aige-Gil, V. and Simkiss, K. (1991) 'Sterilising embryos for transgenic chimaeras', *British Poultry Science*, 32(3), pp. 427–438. Available at: https://doi.org/10.1080/00071669108417368.

Akinyemi, R.O. *et al.* (2021) 'Stroke in Africa: profile, progress, prospects and priorities', *Nature Reviews Neurology*, 17(10), pp. 634–656. Available at: https://doi.org/10.1038/s41582-021-00542-4.

Altgilbers, S. *et al.* (2021) 'Cultivation and characterization of primordial germ cells from blue layer hybrids (Araucana crossbreeds) and generation of germline chimeric chickens', *Scientific Reports*, 11(1), p. 12923. Available at: https://doi.org/10.1038/s41598-021-91490-y.

Anand, M. *et al.* (2018) 'Enhancement of chicken primordial germ cell in vitro maintenance using an automated cell image analyser', *Acta Veterinaria Hungarica*, 66(4), pp. 518–529. Available at: https://doi.org/10.1556/004.2018.046.

Arif, A. *et al.* (2015) 'Production of human interferon alpha-2b in Escherichia coli and removal of N-terminal methionine utilizing archaeal methionine aminopeptidase', *Biologia*, 70(7), pp. 982–987. Available at: https://doi.org/10.1515/biolog-2015-0113.

Babaeipour, V., Shojaosadati, S.A. and Maghsoudi, N. (2013) 'Maximizing Production of Human Interferon-γ in HCDC of Recombinant E. coli', *Iranian journal of pharmaceutical research: IJPR*, 12(3), pp. 563–572.

Baeshen, M.N. *et al.* (2015) 'Production of Biopharmaceuticals in E. coli: Current Scenario and Future Perspectives', *Journal of Microbiology and Biotechnology*, 25(7), pp. 953–962. Available at: https://doi.org/10.4014/jmb.1412.12079.

Bahrami, S. *et al.* (2020) 'Designing A Transgenic Chicken: Applying New Approaches toward A Promising Bioreactor', *Cell Journal*, 22(2), pp. 133–139. Available at: https://doi.org/10.22074/cellj.2020.6738.

Bai, M. *et al.* (2016) 'Spermatogenic Cell-Specific Gene Mutation in Mice via CRISPR-Cas9', *Journal of Genetics and Genomics*, 43(5), pp. 289–296. Available at: https://doi.org/10.1016/j.jgg.2016.02.003.

Bednarczyk, M. *et al.* (2018) 'Generation of transgenic chickens by the non-viral, cell-based method: effectiveness of some elements of this strategy', *Journal of Applied Genetics*, 59(1), pp. 81–89. Available at: https://doi.org/10.1007/s13353-018-0429-6.

van Beers, M.M.C. and Bardor, M. (2012) 'Minimizing immunogenicity of biopharmaceuticals by controlling critical quality attributes of proteins', *Biotechnology Journal*, 7(12), pp. 1473–1484. Available at: https://doi.org/10.1002/biot.201200065.

Bertolini, L.R. *et al.* (2016) 'The transgenic animal platform for biopharmaceutical production', *Transgenic Research*, 25(3), pp. 329–343. Available at: https://doi.org/10.1007/s11248-016-9933-9.

Bhatwa, A. *et al.* (2021) 'Challenges Associated With the Formation of Recombinant Protein Inclusion Bodies in Escherichia coli and Strategies to Address Them for Industrial Applications', *Frontiers in Bioengineering and Biotechnology*, 9, p. 630551. Available at: https://doi.org/10.3389/fbioe.2021.630551.

Bhaya, D., Davison, M. and Barrangou, R. (2011) 'CRISPR-Cas systems in bacteria and archaea: versatile small RNAs for adaptive defense and regulation', *Annual Review of Genetics*, 45, pp. 273–297. Available at: https://doi.org/10.1146/annurev-genet-110410-132430.

Bis, R.L. *et al.* (2014) 'High yield soluble bacterial expression and streamlined purification of recombinant human interferon α-2a', *Protein Expression and Purification*, 99, pp. 138–146. Available at: https://doi.org/10.1016/j.pep.2014.04.010.

Bischoff, N. *et al.* (2020) 'Improving Precise CRISPR Genome Editing by Small Molecules: Is there a Magic Potion?', *Cells*, 9(5), p. 1318. Available at: https://doi.org/10.3390/cells9051318.

Bosques, C.J. *et al.* (2010) 'Chinese hamster ovary cells can produce galactose-α-1,3-galactose antigens on proteins', *Nature Biotechnology*, 28(11), pp. 1153–1156. Available at: https://doi.org/10.1038/nbt1110-1153.

Breitbach, K. and Jarvis, D.L. (2001) 'Improved glycosylation of a foreign protein by Tn-5B1-4 cells engineered to express mammalian glycosyltransferases', *Biotechnology and Bioengineering*, 74(3), pp. 230–239. Available at: https://doi.org/10.1002/bit.1112.

Brogard, J.M., Blickle, J.F. and Paris-Bockel, D. (1985) 'Genetically engineered insulin: five years of experience', *Drugs Under Experimental and Clinical Research*, 11(6), pp. 397–406.

Browne, S.M. and Al-Rubeai, M. (2009) 'Selection Methods for High-Producing Mammalian Cell Lines', in Mohamed Al-Rubeai (ed.) *Cell Line Development*. Dordrecht: Springer Netherlands (Cell Engineering), pp. 127–151. Available at: https://doi.org/10.1007/978-90-481-2245-5_7.

Byun, S.J. *et al.* (2011) 'Oviduct-Specific Enhanced Green Fluorescent Protein Expression in Transgenic Chickens', *Bioscience, Biotechnology, and Biochemistry*, 75(4), pp. 646–649. Available at: https://doi.org/10.1271/bbb.100721.

Carcao, M. *et al.* (2018) 'Recombinant FXIII (rFXIII-A2) Prophylaxis Prevents Bleeding and Allows for Surgery in Patients with Congenital FXIII A-Subunit Deficiency', *Thrombosis and Haemostasis*, 118(03), pp. 451–460. Available at: https://doi.org/10.1055/s-0038-1624581.

Caubet, J.-C. and Wang, J. (2011) 'Current Understanding of Egg Allergy', *Pediatric Clinics of North America*, 58(2), pp. 427–443. Available at: https://doi.org/10.1016/j.pcl.2011.02.014.

Champer, J. *et al.* (2020) 'A CRISPR homing gene drive targeting a haplolethal gene removes resistance alleles and successfully spreads through a cage population', *Proceedings of the National Academy of Sciences*, 117(39), pp. 24377–24383. Available at: https://doi.org/10.1073/pnas.2004373117.

Chen, C.-Y. *et al.* (2011) 'Baculovirus as a gene delivery vector: Recent understandings of molecular alterations in transduced cells and latest applications', *Biotechnology Advances*, 29(6), pp. 618–631. Available at: https://doi.org/10.1016/j.biotechadv.2011.04.004.

Chen, X. *et al.* (2016) 'Probing the impact of chromatin conformation on genome editing tools', *Nucleic Acids Research*, 44(13), pp. 6482–6492. Available at: https://doi.org/10.1093/nar/gkw524.

Cheon, S.A. *et al.* (2012) 'Remodeling of the glycosylation pathway in the methylotrophic yeast Hansenula polymorpha to produce human hybrid-type N-glycans', *The Journal of Microbiology*, 50(2), pp. 341–348. Available at: https://doi.org/10.1007/s12275-012-2097-2.

Choi, B.-K. *et al.* (2003) 'Use of combinatorial genetic libraries to humanize N-linked glycosylation in the yeast Pichia pastoris', *Proceedings of the National Academy of Sciences of the United States of America*, 100(9), pp. 5022–5027. Available at: https://doi.org/10.1073/pnas.0931263100.

Choi, J.W. *et al.* (2010) 'Basic fibroblast growth factor activates MEK/ERK cell signaling pathway and stimulates the proliferation of chicken primordial germ cells', *PloS One*, 5(9), p. e12968. Available at: https://doi.org/10.1371/journal.pone.0012968.

Chojnacka-Puchta, L. *et al.* (2015) 'Obtaining chicken primordial germ cells used for gene transfer: in vitro and in vivo results', *Journal of Applied Genetics*, 56(4), pp. 493–504. Available at: https://doi.org/10.1007/s13353-015-0276-7.

Chrunyk, B.A. *et al.* (1993) 'Inclusion body formation and protein stability in sequence variants of interleukin-1 beta', *The Journal of Biological Chemistry*, 268(24), pp. 18053–18061.

Chu, V.T. *et al.* (2015) 'Increasing the efficiency of homology-directed repair for CRISPR-Cas9-induced precise gene editing in mammalian cells', *Nature Biotechnology*, 33(5), pp. 543–548. Available at: https://doi.org/10.1038/nbt.3198.

Clinton, M. *et al.* (2001) 'Sexing chick embryos: A rapid and simple protocol', *British Poultry Science*, 42(1), pp. 134–138. Available at: https://doi.org/10.1080/713655025.

Cong, L. *et al.* (2013) 'Multiplex Genome Engineering Using CRISPR/Cas Systems', *Science*, 339(6121), pp. 819–823. Available at: https://doi.org/10.1126/science.1231143.

Cooke, S.K. and Sampson, H.A. (1997) 'Allergenic properties of ovomucoid in man', *Journal of Immunology (Baltimore, Md.: 1950)*, 159(4), pp. 2026–2032.

Cox, M.M.J. (2012) 'Recombinant protein vaccines produced in insect cells', *Vaccine*, 30(10), pp. 1759–1766. Available at: https://doi.org/10.1016/j.vaccine.2012.01.016.

Cox, M.M.J. (2021) 'Innovations in the Insect Cell Expression System for Industrial Recombinant Vaccine Antigen Production', *Vaccines*, 9(12), p. 1504. Available at: https://doi.org/10.3390/vaccines9121504.

Cox, M.M.J. and Hollister, J.R. (2009) 'FluBlok, a next generation influenza vaccine manufactured in insect cells', *Biologicals*, 37(3), pp. 182–189. Available at: https://doi.org/10.1016/j.biologicals.2009.02.014.

Dahodwala, H. and Lee, K.H. (2019) 'The fickle CHO: a review of the causes, implications, and potential alleviation of the CHO cell line instability problem', *Current Opinion in Biotechnology*, 60, pp. 128–137. Available at: https://doi.org/10.1016/j.copbio.2019.01.011.

Di Primio, C. *et al.* (2005) 'Potentiation of gene targeting in human cells by expression of Saccharomyces cerevisiae Rad52', *Nucleic Acids Research*, 33(14), pp. 4639–4648. Available at: https://doi.org/10.1093/nar/gki778.

Dingermann, T. (2008) 'Recombinant therapeutic proteins: Production platforms and challenges', *Biotechnology Journal*, 3(1), pp. 90–97. Available at: https://doi.org/10.1002/biot.200700214.

Dix, D.J., Rosario-Herrle, M., *et al.* (1996) 'Developmentally regulated expression of Hsp70-2 and a Hsp70-2/lacZ transgene during spermatogenesis', *Developmental Biology*, 174(2), pp. 310–321. Available at: https://doi.org/10.1006/dbio.1996.0076.

Dix, D.J., Allen, J.W., *et al.* (1996) 'Targeted gene disruption of Hsp70-2 results in failed meiosis, germ cell apoptosis, and male infertility', *Proceedings of the National Academy of Sciences of the United States of America*, 93(8), pp. 3264–3268. Available at: https://doi.org/10.1073/pnas.93.8.3264.

Dix, D.J. *et al.* (1997) 'HSP70-2 is required for desynapsis of synaptonemal complexes during meiotic prophase in juvenile and adult mouse spermatocytes', *Development (Cambridge, England)*, 124(22), pp. 4595–4603. Available at: https://doi.org/10.1242/dev.124.22.4595.

Drury, D.W. *et al.* (2017) 'CRISPR/Cas9 gene drives in genetically variable and nonrandomly mating wild populations', *Science Advances*, 3(5), p. e1601910. Available at: https://doi.org/10.1126/sciadv.1601910.

Dyck, M.K. *et al.* (2003) 'Making recombinant proteins in animals--different systems, different applications', *Trends in Biotechnology*, 21(9), pp. 394–399. Available at: https://doi.org/10.1016/S0167-7799(03)00190-2.

Enguita-Marruedo, A. *et al.* (2019) 'Transition from a meiotic to a somatic-like DNA damage response during the pachytene stage in mouse meiosis', *PLOS Genetics*. Edited by P.E. Cohen, 15(1), p. e1007439. Available at: https://doi.org/10.1371/journal.pgen.1007439.

Esvelt, K.M. *et al.* (2014) 'Concerning RNA-guided gene drives for the alteration of wild populations', *eLife*, 3, p. e03401. Available at: https://doi.org/10.7554/eLife.03401.

Faraghat, S.A. *et al.* (2017) 'High-throughput, low-loss, low-cost, and label-free cell separation using electrophysiology-activated cell enrichment', *Proceedings of the National Academy of Sciences of the United States of America*, 114(18), pp. 4591–4596. Available at: https://doi.org/10.1073/pnas.1700773114.

Farzaneh, M. *et al.* (2017) 'The evolution of chicken stem cell culture methods', *British Poultry Science*, 58(6), pp. 681–686. Available at: https://doi.org/10.1080/00071668.2017.1365354.

Feichtinger, J. *et al.* (2016) 'Comprehensive genome and epigenome characterization of CHO cells in response to evolutionary pressures and over time', *Biotechnology and Bioengineering*, 113(10), pp. 2241–2253. Available at: https://doi.org/10.1002/bit.25990.

Felberbaum, R.S. (2015) 'The baculovirus expression vector system: A commercial manufacturing platform for viral vaccines and gene therapy vectors', *Biotechnology Journal*, 10(5), pp. 702–714. Available at: https://doi.org/10.1002/biot.201400438.

Fernandes, B. *et al.* (2020) 'Adaptive laboratory evolution of stable insect cell lines for improved HIV-Gag VLPs production', *Journal of Biotechnology*, 307, pp. 139–147. Available at: https://doi.org/10.1016/j.jbiotec.2019.10.004.

Ferrer-Miralles, N. *et al.* (2009) 'Microbial factories for recombinant pharmaceuticals', *Microbial Cell Factories*, 8(1), p. 17. Available at: https://doi.org/10.1186/1475-2859-8-17.

Fischer, R. *et al.* (2018) 'Glyco-Engineering of Plant-Based Expression Systems', in E. Rapp and U. Reichl (eds) *Advances in Glycobiotechnology*. Cham: Springer International Publishing (Advances in Biochemical Engineering/Biotechnology), pp. 137–166. Available at: https://doi.org/10.1007/10_2018_76.

Fischer, S., Handrick, R. and Otte, K. (2015) 'The art of CHO cell engineering: A comprehensive retrospect and future perspectives', *Biotechnology Advances*, 33(8), pp. 1878–1896. Available at: https://doi.org/10.1016/j.biotechadv.2015.10.015.

Francis, D.M. and Page, R. (2010) 'Strategies to optimize protein expression in E. coli', *Current Protocols in Protein Science*, Chapter 5, p. Unit 5.24.1-29. Available at: https://doi.org/10.1002/0471140864.ps0524s61.

Fujimoto, T., Ukeshima, A. and Kiyofuji, R. (1976) 'The origin, migration and morphology of the primordial germ cells in the chick embryo', *The Anatomical Record*, 185(2), pp. 139–145. Available at: https://doi.org/10.1002/ar.1091850203.

Gakidou, E. *et al.* (2017) 'Global, regional, and national comparative risk assessment of 84 behavioural, environmental and occupational, and metabolic risks or clusters of risks, 1990–2016: a systematic analysis for the Global Burden of Disease Study 2016', *The Lancet*, 390(10100), pp. 1345–1422. Available at: https://doi.org/10.1016/S0140-6736(17)32366-8.

Gantz, V.M. *et al.* (2015) 'Highly efficient Cas9-mediated gene drive for population modification of the malaria vector mosquito Anopheles stephensi', *Proceedings of the National Academy of Sciences of the United States of America*, 112(49), pp. E6736-6743. Available at: https://doi.org/10.1073/pnas.1521077112.

Gil, G.-C., Velander, W.H. and Van Cott, K.E. (2008) 'Analysis of the N-glycans of recombinant human Factor IX purified from transgenic pig milk', *Glycobiology*, 18(7), pp. 526–539. Available at: https://doi.org/10.1093/glycob/cwn035.

Ginsburg, M. and Eyal-Giladi, H. (1987) ‘Primordial germ cells of the young chick blastoderm originate from the central zone of the area pellucida irrespective of the embryo-forming process’, *Development*, 101(2), pp. 209–219. Available at: https://doi.org/10.1242/dev.101.2.209.

Goeddel, D.V. *et al.* (1979) ‘Expression in Escherichia coli of chemically synthesized genes for human insulin’, *Proceedings of the National Academy of Sciences of the United States of America*, 76(1), pp. 106–110. Available at: https://doi.org/10.1073/pnas.76.1.106.

Grillberger, L. *et al.* (2009) ‘Emerging trends in plasma-free manufacturing of recombinant protein therapeutics expressed in mammalian cells’, *Biotechnology Journal*, 4(2), pp. 186–201. Available at: https://doi.org/10.1002/biot.200800241.

Grunwald, H.A. *et al.* (2019) ‘Super-Mendelian inheritance mediated by CRISPR–Cas9 in the female mouse germline’, *Nature*, 566(7742), pp. 105–109. Available at: https://doi.org/10.1038/s41586-019-0875-2.

Gupta, V. *et al.* (2017) ‘Production of Recombinant Pharmaceutical Proteins’, in Gupta, V. et al., *Basic and Applied Aspects of Biotechnology*. Singapore: Springer Singapore, pp. 77–101. Available at: https://doi.org/10.1007/978-981-10-0875-7_4.

Hamburger, V. and Hamilton, H.L. (1951) ‘A series of normal stages in the development of the chick embryo’, *Journal of Morphology*, 88(1), pp. 49–92.

Hamilton, S.R. *et al.* (2013) ‘Production of sialylated O-linked glycans in Pichia pastoris’, *Glycobiology*, 23(10), pp. 1192–1203. Available at: https://doi.org/10.1093/glycob/cwt056.

Hammond, A. *et al.* (2016) ‘A CRISPR-Cas9 gene drive system targeting female reproduction in the malaria mosquito vector Anopheles gambiae’, *Nature Biotechnology*, 34(1), pp. 78–83. Available at: https://doi.org/10.1038/nbt.3439.

Han, J.Y. and Lee, B.R. (2017) ‘Isolation and Characterization of Chicken Primordial Germ Cells and Their Application in Transgenesis’, in G. Sheng (ed.) *Avian and Reptilian Developmental Biology*. New York, NY: Springer New York (Methods in Molecular Biology), pp. 229–242. Available at: https://doi.org/10.1007/978-1-4939-7216-6_15.

Han, J.Y. and Park, Y.H. (2018) 'Primordial germ cell-mediated transgenesis and genome editing in birds', *Journal of Animal Science and Biotechnology*, 9(1), p. 19. Available at: https://doi.org/10.1186/s40104-018-0234-4.

Harvey, A. and Ivarie, R. (2003) 'Validating the hen as a bioreactor for the production of exogenous proteins in egg white', *Poultry Science*, 82(6), pp. 927–930. Available at: https://doi.org/10.1093/ps/82.6.927.

Hassan, M.S.H. and Abdul-Careem, M.F. (2020) 'Avian Viruses that Impact Table Egg Production', *Animals*, 10(10), p. 1747. Available at: https://doi.org/10.3390/ani10101747.

Hermeling, S. *et al.* (2004) 'Structure-Immunogenicity Relationships of Therapeutic Proteins', *Pharmaceutical Research*, 21(6), pp. 897–903. Available at: https://doi.org/10.1023/B:PHAM.0000029275.41323.a6.

Herron, L.R. *et al.* (2018) 'A chicken bioreactor for efficient production of functional cytokines', *BMC Biotechnology*, 18(1), p. 82. Available at: https://doi.org/10.1186/s12896-018-0495-1.

Heyer, W.-D., Ehmsen, K.T. and Liu, J. (2010) 'Regulation of Homologous Recombination in Eukaryotes', *Annual Review of Genetics*, 44(1), pp. 113–139. Available at: https://doi.org/10.1146/annurev-genet-051710-150955.

Hong, M. *et al.* (2022) 'Genetic engineering of baculovirus-insect cell system to improve protein production', *Frontiers in Bioengineering and Biotechnology*, 10, p. 994743. Available at: https://doi.org/10.3389/fbioe.2022.994743.

Horiuchi, H. *et al.* (2004) 'Chicken leukemia inhibitory factor maintains chicken embryonic stem cells in the undifferentiated state', *The Journal of Biological Chemistry*, 279(23), pp. 24514–24520. Available at: https://doi.org/10.1074/jbc.M313231200.

Houdebine, L.-M. (2009) 'Production of pharmaceutical proteins by transgenic animals', *Comparative Immunology, Microbiology and Infectious Diseases*, 32(2), pp. 107–121. Available at: https://doi.org/10.1016/j.cimid.2007.11.005.

Hwang, H.-G. *et al.* (2016) 'Recombinant Glargine Insulin Production Process Using Escherichia coli', *Journal of Microbiology and Biotechnology*, 26(10), pp. 1781–1789. Available at: https://doi.org/10.4014/jmb.1602.02053.

Inselman, A.L. *et al.* (2009) 'Heat shock protein 2 promoter drives cre expression in spermatocytes of transgenic mice', *genesis*, p. NA-NA. Available at: https://doi.org/10.1002/dvg.20588.

Irons, S.L. *et al.* (2018) 'Protein Production using the Baculovirus Expression System', *Current Protocols in Protein Science*, 91(1). Available at: https://doi.org/10.1002/cpps.45.

Jayathilaka, K. *et al.* (2008) 'A chemical compound that stimulates the human homologous recombination protein RAD51', *Proceedings of the National Academy of Sciences of the United States of America*, 105(41), pp. 15848–15853. Available at: https://doi.org/10.1073/pnas.0808046105.

Jia, B. and Jeon, C.O. (2016) 'High-throughput recombinant protein expression in *Escherichia coli* : current status and future perspectives', *Open Biology*, 6(8), p. 160196. Available at: https://doi.org/10.1098/rsob.160196.

Jinek, M. *et al.* (2012) 'A Programmable Dual-RNA–Guided DNA Endonuclease in Adaptive Bacterial Immunity', *Science*, 337(6096), pp. 816–821. Available at: https://doi.org/10.1126/science.1225829.

Johnson, J. and Merck & Co (2017) 'Evolve With Flexibility - pharmaceutical-technology.com', *Evolve With Flexibility: Advancing Single-Use Technology With Industry Collaboration*. Available at: https://pharmaceutical-technology.com/wp-content/uploads/sites/24/2018/02/Evolve-with-flexibility-single-use-eBook-KA342EB010417EB.pdf (Accessed: 24 December 2022).

Jung, J.G. *et al.* (2005) 'Development of Novel Markers for the Characterization of Chicken Primordial Germ Cells', *STEM CELLS*, 23(5), pp. 689–698. Available at: https://doi.org/10.1634/stemcells.2004-0208.

Kagami, H. *et al.* (1997) 'The developmental origin of primordial germ cells and the transmission of the donor-derived gametes in mixed-sex germline chimeras to the offspring

in the chicken', *Molecular Reproduction and Development*, 48(4), pp. 501–510. Available at: https://doi.org/10.1002/(SICI)1098-2795(199712)48:4<501::AID-MRD11>3.0.CO;2-W.

Keefer, C.L. *et al.* (2001) 'Generation of Dwarf Goat (Capra hircus) Clones Following Nuclear Transfer with Transfected and Nontransfected Fetal Fibroblasts and In Vitro-Matured Oocytes1', *Biology of Reproduction*, 64(3), pp. 849–856. Available at: https://doi.org/10.1095/biolreprod64.3.849.

Kim, J.N. *et al.* (2004) 'Enriched gonadal migration of donor-derived gonadal primordial germ cells by immunomagnetic cell sorting in birds', *Molecular Reproduction and Development*, 68(1), pp. 81–87. Available at: https://doi.org/10.1002/mrd.20051.

Kim, Y.M. and Han, J.Y. (2018) 'The early development of germ cells in chicken', *The International Journal of Developmental Biology*, 62(1-2–3), pp. 145–152. Available at: https://doi.org/10.1387/ijdb.170283jh.

Kovacs-Nolan, J. *et al.* (2000) 'Immunochemical and Structural Analysis of Pepsin-Digested Egg White Ovomucoid', *Journal of Agricultural and Food Chemistry*, 48(12), pp. 6261–6266. Available at: https://doi.org/10.1021/jf000358e.

Kulagina, N. *et al.* (2021) 'Yeasts as Biopharmaceutical Production Platforms', *Frontiers in Fungal Biology*, 2, p. 733492. Available at: https://doi.org/10.3389/ffunb.2021.733492.

Kurihara, T. *et al.* (2020) 'DNA repair protein RAD51 enhances the CRISPR/Cas9-mediated knock-in efficiency in brain neurons', *Biochemical and Biophysical Research Communications*, 524(3), pp. 621–628. Available at: https://doi.org/10.1016/j.bbrc.2020.01.132.

Kwon, M.S. *et al.* (2018) 'Generation of transgenic chickens expressing the human erythropoietin (hEPO) gene in an oviduct-specific manner: Production of transgenic chicken eggs containing human erythropoietin in egg whites', *PLOS ONE*. Edited by X. Tian, 13(5), p. e0194721. Available at: https://doi.org/10.1371/journal.pone.0194721.

Lalonde, M.-E. and Durocher, Y. (2017) 'Therapeutic glycoprotein production in mammalian cells', *Journal of Biotechnology*, 251, pp. 128–140. Available at: https://doi.org/10.1016/j.jbiotec.2017.04.028.

Lamas-Toranzo, I. *et al.* (2020) 'RS-1 enhances CRISPR-mediated targeted knock-in in bovine embryos', *Molecular Reproduction and Development*, 87(5), pp. 542–549. Available at: https://doi.org/10.1002/mrd.23341.

Landgraf, W. and Sandow, J. (2016) 'Recombinant Human Insulins - Clinical Efficacy and Safety in Diabetes Therapy', *European Endocrinology*, 12(1), pp. 12–17. Available at: https://doi.org/10.17925/EE.2016.12.01.12.

van de Lavoir, M.-C. *et al.* (2006) 'Germline transmission of genetically modified primordial germ cells', *Nature*, 441(7094), pp. 766–769. Available at: https://doi.org/10.1038/nature04831.

van de Lavoir, M.-C. *et al.* (2012) 'Interspecific Germline Transmission of Cultured Primordial Germ Cells', *PLoS ONE*. Edited by O. El-Maarri, 7(5), p. e35664. Available at: https://doi.org/10.1371/journal.pone.0035664.

Lee, H.C. *et al.* (2013) 'Compensatory proliferation of endogenous chicken primordial germ cells after elimination by busulfan treatment', *Stem Cell Research & Therapy*, 4(6), p. 136. Available at: https://doi.org/10.1186/scrt347.

Lee, K.Y. *et al.* (2020) 'Highly elevated base excision repair pathway in primordial germ cells causes low base editing activity in chickens', *The FASEB Journal*, 34(12), pp. 15907–15921. Available at: https://doi.org/10.1096/fj.202001065RRR.

Lee, S.-Y. *et al.* (2020) 'Structural and functional characterization of recombinant human growth hormone isolated from transgenic pig milk', *PLOS ONE*. Edited by W.A. Kues, 15(7), p. e0236788. Available at: https://doi.org/10.1371/journal.pone.0236788.

Li, D. *et al.* (2019) 'Chicken Mesenchymal Stem Cells as Feeder Cells Facilitate the Cultivation of Primordial Germ Cells from Circulating Blood and Gonadal Ridge', *Stem Cell Discovery*, 09(01), pp. 1–14. Available at: https://doi.org/10.4236/scd.2019.91001.

Li, G. *et al.* (2017) 'Small molecules enhance CRISPR/Cas9-mediated homology-directed genome editing in primary cells', *Scientific Reports*, 7(1), p. 8943. Available at: https://doi.org/10.1038/s41598-017-09306-x.

Li, H. *et al.* (2011) 'A PCR amplification method without DNA extraction', *ELECTROPHORESIS*, 32(3–4), pp. 394–397. Available at: https://doi.org/10.1002/elps.201000392.

Li, H. *et al.* (2016) 'Genetic analysis of the clonal stability of Chinese hamster ovary cells for recombinant protein production', *Molecular bioSystems*, 12(1), pp. 102–109. Available at: https://doi.org/10.1039/c5mb00627a.

Lieber, M.R. (2010) 'The mechanism of double-strand DNA break repair by the nonhomologous DNA end-joining pathway', *Annual Review of Biochemistry*, 79, pp. 181–211. Available at: https://doi.org/10.1146/annurev.biochem.052308.093131.

Lillico, S.G. *et al.* (2005) 'Transgenic chickens as bioreactors for protein-based drugs', *Drug Discovery Today*, 10(3), pp. 191–196. Available at: https://doi.org/10.1016/S1359-6446(04)03317-3.

Lillico, S.G. *et al.* (2007) 'Oviduct-specific expression of two therapeutic proteins in transgenic hens', *Proceedings of the National Academy of Sciences*, 104(6), pp. 1771–1776. Available at: https://doi.org/10.1073/pnas.0610401104.

Lin, G. *et al.* (2017) 'Verification of mutagen function of Zeocin in Nannochloropsis oceanica through transcriptome analysis', *Journal of Ocean University of China*, 16(3), pp. 501–508. Available at: https://doi.org/10.1007/s11802-017-3231-x.

Lin, S. *et al.* (2014) 'Enhanced homology-directed human genome engineering by controlled timing of CRISPR/Cas9 delivery', *eLife*, 3, p. e04766. Available at: https://doi.org/10.7554/eLife.04766.

Liu, T. *et al.* (2015) 'Oviduct-Specific Expression of Human Neutrophil Defensin 4 in Lentivirally Generated Transgenic Chickens', *PLOS ONE*. Edited by S.V. Pizzo, 10(5), p. e0127922. Available at: https://doi.org/10.1371/journal.pone.0127922.

Llames, S. *et al.* (2015) 'Feeder Layer Cell Actions and Applications', *Tissue Engineering. Part B, Reviews*, 21(4), pp. 345–353. Available at: https://doi.org/10.1089/ten.TEB.2014.0547.

Łojewska, E. *et al.* (2016) 'Extraction and purification methods in downstream processing of plant-based recombinant proteins', *Protein Expression and Purification*, 120, pp. 110–117. Available at: https://doi.org/10.1016/j.pep.2015.12.018.

Lomova, A. *et al.* (2019) 'Improving Gene Editing Outcomes in Human Hematopoietic Stem and Progenitor Cells by Temporal Control of DNA Repair', *Stem Cells*, 37(2), pp. 284–294. Available at: https://doi.org/10.1002/stem.2935.

Loos, A. and Steinkellner, H. (2014) 'Plant glyco-biotechnology on the way to synthetic biology', *Frontiers in Plant Science*, 5, p. 523. Available at: https://doi.org/10.3389/fpls.2014.00523.

Love, J. *et al.* (1994) 'Transgenic birds by DNA microinjection', *Bio/Technology (Nature Publishing Company)*, 12(1), pp. 60–63. Available at: https://doi.org/10.1038/nbt0194-60.

Lundstrom, K. (2018) 'Viral Vectors in Gene Therapy', *Diseases*, 6(2), p. 42. Available at: https://doi.org/10.3390/diseases6020042.

Ma, Y. *et al.* (2016) 'Increasing the efficiency of CRISPR/Cas9-mediated precise genome editing in rats by inhibiting NHEJ and using Cas9 protein', *RNA Biology*, 13(7), pp. 605–612. Available at: https://doi.org/10.1080/15476286.2016.1185591.

Mabashi-Asazuma, H. *et al.* (2014) 'A novel baculovirus vector for the production of nonfucosylated recombinant glycoproteins in insect cells', *Glycobiology*, 24(3), pp. 325–340. Available at: https://doi.org/10.1093/glycob/cwt161.

Macdonald, J. *et al.* (2010) 'Characterisation and Germline Transmission of Cultured Avian Primordial Germ Cells', *PLoS ONE*. Edited by D.S. Milstone, 5(11), p. e15518. Available at: https://doi.org/10.1371/journal.pone.0015518.

Maga, E.A. *et al.* (2006) 'Production and processing of milk from transgenic goats expressing human lysozyme in the mammary gland', *Journal of Dairy Science*, 89(2), pp. 518–524. Available at: https://doi.org/10.3168/jds.S0022-0302(06)72114-2.

Maikawa, C.L. *et al.* (2020) 'Stable Monomeric Insulin Formulations Enabled by Supramolecular PEGylation of Insulin Analogues', *Advanced Therapeutics*, 3(1), p. 1900094. Available at: https://doi.org/10.1002/adtp.201900094.

Mamat, U. *et al.* (2015) 'Detoxifying Escherichia coli for endotoxin-free production of recombinant proteins', *Microbial Cell Factories*, 14, p. 57. Available at: https://doi.org/10.1186/s12934-015-0241-5.

Mao, Z. *et al.* (2008) 'Comparison of nonhomologous end joining and homologous recombination in human cells', *DNA repair*, 7(10), pp. 1765–1771. Available at: https://doi.org/10.1016/j.dnarep.2008.06.018.

Maredza, M. and Chola, L. (2016) 'Economic burden of stroke in a rural South African setting', *eNeurologicalSci*, 3, pp. 26–32. Available at: https://doi.org/10.1016/j.ensci.2016.01.001.

Martínez, J.L. *et al.* (2012) 'Pharmaceutical protein production by yeast: towards production of human blood proteins by microbial fermentation', *Current Opinion in Biotechnology*, 23(6), pp. 965–971. Available at: https://doi.org/10.1016/j.copbio.2012.03.011.

Maruyama, T. *et al.* (2015) 'Increasing the efficiency of precise genome editing with CRISPR-Cas9 by inhibition of nonhomologous end joining', *Nature Biotechnology*, 33(5), pp. 538–542. Available at: https://doi.org/10.1038/nbt.3190.

Massoud, M. *et al.* (1996) 'The deleterious effects of human erythropoietin gene driven by the rabbit whey acidic protein gene promoter in transgenic rabbits', *Reproduction Nutrition Development*, 36(5), pp. 555–563. Available at: https://doi.org/10.1051/rnd:19960511.

Mattanovich, D. *et al.* (2004) 'Stress in recombinant protein producing yeasts', *Journal of Biotechnology*, 113(1–3), pp. 121–135. Available at: https://doi.org/10.1016/j.jbiotec.2004.04.035.

McHugh, M.L. (2013) 'The chi-square test of independence', *Biochemia Medica*, 23(2), pp. 143–149. Available at: https://doi.org/10.11613/bm.2013.018.

Miyahara, D. *et al.* (2014) 'Culture Conditions for Maintain Propagation, Long-term Survival and Germline Transmission of Chicken Primordial Germ Cell-Like Cells', *The Journal of Poultry Science*, 51(1), pp. 87–95. Available at: https://doi.org/10.2141/jpsa.0130077.

Miyaoka, Y. *et al.* (2016) 'Systematic quantification of HDR and NHEJ reveals effects of locus, nuclease, and cell type on genome-editing', *Scientific Reports*, 6, p. 23549. Available at: https://doi.org/10.1038/srep23549.

Motono, M. *et al.* (2008) 'Analysis of chicken primordial germ cells', *Cytotechnology*, 57(2), pp. 199–205. Available at: https://doi.org/10.1007/s10616-008-9156-x.

Mozdziak, P.E. *et al.* (2003) 'Development of transgenic chickens expressing bacterial β-Galactosidase', *Developmental Dynamics*, 226(3), pp. 439–445. Available at: https://doi.org/10.1002/dvdy.10234.

Mozdziak, P.E. *et al.* (2005) 'Isolation of chicken primordial germ cells using fluorescence-activated cell sorting', *Poultry Science*, 84(4), pp. 594–600. Available at: https://doi.org/10.1093/ps/84.4.594.

Naito, M. *et al.* (1994) 'Production of germline chimeric chickens, with high transmission rate of donor-derived gametes, produced by transfer of primordial germ cells', *Molecular Reproduction and Development*, 39(2), pp. 153–161. Available at: https://doi.org/10.1002/mrd.1080390206.

Naito, M., Harumi, T. and Kuwana, T. (2012) 'Expression of GFP Gene in Cultured PGCs Isolated from Embryonic Blood and Incorporation into Gonads of Recipient Embryos', *The Journal of Poultry Science*, 49(2), pp. 116–123. Available at: https://doi.org/10.2141/jpsa.011094.

Naito, M., Harumi, T. and Kuwana, T. (2015) 'Long-term culture of chicken primordial germ cells isolated from embryonic blood and production of germline chimaeric chickens', *Animal Reproduction Science*, 153, pp. 50–61. Available at: https://doi.org/10.1016/j.anireprosci.2014.12.003.

Naito, M., Sakurai, M. and Kuwana, T. (1998) 'Expression of exogenous DNA in the gonads of chimaeric chicken embryos produced by transfer of primordial germ cell transfected in vitro and subsequent fate of the introduced DNA', *Journal of Reproduction and Fertility*, 113(1), pp. 137–143. Available at: https://doi.org/10.1530/jrf.0.1130137.

Nakajima, Y. *et al.* (2011) 'A New Method for Isolating Viable Gonadal Germ Cells from 7-day-old Chick Embryos', *The Journal of Poultry Science*, 48(2), pp. 106–111. Available at: https://doi.org/10.2141/jpsa.010094.

Nakamura, Y. *et al.* (2007) 'Migration and Proliferation of Primordial Germ Cells in the Early Chicken Embryo', *Poultry Science*, 86(10), pp. 2182–2193. Available at: https://doi.org/10.1093/ps/86.10.2182.

Nakamura, Y. *et al.* (2008) 'Increased proportion of donor primordial germ cells in chimeric gonads by sterilisation of recipient embryos using busulfan sustained-release emulsion in chickens', *Reproduction, Fertility, and Development*, 20(8), pp. 900–907. Available at: https://doi.org/10.1071/rd08138.

Nakamura, Y. *et al.* (2009) 'Effects of Busulfan Sustained-release Emulsion on Depletion and Repopulation of Primordial Germ Cells in Early Chicken Embryos', *The Journal of Poultry Science*, 46(2), pp. 127–135. Available at: https://doi.org/10.2141/jpsa.46.127.

Nakamura, Y. *et al.* (2010) 'Germline Replacement by Transfer of Primordial Germ Cells into Partially Sterilized Embryos in the Chicken', *Biology of Reproduction*, 83(1), pp. 130–137. Available at: https://doi.org/10.1095/biolreprod.110.083923.

Nakamura, Y. *et al.* (2011) 'Viability and Functionality of Primordial Germ Cells after Freeze-thaw in Chickens', *The Journal of Poultry Science*, 48(1), pp. 57–63. Available at: https://doi.org/10.2141/jpsa.010085.

Nakamura, Y. *et al.* (2012) 'X-irradiation Removes Endogenous Primordial Germ Cells (PGCs) and Increases Germline Transmission of Donor PGCs in Chimeric Chickens', *Journal of Reproduction and Development*, 58(4), pp. 432–437. Available at: https://doi.org/10.1262/jrd.2012-045.

Nakamura, Y., Kagami, H. and Tagami, T. (2013) 'Development, differentiation and manipulation of chicken germ cells', *Development, Growth & Differentiation*, 55(1), pp. 20–40. Available at: https://doi.org/10.1111/dgd.12026.

Nakano, M. *et al.* (2011) 'Characteristics of Novel Chicken Embryonic Stem Cells Established Using Chicken Leukemia Inhibitory Factor', *The Journal of Poultry Science*, 48(1), pp. 64–72. Available at: https://doi.org/10.2141/jpsa.010102.

Nausch, H. *et al.* (2013) 'Recombinant production of human interleukin 6 in Escherichia coli', *PloS One*, 8(1), p. e54933. Available at: https://doi.org/10.1371/journal.pone.0054933.

New England BioLabs (2017) 'NEBuilder® HiFi DNA Assembly Master Mix/NEBuilder HiFi DNA Assembly Cloning Kit. Instruction Manual'. New England BioLabs.

Nielsen, J. (2013) 'Production of biopharmaceutical proteins by yeast: Advances through metabolic engineering', *Bioengineered*, 4(4), pp. 207–211. Available at: https://doi.org/10.4161/bioe.22856.

Nordt, T.K. and Bode, C. (2003) 'Thrombolysis: newer thrombolytic agents and their role in clinical medicine', *Heart*, 89(11), pp. 1358–1362. Available at: https://doi.org/10.1136/heart.89.11.1358.

Norouzi, N., Bhakta, H.C. and Grover, W.H. (2017) 'Sorting cells by their density', *PLOS ONE*. Edited by V.M. Ugaz, 12(7), p. e0180520. Available at: https://doi.org/10.1371/journal.pone.0180520.

van Oers, M.M., Pijlman, G.P. and Vlak, J.M. (2015) 'Thirty years of baculovirus–insect cell protein expression: from dark horse to mainstream technology', *Journal of General Virology*, 96(1), pp. 6–23. Available at: https://doi.org/10.1099/vir.0.067108-0.

Oishi, I. (2010) 'Improvement of Transfection Efficiency in Cultured Chicken Primordial Germ Cells by Percoll Density Gradient Centrifugation', *Bioscience, Biotechnology, and Biochemistry*, 74(12), pp. 2426–2430. Available at: https://doi.org/10.1271/bbb.100464.

Oishi, I. *et al.* (2016) 'Targeted mutagenesis in chicken using CRISPR/Cas9 system', *Scientific Reports*, 6(1), p. 23980. Available at: https://doi.org/10.1038/srep23980.

Oishi, I. *et al.* (2018) 'Efficient production of human interferon beta in the white of eggs from ovalbumin gene-targeted hens', *Scientific Reports*, 8(1), p. 10203. Available at: https://doi.org/10.1038/s41598-018-28438-2.

Okada, T. *et al.* (2010) 'N-Glycosylation engineering of lepidopteran insect cells by the introduction of the 1,4-N-acetylglucosaminyltransferase III gene', *Glycobiology*, 20(9), pp. 1147–1159. Available at: https://doi.org/10.1093/glycob/cwq080.

Owczarek, B., Gerszberg, A. and Hnatuszko-Konka, K. (2019) 'A Brief Reminder of Systems of Production and Chromatography-Based Recovery of Recombinant Protein Biopharmaceuticals', *BioMed Research International*, 2019, pp. 1–13. Available at: https://doi.org/10.1155/2019/4216060.

Padhi, A., Ghaly, M.M. and Ma, L. (2016) 'Testis-enriched heat shock protein A2 (HSPA2): Adaptive advantages of the birds with internal testes over the mammals with testicular descent', *Scientific Reports*, 6(1), p. 18770. Available at: https://doi.org/10.1038/srep18770.

Paix, A. *et al.* (2017) 'Precision genome editing using synthesis-dependent repair of Cas9-induced DNA breaks', *Proceedings of the National Academy of Sciences*, 114(50). Available at: https://doi.org/10.1073/pnas.1711979114.

Pal, D. *et al.* (2018) 'Antibiotic-free expression system for the production of human interferon-beta protein', *3 Biotech*, 8(1), p. 36. Available at: https://doi.org/10.1007/s13205-017-1056-3.

Palmberger, D. *et al.* (2012) 'SweetBac: A New Approach for the Production of Mammalianised Glycoproteins in Insect Cells', *PLoS ONE*. Edited by Y. Li, 7(4), p. e34226. Available at: https://doi.org/10.1371/journal.pone.0034226.

Park, K.J. *et al.* (2010) 'Gamma-irradiation depletes endogenous germ cells and increases donor cell distribution in chimeric chickens', *In Vitro Cellular & Developmental Biology. Animal*, 46(10), pp. 828–833. Available at: https://doi.org/10.1007/s11626-010-9361-8.

Park, T.S. *et al.* (2003) 'Birth of germline chimeras by transfer of chicken embryonic germ (EG) cells into recipient embryos', *Molecular Reproduction and Development*, 65(4), pp. 389–395. Available at: https://doi.org/10.1002/mrd.10304.

Park, T.S. *et al.* (2015) 'Deposition of bioactive human epidermal growth factor in the egg white of transgenic hens using an oviduct-specific minisynthetic promoter', *The FASEB Journal*, 29(6), pp. 2386–2396. Available at: https://doi.org/10.1096/fj.14-264739.

Park, T.S. and Han, J.Y. (2000) 'Derivation and characterization of pluripotent embryonic germ cells in chicken', *Molecular Reproduction and Development*, 56(4), pp. 475–482. Available at: https://doi.org/10.1002/1098-2795(200008)56:4<475::AID-MRD5>3.0.CO;2-M.

Perry, M.M. (1988) ‘A complete culture system for the chick embryo’, *Nature*, 331(6151), pp. 70–72. Available at: https://doi.org/10.1038/331070a0.

Peternel, S. and Komel, R. (2011) ‘Active protein aggregates produced in Escherichia coli’, *International Journal of Molecular Sciences*, 12(11), pp. 8275–8287. Available at: https://doi.org/10.3390/ijms12118275.

Pinder, J., Salsman, J. and Dellaire, G. (2015) ‘Nuclear domain “knock-in” screen for the evaluation and identification of small molecule enhancers of CRISPR-based genome editing’, *Nucleic Acids Research*, 43(19), pp. 9379–9392. Available at: https://doi.org/10.1093/nar/gkv993.

Pires, M.F. *et al.* (2021) ‘Performance and egg quality of commercial laying hens fed with various levels of protected sodium butyrate’, *South African Journal of Animal Science*, 50(5). Available at: https://doi.org/10.4314/sajas.v50i5.14.

Priola, J.J. *et al.* (2016) ‘High-throughput screening and selection of mammalian cells for enhanced protein production’, *Biotechnology Journal*, 11(7), pp. 853–865. Available at: https://doi.org/10.1002/biot.201500579.

Puetz, J. and Wurm, F.M. (2019) ‘Recombinant Proteins for Industrial versus Pharmaceutical Purposes: A Review of Process and Pricing’, *Processes*, 7(8), p. 476. Available at: https://doi.org/10.3390/pr7080476.

Raju, T.S. *et al.* (2000) ‘Species-specific variation in glycosylation of IgG: evidence for the species-specific sialylation and branch-specific galactosylation and importance for engineering recombinant glycoprotein therapeutics’, *Glycobiology*, 10(5), pp. 477–486. Available at: https://doi.org/10.1093/glycob/10.5.477.

Ran, F.A. *et al.* (2013) ‘Genome engineering using the CRISPR-Cas9 system’, *Nature Protocols*, 8(11), pp. 2281–2308. Available at: https://doi.org/10.1038/nprot.2013.143.

Ranganai, E. and Matizirofa, L. (2020) ‘An analysis of recent stroke cases in South Africa: Trend, seasonality and predictors’, *South African Medical Journal*, 110(2), p. 92. Available at: https://doi.org/10.7196/SAMJ.2020.v110i2.013891.

Rapp, J.C. *et al.* (2003) 'Biologically active human interferon α-2b produced in the egg white of transgenic hens', *Transgenic Research*, 12(5), pp. 569–575. Available at: https://doi.org/10.1023/A:1025854217349.

Rasband, W. (2022) 'ImageJ'. National Institute of Health, USA. Available at: http://imagej.nih.gov/ij/.

Rodgers, K. and McVey, M. (2016) 'Error-Prone Repair of DNA Double-Strand Breaks', *Journal of Cellular Physiology*, 231(1), pp. 15–24. Available at: https://doi.org/10.1002/jcp.25053.

Rosano, G.L. and Ceccarelli, E.A. (2014) 'Recombinant protein expression in Escherichia coli: advances and challenges', *Frontiers in Microbiology*, 5. Available at: https://doi.org/10.3389/fmicb.2014.00172.

Saleh-Gohari, N. and Helleday, T. (2004) 'Conservative homologous recombination preferentially repairs DNA double-strand breaks in the S phase of the cell cycle in human cells', *Nucleic Acids Research*, 32(12), pp. 3683–3688. Available at: https://doi.org/10.1093/nar/gkh703.

Sang, H. (1994) 'Transgenic chickens — methods and potential applications', *Trends in Biotechnology*, 12(10), pp. 415–420. Available at: https://doi.org/10.1016/0167-7799(94)90030-2.

Sang, H. (2004) 'Prospects for transgenesis in the chick', *Mechanisms of Development*, 121(9), pp. 1179–1186. Available at: https://doi.org/10.1016/j.mod.2004.05.012.

Schilit, S.L.P. *et al.* (2016) 'Pronuclear Injection-Based Targeted Transgenesis', *Current Protocols in Human Genetics*, 91, p. 15.10.1-15.10.28. Available at: https://doi.org/10.1002/cphg.23.

Shaaltiel, Y. *et al.* (2007) 'Production of glucocerebrosidase with terminal mannose glycans for enzyme replacement therapy of Gaucher's disease using a plant cell system', *Plant Biotechnology Journal*, 5(5), pp. 579–590. Available at: https://doi.org/10.1111/j.1467-7652.2007.00263.x.

Shao, S. *et al.* (2017) 'Enhancing CRISPR/Cas9-mediated homology-directed repair in mammalian cells by expressing Saccharomyces cerevisiae Rad52', *The International Journal of Biochemistry & Cell Biology*, 92, pp. 43–52. Available at: https://doi.org/10.1016/j.biocel.2017.09.012.

Slaymaker, I.M. *et al.* (2016) 'Rationally engineered Cas9 nucleases with improved specificity', *Science (New York, N.Y.)*, 351(6268), pp. 84–88. Available at: https://doi.org/10.1126/science.aad5227.

Solá, R.J. and Griebenow, K. (2010) 'Glycosylation of therapeutic proteins: an effective strategy to optimize efficacy', *BioDrugs: Clinical Immunotherapeutics, Biopharmaceuticals and Gene Therapy*, 24(1), pp. 9–21. Available at: https://doi.org/10.2165/11530550-000000000-00000.

Soler, E. and Houdebine, L.-M. (2007) 'Preparation of recombinant vaccines', in *Biotechnology Annual Review*. Elsevier, pp. 65–94. Available at: https://doi.org/10.1016/S1387-2656(07)13004-0.

Song, H. *et al.* (2017) 'High purity recombinant human growth hormone (rhGH) expression in Escherichia coli under phoA promoter', *Bioengineered*, 8(2), pp. 147–153. Available at: https://doi.org/10.1080/21655979.2016.1212137.

Song, J. *et al.* (2016) 'RS-1 enhances CRISPR/Cas9- and TALEN-mediated knock-in efficiency', *Nature Communications*, 7(1), p. 10548. Available at: https://doi.org/10.1038/ncomms10548.

Song, Y. *et al.* (2005) 'Production of germline chimeric chickens following the administration of a busulfan emulsion', *Molecular Reproduction and Development*, 70(4), pp. 438–444. Available at: https://doi.org/10.1002/mrd.20218.

Song, Y. *et al.* (2014) 'Characteristics of Long-Term Cultures of Avian Primordial Germ Cells and Gonocytes1', *Biology of Reproduction*, 90(1). Available at: https://doi.org/10.1095/biolreprod.113.113381.

South Africa: Department of Health (2022) 'South African Medicine Price RegistryDatabase Of Medicine Prices 23rd December 2022'. Available at: http://www.mpr.gov.za/PublishedDocuments.aspx.

Steele, K.H. *et al.* (2017) 'Improving the baculovirus expression vector system with vankyrin-enhanced technology', *Biotechnology Progress*, 33(6), pp. 1496–1507. Available at: https://doi.org/10.1002/btpr.2516.

Stolfa, G. *et al.* (2018) 'CHO-Omics Review: The Impact of Current and Emerging Technologies on Chinese Hamster Ovary Based Bioproduction', *Biotechnology Journal*, 13(3), p. e1700227. Available at: https://doi.org/10.1002/biot.201700227.

Strohl, W.R. (2015) 'Fusion Proteins for Half-Life Extension of Biologics as a Strategy to Make Biobetters', *BioDrugs: Clinical Immunotherapeutics, Biopharmaceuticals and Gene Therapy*, 29(4), pp. 215–239. Available at: https://doi.org/10.1007/s40259-015-0133-6.

Szczerba, A. *et al.* (2020) 'In Vitro Culture of Chicken Circulating and Gonadal Primordial Germ Cells on a Somatic Feeder Layer of Avian Origin', *Animals*, 10(10), p. 1769. Available at: https://doi.org/10.3390/ani10101769.

Szczerba, A., Kuwana, T. and Bednarczyk, M. (2021) 'Concentration and total number of circulating primordial germ cells in Green-legged Partridgelike chicken embryos', *Poultry Science*, 100(1), pp. 319–324. Available at: https://doi.org/10.1016/j.psj.2020.08.016.

Tajima, A. *et al.* (1998) 'Production of germ-line chimeras by transfer of cryopreserved gonadal primordial germ cells (gPGCs) in chicken', *The Journal of Experimental Zoology*, 280(3), pp. 265–267.

Tang, X. *et al.* (2007) 'Pro-proliferating effect of homologous somatic cells on chicken primordial germ cells', *Cell Biology International*, 31(9), pp. 1016–1021. Available at: https://doi.org/10.1016/j.cellbi.2007.03.014.

Tihanyi, B. and Nyitray, L. (2020) 'Recent advances in CHO cell line development for recombinant protein production', *Drug Discovery Today: Technologies*, 38, pp. 25–34. Available at: https://doi.org/10.1016/j.ddtec.2021.02.003.

Tonus, C. *et al.* (2016) 'Long term-cultured and cryopreserved primordial germ cells from various chicken breeds retain high proliferative potential and gonadal colonisation competency', *Reproduction, Fertility and Development*, 28(5), p. 628. Available at: https://doi.org/10.1071/RD14194.

Trefil, P. *et al.* (2017) 'Male fertility restored by transplanting primordial germ cells into testes: a new way towards efficient transgenesis in chicken', *Scientific Reports*, 7(1), p. 14246. Available at: https://doi.org/10.1038/s41598-017-14475-w.

Tripathi, N.K. and Shrivastava, A. (2019) 'Recent Developments in Bioprocessing of Recombinant Proteins: Expression Hosts and Process Development', *Frontiers in Bioengineering and Biotechnology*, 7, p. 420. Available at: https://doi.org/10.3389/fbioe.2019.00420.

Tsukahara, T. *et al.* (2015) 'The Tol2 transposon system mediates the genetic engineering of T-cells with CD19-specific chimeric antigen receptors for B-cell malignancies', *Gene Therapy*, 22(2), pp. 209–215. Available at: https://doi.org/10.1038/gt.2014.104.

Tsukuda, M. and Miyazaki, K. (2013) 'DNA fragmentation caused by an overdose of Zeocin', *Journal of Bioscience and Bioengineering*, 116(5), pp. 644–646. Available at: https://doi.org/10.1016/j.jbiosc.2013.05.004.

Usmani, S.S. *et al.* (2017) 'THPdb: Database of FDA-approved peptide and protein therapeutics', *PLOS ONE*. Edited by Q.-X.A. Sang, 12(7), p. e0181748. Available at: https://doi.org/10.1371/journal.pone.0181748.

van Veen, H.A. *et al.* (2012) 'Characterization of recombinant human C1 inhibitor secreted in milk of transgenic rabbits', *Journal of Biotechnology*, 162(2–3), pp. 319–326. Available at: https://doi.org/10.1016/j.jbiotec.2012.09.005.

Vieira Gomes, A.M. *et al.* (2018) 'Comparison of Yeasts as Hosts for Recombinant Protein Production', *Microorganisms*, 6(2), p. E38. Available at: https://doi.org/10.3390/microorganisms6020038.

Vos, T. *et al.* (2020) 'Global burden of 369 diseases and injuries in 204 countries and territories, 1990–2019: a systematic analysis for the Global Burden of Disease Study 2019', *The Lancet*, 396(10258), pp. 1204–1222. Available at: https://doi.org/10.1016/S0140-6736(20)30925-9.

Wang, B. *et al.* (2015) 'Highly efficient CRISPR/HDR-mediated knock-in for mouse embryonic stem cells and zygotes', *BioTechniques*, 59(4), pp. 201–208. Available at: https://doi.org/10.2144/000114339.

Wang, L. *et al.* (2017) 'Derivation and characterization of primordial germ cells from Guangxi yellow-feather chickens', *Poultry Science*, 96(5), pp. 1419–1425. Available at: https://doi.org/10.3382/ps/pew387.

Wang, Ling *et al.* (2017) 'Enhancing Targeted Genomic DNA Editing in Chicken Cells Using the CRISPR/Cas9 System', *PLOS ONE*. Edited by W. Shen, 12(1), p. e0169768. Available at: https://doi.org/10.1371/journal.pone.0169768.

Wang, X.J. *et al.* (2017) 'Stress impairs the reproduction of laying hens: an involvement of energy', *World's Poultry Science Journal*, 73(4), pp. 845–856. Available at: https://doi.org/10.1017/S0043933917000794.

Warach, S.J., Dula, A.N. and Milling, T.J. (2020) 'Tenecteplase Thrombolysis for Acute Ischemic Stroke', *Stroke*, 51(11), pp. 3440–3451. Available at: https://doi.org/10.1161/STROKEAHA.120.029749.

Weitzel, A.J. *et al.* (2021) 'Meiotic Cas9 expression mediates gene conversion in the male and female mouse germline', *PLoS biology*, 19(12), p. e3001478. Available at: https://doi.org/10.1371/journal.pbio.3001478.

Whyte, J. *et al.* (2015) 'FGF, Insulin, and SMAD Signaling Cooperate for Avian Primordial Germ Cell Self-Renewal', *Stem Cell Reports*, 5(6), pp. 1171–1182. Available at: https://doi.org/10.1016/j.stemcr.2015.10.008.

Woodcock, M.E. *et al.* (2019) 'Reviving rare chicken breeds using genetically engineered sterility in surrogate host birds', *Proceedings of the National Academy of Sciences*, 116(42), pp. 20930–20937. Available at: https://doi.org/10.1073/pnas.1906316116.

Woodfint, R.M., Hamlin, E. and Lee, K. (2018) 'Avian Bioreactor Systems: A Review', *Molecular Biotechnology*, 60(12), pp. 975–983. Available at: https://doi.org/10.1007/s12033-018-0128-x.

Wright, G. *et al.* (1991) 'High Level Expression of Active Human Alpha-1-Antitrypsin in the Milk of Transgenic Sheep', *Nature Biotechnology*, 9(9), pp. 830–834. Available at: https://doi.org/10.1038/nbt0991-830.

Yamamoto, Y. *et al.* (2007) 'A Novel Method to Isolate Primordial Germ Cells and Its Use for the Generation of Germline Chimeras in Chicken', *Biology of Reproduction*, 77(1), pp. 115–119. Available at: https://doi.org/10.1095/biolreprod.107.061200.

Yang, H. *et al.* (2020) 'Methods Favoring Homology-Directed Repair Choice in Response to CRISPR/Cas9 Induced-Double Strand Breaks', *International Journal of Molecular Sciences*, 21(18), p. 6461. Available at: https://doi.org/10.3390/ijms21186461.

Yang, P. *et al.* (2008) 'Cattle Mammary Bioreactor Generated by a Novel Procedure of Transgenic Cloning for Large-Scale Production of Functional Human Lactoferrin', *PLoS ONE*. Edited by H.A. El-Shemy, 3(10), p. e3453. Available at: https://doi.org/10.1371/journal.pone.0003453.

Yao, J. *et al.* (2015) 'Plants as Factories for Human Pharmaceuticals: Applications and Challenges', *International Journal of Molecular Sciences*, 16(12), pp. 28549–28565. Available at: https://doi.org/10.3390/ijms161226122.

Yao, X. *et al.* (2018) 'Tild-CRISPR Allows for Efficient and Precise Gene Knockin in Mouse and Human Cells', *Developmental Cell*, 45(4), pp. 526-536.e5. Available at: https://doi.org/10.1016/j.devcel.2018.04.021.

Yee, C.M. *et al.* (2018) 'The Coming Age of Insect Cells for Manufacturing and Development of Protein Therapeutics', *Industrial & Engineering Chemistry Research*, 57(31), pp. 10061–10070. Available at: https://doi.org/10.1021/acs.iecr.8b00985.

Zeng, H. and Yang, A. (2019) 'Quantification of proteomic and metabolic burdens predicts growth retardation and overflow metabolism in recombinant Escherichia coli', *Biotechnology and Bioengineering*, 116(6), pp. 1484–1495. Available at: https://doi.org/10.1002/bit.26943.

Zhang, J. *et al.* (2008) 'Expression of active recombinant human lactoferrin in the milk of transgenic goats', *Protein Expression and Purification*, 57(2), pp. 127–135. Available at: https://doi.org/10.1016/j.pep.2007.10.015.

Zhang, J.-P. *et al.* (2017) 'Efficient precise knockin with a double cut HDR donor after CRISPR/Cas9-mediated double-stranded DNA cleavage', *Genome Biology*, 18(1), p. 35. Available at: https://doi.org/10.1186/s13059-017-1164-8.

Zhang, X. *et al.* (2021) ‘Improvement of protein production by engineering a novel antiapoptotic baculovirus vector to suppress the expression of *Sf-caspase-1* and *Tn-caspase-1*’, *Biotechnology and Bioengineering*, 118(8), pp. 2977–2989. Available at: https://doi.org/10.1002/bit.27807.

Zhang, X. *et al.* (2022) ‘Homology-based repair induced by CRISPR-Cas nucleases in mammalian embryo genome editing’, *Protein & Cell*, 13(5), pp. 316–335. Available at: https://doi.org/10.1007/s13238-021-00838-7.

Zhao, D.F. and Kuwana, T. (2003) ‘Purification of avian circulating primordial germ cells by nycodenz density gradient centrifugation’, *British Poultry Science*, 44(1), pp. 30–35. Available at: https://doi.org/10.1080/0007166031000085382.

Zitek, T., Ataya, R. and Brea, I. (2020) ‘Using Tenecteplase for Acute Ischemic Stroke: What Is the Hold Up?’, *The Western Journal of Emergency Medicine*, 21(2), pp. 199–202. Available at: https://doi.org/10.5811/westjem.2020.1.45279.

Appendices

Table 2.22. LB liquid and LB agar recipes. The following components are added to 500ml distilled water. Agar can be added for making LB agar.

Component	Weight (g)
Tryptone/Peptone	10
NaCl	10
Yeast Extract	5

Table 2.23. Buffer compositions for Alkaline lysis plasmid extraction.

Stock solution	Final concentration
Alkaline lysis solution I	
1M Glucose	50 mM
1M Tris pH 8.0	25 mM
0.5M EDTA pH 8.0	5 mM
dH_20	Up to desired volume
Alkaline lysis solution II	
10N NaOH	0.2N
1% SDS	0.01%
dH_2O	Up to desired volume
Alkaline lysis solution III	
5M potassium acetate	3M
Glacial acetic acid (100%)	11.5%
dH_2O	Up to desired volume
Tris-EDTA	
1M Tris (pH 8.0)	10mM
0.5M EDTA (pH 8.0)	1mM
dH_2O	Up to desired volume

Table 2.24. CEF culture media.

Component	Concentration
Fetal bovine serum	10%
Chicken Serum	2%
L-Glutamine	1%
NEAA	1%
Primocin	0.2%
DMEM	Up to 250ml

Table 2.25. CEF freezing media.

Component	Concentration
Fetal bovine serum	10%
Chicken Serum	2%
DMSO	10%
DMEM	78%

Table 2.26. PGC culture media composition. Media was supplemented with basic fibroblast growth factor (10ng/ml), Leukemia inhibitory factor (10ng/ml), and Stem cell factor (5 ng/ml).

Component	Concentration
Fetal bovine serum	10%
Chicken Serum	2.5%
L-Glutamine	2mM
NEAA	1X
Primocin	1X
β-Mercaptoethanol	0.1mM
DMEM	Up to 250ml

Table 2.27. Lysis buffers used for sex determination. The buffers when using blood or tissue samples are shown.

Component	M/V
Blood	
Citric acid	0.48%
Sodium Citrate	1.32%
Dextrose/D-glucose	1.47%
Head tissue	
Tris-HCl/Base	1M
EDTA	0.5M
NaCl	1mol
dH_2O	Up to desired volume

Table 2.28. Terrific Broth Medium composition

Component	Quantity
Tryptone/Peptone	20g
Glycerol	4ml
Yeast Extract	24g
Distilled water	900ml
Phosphate buffer (0.17M KH_2PO4, 0.72M K_2HPO4)	100ml